Evaluation of methodologies for risk assessment of combined toxic actions of chemical substances and establishment of PBTK/TD models for pesticides

Reffstrup, Trine Klein

Publication date:
2012

Document Version
Publisher's PDF, also known as Version of record

Evaluation of methodologies for risk assessment of combined toxic actions of chemical substances and establishment of PBTK/TD models for pesticides

Ph.D. Thesis

Trine Klein Reffstrup

Division of Toxicology and Risk Assessment
National Food Institute
Technical University of Denmark

Evaluation of methodologies for risk assessment of combined toxic actions of chemical substances and establishment of PBTK/TD models for pesticides

Søborg, 2012

Photo on front-page: Painting by Lena Klein Reffstrup
ISBN: 978-87-92736-17-4

Supervisors: John Christian Larsen and Otto Meyer, Division of Toxicology and Risk Assessment, National Food Institute, Technical University of Denmark

Division of Toxicology and Risk Assessment
National Food Institute
Technical University of Denmark
Mørkhøj Bygade 19
DK-2860 Søborg

Tel: +45 35 88 70 00
Fax: +45 35 88 70 01

PREFACE AND ACKNOWLEDGEMENT

This thesis is carried out at Division of Toxicology and Risk Assessment, National Food Institute, Technical University of Denmark. The two supervisors were John Christian Larsen and Otto Meyer, Division of Toxicology and Risk Assessment, National Food Institute, Technical University of Denmark.

The thesis provides an overview of the present methods for risk assessment of mixtures of chemicals in food focusing on residues of pesticides. Further, it examines the applicability of physiologically based toxicokinetic/toxicodynamic (PBTK/TD) models in risk assessment. The thesis represents the initial work on implementing PBTK/TD modeling in the risk assessment of combined actions of chemicals at the institute.

I would like to thank my two supervisors John Christian Larsen and Otto Meyer for fruitful discussions, constructive criticism as well as their encouragement during the process.

My two proofreaders Kirsten Pilegaard and Svava Osk Jonsdottir are thanked for their quick response, beneficial comments on the manuscript and their linguistic enthusiasm.

Thanks to all my colleagues in the division for a positive and inspiring working environment.

Thanks to my family and friends for their patience and support.

"Every aspect of the development of a new model should be subject to skeptical criticism and careful evaluation by experimental measurement and simulation, rather than by reference to a previous model" (Clewell and Clewell, III, 2008).

CONTENT

1 ABBREVIATIONS

A list of abbreviations used in the model can be found at the end of Annex II.

AChE: acetylcholinesterase
ADI: acceptable daily intake
ADME: absorption, distribution, metabolism and excretion
ATSDR: Agency for Toxic Substances and Disease Registry in USA
BBDR: biologically based dose response modelling
BINWOE: binary weight of evidence
BMD: benchmark dose
BuChE: butyrylcholinesterase
bw: body weight
CaE: carboxylesterase
CAG: cumulative assessment groups
ChE: cholinesterase
CMG: common mechanism group
CNS: central nervous system
CPF: chlorpyrifos
CRI: cumulative risk index
DCE: 1,1-dichloroethylene
DFP: diisopropylfluorophosphate
EFSA: European Food Safety Authority
HI: hazard index
HI_I: interaction hazard index
HQ: hazard quotient
ILSI: International Life Sciences Institute
IPCS: International Programme on Chemical Safety
JMPR: FAO/WHO Joint Meeting on Pesticide Residues
LOAEL: lowest observed adverse effect level
MOE: margin of exposure
MOE_T: combined margin of exposure
NOAEL: No observed adverse effect level
OP: organophosphorus pesticide or organophosphate
PBPD: physiologically based pharmacodynamic
PBPK: physiologically based pharmacokinetic
PBTD: physiologically based toxicodynamic
PBTK: physiologically based toxicokinetic
PCB: polychlorinated biphenyls
p_{mix}: probability for an adverse effect from a mixture (Bliss independence)
POD: point of departure
PODI: point of departure index
PON-1: paraoxonase 1
PPR Panel: Scientific Panel on Plant Protection Products and their Residues
QSAR: quantitative structural activity relationship

RBC: red blood cells, erythrocytes
RfD: reference dose
RIVM: Rijksinstituut voor Volksgezondheid en Milieu (in English: National Institute for Public Health and the Environment)
RPF: relative potency factor
TCE: trichloroethylene
TCP: 3,5,6-trichloro-2-pyridinol
TEF: toxicity equivalency factor
TEQ: Toxicity equivalent
U.S. EPA: USA Environmental Protection Agency
UF: uncertainty factor
WOE: weight of evidence

2 SUMMARY

Humans are simultaneously exposed to a number of chemicals via food and environment. These chemicals may have a combined action that causes a lower or higher toxic effect than would be expected from knowledge about the single compounds. Therefore, combined actions need to be addressed in the risk assessment process.

This Ph.D.-thesis provides an overview of the current knowledge on methods for risk assessment of combined actions of chemicals focussing on pesticides. Some of the methods are based on knowledge on the whole mixture and others are based on data on the single compounds in the mixture. The whole mixture approaches would be the ideal choice for assessment of e.g. pesticide residues in food. However, they are normally not applicable since they require a large number of experimental data that are rarely available. This leaves the single compound approaches as the more realistic ones.

The first step in the risk assessment of a mixture is to evaluate whether a group of compounds can be identified that induce a common toxic effect by a common mechanism of toxicity and therefore is suited for a cumulative risk assessment based on additivity. Ideally the identification of a group of pesticides for cumulative risk assessment should be based on criteria providing the best and most robust grouping such as chemical structure, mechanism of action, common toxic mode of action or common toxic effect. Unfortunately, such data are seldom available for all of the compounds of concern. Instead for pragmatic reasons, it is often more appropriate to consider the individual compounds as possible candidates for one (or more) cumulative assessment group(s).

The cumulative risk assessment of this group will then be performed assuming simple similar action using one of the single compound approaches. The hazard index based on a health based guidance value e.g. the acceptable daily intake (ADI) would normally be sufficient. However, the point of departure index is the most preferably method because it does not make use of a policy driven uncertainty factor and instead it is based on the most relevant toxicity data.

In case that more than one common mechanism group based on different simple similar actions are identified, they should be assessed separately. In addition, the potential for interactions between the groups (or single compounds) has to be considered. If no interactions are identified, simple dissimilar action can be anticipated and the response addition method should be used to assess the effect of the mixture.

In many cases the evaluators will probably tend to use very pragmatic approaches if lack of interaction between the compounds at the actual dose level can be assumed. This includes assuming all compounds in the mixture show dose additivity (simple similar actions). The hazard index or point of departure index would then be the preferred methods.

A crucial point in the assessment is whether there is interaction or no interaction between the compounds in the mixture. Although interactions among chemicals at high doses are well-known, no single simple approach is currently available to judge upon potential interactions at the low dose levels of pesticide residues that humans are exposed to in food. For this

purpose, physiologically based toxicokinetic/toxicodynamic (PBTK/TD) modelling has been recommended as a tool to assess combined tissue doses and to help predict potential interactions including thresholds for such effects. Therefore, this thesis also focuses on such models and their applicability for use in risk assessment. This type of model has been used for several years in the area of pharmacology but the use in the area of toxicology is relatively new.

In a PBTK model the animal or man is described as a set of tissue compartments which is combined by mathematical descriptions of biological tissues and physiological processes in the body. Thereby it is possible to quantitatively simulate the absorption, distribution, metabolism and excretion of chemicals and to predict the internal dose after exposure to the chemical (or metabolite) of concern.

The PBTK models make it possible to extrapolate between species, from high-dose to low-dose, from route-to-route and between exposure scenarios. In this way the risk assessor can simulate various scenarios including scenarios which cannot be studied experimentally. Models can be developed for subpopulations such as children and this may help the risk assessor determine whether special care should be taken for such groups.

It is also possible to incorporate mechanistic information on interactions in the model and as mentioned above interaction threshold can be determined. This would provide a helpful tool in the risk assessment of combined actions of chemicals.

The PBTK model can be coupled with a toxicodynamic part in which the model attempts to estimate the effect resulting from the internal dose. The output of a PBTK model is linked to a toxicodynamic model by mathematical descriptions of the hypothesis of how compounds contribute to the initiation of cellular changes leading to the toxic responses.

In the present Ph.D. project a PBTK/TD model was established based on a previous published model. The model describes the organophosphorus pesticide chlorpyrifos and its metabolism to chlorpyrifos-oxon and 3,5,6-trichloro-2-pyridinol as well as the toxicodynamic of the chlorpyrifos-oxon i.e. inhibition of acetylcholinesterase activity in various tissues. This paper was chosen because the model is on a relevant compound (a pesticide that is widely used) and one had the impression that the model work was described in details.

The work in establishing this model clearly pointed out the importance that authors of such publications report their results with a high degree of transparency in order to enable colleagues to reproduce their work and e.g. evaluate it for further developing the model. The model description should include model structure and equations as well as documentation of the choice of parameters and their origin. At present there is a lack of adequate data for use in the PBTK models and further studies in order to determine parameters for use in PBTK models are needed. The model developer is also forced to make assumptions and extrapolations. It is of great importance that these are biologically based and explained.

The PBTK/TD model on chlorpyrifos in the present project was used to illustrate how a no observed adverse effect level (NOAEL) can be established by the model and how to make extrapolations between species (rats and humans). The model underestimated the inhibition

of acetylcholinesterase compared to experimental data. Therefore, the model needs improvement before it can be used in risk assessment.

The PBTD modelling is still in its infancy and it will probably be better to put more effort into improving the toxicokinetic part especially including establishment of internationally acceptable reference values for various parameters before extending the model with a toxicodynamic part.

PBTK models can be used to evaluate combined actions of a mixture of compounds. In case of a mixture of compounds that do not interact (e.g. simple similar action) the PBTK modelling tool is useful to predict the combined doses in the target organ taking metabolism of the compounds into account. Such compounds should be dealt with in the PBTK models in the same way as single compounds.

In case of a mixture of interacting compounds mechanistic information on interactions can be incorporated in the PBTK/TD model and thereby it can be used e.g. to determine the interaction threshold. Such a model will consists of sets of identical equations, one set for each chemical as well as equations that specifically accounts for the interactions (e.g. competitive inhibition of metabolism in liver or induction of hepatic metabolism).

The development of PBTK models is complex and should only be used when it is considered essential. If adequate models are developed, they can provide better knowledge and understanding of the effects of mixtures in the organism and provide improved information on tissue dose levels and variations between species and within a population. Moreover, scientifically supportable results about possible combined actions in humans after exposure to mixtures of pesticide residues in food would help making more reliable risk assessment.

The PBTK models thus have a potential as an important tool in the risk assessment. Adequate documentation of the model is fundamental in order to increase the credibility of PBTK modelling. Such credibility is crucial for a spreading of its use in risk assessment.

This Ph.D.-project constitutes the initial work on implementing PBTK/TD models in the risk assessment of combined toxic action of chemical substances in food at the DTU National Food Institute. The work has revealed some major problems and pitfalls in the developing process. However if reliable, these models will provide knowledge of the relationship between internal doses of the chemicals and the observed toxic effects and this knowledge will reduce the uncertainty in the risk assessment. Therefore, the work will continue implementing these models as a helpful tool in future risk assessment.

3 DANSK RESUMÉ

Mennesker er udsat for en række kemiske stoffer samtidigt fra fødevarer og miljø. Disse kemikalier kan have en kombinationseffekt, der fører til en lavere eller højere toksisk effekt, end man ville forvente ud fra viden om de enkelte stoffer. Derfor er det nødvendigt at se på kombinationseffekter i risikovurderingsprocessen.

Denne ph.d.-afhandling giver et overblik over den nuværende viden om metoder til risikovurdering af kombinationseffekter af kemiske stoffer med fokus på pesticider. Nogle af disse metoder er baseret på data for hele blandingen, mens andre er baseret på data for de enkelte stoffer i en blanding.

Metoderne baseret på data for hele blandinger ville være det ideelle valg til risikovurdering af pesticider i fødevarer, men de kræver en stor mængde eksperimentelle data, som sjældent er til rådighed, og derfor er deres anvendelighed begrænset. Metoderne baseret på data for enkelt stoffer er mere brugbare.

Det første trin i risikovurderingen af en blanding er at se på, om der kan identificeres en gruppe af stoffer, der inducerer samme toksiske effekt ved samme virkningsmekanisme, og som derfor er egnet til at blive vurderet sammen baseret på "dosis addition". Ideelt set skal identifikationen af grupper af pesticider til en sådan kumulativ risikovurdering baseres på kriterier, der giver den bedste og mest robuste gruppering. Det kan være samme kemiske struktur, virkningsmekanisme, virkemåde eller toksiske effekt. Sådanne data er dog sjældent tilgængelige for alle stoffer i en blanding, og af praktiske grunde er det derfor ofte mere relevant at undersøge, om de enkelte stoffer kan grupperes i en (eller flere) såkaldt "cumulative assessment group".

Det næste trin i den kumulative risikovurdering vil blive baseret på en antagelse om, at stofferne agerer med samme virkningsmåde (såkaldt "simple similar action"), og en af metoderne baseret på data for enkelt stoffer vil blive benyttet i vurderingen. I mange tilfælde vil brug af "hazard index" baseret på en sundhedsbaseret "guidance value", f.eks. acceptabelt dagligt indtag (ADI), være tilstrækkeligt. Den foretrukne metode vil dog være "point of departure index", da denne ikke involverer en politisk styret usikkerhedsfaktor men i stedet er baseret på de mest relevante toksikologiske data.

Hvis der identificeres mere end én fælles mekanisme gruppe baseret på "simple similar action", bør de vurderes hver for sig. Muligheden for kombinationseffekter mellem grupper (og enkeltstoffer) skal også vurderes. Hvis der ikke kan forventes interaktioner mellem stofferne i blandingen, kan man antage, at der er tale om såkaldt "simple dissimilar action" og metoden "response addition" kan bruges til at vurdere effekten af blandingen.

Hvis der ikke er fundet tegn på interaktion mellem stoffer ved de aktuelle dosisniveauer i en blanding vil det antages, at alle stofferne i blandingen viser "simple similar action". I mange tilfælde vil der blive valgt en pragmatisk løsning, og de foretrukne metoder ofte være "hazard index" eller "point of departure index".

I en risikovurdering er det vigtigt at fastslå, om stofferne i blandingen interagerer eller ej. Interaktioner er velkendte mellem stoffer ved høje doser, men der er ikke nogen simpel metode til at vurdere muligheden for potentielle interaktioner mellem stofferne ved de lave dosisniveauer, som mennesker bliver udsat for af pesticider via fødevarer. Det er blevet foreslået at de såkaldte fysiologisk baserede toksikokinetiske/toksikodynamiske ("physiologically based toxicokinetic/toxicodynamic", PBTK/TD) modeller kunne være et nyttigt redskab til vurdering af en samlet dosis fra en kemisk blanding til et væv eller organ. Dermed vil disse modeller kunne hjælpe med at forudsige potentielle interaktioner herunder bestemme tærskler, hvorunder der ikke vil ses kombinationseffekter. Denne afhandling fokuserer derfor også på sådanne modeller og deres anvendelighed i risikovurderingssammenhæng. Denne type modeller har i mange år været brugt indenfor farmakologien, men det er relativt nyt at anvende dem indenfor toksikologien.

I en PBTK model er et dyr eller menneske beskrevet som et sæt af kasser (compartments), der beskriver de fysiologiske processer i væv eller organer vha. matematiske ligninger. Et kemisk stofs absorption, fordeling, metabolisme og udskillelse beskrives kvantitativt, og modellen kan forudsige den interne dosis efter eksponering for det pågældende stof.

PBTK modeller gør det muligt at ekstrapolere mellem arter, fra høje doser til lave doser, fra eksponeringsrute til eksponeringsrute og mellem forskellige eksponerings scenarier. På denne måde kan forskellige scenarier simuleres – også scenarier, som det ikke er muligt at studere eksperimentelt. Modeller kan også udvikles for del-populationer af befolkningen f.eks. for børn, og kan på den måde hjælpe til at bestemme, om det er nødvendigt at tage hensyn til en særlig følsom gruppe i risikovurderingen.

Det er muligt at inkorporere mekanistisk information om interaktioner i modellen, og som nævnt ovenfor, kan tærskelværdier for interaktioner dermed fastlægges. Dette vil være et nyttigt værktøj i risikovurderingen af kombinationseffekter af kemiske stoffer.

En PBTK model kan kobles til en toksikodynamisk del, hvori modellen forsøger at estimere den effekt, som den interne dosis forårsager. Outputtet fra PBTK modellen kobles sammen med den toksikodynamiske model vha. matematiske beskrivelser af hypotesen om, hvordan stofferne bidrager til initiering af de cellulære ændringer, der fører til det toksiske respons.

I dette ph.d.-projekt blev en PBTK/TD model etableret på baggrund af en tidligere publiceret model. Modellen beskriver pesticidet chlorpyrifos (en organofosfat) og dets metabolisme til chlorpyrifos-oxon og 3,5,6-trichloro-2-pyridinol. Den beskriver også toksikodynamikken for chlorpyrifos-oxon som hæmmer aktiviteten af acetylcholinesterase i forskellige væv. Artiklen, der beskriver denne model, blev valgt, fordi modellen beskriver et relevant stof (nemlig et meget udbredt pesticid), og fordi det så ud til, at modellen var beskrevet i detaljer i artiklen.

Arbejdet med at etablere denne model har tydeligt vist vigtigheden af, at forfattere til sådanne publikationer er omhyggelige med at beskrive, hvad de har gjort, således at kolleger kan reproducere deres resultater og f.eks. videreudvikle modellen. Modelbeskrivelsen skal indeholde modelstruktur og ligninger men også dokumentation for valget af parametre og en beskrivelse af, hvor disse kommer fra. Der er på nuværende tidspunkt en mangel på anvendelige data til brug i modellerne, og det er derfor nødvendigt med flere studier til at

bestemme parametre, der kan benyttes i PBTK modeller. Det vil dog fortsat være nødvendigt at lave antagelser og ekstrapoleringer i forbindelse med model udviklingen. I denne sammenhæng er det meget vigtigt, at disse er biologisk baserede og at det er forklaret, hvad der ligger bag.

Den opstillede PBTK/TD model for chlorpyrifos er i denne afhandling brugt til at vise, hvordan et nul-effekt-niveau (NOAEL) kan bestemmes ved hjælp en model, og hvordan man kan ekstrapolere mellem arter (her rotter og mennesker). Modellen underestimerede hæmningen af acetylcholinesterase sammenlignet med eksperimentelle data. Derfor skal denne model forbedres, før den kan anvendes indenfor risikovurdering.

PBTD modellering er stadig meget nyt, og det vil formentligt være bedre at bruge kræfter på at forbedre den toksikokinetiske del af modelleringen, herunder at etablere et sæt af internationalt accepterede referenceværdier for forskellige parametre til brug i modelleringen, frem for at udvide modellerne med en toksikodynamisk del.

PBTK modeller kan bruges til at evaluere kombinationseffekter af en blanding af stoffer. I tilfælde af at stofferne i blandingen ikke interagerer (f.eks. "simple similar action"), vil PBTK modellering være et godt værktøj til at forudsige den samlede dosis, der når frem til målorganet herunder at tage højde for metaboliseringen af stofferne. PBTK modeller for disse stoffer vil skulle opstilles på samme måde som for enkeltstoffer.

Hvis stofferne i blandingen interagerer, kan mekanistisk information om interaktionerne inkorporeres i modellen, og dermed kan denne bruges til at bestemme f.eks. en tærskelværdi for interaktioner. En sådan model vil bestå af et sæt af identiske ligninger for hvert stof samt en række ligninger, der beskriver interaktioner (f.eks. kompetitiv hæmning af metabolismen i leveren eller induktion af levermetabolismen).

Udviklingen af PBTK modeller er indviklet, og de bør derfor kun bruges, når det anses for nødvendigt. Hvis de udviklede modeller er troværdige, vil de kunne bidrage med bedre viden og forståelse af effekter af blandinger i organismen, give bedre informationen of dosisniveauer i væv samt variationen mellem arter og indenfor en population. Videnskabeligt dokumenterede resultater om eventuelle kombinationseffekter i mennesker efter indtagelse af relevante blandinger af pesticidrester i fødevarer vil kunne bidrage til, at der kan foretages en pålidelig risikovurdering.

PBTK modeller har et potentiale som et vigtigt redskab i risikovurderingen. Tilstrækkelig dokumentation for modellen er grundlæggende for at øge troværdigheden af PBTK modelleringen, og en sådan troværdighed er afgørende for en spredning af anvendelsen af modellering i risikovurderingen.

Dette ph.d.-projekt udgør det indledende arbejde i implementeringen af PBTK/TD modeller i risikovurderingen af kombinationseffekter af kemiske stoffer i fødevarer ved DTU Fødevareinstituttet. Arbejdet har afsløret mange problemer og faldgruber i udviklingsprocessen. Hvis modellerne er troværdige, vil de kunne give en viden om sammenhængen mellem interne doser af et kemisk stof og observerede toksiske effekter, og denne viden vil kunne reducere usikkerheden i risikovurderingen. Derfor vil arbejdet

fortsætte med at implementere disse modeller som et nyttigt værktøj i den fremtidige risikovurdering.

4 INTRODUCTION

4.1 OBJECTIVE

The objectives of this thesis were to:

1) provide an overview of the existing knowledge on methods for risk assessment of combined actions of chemicals focussing on pesticides found as residues in food
2) establish physiologically based toxicokinetic / toxicodynamic (PBTK/TD) models in order to improve methods for risk assessment of mixtures of chemicals.
3) examine the applicability of PBTK/TD models in risk assessment of mixtures.

The overview of the current methods for risk assessment of mixtures was published in a review article (see Appendix III):

Trine Klein Reffstrup, John Christian Larsen, Otto Meyer, 2010. Risk assessment of mixtures of pesticides. Current approaches and future strategies. Regul. Toxicol. Pharmacol., 56, 174-192.

Physiologically based toxicokinetic /toxicodynamic modelling is a new tool at DTU National Food Institute. As a starting point it was planned to build a model based on an already published model in order to be familiar with the tool and software. The model that was chosen for this purpose was published by Timchalk and co-workers (Timchalk et al., 2002b). It describes the organophosphorus pesticide chlorpyrifos and its metabolism to chlorpyrifos-oxon and 3,5,6-trichloro-2-pyridinol as well as the toxicodynamic of the oxon i.e. inhibition of acetylcholinesterase activity in various tissues. This paper was chosen because the model is on a relevant compound and one had the impression that the model work was described in details.

However, the work on this model made it clear that the re-building as an initial step in the development of an appropriate model was not as straight forward as expected. In fact many problems occurred especially in the toxicodynamic part of the model. This was primarily due to insufficient description of which parameter values (i.e. constants) to be used (and the background for these) and some lack in the description of the equations used. These problems had the consequence that the above mentioned objective of this Ph.D.-project point 2) could not be fulfilled within the time limit of the project. Therefore, the Ph.D.-project has focused on a critical evaluation of the already published model and has examined the applicability of this model as a basis for a development of feasible model for the risk assessment for combined actions of substances in food e.g. pesticide residues.

Since 2005 the European Union member states have been obliged to evaluate and if possible refine existing methodologies in order to take combined actions of pesticides into account during risk assessment and especially when establishing maximum residue levels (MRLs) (European Parliament and Council, 2005). The European Food Safety Authority (EFSA) has suggested to use PBTK models as a higher tier in risk assessment of mixtures of pesticides found as residues in food (EFSA, 2008). Therefore, point 3) in the present Ph.D. –project was to examine the applicability of PBTK models in risk assessment of mixtures.

4.2 BACKGROUND

During the last decades there has been increasing focus on the fact that humans are concurrently exposed to a number of chemicals via food and environment. These chemicals may have a combined action that causes a lower or higher toxic effect than would be expected from knowledge about the single compounds (Larsen et al., 2003). Consequently, combined actions need to be addressed in the risk assessment process. This thesis will focus on risk assessment of combined actions of pesticide residues in food.

Ideally, the evaluation of the toxicological properties of a pesticide mixture requires detailed information on the composition of the mixture and the mechanism of action of each of the individual compounds. In order to perform a risk assessment, proper exposure data are also needed. However, sufficient detailed information is often not available. The mixture of pesticide residues that a person would be exposed to via the food chain may change over time in composition and quantity. Adequate experimental testing of mixtures is often not possible because the number of theoretical possible combinations is enormous and furthermore the use of a sufficient number of dose levels is not feasible. A full study design would require 2^n-1 test groups to identify interactions between all compounds of interest (n is the number of chemicals in the mixture). In addition, high dose levels of a pesticide mixture as used in toxicological studies may have different types of effects than low dose levels (Groten et al., 1997).

During the last two decades several suggestions have been published on how to perform risk assessment on mixtures of pesticides. In 1986 the Environmental Protection Agency in USA (U.S. EPA) published a guideline for health risk assessment of chemical mixtures (U.S.EPA, 1986). However, what really put focus on this topic was the Food Quality Protection Act of 1996 which in relation to pesticide residues requires U.S. EPA to consider ”available information concerning the cumulative effects of such residues and other substances that have a common mechanism of toxicity” (United States of America in Congress, 1996). Since then U.S. EPA has published several reports and guidelines on health risk assessment of chemical mixtures (U.S.EPA, 1999a; U.S.EPA, 2000; U.S.EPA, 2002; U.S.EPA, 2003).

The Agency for Toxic Substances and Disease Registry in USA (ATSDR) has published two guidelines with instructions to users on how to apply current methodologies for risk assessment of combined actions of chemicals (ATSDR, 2001; ATSDR, 2004). In 2002 the Health Council of The Netherlands as well as the Committee on Toxicity of Chemicals in Food, Consumer Products and the Environment in the United Kingdom published advisory reports dealing with risk assessment of mixtures (Committee on Toxicity, 2002; Feron et al., 2004; Health Council of the Netherlands, 2002).

The Danish Veterinary and Food Administration has published the reports “Combined Actions of Pesticides in Food” (Reffstrup, 2002) and “Combined Actions and Interactions of Chemicals in Mixtures” (Larsen et al., 2003) which summarised and evaluated the present knowledge about combined toxic effects of mixtures of chemicals. One of the main conclusions was that the existing methods were uncertain and crude.

Since then, several international initiatives have been taken in order to more closely explore what approaches can be used to evaluate chemical mixtures. Most notably, the EFSA organised a workshop on cumulative risk assessment in 2006 (EFSA, 2007). More recently the Norwegian Scientific Committee for Food Safety and EFSA have published opinions on risk assessment of combined actions on chemicals (EFSA, 2008; Norwegian Scientific Committee for Food Safety, 2008).

These organizations and workshops recommended introducing PBTK/TD modelling as a tool in the risk assessment of chemical mixtures. These models can be used as a tool to predict internal dose levels at different exposure levels and thereby be useful in predicting concentration levels at the target site. In addition, kinetic overload leading to changes in metabolic patterns at high doses can also be modelled. The models require a large amount of data for construction and therefore they should only be used for higher tier assessment. However, when the models are constructed and evaluated they can reduce the need for data on specific scenarios (they can e.g. be used for exposure scenario extrapolation, interspecies extrapolation or high-dose to low-dose extrapolation).

4.3 STRUCTURE OF THE THESIS

The first part of this thesis provides an overview of the existing methods for risk assessment of mixtures of chemicals focussing on pesticides. This includes flow charts proposed by various authors and institutions. This part of the thesis is based on the review paper compiled in this project (see Appendix III):

Trine Klein Reffstrup, John Christian Larsen, Otto Meyer, 2010. Risk assessment of mixtures of pesticides. Current approaches and future strategies. Regul. Toxicol. Pharmacol., 56, 174-192.

Several scientists and organizations have recommended using PBTK/TD modelling as a tool in the risk assessment of mixtures. Development and use of such models in the risk assessment are the topics in the second part of the thesis, from chapter 10 and onwards. Firstly, the development and possibilities of using PBTK/TD models in general will be described. In this thesis the re-building of a PBTK/TD model on chlorpyrifos and its metabolite chlorpyrifos-oxon will be described in details. The problems that arised during this process will be explained and discussed. Finally, the use of PBTK/TD models in the risk assessment of mixtures will be discussed.

5 TYPES OF COMBINED ACTIONS

When evaluating a mixture of compounds one of the main points to consider is whether there will be either no interaction or interaction in the form of either synergism or antagonism. These basic principles of combined actions of chemical mixtures are purely theoretical and one often has to deal with more than one of the concepts at the same time when mixtures consist of more than two compounds and when the toxicity targets are more complex.

In case of no interaction the combined effect can either be in the form of simple similar action (dose addition) or simple dissimilar action (response addition). Many other terms have been

used for additivity, but it seems as the terminology that has become fairly common includes the terms simple similar action and simple dissimilar action to describe additivity (Teuschler, 2007).

5.1 NO INTERACTIONS

The model for simple similar action (synonyms: dose additivity, Loewe additivity) assumes that the compounds in the mixture behave as if they are dilutions of each other (Krishnan et al., 1997); (Svendsgaard and Hertzberg, 1994). This means that the compounds act on the same biological site by the same mechanism/mode of action and differ only in their potencies. The dose-response curves for the single compounds in a mixture are allowed to be nonparallel (on a linear-log graph) (Svendsgaard and Greco, 1995).

The theoretical basis for the simple dissimilar action (synonyms: response additivity, Bliss independence) is probabilistic independence. This means that the compounds in the mixture do not interfere with each other but they all contribute to a common result. The model assumes that the compounds in the mixture do not act by the same mechanism/mode of action and the nature and site of action may also differ among the compounds.

5.2 INTERACTIONS

Interactions are defined as combined actions resulting in a stronger (synergism) or weaker (antagonism) effect than would be expected based on the assumption of additivity. Interactions can be divided into direct chemical-chemical, toxicokinetic, or toxicodynamic interactions (ATSDR, 2001; Norwegian Scientific Committee for Food Safety, 2008).

In direct chemical-chemical interactions, one chemical interacts directly with another chemical causing a chemical change (i.e. a chemical reaction) which will lead to a change in the toxicity causing a stronger or weaker effect than expected from exposure to either of the chemicals alone. Toxicokinetic-based interactions may result in effects on absorption, distribution, metabolism or elimination of the compounds. Toxicokinetic-based interaction is of particular concern when it results in an increase in the internal dose of the active form of another compound. Toxicodynamic interactions occurs when the presence of two (or more) compounds change the response without affecting the tissue dose of each of the compounds. Toxicodynamic interaction can occur at the cellular receptor site or target molecule, at different sites on the same molecule or among different receptor sites or targets. When interaction takes place at the same receptor site this usually results in antagonism (ATSDR, 2001; ATSDR, 2004; Norwegian Scientific Committee for Food Safety, 2008).

It is difficult to predict interactions leading to toxicity at very low exposure levels. Knowledge about combined actions has normally been obtained for considerably higher concentrations than for the levels of chemical residues actually found in food and it is often unclear whether knowledge about the combined action at higher concentrations are relevant for the low exposure level. For example, a combined toxic action observed at high dose levels may be based on mechanisms that are not relevant at low dose levels and high to low dose extrapolation may be meaningless (Borgert et al., 2004). Overall, interactions appear less

often at relatively low exposure levels compared to high exposure levels since they are primarily caused by various thresholds and saturation phenomenon (saturation of activating, detoxification or reparative processes). The main mode of toxicologic interaction is the alteration of the toxicokinetic process, which strongly depends on the exposure levels of the compounds in the mixture (U.S.EPA, 2000). Slikker et al. (2004) have given examples in which dose-dependent transition in the underlying kinetic and/or dynamic factors behind the toxicity occurs. It is often difficult to interpret the relevance of effects at high dose levels in animal studies and the results may not reflect the actual toxicity at relevant human exposure levels. This is particularly the case if dose-dependent transitions in the principal mechanism of toxicity occur (Slikker, Jr. et al., 2004).

5.3 EARLY EXPERIMENTAL WORK ON MIXTURE TOXICOLOGY

From the results of experimental short-term toxicity studies Feron and co-workers concluded that combined exposure to arbitrarily chosen chemicals demonstrated less than an additive effect when all chemicals in the mixture were administrated at their own individual no observed adverse effect levels (NOAELs) whereas no clear evidence of toxicity was found at slightly lower dose levels. The examined compounds had either different target organs and/or differed in their mode of action. Exposure levels at or below the individual NOAELs of the compounds having different target organs and/or differed in the mode of action in a mixture are therefore not expected to be associated with a greater hazard than exposure to the individual chemicals. However, both synergistic and antagonistic effects may be seen at exposure levels higher than the NOAELs, i.e. at their respective LOAELs (Feron et al., 1995b; Groten et al., 1997; Jonker et al., 1996; Jonker et al., 1990; Jonker et al., 1993).

Feron and co-workers were of the opinion that the use of the “dose addition” approach to the risk assessment of chemical mixtures is only scientifically justifiable when the chemicals in the mixture act in the same way, by the same mechanism and thus differ only in their potencies. Application of the “dose addition” model to mixtures of chemicals that act by mechanisms for which the additivity assumptions are invalid could greatly overestimate the risk (Cassee et al., 1998; Feron et al., 1995a). This group found it reasonable to use the approaches based on toxicological similarity and toxicological independency for risk assessment of pesticide residues in food since these compounds are found at levels well below the NOAELs for the compounds.

However, the group did not define the criteria used to judge whether two compounds in a mixture share a common mode of action. This means that when looking on the same data other scientists may come to other conclusions as to whether the compounds are similar with respect to mode of action. Therefore, the conclusions from these studies are not totally unambiguous.

6 GENERAL PROCESS OF RISK ASSESSMENT FOR MIXTURES

There are four steps in the general process of risk assessment for mixtures: 1) the hazard identification, 2) hazard characterisation or dose-response assessment, 3) exposure

assessment and 4) risk characterisation (IPCS, 2009b). The use of these steps for mixtures will be described in the following.

- The hazard identification step identifies the mixtures and the potential human health effects that the chemicals can cause. Firstly, chemicals acting by a common mechanism of toxicity should be identified. U.S. EPA described a procedure for that in "Guidance for identifying pesticide chemicals and other substances that have a common mechanism of toxicity" (U.S.EPA, 1999a). Secondly, the conditions for expression of the risk via route, use pattern and duration of exposure should be described. A specific toxicity endpoint for a certain exposure duration shared by each chemical in the mixture should be specified. U.S. EPA uses the weight of evidence approach to evaluate and characterise the toxicity endpoints of concern and for evaluation of risk to the human population. If one has observed clear species (strain or sex) differences, data from the most sensitive test animal should be used (U.S.EPA, 2000).
- The dose-response assessment step determines the health effects that occur at different levels of exposure. A uniform point of departure must be selected, normalised, and adjusted. Then a method for combining common toxicity must be selected. U.S. EPA considers dose addition (simple similar action) to be an appropriate approach of risk assessment of mixtures because it assumes that the chemicals act on similar biological systems and produce a common response. Both the margin of exposure (MOE) method and the relative potency factor (RPF) method can be used to evaluate the toxicity of a mixture assuming that the compounds act additively. The margin of exposure is calculated by dividing the point of departure (POD) by the measured or estimated exposure from a given route. The point of departure on each compound's dose-response curve can be determined as the toxic potency of the compound relative to the other compounds. In the relative potency factor method the potency of each compound is expressed in relation to the potency of an index chemical. These methods will be described in more detail below (U.S.EPA, 2000).
- The exposure assessment step expresses how much of the chemicals humans are exposed to via different exposure routes (oral, gavage, inhalation, dermal). First the sources of exposure (food, drinking water, and various non-agricultural uses) are identified and then the frequencies, durations, and magnitude of exposures are determined. Based on these data realistic exposure scenarios must be developed (U.S.EPA, 2000).
- In the risk characterisation step the risk of health effects that could result from exposure to the chemicals are identified. The exposure should be matched with the relevant toxicological values in terms of route and duration. Then the cumulative risk of each individual compound on a daily basis should be calculated by maintaining appropriate spatial, temporal and demographic characteristics of data. U.S. EPA uses Monte Carlo analysis to make an iterative process of multiplication of residue concentrations in foods by one-day consumption of these foods. The results are characterised and interpreted. The major chemical contributors to risk, the exposure scenarios of concern and the sensitive subpopulations are identified and it is discussed how well the data support the conclusions. Finally the uncertainties and the uses of assumptions are identified (U.S.EPA, 2000).

7 METHODS FOR RISK ASSESSMENT OF MIXTURES OF PESTICIDES IN FOODS

Various approaches have been suggested in the scientific literature for use in the evaluation of the health risks from exposure to mixtures of chemicals but there is no internationally accepted procedure. The most important approaches are summarised in this section.

The first step in the cumulative risk assessment of mixtures is to identify a group of compounds that induce a common toxic effect by a common mechanism of toxicity. U.S. EPA has described a procedure for that in "Guidance for identifying pesticide chemicals and other substances that have a common mechanism of toxicity" (U.S.EPA, 1999a). In this guidance U.S. EPA defined a common mechanism to be caused "by the same, or essentially the same, sequence of major biochemical events." This definition is equivalent to the definition of the term mode of action (U.S.EPA, 2002). In other reports U.S. EPA distinguished between mechanism of action and mode of action: The term mode of action describes the key events and processes starting with interaction of a compound with a cell via operational and anatomical changes, resulting in the toxic effect. Mechanism of action implies a more detailed understanding and description of steps at the molecular level (U.S.EPA, 2000; U.S.EPA, 2005).

The International Life Sciences Institute (ILSI) convened a group of experts to consider the definition of the term common mechanism. They concluded that chemicals act via a common mechanism of toxicity if they cause the same critical effect, act on the same molecular target tissue, act by the same biochemical mechanism of action, or share a common toxic intermediate (Botham et al., 1999; Mileson et al., 1998).

ATSDR does not define the terms mode of action and mechanism of action. However, they point out that for mixtures of compounds that have an effect on the same endpoint by the same mode of action dose addition is the most appropriate method (ATSDR, 2001; ATSDR, 2004).

The requirement of knowledge on the mode of action is an assumption made for the purpose of being able to perform the risk assessment process for mixtures. However, the theoretical and empirical basis for the term mode of action has yet to be established. Thus, Borgert et al. (2004) have questioned the use of the mode of action to predict combined actions of mixtures. They stated that in order to use mechanistic information for predicting combined action on a scientific basis more research is needed to better understand how mode of action for individual compounds is related to the toxicity of the whole mixture. They concluded that until then the use of mode of action to predict mixture toxicity will remain tenuous (Borgert et al., 2004). Berenbaum (1989) states that interactions cannot usefully be defined as departures from what is expected from mechanism of action. New knowledge on the mechanism of action of the same compounds may lead to derivation of a different eqation which again may lead to another conclusion concerning interactions. That is in this case, Berenbaum discharge the use of mechanism of action and recommends using observed effects as basis for evaluating interactions because this will not change. Such an approach is applicable also for compounds with unknown modes of action. Interactions is then defined as being present when the effect

of a mixture differs from that expected from their individual dose-response curves (Berenbaum, 1989).

Ideally the identification of a group of pesticides for cumulative risk assessment should be based on criteria providing the best and most robust grouping such as chemical structure, mechanism of action, common toxic mode of action or common toxic effect. Unfortunately, such data are seldom available for all of the compounds of concern. Therefore, EFSA has suggested to group compounds for cumulative assessment even in the absence of such detailed data and make cumulative assessment groups (CAG) based on a less refined evaluation of the mode of action e.g. only on target organ toxicity (EFSA, 2008).

The next step is to select an appropriate method and dataset for combining the risks of the compounds in the group. In 1986, the U.S. EPA recommended three approaches for health risk assessment of chemical mixtures (Mumtaz, 1995; U.S.EPA, 1986): 1) the mixture of concern approach, 2) the similar mixture approach and 3) the single compounds approach.

The choice of method depends on the toxic effect, the available data on toxicity of the mixture or the compounds in the mixture, the predicted interactions among the compounds in the mixture and on the quality of the exposure data. However, the U.S. EPA points out that it is ideal to conduct all three assessments when possible in order to make the best risk assessment and to use all the available data – in particular the incorporation of interaction data when available. The uncertainties for the risk assessment should be clearly discussed and the overall quality of the risk assessment should be characterised (U.S.EPA, 1986).

7.1 MIXTURE APPROACHES

The U.S. EPA guidance was supplemented in 2000 (U.S.EPA, 2000) and the flow chart for the different types of mixture assessments shown in Figure 1 was suggested. In this guidance three methods for whole mixture assessment and four compound-based methods were presented. The first step in the flow chart is to assess the quality of the available data of the compounds of interest. When the data are adequate for an assessment, it should be decided whether there are data available for an assessment on the whole mixture or only on the single compounds.

The assessment based on data on whole mixtures can be done on the mixture of concern, on a sufficiently similar mixture (almost the same compounds and in almost the same proportions as in the mixture of concern) or on a group of similar mixtures (same compounds but slightly different ratios, or lacking one or more compounds or having one or more additional compounds compared with the mixture one wants to evaluate). These assessments would be the most appropriate for risk assessment of pesticide residues in food; however, they are very data intensive and data for these methods are rarely available.

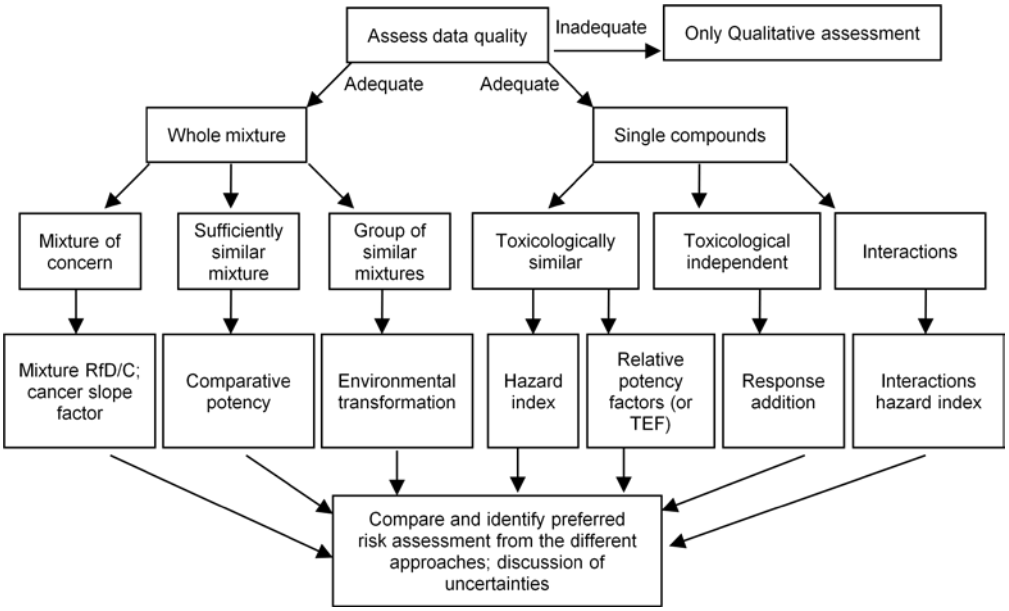

Figure 1. Flow chart of the risk assessment approach used by U.S. EPA. Modified from (U.S.EPA, 2000).

7.2 SINGLE COMPOUND APPROACHES

U.S. EPA has proposed guidance on how to perform a risk assessment on a mixture of pesticides that act by a common mechanism (U.S.EPA, 2002). For mixtures of compounds that are toxicologically similar, U.S. EPA suggested three methods based on simple similar action: the hazard index method (HI), the relative potency factor method (RPF) and the special type of the relative potency factor method named the toxicity equivalency factor method (TEF) (U.S.EPA, 2000).

The point of departure index (PODI) has also been suggested for estimating the risk of a group of compounds which are toxicologically similar. Also the margin of exposure (MOE) as wells as the cumulative risk index (CRI) have been suggested. These two methods are reciprocals of the point of departure and the hazard index, respectively (U.S.EPA, 2003).

These six methods based on simple similar action use the same underlying data but they express the information differently. The exposure levels are added after having been multiplied by a scaling factor that accounts for differences in the toxicological potency (for instance acceptable daily intake (ADI) or reference dose (RfD)) or point of departure doses (e.g. benchmark dose at 10 % effect level, BMD_{10}). For compounds acting independently by simple dissimilar action the response addition (Bliss independence) approach may be used, and for compounds that interact, use of the interaction hazard index is applicable (U.S.EPA, 2000).

When making a risk assessment of exposure to a mixture the need to perform a comprehensive risk assessment should be determined early in the process and the most

appropriate method should be used (U.S.EPA, 2002). The single compound approaches are described in more details in the following.

7.2.1 HAZARD INDEX

In the hazard index approach the doses are standardised by using health based guidance values such as the ADI. The hazard index is calculated by the following equation:

$$HI = \frac{E1}{AL1} + \frac{E2}{AL2} + ... + \frac{En}{ALn} = \sum_{i=1}^{n} \frac{Ei}{ALi} \qquad (1)$$

where E_1, E_2, E_n and E_i are the levels of exposure to each individual compound (i) in a mixture of n compounds. AL_1, AL_2, AL_n and AL_i are the maximum acceptable level for each compound. The "acceptable level" is often a regulatory health based guidance value for exposure to the i^{th} compound e.g. ADI or RfD (as used by U.S. EPA) (U.S.EPA, 1986; U.S.EPA, 2000). If the hazard index exceeds 1, the exposure to the mixture has exceeded the maximum acceptable level (e.g. ADI or RfD) and there may thus be a risk. The fractions (E_1/AL_1 etc.) are sometimes called the hazard quotients, HQ. In cases where the compounds in the mixture act by different mechanisms or affect different target organs, the interaction based hazard index should be calculated for each end point (Haddad et al., 2001). Since this method is based on an assumption of additivity it can lead to errors if a synergistic or antagonistic action occurs.

As an example of how to use the HI method, a mixture of three pesticides will be examined, see Table 1. Chlorpyrifos, methidathion and malathion are chosen for the example as they are the three most frequently found pesticides in the Danish monitoring programme (Jensen et al., 2003). All three compounds can be found in oranges and the residues used in the calculations are the highest amount found in oranges in the Danish survey from 2005 (Christensen et al., 2006). The same uncertainty factor (UF=100) was used to derive the ADI for the three compounds. The hazard index is then calculated from the values of exposure levels and ADIs given:

$$HI = \left(\frac{2.6x10^{-5}}{0.01} + \frac{6.8x10^{-6}}{0.001} + \frac{1.7x10^{-5}}{0.3} \right) \left(\frac{mg/kgbw/day}{mg/kgbw/day} \right) \cong 0.0095$$

The calculated HI is well below one and the mixture is therefore not expected to constitute a risk.

Table 1: Data on three pesticides found as residues in oranges imported to Denmark. The residues are among the highest amount found in oranges in the Danish survey from 2005. TEF values from Jensen et al. (2003).

Compound	Residue [a] (mg/kg)	Exposure [b] (mg/kg bw/day)	NOAEL based in inhibition of AChE in brain or red blood cells (mg/kg bw/day) [c]	ADI (mg/kg bw)	Acute RfD (mg/kg bw)	TEF is based on NOAEL for inhibition of AChE in brain or red blood cells (Jensen et al., 2003)
Chlorpyrifos	0.19	$2.6*10^{-5}$	1	0.01 [d]	0.1 [d]	1
Methidathion	0.049	$6.8*10^{-6}$	0.5	0.001 [e]	0.01 [e]	0.2
Malathion	0.12	$1.7*10^{-5}$	0.15	0.3 [f]	2 [f]	2

a) Residues in oranges imported to Denmark found in the Danish survey from 2005. (Christensen et al., 2006)
b) Exposure = (residue x intake) / (weight of person), where "weight of person" = 72 kg and "intake" (of orange) = 0.01 kg/day (Jensen et al., 2003)
c) NOAEL for chlorpyrifos and methidathion is based on inhibition on AChE in rat brain and NOAEL for malathion is based on inhibition of AChE in red blood cells in dogs (Luijk et al., 2000)
d) Chlorpyrifos: ADI based on a NOAEL of 1 mg/kg bw/day. Acute RfD from (JMPR, 2000).
e) Methidathion: ADI based on a NOAEL of 0.1 mg/kg bw/day (JMPR, 1993). Acute RfD from (JMPR, 1998)
f) Malathion: ADI based on a NOAEL of 29 mg/kg bw/day (JMPR, 1998). Acute RfD from (JMPR, 2004). It should be noted that an ADI for malathion of 0.03 mg/kg bw and an acute Rfd = 0.3 mg/kg bw in EU have been set more recently based on the same study but with an uncertainty factor of 1000 and 100, respectively (EFSA, 2006)

7.2.2 RELATIVE POTENCY FACTOR AND TOXICITY EQUIVALENCY FACTOR APPROACH

The relative potency factor method has been applied to mixtures of a single class of chemicals for which extensive information are available for one of the chemicals in the group but less for the other members. The method assumes simple similar action and that the potency ratios between each chemical in the group remain constant at all dose levels. It requires toxicological similarity for specific conditions i.e. endpoint, route of exposure and duration. In cases where data indicate that different modes of action may apply to different target organs or under different exposure conditions or in cases where data are insufficient, endpoint specific RPFs may be derived for each effect or exposure condition (Advisory Committee on Hazardous Substances, 2007; U.S.EPA, 2000).

The potency of each compound is expressed in relation to the potency of an index chemical which is typically the most extensively studied chemical in the mixture. To evaluate a set of data of combined effects it is necessary to know the dose-response curve for the index compound and to know the effect of the other compounds in the mixture (Seed et al., 1995; U.S.EPA, 2000).

Recently the RPF method has been used in cumulative risk assessment of effects of pesticides by combining it with an Integrated Probabilistic Risk Assessment (IPRA) model. The RPF values were estimated with the use of one or two index compounds and the RPF for each compound were used to calculate the cumulative residue level of each sample expressed as equivalents of the index compound. Then the probabilistic approach was used to calculate the distribution of the cumulative dietary exposure from consumption data and residue data of a group of pesticides in a population. The use of this approach has been demonstrated for a group of 40 acetylcholinesterase inhibiting pesticides (Boon and van Klaveren, 2003), for a group of 31 organophosphorus pesticides (Bosgra et al., 2009) as well as in a study of three anti-androgenic pesticides (Müller et al., 2009). This method makes it possible to better

describe the uncertainties that are present in the data (Advisory Committee on Hazardous Substances, 2007).

The toxicity equivalency factor method is a special case of RPF in which a single TEF is derived for each chemical in the mixture across all endpoints and all exposure conditions. Therefore, it requires a strong degree of toxicologically similarity as well as toxicological equivalence across all endpoints, i.e. it is assumed that all the toxic effects of concern share a common mode of action (U.S.EPA, 2000). Other assumptions are that the effects of each compound in the mixture are essentially additive at sub-maximal levels of exposure and that the dose-response curves are parallel (Advisory Committee on Hazardous Substances, 2007; Safe, 1998; U.S.EPA, 2000). The assumptions for the TEF model imply that a large amount of data is collected for the group of compounds under evaluation. So far the TEF approach has only been implied for a few mixtures of pesticides e.g. for assessment of combined risk from exposure to mixtures of organophosphorus compounds and carbamates (Boon and van Klaveren, 2003; Jensen et al., 2003; Mileson et al., 1999; National Research Council, 1993).

The TEF method was originally developed during the 1980ies to express the toxicological potency of mixtures of polychlorinated dibenzo-p-dioxins and dibenzofurans by several authorities (U.S.EPA, 1989a). According to Safe (1990), TEF values should be derived from data available for more than one response. These criteria were used by Safe for deriving TEF values for (dioxin-like) polychlorinated biphenyls, polychlorinated dibenzo-p-dioxins and dibenzofurans ("dioxins") as well as related compounds (Safe, 1990). Based on the experience from the development of TEFs for dioxins in the beginning of the 1990ies seven guiding criteria were developed for the TEF approach for application to dioxins and dioxin-like compounds (U.S.EPA, 2000). In this report EPA also described a procedure for developing a RPF approach for more general use. Similar criteria were used at an expert meeting organised by WHO in 1997 with the purpose to derive consensus TEF values for polychlorinated dibenzo-p-dioxins, dibenzofurans and dioxinlike polychlorinated biphenyls. They followed a ranking order for weighting different types of studies: *in vivo* studies were higher ranked than *in vitro* studies and/or quantitative structural activity relationship (QSAR) data. In accordance with the approach used by Safe, the studies were then further ranked due to the type of study (chronic > subchronic > subacute > acute) (Van den Berg et al., 1998). The TEF values for "dioxins" were re-evaluated at another WHO meeting in 2005 (Van den Berg et al., 2006).

The toxicity equivalent (TEQ) concentration is calculated by multiplying the concentration of each compound (C_i) in a mixture with the TEF value of the individual compounds in the mixture (TEF_i):

$$TEQ = \sum C_i \times TEF_i \qquad (2)$$

The resulting TEQ is assumed to be an equivalent concentration of the index compound and it can therefore be compared to the RfD of the index compound (Botham et al., 1999). If the TEQ is greater than the RfD, the mixture may constitute a risk.

In order to improve the application of relative potency factors to pesticide mixtures U.S. EPA has published a report with information concerning biological concepts and statistical procedures (U.S.EPA, 2003).

In the following the mixture of the three pesticides in Table 1 is used to illustrate the use of the TEF method. The TEQ dose is calculated by the above equation in which the exposure data (from Table 1) are inserted instead of the concentration of each compound:

$$\mathrm{TEQ} = ((2.6\times10^{-5}\times1)+(6.8\times10^{-6}\times0.2)+(1.7\times10^{-5}\times2))\mathrm{mg/kgbw/day}$$
$$\cong 6.1\times10^{-5}\,\mathrm{mg/kgbw/day}$$

The ADI for the index compound chlorpyrifos is 0.01 mg/kg bw/day (see Table 1) and the TEQ is then a factor of 165 below ADI. Therefore, the mixture is not expected to constitute a risk.

7.2.3 POINT OF DEPARTURE, MARGIN OF EXPOSURE, CUMULATIVE RISK INDEX

In the ***point of departure index*** (PODI) method the exposures of each compound in the mixture are summed and expressed as a fraction of their respective PODs.

$$\mathrm{PODI} = \frac{E_1}{POD_1} + \frac{E_2}{POD_2} + \ldots + \frac{E_n}{POD_n} = \sum_{i=1}^{n} \frac{E_i}{POD_i} \qquad (3)$$

The point of departure can be a data point (typically the NOAEL) or an estimated point derived from observed dose response data (e.g. benchmark dose at 10 % effect level, BMD_{10}). Thus in contrast to the HI method the PODI method does not employ an uncertainty factor. The point of departure on each compound's dose-response curve can be determined as the toxic potency of the compound relative to the other compounds (Larsen et al., 2003; U.S.EPA, 2002).

An EFSA colloquium (EFSA, 2007) recommended the use of the PODI instead of the less transparent HI method because it does not involve a policy driven uncertainty factor. However, they state that HI is a practical tool for screening purposes.

EFSA uses the term reference point (RP or RfP) to replace the term point of departure (EFSA, 2008). Barlow et al. distinguish between the term reference point and point of departure in the way that the reference point is used in description of the margin of exposure approach and the point of departure is used in descriptions of extrapolation approaches (Barlow et al., 2006).

Data from Table 1 is used to calculate PODI with the NOAEL as the POD:

$$\mathrm{PODI} = \left(\frac{2.6\mathrm{x}10^{-5}}{1} + \frac{6.8\mathrm{x}10^{-6}}{0.5} + \frac{1.7\mathrm{x}10^{-5}}{0.15}\right)\left(\frac{\mathrm{mg/kgbw/day}}{\mathrm{mg/kgbw/day}}\right) \cong 1.5\times10^{-4}$$

No international consensus exists on how to evaluate the PODI. However, the PODI can be converted into a "risk cup" unit by multiplying with a group UF. A suggestion could be to use a group UF of 100 and an acceptable risk cup unit should be below 1 (Wilkinson et al., 2000). In the above example a risk cup unit of 0.015 is obtained which is well below 1 and therefore is considered acceptable.

In the ***margin of exposure*** (MOE) method the point of departure (POD) is divided by the measured or estimated exposure (E) from a given route:

$$MOE_i = \frac{POD_i}{E_i} \qquad (4)$$

The margin of exposure approach has been used by EPA to determine the acceptability of acute risks for single chemicals. MOEs of >10 or >100 are usually considered acceptable when derived from toxicological data from human and animal studies, respectively. These levels are chosen since they are numerically the same as the typical uncertainty factors that are used in calculating e.g. a RfD from NOAEL (Wilkinson et al., 2000).

The combined margin of exposure (MOE_T) is the reciprocal of the sum of the reciprocal of MOEs of each compound in the mixture. Using equation (4) and (3) illustrate that MOE_T is the reciprocal of PODI as shown in the second line:

$$MOE_T = \frac{1}{1/MOE_1 + 1/MOE_2 + ... + 1/MOE_n} = \frac{1}{\sum_{i=1}^{n} 1/MOE_i}$$
$$= \frac{1}{\sum_{i=1}^{n} E_i/POD_i} = \frac{1}{PODI} \qquad (5)$$

A MOE_T higher than 100 is usually considered acceptable when derived from toxicological data from animal studies (Wilkinson et al., 2000).

For the example in Table 1 the MOE_T can be calculated by inserting MOE from each of the three compounds in the above equation:

$$MOE_T = \frac{1}{E_1/POD_1 + E_2/POD_2 + E_3/POD_3} = \frac{1}{PODI} = \frac{1}{1.5 \times 10^{-4}} \cong 6500$$

As MOE_T is higher than 100, it is considered acceptable.

U.S. EPA has suggested to derive a ***cumulative risk index*** from the MOE for compounds with different uncertainty factors. The risk index (RI) can be calculated as follows:

$$RI = \frac{POD}{E \times UF} = \frac{RfD}{E} = \frac{1}{HQ} \qquad (6)$$

The cumulative risk index is the reciprocal of the sum of the reciprocal of the RIs and thereby of HI:

$$CRI = \frac{1}{1/RI_1 + 1/RI_2 + ... + 1/RI_n}$$
$$= \frac{1}{E_1/RfD_1 + E_2/RfD_2 + ... + E_n/RfD_n} = \frac{1}{\sum_{i=1}^{n} E_i/RfD_i} = \frac{1}{HI} \qquad (7)$$

The risk increases as the CRI falls below 1, equal to situations where the exposure is higher than the RfD (Larsen et al., 2003; U.S.EPA, 1999b; Wilkinson et al., 2000).

The data from Table 1 will be used in this example showing how to calculate the cumulative risk index for the three compounds:

$$CRI = \frac{1}{E_1/RfD_1 + E_2/RfD_2 + E_3/RfD_3}$$
$$= \frac{1}{2.6\times10^{-5}/0.1 + 6.8\times10^{-6}/0.01 + 1.7\times10^{-5}/2} \cong 1050$$

This is well above one and therefore the mixture is not expected to constitute a risk.

7.2.4 SIMPLE DISSIMILAR ACTION, RESPONSE ADDITION

The model for simple dissimilar action assumes that the compounds in the mixture do not act by the same mode of action and the model does not assume that the dose-response curves have a similar shape. The nature and site of action may also differ among the compounds and every compound in the mixture is thought to provoke effects (response) independent of the other compounds present i.e. the effect of one compound is the same whether or not another compound is present. An example of simple dissimilar action is the combined risk of any kind of reproductive toxicity for a set of chemicals with different modes of action (U.S.EPA, 2000).

If compound 1 in a mixture of two compounds has a probability for adverse effect, p_1, then compound 2 can act only on the remaining fraction 1- p_1 assuming that the maximum fraction of total possible effect is 1 (Svendsgaard and Hertzberg, 1994). Then the probability for adverse effect of compound 2 will be $p_2 \times (1- p_1)$ and the expected probability for an adverse effect from the mixture according to the model of Bliss independence, p_{mix}, at the doses d_1 and d_2, respectively, will be:

$$p_{mix}(d_1, d_2) = p_1(d_1) + p_2(d_2) \times (1 - p_1(d_1))$$
$$= p_1(d_1) + p_2(d_2) - p_1(d_1) \times p_2(d_2) \qquad (8)$$
$$= 1 - [(1 - p_1(d_1)) \times (1 - p_2(d_2))]$$

Bliss independence occurs if the measured effect of the mixture (stated as a probability for an adverse effect) equals $p_{mix}(d_1,d_2)$ (Bliss, 1939; Könemann and Pieters, 1996; National Research Council, 1989; U.S.EPA, 2000).

In a more general form, the probability for an adverse effect to arise from a mixture with more than two compounds is 1 minus the probability of not responding to any of the single compounds:

$$p_{mix}(d_1,...,d_n) = 1 - [(1 - p_1(d_1)) \times (1 - p_2(d_2)) ... \times ... (1 - p_n(d_n))] = 1 - \prod_{i=1}^{n} (1 - p(d_i)) \quad (9)$$

(Advisory Committee on Hazardous Substances, 2007; U.S.EPA, 2000).

The response to a mixture depends on the dose and on the correlation of tolerances. This correlation can vary between -1 and 1. The equation above corresponds to no correlation of tolerances and it is the standard formula for statistical independence (Könemann and Pieters, 1996). If the organisms most sensitive to chemical 1 are also most sensitive to compound 2 then the compounds are completely positively correlated. In case of complete positive correlation (r = 1) the effect of the mixture will depend on the most toxic compound in the mixture, that is:

$$\begin{aligned} p_{mix} &= p_1(d_1) \text{ if } p_1(d_1) > p_2(d_2) \\ p_{mix} &= p_2(d_2) \text{ if } p_1(d_1) < p_2(d_2) \end{aligned} \quad (10)$$

In case of complete negative correlation (r = -1), the probability of an adverse effect from a mixture of compound 1 and 2 equals to the sum of the individual responses:

$$p_{mix} = p_1(d_1) + p_2(d_2) \text{ if } p_{mix} \leq 1 \quad (11)$$

In this case the organisms most sensitive to compound 1 is least sensitive to compound 2 and vice versa (ATSDR, 2004; Könemann and Pieters, 1996; U.S.EPA, 2000).

The last equation is the most conservative approach to describe simple dissimilar action and U.S. EPA has recommended it to be used in risk assessment of mixtures of carcinogens. They use the following equation to estimate the risk (unit-less probability that an individual will develop cancer) for the mixture:

$$Risk = \sum_{i=1}^{n} Risk_i = \sum_{i=1}^{n} d_i B_i \quad (12)$$

where $Risk_i$ is the risk estimate for the i^{th} compound, d_i is the dose and B_i is the potency parameter for the i^{th} carcinogen (U.S.EPA, 1986). According to U.S. EPA the equation is appropriate to use when the risks of the individual compounds are less than 0.01 and the sum of the individual risks is less than 0.1 (ATSDR, 2004; U.S.EPA, 1989b; U.S.EPA, 2000).

In a hypothetical mixture of four compounds, I, II, III and IV the compounds are present at concentrations providing the following doses: 1.5, 2.0, 2.5 and 3.0 mg/kg/day. The corresponding responses are derived from the hypothetical dose-response curves in Figure 2: 0.3, 0.16, 0.11 and 0.

The probability for an adverse effect to arise from the mixture is calculated from equation (9):

$$p_{mix}=1-(1-0.3)x(1-0.16)x(1-0.11)x(1-0)=0.48$$

This is called the "true response" by U.S. EPA (U.S.EPA, 2000).

Using the more conservative method (equation (11)) will give an unadjusted mixture risk (corresponding to complete negative correlation) of:

$$p_{mix}=0.3+0.16+0.11+0=0.57$$

This gives a "relative error" of:

$$(0.57-0.48) / (0.48) = 0.20$$

The results from using the two different approaches give a "relative error" of 20 %. In both cases the risk of an adverse effect arising from the mixture is around 50 %.

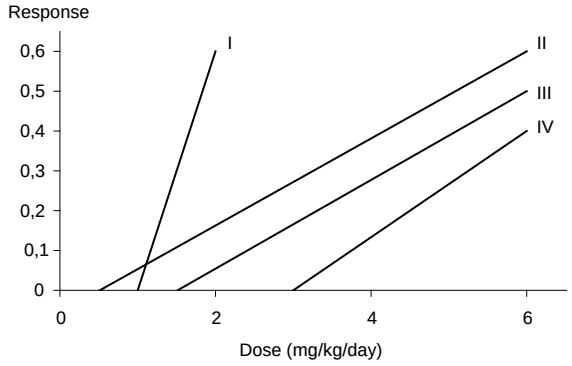

Figure 2. Hypothetical dose-response curve for four compounds I, II, III and IV.

The response addition is based on the principle that each organism will have a certain level of susceptibility to each compound and the threshold of susceptibility has to be exceeded in order to perform a response. This means that the response addition method cannot estimate a toxic effect from a mixture when the individual compounds in the mixture do not lead to an effect. Based on this assumption EFSA concluded, that response addition will rarely if ever be relevant for pesticide residues in food since they generally are found at levels well below their respective toxic levels (EFSA, 2008).

7.2.5 INTERACTIONS

U.S. EPA has suggested the interaction hazard index approach for mixtures consisting of interacting compounds in order to take antagonistic and synergistic interactions into account

in the derivation of a hazard index. The interaction-based hazard index uses the weight of evidence (WOE) approach as a quantitative modifier to the hazard index in risk assessments involving interactions of multiple compounds (Mumtaz et al., 1998; Mumtaz and Durkin, 1992; U.S.EPA, 2000). It assumes that binary interactions are the most important and information on binary interactions is used to modify the hazard index using binary weight of evidence (BINWOE). It is also assumed that compounds in a mixture act by similar mechanisms (U.S.EPA, 2000).

There are four important features in the interaction hazard index approach (Seed et al., 1995). Firstly, the interaction mechanism should be well understood. Secondly, the data from other related compounds should be consistent with the proposed mechanism. Thirdly, the toxicological significance of this interaction should be demonstrated and fourthly, the *in vivo* data of the interaction should be available from long-term studies using a route of exposure relevant for humans.

In the first steps of the interaction-based hazard index approach, the mechanistic understanding and the toxicological significance is connected. This forms the basis of the risk assessment. Thereafter, the binary mixtures are grouped in three modifying categories used to alter the rating of the risk assessment. The three modifying categories are duration/sequence of exposure, *in vivo*/*in vitro* and route of exposure.

This classification is used to set up a quantitative interaction matrix by the aid of a set of default weighting factors and many calculations. The calculations include the hazard index and interaction factors for each binary mixture. The normalised site-specific weight of evidence is calculated and used to adjust the hazard index for the uncertainty of interactions. And finally the adjusted hazard index can be evaluated.

The dose-additive hazard index can be modified by using a scaled BINWOE (WOE_N) giving the interaction hazard index, HI_I:

$$HI_I = HI_{ADD}(UF_I)^{WOE_N} \quad (13)$$

where HI_{ADD} is the non-interactive HI based on dose addition and UF_I is the uncertainty factor for the interactions (Mumtaz and Durkin, 1992; U.S.EPA, 2000).

U.S. EPA has pointed out some very important weaknesses of the interaction hazard index approach (U.S.EPA, 2000): There is no guidance for selection of the uncertainty factors for interactions used in the method, and the steps in determining the BINWOE are complex. The weighting factors used in the method lack support from empirical assessments of key experimental variables. Further the interaction hazard index approach is supposed to account for (pair wise) interactions, but the method may be too simple in that the interaction information is only represented by the uncertainty factor, which is multiplied with the entire additive hazard index. The magnitude of the interaction is not included in the method. The fact that a qualitative/subjective evaluation of data is used as the basis for quantitative modelling makes this model less applicable.

Neither the approaches for toxicologically similar compounds nor the approach for toxicologically independent compounds presented earlier in the text will accurately predict risks for compounds that exhibit toxicological interactions. The interaction-based hazard index approach introduced by Mumtaz and co-workers (Mumtaz and Durkin, 1992) seems to be the only method at present that take toxicological interactions into account. However, this method is complicated to use and it requires a great deal of data, calculations and assumptions concerning the interactions of the compounds. Conolly has stated that one of the greatest dangers in trying to describe mechanisms quantitatively is the use of speculative assumptions about the mechanisms rather than the lack of knowledge as such (Conolly, 2001).

The method described by Mumtaz and Durkin (1992) requires an evaluation of data quality for mechanistic information. However, it does not provide guidance on evaluating interactions data themselves. Borgert et al. (2001) has presented five criteria to evaluate the quality of data and interpretations in studies of chemical mixtures:

"Criterion 1. Dose response curves (DRCs) for the mixture components should be adequately characterized.

Criterion 2. An appropriate "no-interaction" hypothesis should be explicitly stated and used as the basis for assessing synergy and antagonism.

Criterion 3. Combinations of mixture components should be assessed across a sufficient range to support the goals of the study.

Criterion 4. Formal statistical tests should be used to distinguish whether the response produced by a dose combination is different (larger or smaller) from that predicted by the "no-interaction" hypothesis.

Criterion 5. Interactions should be assessed at relevant levels of biological organization."

The criteria are intended to assist the risk assessor in the evaluation of interactions studies for use in risk assessment of chemical mixtures (Borgert et al., 2001). EPA has also pointed out statistical deficiencies in handling and interpretation of data from interaction studies (U.S.EPA, 1988b).

The quality of studies and the uncertainty in the interpretation of studies on combined actions of compounds in mixtures is a very important point since it makes the basis for deciding whether there will be no interaction or interaction between the compounds in the mixture. Information on interaction or not is used for deciding which method to use in the evaluation process.

7.3 ADVANTAGES AND DISADVANTAGES OF THE METHODS

Eight methods for risk assessment of mixtures based on data on single compounds are shown in Table 2. The required data, applicability, assumptions, advantages and disadvantages of each method are summarised.

Table 2: Overview of eight methods for risk assessment of mixtures based on data on single compounds. Advantages and disadvantages of the methods.

Procedure	Required data	Applicability	Assumptions	Advantages	Disadvantages
Hazard Index (HI)	Maximum acceptable level for each compound (e.g. RfD or ADI). Exposure data.	Compounds having adequate dose-response data, as well as exposure data at low levels. HI is also used for compounds with similar target organ	Simple similar action – toxicological similarity	Transparent, understandable, relates directly to long-used and well-understood measure of acceptable risk e.g. RfD or ADI	RfD (or ADI) is not an appropriate point of departure – it involves an UF (subjective). If the UFs are not the same for all compounds in the mixture, this will affect the result
Relative Potency Factor (RPF)	Toxicity data for each compound, dose-response data for the index compound. Exposure data.	Some data available – restricted by similarity and to specific conditions	Simple similar action – toxicological similarity, but for specific conditions (end point, route, duration). It is supposed to account for mixtures with different mode of action	Transparent, understandable, relates directly to real exposure and toxicity data	Complicated to use. Relies on the availability of dose-response data for the index compound.
Toxicity Equivalency Factor (TEF)	Toxicity data for each compound, dose-response data for the index compound. Exposure data.	Seldom applicable as data seldom available. A TEF value is applied to all end points; therefore, method restricted to mixtures of compounds with strong similarity – few chemical classes will qualify	Simple similar action – toxicological similarity across endpoints	Transparent, understandable, relates directly to real exposure and toxicity data	Data seldom available. In some cases complicated to use. Relies on the availability of dose-response data for the index compound
Margin of Exposure for mixtures (MOE_T)	Point of departure (e.g. NOAEL or BMD_{10}). Exposure data.	Compounds having adequate dose-response data, as well as exposure data	Simple similar action – toxicological similarity	Relates directly to real exposure and toxicity data - not based on a policy driven parameter like ADI.	No criteria for defining the magnitude for an acceptable MOE_T
Point of Departure Index (PODI)	Point of departure (e.g. NOAEL or BMD_{10}). Exposure data.	Compounds having adequate dose-response data, as well as exposure data	Simple similar action – toxicological similarity	Relates directly to real exposure and toxicity data - not based on a policy driven parameters like ADI.	No criteria for defining the magnitude for an acceptable PODI
Cumulative Risk Index (CRI)	Point of departure (e.g. NOAEL or BMD_{10}) or maximum acceptable level for each compound (e.g. RfD or ADI). Exposure data.	Compounds having adequate dose-response data, as well as exposure data	Simple similar action – toxicological similarity	Combines MOEs for chemicals with different UFs	RfD (or ADI) is not an appropriate POD – it involves an UF (subjective). Not as transparent and understandable as the HI. Complex calculations
Response Addition	Toxicity data measured as a fraction of responding. Good dose-response data. Exposure data	Seldom applicable as data seldom available	Simple dissimilar action – Bliss independence	Mathematically easy	Data seldom available
Interaction Hazard Index (HI_I)	Maximum acceptable level for each compound, a	Seldom applicable as data seldom available: limited data on interactions	Binary interactions are most important. Magnitude of interaction depends	Supposed to account for interactions (binary)	Data seldom available. Complex to determine the BINWOE. Weighting

Procedure	Required data	Applicability	Assumptions	Advantages	Disadvantages
	number of weighting factors. Exposure data.		on proportions of the compounds – not dose-dependent		factors are not supported by experimental data. No guidance for selecting UFs for interactions and interactions are only represented by these

8 PROPOSED FLOW CHARTS FOR RISK ASSESSMENT OF MIXTURES OF CHEMICALS

In 2001 ATSDR published the report "Guidance for the Preparation of an Interaction Profile" including flow charts for a step-by-step procedure for assessing effects (including carcinogenicity) (ATSDR, 2001). These flow charts were revised in the report "Guidance Manual for the Assessment of Joint Toxic Action of Chemical Mixtures" in 2004 (ATSDR, 2004). The flow charts are shown in Figure 3 and 4. The two methods are especially concerned with how public health is affected by exposure to chemical mixtures at hazardous waste sites.

The two flow charts for non-carcinogenic and carcinogenic effects, respectively, are similar. In the first steps it is considered which information is available on the mixture: - An interaction profile? - A toxicological profile? - A minimal risk level? - Other health guideline values? If no such information is available the single compounds approach should be used. ATSDR recommends using PBPK/PD models, if available, to predict the potential for interactions or effects from the mixture. The hazard index method is recommended to be used for screening for non-cancer hazards from potential additivity of the compounds in the mixture (Figure 3).

In case of carcinogenic effects the compounds in the mixture are summed to screen for hazards from potential additivity (Figure 4). The potential impact of interactions on non-cancer and cancer health effects is evaluated by a weight-of-evidence method.

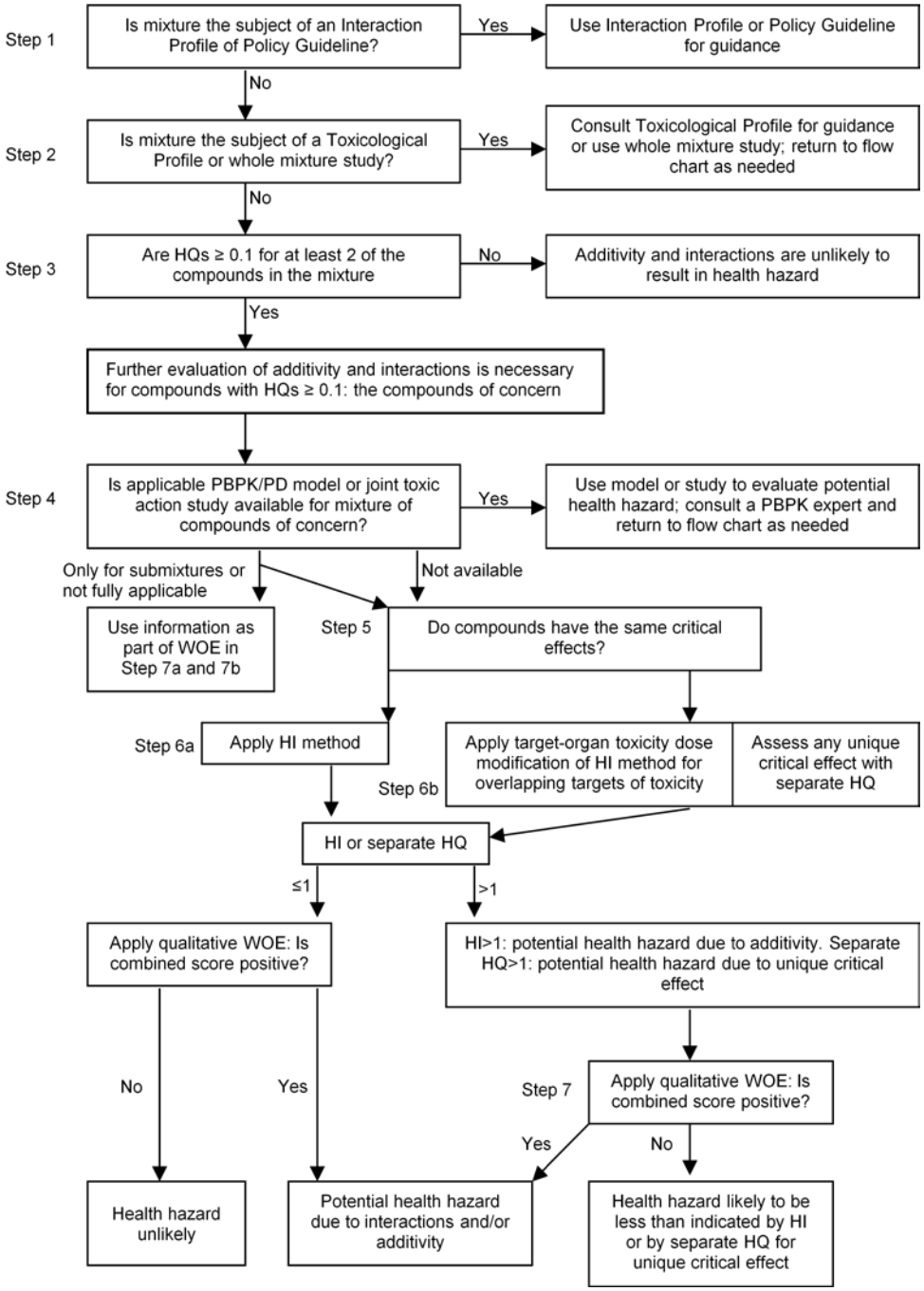

Figure 3. Flow chart proposed by ATSDR for a step-by-step procedure for assessment of combined action of mixtures of non-carcinogenic chemicals. Modified from (ATSDR, 2004).

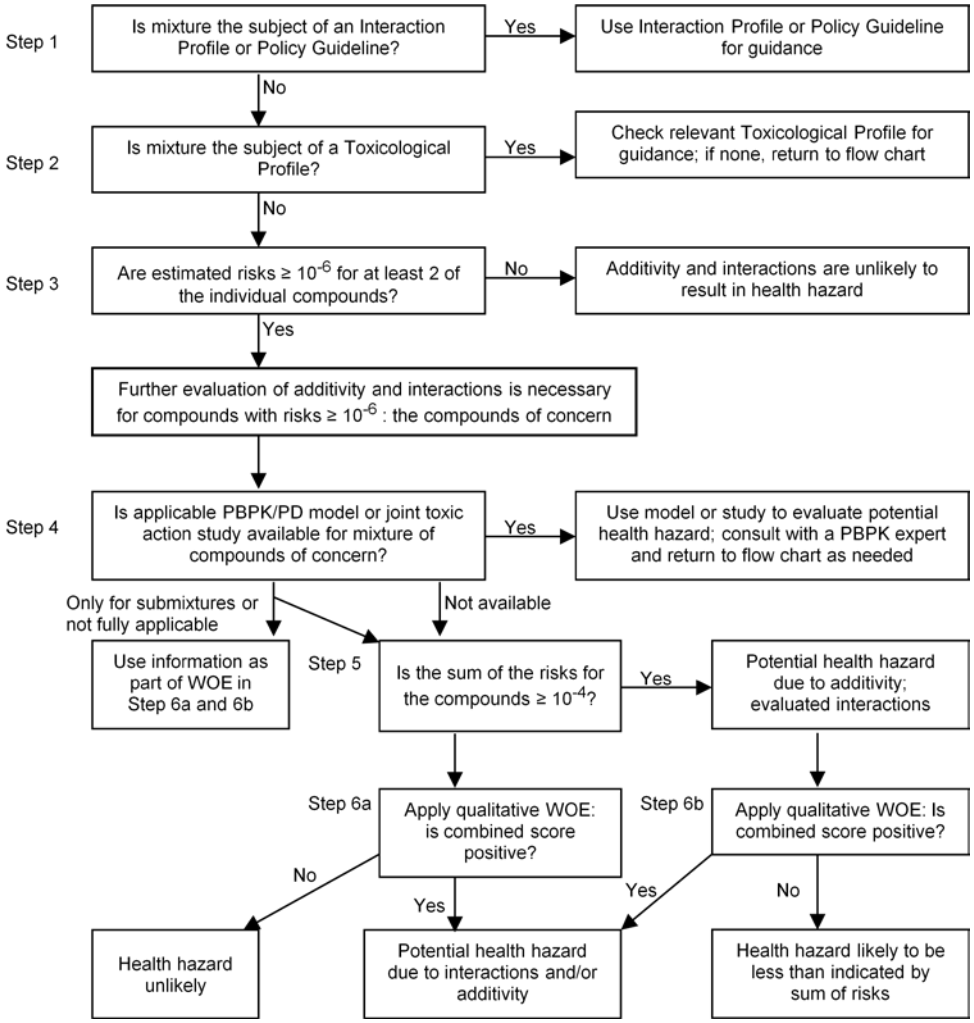

Figure 4. Flow chart proposed by ATSDR for a step-by-step procedure for assessment of combined action of mixtures of carcinogenic chemicals. Modified from (ATSDR, 2004).

In 2002 a committee of the Health Council of The Netherlands published an advisory report which included a flow chart for safety evaluation of combined exposures using the so-called "top n" and "pseudo top n" approaches in which the most toxic compounds in the mixture are selected and assessed for toxicity, see Figure 5 (Feron et al., 2004; Health Council of the Netherlands, 2002). This approach is especially suitable for the toxicological evaluation of workplace and hazardous waste site atmospheres. The report recommends use of Mumtaz-Durkin weight of evidence method for prioritisation of the combined exposures according to their potential risk (Feron et al., 2004). The intention is that the flow chart should be walked through in its entirety in order to select the best method. In the upper part of Figure 5 it is decided whether the data on toxicity is available on a mixture or on single compounds, that is to say corresponding with the upper part of the flow chart suggested by U.S. EPA shown in Figure 1. The lower part of Figure 5 is intended for specified mixtures of compounds concentrating on pairs of compounds in the mixture. The first step is to consider whether the compounds in the mixture act by similar action or dissimilar action and thereafter consider whether interactions occur or not. If the compounds act by similar action without interaction

the scheme recommends dose addition and toxicity equivalency factor for assessing the joint toxicity. If the compounds act by dissimilar action without interaction, response addition should be used.

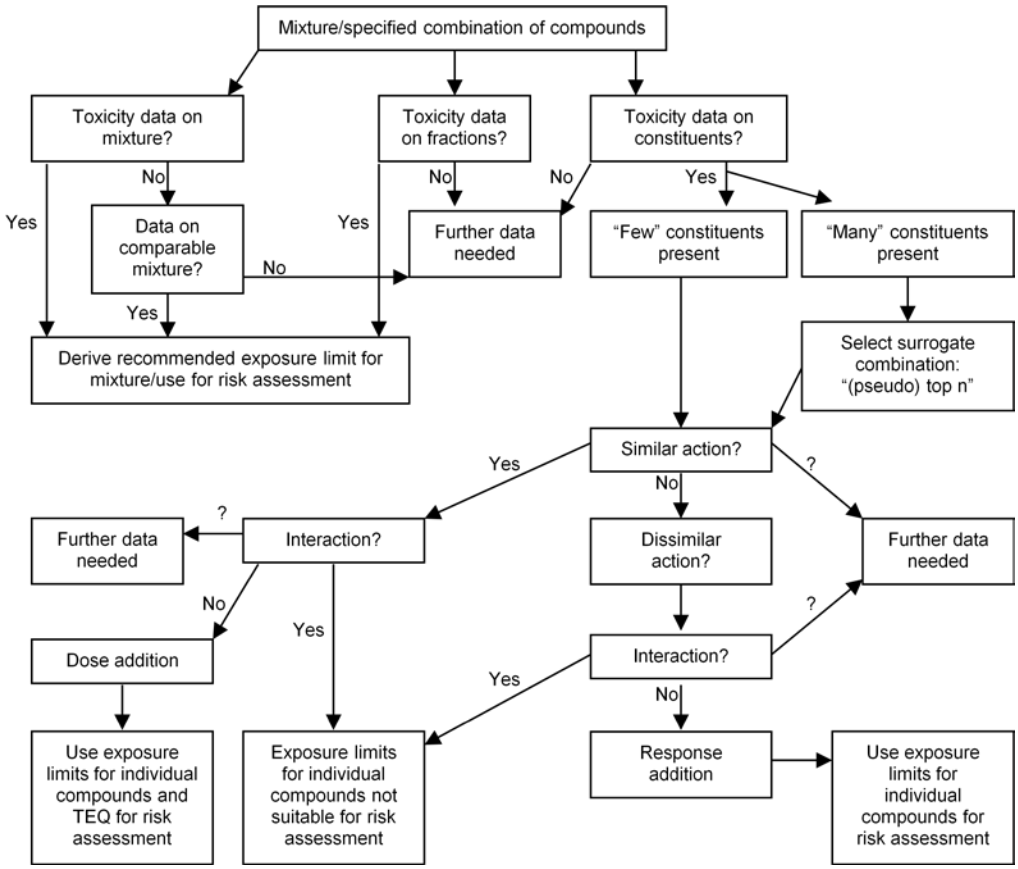

Figure 5. Flow chart suggested by Health Council of the Netherlands for assessing combined actions of two compounds. Modified from (Feron et al., 2004; Health Council of the Netherlands, 2002).

Use of a hazard index is also recommended for mixtures of compounds without interactions: in the case of similar action the hazard quotients are added and in the case of dissimilar action the highest hazard quotient is chosen even though the latter is not following the theory stringent (Health Council of the Netherlands, 2002). In cases with similar action with interactions or dissimilar action with interactions, it is necessary to examine whether the data available can be used for a quantitative conclusion; the Committee concluded that it is not able to give universal criteria for this.

The flow chart in Figure 6 is an expansion of the method proposed by U.S. EPA in Figure 1: one method has been added to the methods based on data on single compound. In the case of a mixture of compounds having different modes of action but causing the same toxic effect it is suggested to combine the response and dose addition methods in what they call the cumulative relative potency factors (CRPF). The compounds in the mixture which have the same mode of action are put together in subclasses. Then the RPF can be used to estimate the risk of each subclass. These subclasses are expected to act independently of each other (that is

simple dissimilar action) and therefore the calculated RPFs can be added to give the total mixture risk (Teuschler, 2007).

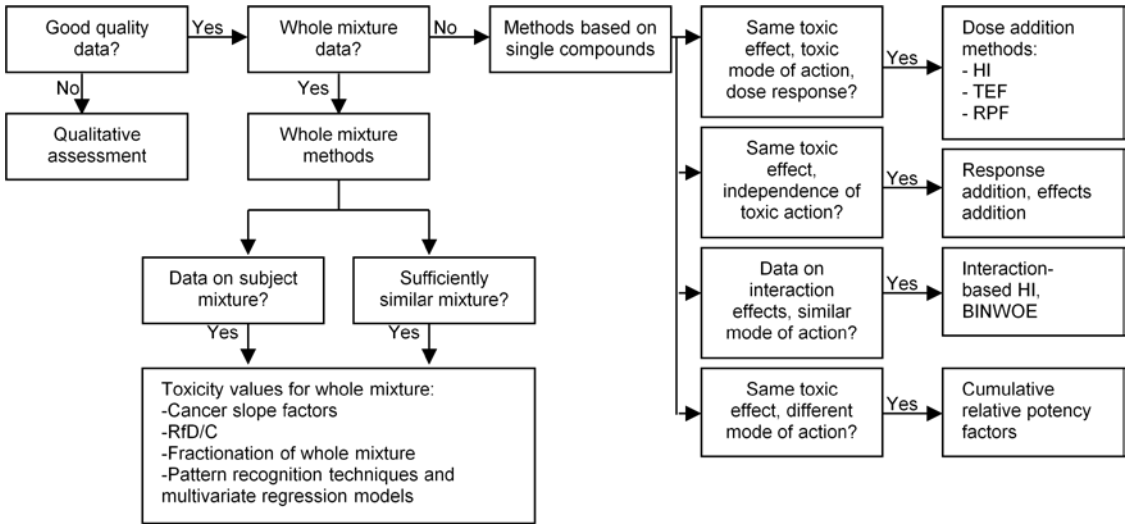

Figure 6. Flow chart for assessment of combined actions of chemical mixtures. Adapted from (Teuschler, 2007).

The Norwegian Scientific Committee for Food Safety has suggested a step-wise case-by-case evaluation of the toxicological data on the compounds and the exposure data, see Figure 7 (Norwegian Scientific Committee for Food Safety, 2008). They assume that if exposure to compounds is below the individual NOAELs and they act by similar mode of action then no more than an additive effect is expected. If exposure to compounds is above the NOAELs, interaction may occur. Interactions are taken into account in the two boxes with dotted lines in the figure.

On the left hand side in Figure 7, it should be considered whether the compounds act on the same target organ, whether the compounds in the mixture act by the same mode of action and finally in the refinement it should be considered whether the compounds act by the same mechanism of action. If data are available and indicate that the compounds act by the same mechanism of action, the toxicity equivalency factor method should be used, otherwise (i.e. the compounds act by the same mode of action) the hazard index, the margin of safety or the point of departure index method should be used. On the right hand side it should be considered whether the compounds in the mixture act by simple dissimilar action.

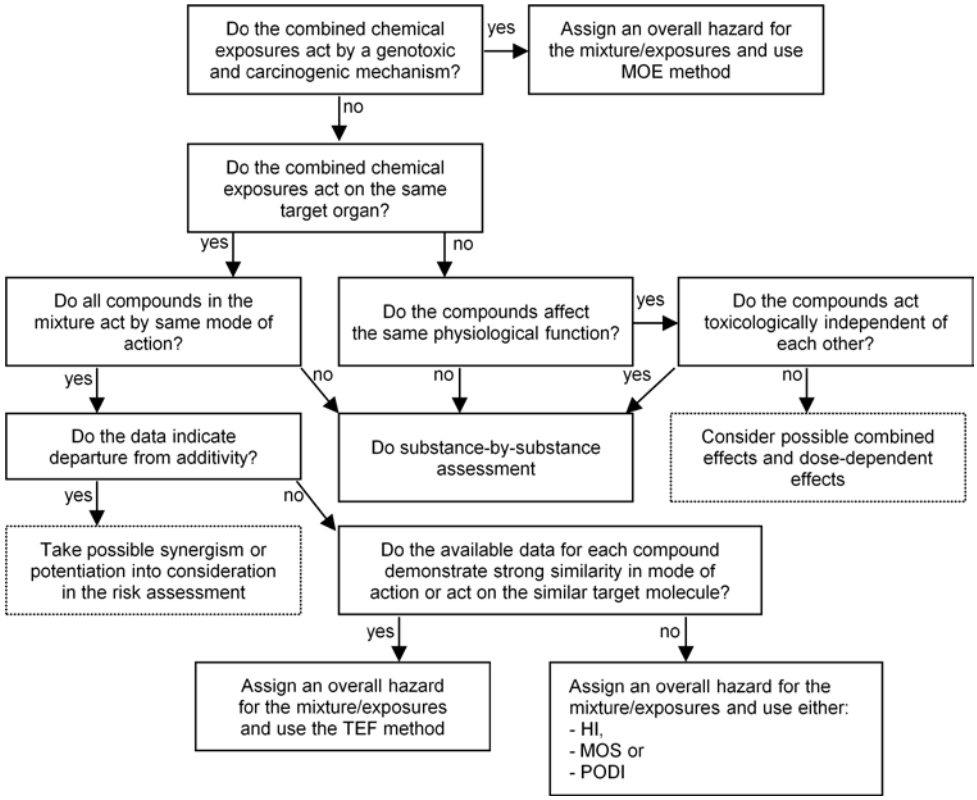

Figure 7. Flow chart proposed by Norwegian Scientific Committee for Food Safety. Adapted from (Norwegian Scientific Committee for Food Safety, 2008).

In 2002, the Danish Veterinary and Food Administration suggested to use the flow chart shown in Figure 8 for risk assessment of pesticide mixtures found as residues in food (Reffstrup, 2002). The risk assessment must be done on a case-by-case evaluation in which the available chemical and toxicological data on the pesticides are evaluated in a weight of evidence process. Then the hazard index with the ADI as the acceptable level in the denominator should be used. However, in cases where the weight of evidence points out that the compounds in the mixture share a common mechanism the toxicity equivalency factor should be used instead of the hazard index. This concerns for instance the organophosphorus pesticides, the chloroacetanilides, the dithiocarbamates and the thiocarbamates. This is a rough and pragmatic method. In Denmark, this method has been used for evaluating mixtures of pesticides in foods since 2002. In most cases, the hazard index has been used with ADI as the acceptable level. In only a few cases the ADI were exceeded and this was often due to only one compound in the mixture.

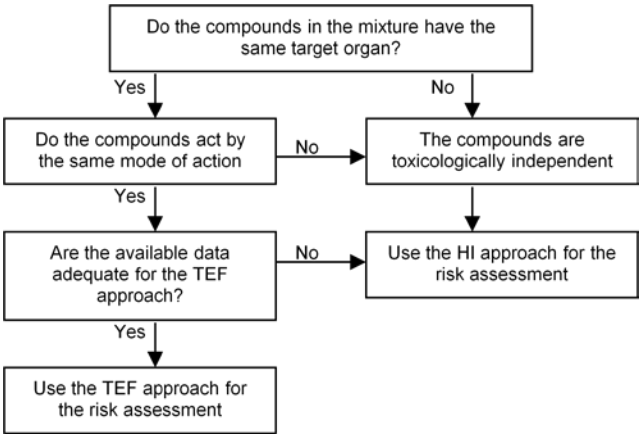

Figure 8. Flow chart of the risk assessment approach for pesticide mixtures found in food (Reffstrup, 2002).

The Scientific Panel on Plant Protection Products and their Residues (PPR Panel) has recommended the flow chart shown in Figure 9 mentioning what they consider the most useful methods (EFSA, 2008). Going from the top and down through the flow chart there are an increasing level of complexity and refinement: the hazard index, the reference point index (i.e. PODI), the relative potency factor method and physiologically based toxicokinetic modelling.

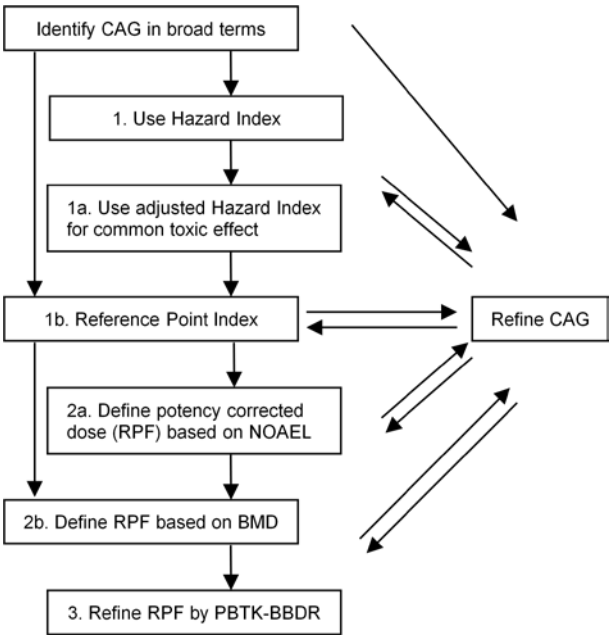

Figure 9. Tiered hazard assessment proposed by EFSA. Modified from (EFSA, 2008). BBDR = biologically based dose response modelling.

An overview of the required data and assumptions for these eight flow charts are shown in Table 3 as well as the advantages and disadvantages of the different strategies.

Table 3: Overview of the required data, assumptions, advantages and disadvantages for the eight flow charts / assessment strategies shown in this thesis.

Flow chart	Required data	Methods suggested	Assumptions	Advantages	Disadvantages
Figure 1. Flow chart of the risk assessment approach used by U.S. EPA (U.S.EPA, 2000). Developed for environmental contaminant mixtures	Either data on mixture or on single compounds	Mixture: RfD/C, cancer slope factor, comparative potency, environmental transformation. Single compounds: HI, RPF/TEF, response addition, interaction based HI	For single compound approaches (except interaction based HI): no or insignificant interaction effects at low dose levels. In some cases the requirement of similar mode of action is relaxed to require only same target organ	Flow chart is straight forward. Very broad flow chart that covers many approaches/situations and can therefore be used in many cases. Allows risk assessment based on whole mixtures as well as single compounds with a wide range of methods suggested	Comprehensiveness makes the flow chart complicated. Some of the methods are complicated and requires many data. In case of interaction no universal criteria for deciding whether the data permits a quantitative conclusion to be drawn
Figure 3. Flow chart proposed by ATSDR for assessment of non-carcinogenic chemicals from hazardous waste sites (ATSDR, 2004)	Either data on mixture or on single compounds	Mixture: use of interaction profile (if available) incl. minimal risk level. Single compounds: HI, PBTK/PD, BINWOE, target-organ toxicity dose (TTD) modification of HI (for compounds not having same critical effect but having overlapping target organ)	The mechanism of toxicity is well enough known to assume which compounds will be additive and which will not (McCarty and Borgert, 2006). If two or more compounds have HQ≥0.1 the mixture requires more evaluation of additivity and interactions	Flow chart is comprehensive and allows use of different approaches including newer modelling techniques. Depending on the available data and exposure level the risk assessment can stop after only a few steps	Criteria for judging whether the compounds act additively or not are not defined or validated (McCarty and Borgert, 2006). Comprehensiveness makes the flow chart complicated. Some of the methods are complicated and requires many data
Figure 4. Flow chart proposed by ATSDR for assessment of carcinogenic chemicals from hazardous waste sites (ATSDR, 2004)	Either data on mixture or on single compounds	Mixture: use of interaction profile (if available). Single compounds: cancer risk estimates (cancer slope factors times exposure of the population of concern)	Cancer is regarded as same critical effect not considering the tumour type or location. The mechanism of toxicity is well enough known to assume which compounds will be additive and which will not (McCarty and Borgert, 2006). If two or more compounds have estimated risk ≥ 10^{-6} the mixture requires more evaluation of additivity and interactions	Flow chart easily understandable although it requires many data. Depending on the available data and exposure level the risk assessment can stop after only a few steps	Criteria for judging whether the compounds act additively or not are not defined or validated (McCarty and Borgert, 2006). Some of the methods are complicated and requires many data
Figure 5. Flow chart suggested by Health Council of the Netherlands for assessing risk from contaminated soil. The Committee recommends use in e.g. consumption of contaminated food or inhalation of polluted air (Feron et al., 2004; Health Council of the Netherlands, 2002)	Either data on mixture or on single compounds	Mixture: recommended exposure limits for mixture. Single compounds: TEQ, exposure limits for individual compounds. HI (not shown in flow chart) is also recommended in the report for similar and dissimilar acting compounds even though the latter is	Assesses the combined effect per pair in the mixture. Concerning exposure limits: harmfulness only manifests itself above a certain concentration	Flow chart straight forward. Broad flow chart that covers many approaches/situations and can therefore be used in many cases. Allows risk assessment based on whole mixtures as well as single compounds	Even though flow chart is broad it does not directly concretize many methods (e.g. method(s) for dissimilar acting compounds). The Committee concludes that in case of interaction there are no universal criteria for deciding whether the data permits a

Flow chart	Required data	Methods suggested	Assumptions	Advantages	Disadvantages
		not following the theory stringent			quantitative conclusion to be drawn.
Figure 6. Flow chart for assessment of combined actions from environmental contaminant mixtures (Teuschler, 2007)	Either data on mixture or on single compounds	Mixture: RfD/C, cancer slope factor, fractionation of whole mixture, pattern recognition techniques and multivariate regression Single compounds: HI, TEF, RPF, response addition, interaction based HI, BINWOE, cumulative relative potency factors	Departure from additivity is more likely at "high" concentrations than at "low"	Flow chart is straight forward – even though this is not always the case for the answers (Teuschler, 2007). Very broad flow chart that covers many approaches/situations and can therefore be used in many cases. Allows risk assessment based on whole mixtures as well as single compounds with a wide range of methods suggested	Comprehensiveness makes the flow chart complicated. Some of the methods are complicated and requires many data. Missing criteria to assess whether mixtures are sufficiently similar (Teuschler, 2007). In case of interaction data for a group of compounds with different modes of action there is no quantitative method.
Figure 7. Flow chart proposed by Norwegian Scientific Committee for Food Safety for risk assessment of chemical mixtures in food, feed and cosmetics (Norwegian Scientific Committee for Food Safety, 2008)	Data on single compounds	MOE, HI, MOS, PODI, TEF, response addition	Uses the term "same mode of action" which does not require knowledge about precise molecular mechanism but dose addition may be used anyway. No more than additive effect is expected for compounds at concentrations below individual NOAELs; above NOAEL interactions may occur	Flow chart straight forward. Can be used for many types of compounds / situations. The first step sorts out genotoxic and carcinogenic chemicals	Does not suggest methods in case of data on mixtures, if compounds act independently and in case of interactions (but report suggests: case-by-case basis – ideally based on test on the mixture). Flow chart encourage to consider whether the compounds affect the same physiological function but do not explain what is meant by that and how to deal with it
Figure 8. Flow chart for risk assessment of pesticide mixtures found as residues in food (Reffstrup, 2002)	Data on single compounds	HI, TEF	No more than additive effect is expected since pesticides are present in food at concentrations below individual NOAELs, and available evidence supports the view that significant toxic interactions are less likely to occur at these levels than at higher.	Very simple to use – few and simple steps in the flow chart. Simplified to cover pesticide residues in food. Valuable as a first step in the risk assessment	Pragmatic. Deals only with compounds present at low concentrations. Not scientific comprehensive, e.g. do not take interactions and dissimilar actions into account. Do not deal with data on whole mixtures (however seldom available for mixtures of pesticides)
Figure 9. Flow chart proposed by EFSA for risk assessment of pesticide mixtures found as residues in food (EFSA, 2008)	Data on single compounds	HI, reference point index (PODI), RPF, PBTK-BBDR	No more than additive effect (similar action) is expected since pesticides are present in food at concentrations below individual NOAELs, and available	Flow chart straight forward. Simplified to cover pesticide residues in food	Deals only with compounds present at low concentrations. Do not take interactions and dissimilar actions into account.

Flow chart	Required data	Methods suggested	Assumptions	Advantages	Disadvantages
			evidence supports the view that significant toxic interactions are less likely to occur at these levels than at higher.		Do not deal with data on whole mixtures (however seldom available for mixtures of pesticides). Some of the methods are complicated and requires many data

9 DEFINED CUMULATIVE ASSESSMENT GROUPS / COMMON MECHANISM GROUPS FOR PESTICIDES

As mentioned earlier the Food Quality Protection Act of 1996 requires U.S. EPA to take cumulative effects into account in the risk assessment of mixtures of pesticide residues in food. On that background U.S. EPA has up till now evaluated data on four common mechanism groups (CMGs): organophosphates (U.S.EPA, 2006c), N-methyl carbamates (U.S.EPA, 2007), triazines (U.S.EPA, 2006d) and chloroacetanilides (U.S.EPA, 2006b):

- Evaluation of the group of organophosphorus pesticides was prioritized as they are expected to be one of the classes of pesticides that poses the greatest risk. In the group of organophosphorus compounds methamidophos was selected as the index chemical to standardize the toxic potencies of the compounds. U.S. EPA used the relative potency factor method to determine the cumulative risk. Benchmark dose estimates at a level of 10 % brain acetylcholinesterase inhibition in studies on female rats were used to determine relative potencies for the organophosphorus compounds (U.S.EPA, 2006c).
- The N-methyl carbamate pesticides were found to share a common mechanism of action. The ten carbamates all inhibit acetylcholinesterase. In this group, oxamyl was selected as the index chemical. Benchmark dose estimates at a level of 10 % brain acetylcholinesterase inhibition was used to estimate the relative potencies for the compounds (U.S.EPA, 2007).
- Six triazines (atrazine, propazine, simazine and three of their metabolites) have been defined as a group based on a common mechanism causing neuro-endocrine and endocrine-related developmental, reproductive and carcinogenic effects. The compounds were included in the cumulative assessment group based on use patterns and the likelihood of exposure. The primary exposure route for these triazines is drinking water. Propazine, simazine and the three metabolites in the group are considered to be equivalent in toxicity to atrazine, per se, based on the evaluation of endocrine-related data on the triazines demonstrating either equal potency or potency less than atrazine (U.S.EPA, 2006d).
- U.S. EPA has defined a group of chloroacetanilides consisting of acetochlor, alachlor and butachlor based on the common mode of action that cause nasal olfactory epithelium tumours in rats. Due to knowledge on the capacity to induce adverse effects by a common mechanism of toxicity, this group of pesticides was prioritized. Alachlor was selected as the index chemical. Butachlor was excluded from the risk assessment since there was no registered use of the compound in the US. The point of departure was chosen at the NOAEL for tumour formation for each compound and the margin of exposure for the cumulative exposure was calculated (U.S.EPA, 2006b).

The Pesticides Safety Directorate in the United Kingdom went through the data concerning carbamates and organophosphorus pesticides in order to consider whether there are scientifically valid justification for grouping N-methyl carbamates and organophosphates separately. They concluded that carbamates and organophosphorus pesticides share the ability to inhibit acetylcholinesterase at the same binding site. However, the enzyme recovers its activity much faster in case of inhibition by a carbamate compared to an organophosphorus pesticide. This difference in rate of recovery was the reason for the U.S. EPA to establish two separate groups. However, the Pesticides Safety Directorate in the United Kingdom concluded that as humans are often co-exposed to carbamates and organophosphates there is no scientific justification to establish separate groups for these compounds. This represents a more precautionary approach (Food Standards Agency, 2005).

The United Kingdom performed cumulative risk assessment of carbamates and organophosphorus pesticides. They assessed various options for assessing relative potency. The RPFs using chlorpyrifos as the reference compound were derived from NOAELs for inhibition of RBC or brain cholinesterase in studies of various durations or from estimated benchmark doses (BMD_{10}). The hazard index using ADI or acute RfD was also calculated (EFSA, 2008; IPCS, 2009a).

EFSA has evaluated data on 25 compounds with a triazole-ring as a cumulative assessment group. From the literature they found that concerning acute toxicity seven of the compounds were producing crania facial malformation via a common mechanism of toxicity. Further, for chronic assessment 11 compounds were found to cause hepatotoxicity as a common effect (EFSA, 2009).

10 USE OF PBTK/TD MODELLING IN NEWER APPROACHES IN THE RISK ASSESSMENT OF MIXTURES

As mentioned in the previous sections several scientists, organizations and workshops have recommended the use of PBTK/TD modelling as a tool in the risk assessment of chemical mixtures. Thus the EFSA workshop on cumulative risk assessment of pesticides strongly encouraged the introduction of PBTK/TD models in the cumulative risk assessment (EFSA, 2007) and in the EFSA opinion concerning risk assessment of pesticide mixtures PBTK/TD modelling is mentioned as the most refined model (EFSA, 2008).

Simmons (1996) mentioned that there is a clear need for the development of PBTK models for mixtures. This development should be performed for the same mixtures by several laboratories in order to determine inter-laboratory consistency and variability. Scientists should also focus on extrapolation across species and development of human PBTK models for mixtures (Simmons, 1996).

The US National Research Council has provided “guidance on new directions in toxicity testing, incorporating new technologies such as genomics and computational systems biology into a new vision for toxicity testing” (Andersen and Krewski, 2009). They recommend further development and use of *in vitro* methods instead of *in vivo* studies as well as improvement and use of computational methods to extrapolate from *in vitro* to *in vivo*

systems to predict tissue and blood concentrations in humans after exposure to chemicals in specific circumstances. They suggested PBTK models as a good answer to this.

Teuschler pointed out the necessity to develop PBTK models for common mixtures of concern in order to use such models routinely in future risk assessments (Teuschler, 2007). As a helping tool for risk assessors and PBTK modellers, U.S. EPA has published a report describing different aspects of use and evaluation of PBTK models in risk assessment (U.S.EPA, 2006a). Further, some basic considerations for evaluation of PBTK models intended for risk assessment are nicely described by Chiu and co-workers (Chiu et al., 2007).

11 WHAT IS A PBTK/TD MODEL?

Physiologically based pharmacokinetic/pharmacodynamic (PBPK/PD) modelling is used in pharmacology as a technique for prediction of the internal dose after exposure to a certain compound (PBPK) and for prediction of the tissue response due to this tissue dose (PBPD). Broadly speaking pharmacokinetic describes what the body does to the compound whereas pharmacodynamic describes what the compound does to the body. The development of PBPK models arose from the need to predict the correlation between doses of a chemical (pharmaceutical) given to an animal or human and the actual internal concentration at the target site.

In the area of pharmacology, Torben Teorell used physiological considerations as the basis for a pharmacokinetic description. However, his work was done in the 1930s and the computational resources necessary for solving the differential equations were not available at that time (Rowland et al., 2004). Further, description of interactions of compounds with molecular targets at the necessary level of detail was not attainable in the 1930s. Therefore, the equations were replaced by simpler ones and for many years these more simple pharmacokinetic approaches continued to be in use even after the computational resources became available. Kenneth Bischoff and Robert Dedrick are generally credited for being the pioneers in the development of PBPK models by incorporating physiology, physical-chemistry and biochemistry into a computer modelling platform in the early 1970ies (Andersen and Krishnan, 2010).

During the latest decades more research has been done on PBPK/PD models in which the data on both physiology and biochemistry of the chemical(s) of interest are incorporated into the conceptual model for computer simulation.

In the area of toxicology several scientists have used the term physiologically based toxicokinetic/toxicodynamic (and PBTK/TD) models; however the principles of the models are the same as for PBPK/PD models. The term physiologically based toxicokinetic/ toxicodynamic and the abbreviation PBTK/TD will be used in this thesis.

In a PBTK model the animal or man is described as a set of tissue compartments combined by mathematical descriptions (differential equations) of biological tissues and physiological processes in the body. Thereby it is possible to quantitatively simulate the absorption, distribution, metabolism and excretion (ADME) of chemicals and to predict the internal

concentration of the chemical (or metabolite) of concern. A conceptual representation of a PBTK model is shown in Figure 10

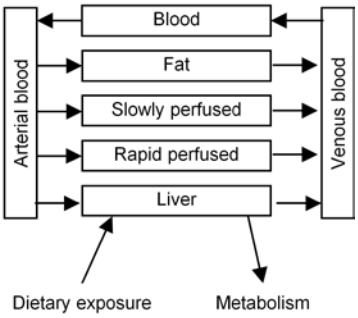

Figure 10: Conceptual representation of a PBTK model.

The PBTK model is sometimes coupled with a toxicodynamic part in which the model attempts to estimate the effect resulting from the internal dose. The output of a PBTK model is linked to a toxicodynamic model by mathematical description of the hypothesis of how compounds contribute to the initiation of cellular changes leading to the toxic responses. Such a model is sometimes called a biologically based dose-response model (BBDR) (EFSA, 2008; National Research Council, 2007; U.S.EPA, 2006a). The relationship between external dose, internal dose and observed toxic effect is shown in Figure 11.

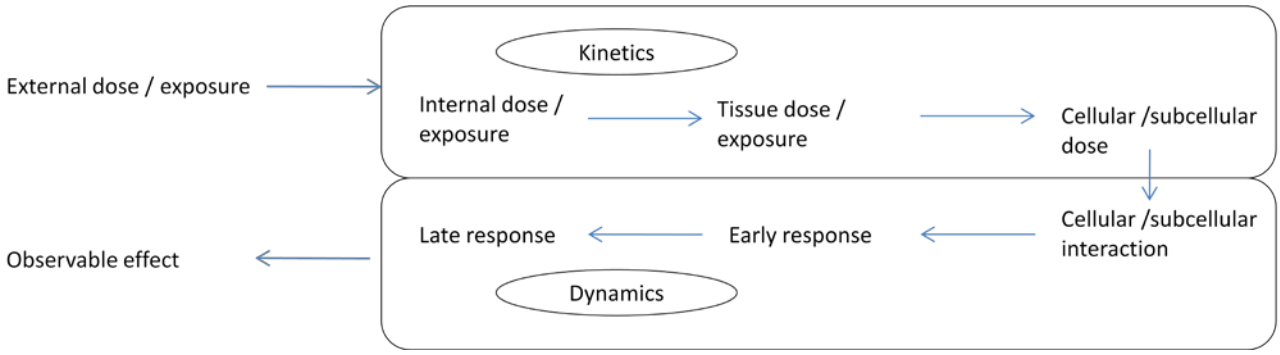

Figure 11. Relationship between exposure, internal dose and observable effect. Modified from (IPCS, 2010).

Figure 12 shows an overview of different steps in modelling representing increasing levels of information on the link between external dose, internal dose of the compound and its metabolites and their toxic response:

- Basic data set: only knowledge on external dose and toxic response from experiments
- Kinetic parameters: in this case simple calculations are made of the internal dose (possibly concentration of the compound in blood) i.e. the link between the external dose and toxic response
- Physiologically based toxicokinetic (PBTK) model: in addition to the internal dose (which is possibly the concentration in blood) the target organ dose is calculated taking metabolism in the liver into account

- PBTK model with target organ metabolism: in this model both concentration in the target organ as well as metabolism of the compound in the target organ is modelled
- Biologically based dose-response model: is the most refined model which combine PBTK and PBTD models to predict biological processes at the cellular and molecular levels by linking the concentration in the target organ to the adverse effect (Andersen and Krishnan, 2010; U.S.EPA, 2006a).

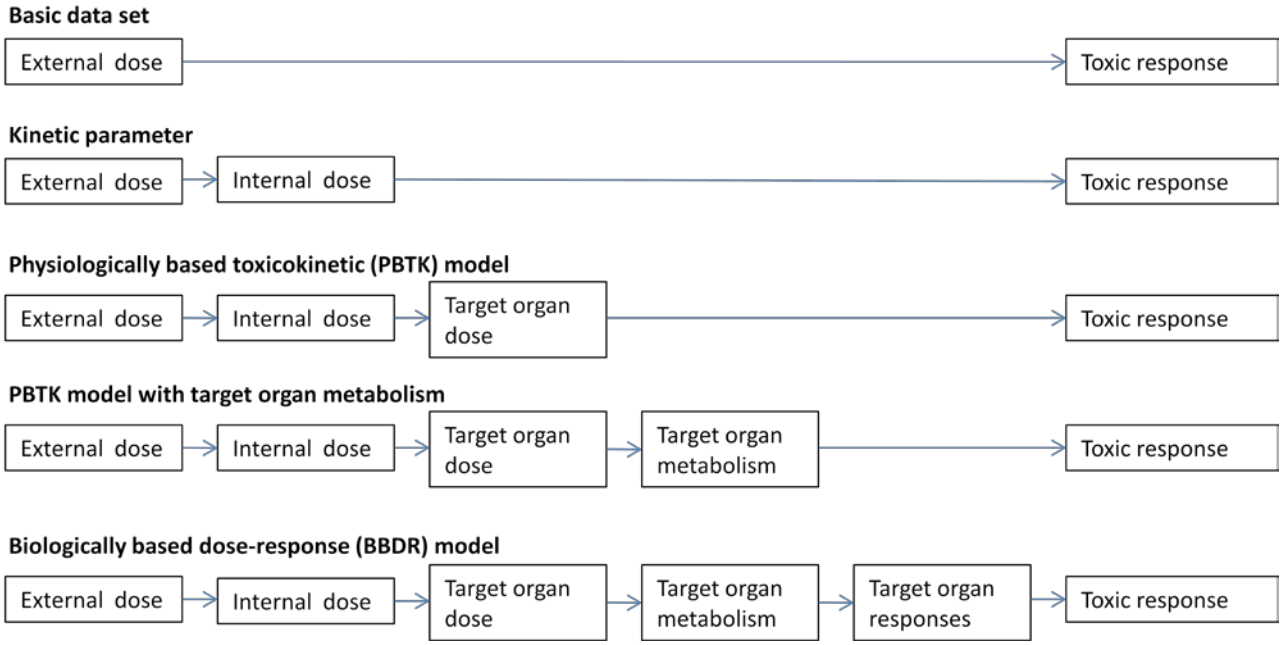

Figure 12. Relationship between exposure, internal concentration and effect in dose-response analysis with increasing level of data-information. Figure modified from (IPCS, 2010).

There are two main modes of implementing a PBTK model: descriptive and predictive. In a descriptive model the point of departure is a set of observed data i.e. knowledge about input and output, however, knowledge about the biology of the system is not required. A model is chosen and the job is then to fit the model to the data, i.e. making an interpolation. Such a model is also called empirical or data based. Unlike this, a predictive model is developed from knowledge on biology and the prediction from the model is afterwards validated against observed data. It is also called a mechanistic model. This kind of model is useful for extrapolations. A descriptive model has the fewest assumptions but it cannot be used for extrapolations to other species, types of exposure etc. Often both the descriptive and the predictive methods are used in the development of PBTK models in practice (Andersen and Krishnan, 2010; Nestorov, 2003).

12 DEVELOPMENT OF A PBTK MODEL

In order to develop a PBTK model for a certain chemical it is necessary to understand the anatomical and physiological characteristics of the species and the pathways of absorption, distribution, metabolism and elimination of the chemical in the body.

In the development of a PBTK model the Law of Parsimony should always be applied i.e. keep the model as simple as possible but still biological plausible. It is important to consider which compartments can be lumped together due to e.g. similar concentration-time courses. A large number of compartments are not necessarily equal to accuracy and usefulness of the model since the complexity requires a multitude of parameters to be estimated and thereby create greater uncertainty in the model description (Krishnan and Andersen, 2001; Yang and Lu, 2007).

The necessity for including a particular tissue as a separate compartment depends on the toxicokinetic properties, mode of action and toxicity of the compound being modelled. Common criteria for selecting a tissue is whether it has significant metabolizing enzyme activities or the solubility of the chemical plays an important role within the tissue (as for lipophilic compounds). Target organs and eliminating organs have to be described as separate compartments. For instance the liver is a major site of biotransformation and should therefore always be described separately (Krishnan et al., 2010; Krishnan and Andersen, 2001).

Tissues such as kidney, brain, heart, lung, thyroid, testis, and the hepatoportal system are often lumped into one compartment called rapidly (or richly) perfused tissue. In the same way slowly (or poorly) perfused tissues such as muscle and skin are often lumped into one compartment. Fat tissues in the whole body are also often lumped into one compartment. During the model development the complexity of the model can be increased (splitting or adding of compartments) if necessary in order to adequately describe data (Krishnan et al., 2010; Krishnan and Andersen, 2001; Yang and Lu, 2007).

The blood is not always described in the PBTK model as a separate compartment even though the blood concentrations are calculated. Instead the total blood volume is divided among the tissues (Krishnan and Andersen, 2001).

The steps in developing a PBTK model for estimating tissue dose metrics for use in chemical risk assessment is as follows (see also Figure 13) (Andersen, 2003; Clewell and Clewell, III, 2008; U.S.EPA, 2006a):

1. identify toxic effects in animals (and humans) and determine the critical effect(s)
2. search the literature and organise available data in order to determine the mode of action, metabolism, as well as physiological constants for the relevant animal species
3. suggest relationships between response and tissue dose
4. model formulation: develop a PBTK model to estimate the tissue dose metric at various doses
5. run the model (that is, solve the equations)
6. compare output from the model-simulation with available experimental data. If the result from the simulation deviates from the experimental data go to point 7) otherwise go to point 9)
7. refine the model
8. repeat point 5) and 6)
9. application in risk assessment

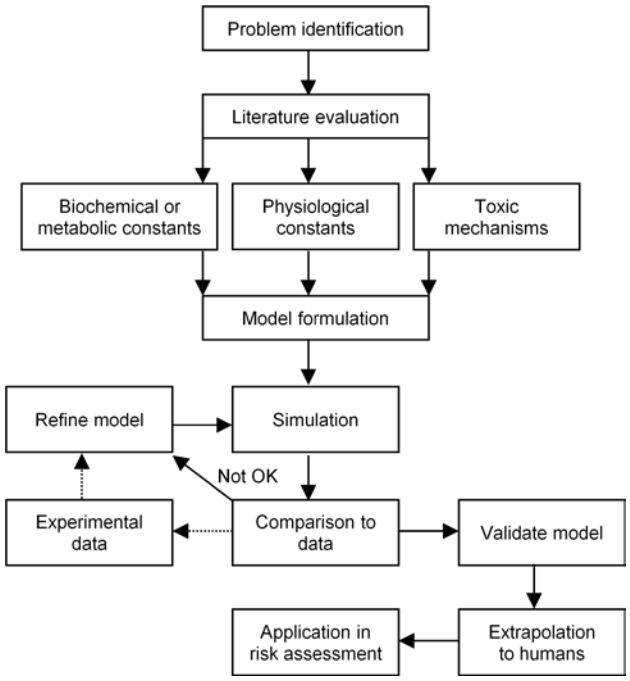

Figure 13: Flow chart for development of a PBTK model. Adapted from (U.S.EPA, 2006a).

13 MATHEMATICAL DESCRIPTIONS IN PBTK MODELS

Examples of descriptions of absorption, distribution, metabolism and elimination used in PBTK models are shown in Table 4. Other equations are also used. In the section concerning the model-work performed in this thesis the equations used here are further outlined (see section 21.1).

The equations most often used for description of metabolism in PBTK modelling will be described in the following sections.

Table 4. Examples of mathematical representation of absorption, distribution and excretion. Only oral absorption and urinary excretion are shown. Modified from (Krishnan et al., 2010).

Toxicokinetic process		**Mathematical description**
Absorption	Oral	$\frac{dA_o}{dt} = K_o * D_o * e^{-K_o * t}$ A_o: amount of compound absorbed orally(mg), K_o: oral absorption rate constant (1/hr), D_o: Oral dose (mg), t: time (hr)
Distribution	Protein binding	$C_b = \frac{n * \beta * K_d * C_f}{1 + K_d * C_f}$ Cb: concentration of bound compound (mg/l), n*α: binding maximum, K_d: dissociation constant (mg/l), C_f: concentration of free compound (mg/l)
	Diffusion limited tissue distribution	$\frac{dA_t}{dt} = PA_t * \left(C_{vt} - \frac{C_t}{P_t} \right)$ A_t: amount of compound in tissue t (mg), PA_t: permeation area cross product for tissue t (l/hr), C_{vt}: concentration in venous blood leaving tissue t (mg/l), C_t: concentration in tissue t (mg/l) P_t: tissue:blood partition coefficient
	Perfusion limited tissue distribution	$\frac{dA_t}{dt} = Q_t * (C_a - C_{vt})$ A_t: amount of compound in tissue t (mg), Qt: blood flow to tissue (l/hr), Ca: concentration in arterial blood (mg/l), C_{vt}: concentration in venous blood leaving tissue t (mg/l)
Metabolism	First order	$\frac{dA_{met}}{dt} = K_f * C_{vt} * V_t = CL_{int} * C_{vt}$ A_{met}: amount of compound metabolised (mg), K_f: first-order metabolism rate constant (1/hr), C_{vt}: concentration in venous blood leaving tissue t (mg/l), V_t: tissue volume (l), CL_{int}: intrinsic clearance (l/hr)
	Second order	$\frac{dA_{met}}{dt} = K_s * C_{vt} * V_t * C_{cf}$ A_{met}: amount of compound metabolised (mg), Ks: second-order metabolism rate constant (l/mg/hr), C_{vt}: concentration in venous blood leaving tissue t (mg/l), V_t: tissue volume (l), C_{cf}: concentration cofactor in tissue t
	Saturable process	$\frac{dA_{met}}{dt} = \frac{V_{max} * C_{vt}}{K_m + C_{vt}}$ A_{met}: amount of compound metabolised (mg), V_{max}: maximum velocity of enzymatic reaction (mg/hr), C_{vt}: concentration in venous blood leaving tissue t (mg/l), K_m: Michaelis-Menten constant (mg/l)
Excretion	Urinary	$\frac{dA_{rc}}{dt} = GFR * \frac{T_m}{K_t + C_p} * C_p$ A_{rc}: amount of compound in renal compartment (mg), GFR: glomerular filtration rate (l/hr), T_m: apparent maximum transport of the carrier system (mg/hr), K_t: apparent Michaelis-Menten constant with respect to secretary carrier (mg/l), C_p: plasma concentration (mg/l)

13.1 MIXTURES WITH NO INTERACTION

In case of a mixture of compounds that do not interact (e.g. simple similar action) the PBTK modelling tool is useful to predict the dose in the target organ taking metabolism of the compounds into account. Compounds in a mixture where no interaction appears should be dealt with in PBTK models in the same way as single compounds (Haddad et al., 2010).

PBTK models are increasingly being used in supporting the derivation of health based guidance values such as ADI or RfDs for use in risk assessment. In the absence of adequate human data to assess the risk for humans directly, the reference value is typically derived from animal data. Uncertainty factors are then used to fill in the data gaps between the species as well as the intra-species variability. When a PBTK model is developed and tested

adequately, it will provide a more scientifically supportable result for these data gaps than use of uncertainty factors will give (DeWoskin and Thompson, 2008).

Metabolism of a compound is usually described by the Michaelis-Menten equation in PBTK models. This model is known from basic biochemistry describing the enzyme kinetic of substrate S binding to enzyme, E, forming a complex, ES, which is an intermediate in the formation of product, P:

$$E + S \underset{k_{-1}}{\overset{k_1}{\leftrightarrow}} ES \xrightarrow{k_2} E + P$$

k_1, k_{-1} and k_2 are the rate constants for the three possible steps in the reaction.

The initial rate of the reaction increases hyperbolically as a function of substrate concentration until it reaches a maximum, V_{max}. Initially the rate of reaction follows a linear course with the pseudo-first order rate constant V/K. The Michaelis-Menten constant, Km, can be read as the intersection of the curves V/K and V_{max}, see Figure 14.

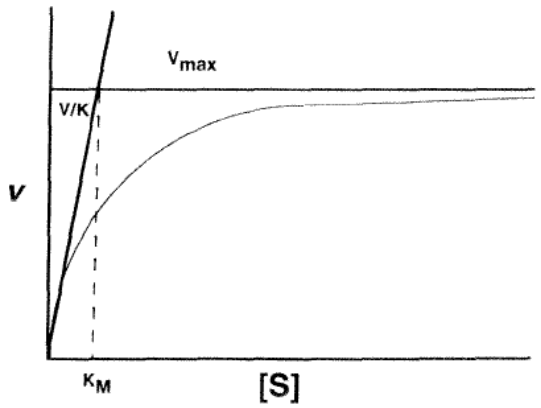

Figure 14. Michaelis-Menten saturation curve: the initial rate (v) plotted as a function of substrate concentration [S]. Vmax represents the maximum of the curve and V/K is the pseudo-first order rate constant (the slope of the linear curve at low [S]). Adapted from (Kedderis, 1997)

Mathematically the Michaelis-Menten equation can be written as:

$$RAM = \frac{V_{max} * [S]}{K_m + [S]} \qquad (14)$$

RAM is the rate of metabolism, V_{max} represents the maximal rate for the system at the maximum substrate concentration, [S], and the Michaelis-Menten constant K_m is:

$$K_m = \frac{k_{-1} + k_2}{k_1} \qquad (15)$$

(Kedderis, 1997)

The Michaelis-Menten equation makes the steady-state assumption that the amount of complex between enzyme and substrate is constant (i.e. the complex is formed at the same rate as it is decomposed). This assumption is only valid when the concentration of substrate is much greater than the total enzyme concentration (Kedderis, 1997).

13.2 TYPES OF TOXICOKINETIC INTERACTIONS AND MATHEMATICAL DESCRIPTIONS OF THESE

The PBTK model can be used to investigate hypotheses regarding mechanisms of interaction between chemicals i.e. toxicokinetic interactions can be described in the model.

A PBTK model describing interactions consists of sets of identical equations, one set for each chemical as well as equations that specifically accounts for the interactions (e.g., competitive inhibition of metabolism in liver or induction of hepatic metabolism) (ATSDR, 2001). These equations are based on knowledge or hypothesised mathematical descriptions of their interaction mechanisms (Haddad et al., 2010).

Exposure to multiple chemicals may cause alterations in the toxicokinetics of the individual chemicals resulting in a change in the predicted toxicity based on effects of the single compounds. Toxicokinetic interactions occur as a result of one compound altering the absorption, distribution, metabolism or elimination of other compounds. They may affect the relationship between administered dose and the dose delivered to the target site (Krishnan et al., 1994; Krishnan et al., 2002). Toxicokinetic interactions can be caused by changes in either the physiological, physicochemical or biochemical parameters (Haddad et al., 2010).

Physiological changes (e.g. changing in cardiac output and tissue blood flow) altering the toxicokinetics of one compound by another have been seen for many binary chemical mixtures. ***Physicochemical*** interactions such as solubility in lipid or water (e.g. by altering the pH) or permeability across biological membranes (by formation of more lipophilic complexes than either chemical itself) can result in changes in distribution or rates of absorption. However, models incorporating changes in physiological or physicochemical parameters caused by co-exposures have not yet been published (Haddad et al., 2010).

The most frequently reported toxicokinetic interactions are at the metabolic and transporter levels (***interaction at the biochemical level***). These kinds of interactions occur when one chemical alters the binding, the biotransformation or the active transport of another chemical and they are either a result of changes in the affinity or maximal velocity. Interactions at the biochemical level are divided into: reversible metabolic inhibition, irreversible metabolic inhibition, reversible protein binding interaction and enzyme induction.

The most often seen type of interaction in PBTK models is ***reversible metabolic inhibition*** and this can be divided into three cases: competitive, non-competitive and uncompetitive reversible enzyme inhibition (Haddad et al., 2010). Competitive inhibition takes place when chemicals compete for the same active site of the enzyme resulting in decreased apparent affinity (and increased Km) which again leads to a decrease in the rate of metabolism at lower substrate concentrations. Non-competitive inhibition results when a chemical binds to the enzyme at a site away from the catalytic active site. This leads to decreased catalytic activity

(and decreased Vmax). Uncompetitive inhibition occurs when a chemical binds to the enzyme-substrate complex and thereby affects the catalytic function without interfering with the substrate binding. The inhibiting chemical causes a structural distortion of the active site which becomes inactivated. The available enzyme is reduced (and Vmax is decreased) and the reaction E+S->ES is driven to the right (and Km lowered) (Haddad et al., 2010). The mathematically description of competitive, non-competitive and uncompetitive reversible enzyme inhibition is shown in Table 5. The derivation of these equations are nicely described in (Campbell et al., 2010).

Table 5. Metabolic inhibition hypotheses, equilibrium equations and mathematical equations for the rate of metabolism (velocity) for compound 1 (Comp1) as well as the effect on K_m and V_{max}. Comp1 is the substrate with concentration C_1, Comp2 is the inhibitor with concentration C_2. V_{max1} and K_{m1} are the maximum velocity and Michaelis-Menten constant respectively for compound 1. Ki_{21} is the inhibition constant which is determined as the concentration of compound 2 at which 50 % inhibition occur. α is the factor by which K_m and V_{max} are changed, $\alpha=1+C_2/K_{21}$. Table based on (Haddad et al., 2010) and (Campbell et al., 2010). A similar set of equations can be set up for compound 2.

Hypothesis	**Equilibrium equation**	**Equation for the rate of metabolism of compound 1 (RAM1)**	**Apparent K_m**	**Apparent V_{max}**
No metabolic interaction	$E + Comp1 \underset{}{\overset{K_{M1}}{\rightleftharpoons}} E\text{-}Comp1 \xrightarrow{K_{p1}} E + P$	$RAM_1 = \frac{Vmax1 * C_1}{K_{m1} + C_1}$		
Competitive interaction	$E + Comp1 \overset{K_{M1}}{\rightleftharpoons} E\text{-}Comp1 \xrightarrow{K_{p1}} E + P$ $+$ $Comp2 \updownarrow Ki_{21}$ $E\text{-}Comp2$	$RAM_1 = \frac{Vmax1 * C_1}{C_1 + K_{m1} * (1 + C_2/Ki_{21})}$	$\alpha * K_m$	V_{max}
Non-competitive interaction	$E + Comp1 \overset{K_{M1}}{\rightleftharpoons} E\text{-}Comp1 \xrightarrow{K_{p1}} E + P$ $+ \quad +$ $Comp2 \updownarrow Ki_{21} \quad Comp2 \updownarrow Ki_{21}$ $E\text{-}Comp2 + Comp1 \rightleftharpoons E\text{-}Comp1\text{-}Comp2$	$RAM_1 = \frac{Vmax1 * C_1}{(C_1 + K_{m1}) * (1 + C_2/Ki_{21})}$	K_m	V_{max}/α
Uncompetitive interaction	$E + Comp1 \overset{K_{M1}}{\rightarrow} E\text{-}Comp1 \xrightarrow{K_{p1}} E + P$ $+$ $Comp2 \updownarrow Ki_{21}$ $E\text{-}Comp1\text{-}Comp2$	$RAM_1 = \frac{Vmax1 * C_1}{K_{m1} + C_1 * (1 + C_2/Ki_{21})}$	K_m/α	V_{max}/α

Irreversible metabolic inhibition occurs when the inhibitor binds irreversibly to the enzyme at the active site. This binding decreases the concentration of functional enzyme (and thus decreases Vmax). The level of enzyme is decreased by a rate of enzyme interaction:

$$\frac{dInact}{dt} = \frac{k_{inact} * E_a * f_{ub} * I_h / K_p}{K_{i,app} + f_{ub} * I_h / K_p} \qquad (16)$$

where k_{inact} is the maximum inactivation rate constant, E_a is the amount of active enzyme, K_p is the liver:blood partition coefficient, f_{ub} is the unbound fraction in blood, $K_{i,app}$ is the apparent inactivation constant and I_h is the concentration of the inactivator in the liver (Haddad et al., 2010).

Reversible protein binding interaction can occur either by competition for the binding site or induction of binding protein levels. The concentration of bound compound, C_b, can be calculated by the following equation:

$$C_b = \frac{n * \beta * K_d * C_f}{1 + K_d * C_f} \qquad (17)$$

where C_f is the concentration of free compound, K_d is the dissociation constant and $n*\beta$ is the binding capacity. If a competitive inhibitor is present, then K_d in the above equation will be increased by a factor α:

$$\alpha = 1 + \frac{[I]}{K_i} \qquad (18)$$

where [I] is the concentration of the inhibitor and K_i is the inhibition constant (Haddad et al., 2010).

Enzyme induction leads to increased enzyme synthesis and/or decreased enzyme degradation (and thus increased Vmax). Enzyme induction has been described by:

$$\frac{dSyn}{dt} = Ksyn_{basal} + (Ksyn_{max} Ksyn_{basal}) * \frac{[RL]^n}{[RL]^n + Kd^n} \qquad (19)$$

where $Ksyn_{basal}$ is the basal rate of enzyme synthesis, $Ksyn_{max}$ is the maximal rate of enzyme synthesis, [RL] is the concentration of the receptor-ligand complex and n is the Hill coefficient (Haddad et al., 2010).

14 PARAMETER VALUES FOR PBTK MODELS

For the development of PBTK models a set of physiological, physicochemical as well as biochemical parameters are needed. The physiological parameters are parameters like tissue weight, tissue blood flow rates, ventilation rates (for modelling inhaled/exhaled compounds) and cardiac output and these are independent of the chemical of concern (but they can be affected due to interactions). The physicochemical and biochemical parameters are chemical specific. Physicochemical parameters required are e.g. tissue partition coefficients of the chemical between various media (typically tissue:blood partition coefficients). Biochemical parameters are e.g. used to describe metabolism (e.g. Km and Vmax) and protein binding

(Brown et al., 1997; Yang and Lu, 2007). These parameters can be measured *in vivo* and/or *in vitro*. OECD has published a test guideline on toxicokinetic studies, TG 417 (OECD, 2010).

No international accepted set of reference values of physiological parameters have been compiled. Several groups of scientists have created compendia of reference values of physiological parameters for adult as well as for young animals and humans for use in PBTK modelling e.g. (Brown et al., 1997; Davies and Morris, 1993; Thompson et al., 2009; U.S.EPA, 1988a). Most recently U.S. EPA has published a database of physiological parameters for adult humans and rodents (U.S.EPA, 2009) and Thompson and co-workers have published description of a database of physiological parameters for elderly humans (Thompson et al., 2009).

Among others Johns et al. (2010) point out the lack of biological and experimental variability associated with the reference values in many of the published compendia (Johns et al., 2010). On the other hand other scientists have mentioned that the reference works presenting several values for each parameter cause a tendency for modellers to use their "favourite" values (Davies and Morris, 1993). Due to this discussion on balancing simplicity in the set of reference values and the wish to know the variability associated with the parameters it will probably take some time before different modellers will agree on using the same reference values of physiological parameters in PBTK models.

Some parameters have greater impact on the predictive ability of the model than others. Accuracy of these parameter values are of course of the greatest concern. This topic will be addressed and discussed in more detail in the chapters concerning the model-work in this thesis (see chapter 21-24).

A very important, general statement to keep in mind working with models is: "The model is only as good as the input parameters." (Krishnan and Andersen, 2010)

15 SOFTWARE

When all the equations for the model have been set up and the parameters defined, the equations should be put into a differential equation solver. There are many such programs on the market which have been used for PBTK modelling. Krishnan and Andersen have set up the following criteria for selection of simulation language:

"(a) provides a convenient means for initializing the status of the model (e.g., generating random numbers in case of stochastic models),

(b) permits the introduction of changes in both the status and temporal structure of the model as simulation time evolves (i.e., scheduling the occurrence of events),

(c) provides simple methods by which model results and statistical summaries can be obtained,

(d) allows considerable flexibility in conducting sensitivity and other types of model analyses, and

(e) contains error detection facilities." (Krishnan and Andersen, 2001)

The software Berkeley-Madonna has been used in the present thesis. It is a fast differential equation solver developed by Robert Marcey and George Oster at the University of California at Berkeley. It is a user-friendly program for modelling and analysis of dynamic systems and some universities offers good courses in the use of it.

16 EVALUATION OF PREDICTIVE CAPACITY

Before using a model in risk assessment, the model should be evaluated. The purpose of this is to assess the available toxicokinetic and dose-response data of the chemical-biological system and also to depict the uncertainty associated with the parameter values used. Further, in the context of risk assessment the suitability and the applicability of the model for regulatory purposes should be assessed (U.S.EPA, 2006a). Model evaluation consist of validation and verification, that is whether the model is correctly build and whether it is the right model, respectively (Balci, 1997; U.S.EPA, 2006a).

The model verification includes checking the biological plausibility of the model structure and parameters (U.S.EPA, 2006a).

The purpose of the validation process is to verify whether the biological system is described adequately by the chosen compartments and parameters in the model, i.e. answer the question: is the model correctly build? This can be done by comparing model predictions with experimental data by visual inspection, statistical tests or discrepancy measures (a quantitative representation of the deviation between model prediction and experimental data) (Krishnan and Andersen, 2001).

A validated model is a model that has been calibrated against one dataset and afterwards has adequately simulated another dataset. However, this only means that the model is capable to simulate within the domain that these two dataset covers (U.S.EPA, 2006a).

17 APPLICATION OF PBTK MODELS IN RISK ASSESSMENT

A PBTK model is useful for predicting internal dose levels for hypothetical exposure regimens and this is the main application of PBTK models. It is possible to simulate the dose metrics in the test species and/or humans for the actual exposure route and exposure scenario of concern. The internal concentration of the chemical will provide a better relationship to the observed toxic effects than the external or exposure concentration of the chemical and this knowledge will reduce the uncertainty in risk assessment. It is also possible to predict overload of toxicokinetic pathways and to do high-dose to low-dose extrapolation. Further, PBTK models can improve the estimation of risk from chemical mixtures. These are all useful tools that can offer an improvement when applied to risk assessment.

Route-to-route extrapolation
With a PBTK model it is possible to simulate exposure from different routes, e.g. dietary or gavage intake, dermal uptake or inhalation, that is, to extrapolate from one route to another in animals using equivalent dose metric. This can be performed by adding appropriate equations to represent each exposure pathway.

Route-to-route extrapolation can also be used to predict target tissue dose in humans for one route based on available data from an animal toxicity study for another route on the basis of equivalent dose metric (Clewell, 2010; U.S.EPA, 2006a).

Exposure scenario extrapolation
Exposure scenario extrapolations are done by introducing a mathematical function that explains the temporal change in exposure level and time frame. Thereby it is possible to predict tissue dose during short-duration exposure to higher concentrations or during variable-exposure concentrations (Krishnan and Andersen, 2001). Clewell points out that PBTK modelling is generally not very useful for extrapolating from acute to subchronic or from subchronic to chronic exposure scenarios primarily due to toxicodynamic factors (such as damage accumulation, repair and compensation) during the different time frames. Therefore, Clewell suggests to use an uncertainty factor to account for the differences in duration of exposure as it is common in the default approach for non-cancer risk assessment (Clewell, 2010).

High-dose to low-dose extrapolation
High-dose to low-dose extrapolation in PBTK models is accomplished by a description of the nonlinear kinetic behaviour of chemicals. The often used Michaelis-Menten equation describes how the rate of metabolism varies with substrate concentration by a nonlinear curve where the rate of metabolism increases toward a maximum. Two metabolic pathways are described in the Michaelis-Menten model: first-order kinetic at low concentrations and saturation at high concentrations – this makes the model suitable for the high-dose to low-dose extrapolation (National Research Council, 1987; U.S.EPA, 2006a).

Interspecies extrapolation
When a model has been built and evaluated in for instance rats, the model is ready for extrapolation to other species including humans. The steps in developing a PBTK model for interspecies extrapolation is as follows: 1) the model is built for the appropriate species (e.g. rats), 2) the a priori predictions are compared with experimental data and the structure and parameters in the model are evaluated. If necessary the parameters may be adjusted. 3) The species specific model parameter values (i.e. partition coefficients, physiological parameters and metabolic rate constants) should be replaced by appropriate estimates for the species of interest (e.g. humans) (U.S.EPA, 2006a). This extrapolation between species can however be difficult due to an often unpredictable pattern for metabolic rate constants between the species. The metabolic rate constants should therefore most preferably be obtained in the species of interest. However, *in vivo* approaches for determining these constants are not always possible for application in humans. Therefore, in many cases the solution is to either

obtain such data by scaling from *in vitro* assays (using rodents or human tissue fractions) or from *in vivo* rodent data (Krishnan and Andersen, 2001).

17.2 METHODS FOR DEVELOPMENT OF MIXTURE PBTK MODELS

Different ways to describe interactions in PBTK models have been suggested: 1) describing each binary interaction in the mixture, 2) modelling of the maximal effect of metabolic interactions in the mixture, 3) lumping of chemicals in the mixture, 4) using Km as Ki for competing substrates in the mixture, and 5) fitting parameter values to experimental mixture data. These methods are described in more details below.

Binary interaction-based PBTK model

The first step in the development of a PBTK model for a binary mixture is to develop PBTK models for the individual compounds and the next step is to include descriptors that account for the interactions. As mentioned previously the most frequently seen type of interaction in PBTK models is metabolic inhibition. The rate of metabolism of compound 1 (RAM_1) is calculated by a modified Michaelis-Menten equation including a modulation factor reflecting the effect of interaction (e.g. competitive inhibition):

$$RAM_1 = \frac{Vmax1 * C_1}{C_1 + K_{m1} * (1 + C_2/Ki_{21})} \qquad (20)$$

where the Vmax1 and K_{m1} are the maximum velocity and Michaelis-Menten constant for compound 1, C_1 is the concentration of compound 1 and C_2 is the concentration of the competing compound – both at the site of metabolism. The inhibition constant Ki_{21} reflects the concentration of compound 2 (C_2) at which 50 % inhibition occurs (Krishnan et al., 2002).

A similar equation can be set up for compound 2 (Haddad et al., 2010):

$$RAM_2 = \frac{Vmax2 * C_2}{C_2 + K_{m2} * (1 + C_1/Ki_{12})} \qquad (21)$$

where Vmax2 and K_{m2} are the maximum velocity and Michaelis-Menten constant for compound 2, and Ki_{12} corresponds to the concentration of compound 1 at which 50 inhibition occurs.

Krishnan and co-workers have very nicely described how to extend the method for extrapolation of interactions from binary to more complex mixtures (Krishnan et al., 2002).

In a ternary mixture of compound 1, 2 and 3, the compounds interact with each other in pairs (1-2, 1-3 and 2-3) as shown in Figure 15. Further, compared to a binary mixture compound 3 not only interacts directly with compound 1 and 2 but it also influences the interaction between 1 and 2 by inhibiting their metabolism.

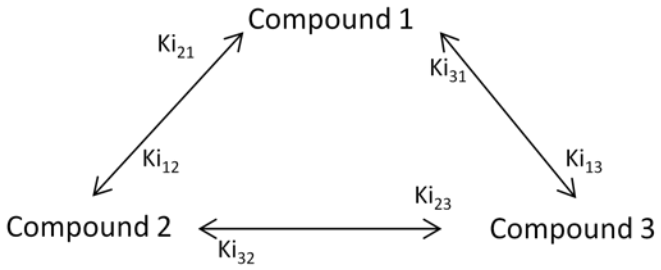

Figure 15. Ternary mixture. Interactions among the three compounds are shown with arrows. The inhibition constants Ki_{XY} of compound X on compound Y are shown (X and Y denotes the three compounds 1, 2, and 3).

In a similar way a network of binary toxicokinetic interactions is created for a mixture of five compounds as shown in Figure 16. Each binary interaction will affect the kinetics of all other compounds in the network.

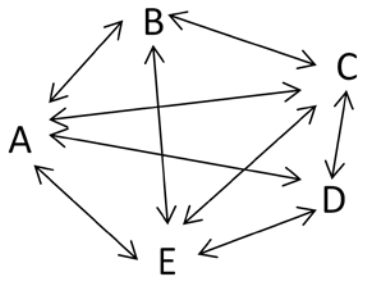

Figure 16. Network of binary toxicokinetic interactions between five compounds, A, B, C, D and E. The arrows represent the connection between the compounds. Modified from (Haddad et al., 2010).

With a more complex mixture of n compounds the equation above is expanded to account for binary inhibition between the other compounds in the mixture and the rate of metabolism of compound 1 can be calculated as:

$$RAM_1 = \frac{V\max 1 * C_1}{C_1 + Km_1 * (1 + C_2 / Ki_{21} + C_3 / Ki_{31} + ... + C_n / Ki_{n1})} \quad (22)$$

Similar equations should be included for each compound in the mixture (Krishnan et al., 2002).

In this way PBPK models for complex mixtures can be developed as long as the quantitative information of the mechanism of interaction for each interacting pair is available or can be hypothesised. However, this is also the limitation of the technique as this requires knowledge (from studies) for a great number of binary interactions. The number of binary interactions, N, in a mixture of n compounds is: N=n(n-1)/2) (Haddad et al., 2010; Krishnan et al., 2002).

Until now this method has only been used on volatile organic compounds and its broader applicability still remains to be evaluated.

Modelling of maximal effect of metabolic interactions

For PBTK models to be used for risk assessment purposes a pragmatic approach has been suggested in cases where insufficient information on mechanisms of binary interactions is available (Haddad et al., 2000; Krishnan et al., 2002). The method assumes that interactions only occur at the level of hepatic metabolism. The rate of metabolism is calculated by:

$$RAM=Ql*E*Ca \qquad (23)$$

where Ql is the blood flow in liver, E is the hepatic extraction ratio and Ca is the arterial blood concentration. This equation expresses the same as the Michaelis-Menten equation but it makes it possible to simulate the theoretical limits of the impact of metabolic interactions. This is done by varying the value for the hepatic extraction ratio. The maximum value of E is 1 (corresponding to a maximum organ blood flow) and this value constitutes the maximal value for enzyme induction. In case of metabolic inhibition the E value is decreased to the minimal hepatic extraction ratio (E=0). The results from the PBTK simulations using these two limits for the hepatic extraction ratio make it possible to predict the corresponding theoretical limits of blood concentrations due to metabolic interactions: E=1 constitutes the theoretically plausible lower limit and E=0 the upper limit of the blood concentration.

The applicability of the method was tested on data for mixtures of up to ten volatile organic chemicals (rat inhalation). The authors found that the limits were well predicted for nine out of the ten volatile organics and the method is useful for identifying compounds for which metabolic interactions are likely to be important (Haddad et al., 2000).

Lumping of chemicals in mixtures

For modelling of very complex mixtures such as gasoline, it has been suggested to lump the chemicals in groups of similar compounds so that a group of compounds are handled as if it was only one compound. This method can be used when the compounds in the mixture act in the same way so that their properties can be described by a central estimate and when it is not necessary to distinguish one compound in the lump from another. The simplest lumping approach is to split those compounds where individual toxicokinetic information is needed and then lump the rest of the compounds (Dennison et al., 2004; Dennison et al., 2003).

Dennison and co-workers developed a six lump PBTK model to describe exposure to gasoline in an inhalation study with rats. Five of the six lumps were single compounds (benzene, toluene, n-hexane, ethylbenzene, o-xylene (i.e. BTHEX)) and the sixth lump consisted of the rest of the compounds in the mixture (aromatics, isoparaffins, naphthalenes etc.). The five single compounds have different modes of toxicity and they represent different chemical structures and therefore they were chosen to be treated separately. The authors determined parameter values for the lump as a whole. The metabolic interactions between the six compounds / pseudo-compounds in the mixture were simulated using the binary interaction-based approach described above. The model simulations were in good agreement with experimental data for the single compounds, the pseudo-compound and the mixtures. They found the lumping method useful to predict the toxicokinetic of the compounds in gasoline

and recommended the method to be used for other mixtures and for other routes of exposure (Dennison et al., 2004; Dennison et al., 2003).

Use of QSAR for estimating Km and Vmax

Another method for PBTK modelling of mixtures in the absence of data for binary interaction studies was presented by Price and Krishnan. They used QSAR to predict values for Km, Vmax and partition coefficients for single compounds based on data for 53 volatile organic compounds. These values were then used as input in interaction-based PBTK models in order to predict toxicokinetics for mixtures of up to ten compounds (benzene, toluene, m-xylene, o-xylene, p-xylene, ethylbenzene, dichloromethane, trichloroethylene, tetrachloroethylene, and styrene). They also assumed that the Michaelis-Menten constants, Km, were equal to the metabolic inhibition constant, Ki, for competing compounds and compared the simulation results based on this assumption with simulations using experimental data for Ki. The authors conclude that the method is useful as a first step in identifying the assumption of competitive inhibition in cases where the compounds in the mixture compete at the metabolic level, and that QSAR is a helpful tool in deriving parameters for PBTK modelling (Haddad et al., 2010; Price and Krishnan, 2011).

Obtaining parameter values by fitting to data on mixtures

PCB congeners are highly lipophilic and kinetic data are available. Due to the known lipophilicity of these compounds Emond and co-workers (2005) assumed that the lipid content was determining for the distribution of the compounds to the tissue compartments and that their solubility in water and water-like fractions of tissues and blood is negligible. Instead of modelling every binary interaction in the mixture, they obtained toxicokinetic data for these compounds from studies on a mixture of PCBs.

They developed a model for simulating the PCB concentration in blood and lipid tissue based on data estimated in rats exposed to an environmentally relevant mixture of PCB congeners. Equations describing the elimination due to metabolism were included in the liver comparment.

The concentration of PCBs in adipose tissue and plasma lipids of rats were simulated at four different exposure scenarios at three dose levels. The elimination rate constant for each PCB were determined based on fit of the model to hepatic concentrations of PCBs measured on day 41 and 90 following exposure of rats to a mixture of PCBs by various doses and exposure scenarios.

The authors concluded that the model based on the neutral lipid content of tissues alone (without the use of tissue:blood partition coefficients) was sufficient to simulate the accumulation and elimination kinetics of PCBs as well as the lipid concentrations of PCBs in the mixture (Emond et al., 2005).

This is an example of the use of a PBTK model to obtain parameter values based on data from exposure of a mixture. The method is only expected to be of value in conducting interpolations covering the range of doses and exposure scenarios for which the metabolic rates were optimized (Emond et al., 2005; Haddad et al., 2010).

17.3 INTERACTION BASED HAZARD INDEX USING PBTK MODELS

Haddad et al. have shown how estimates from PBTK models can be used successfully in the risk assessment. They used the PBTK model approach to account for interactions in occupational inhalation exposure of mixtures of five volatile organic chemicals (benzene, dichloromethane, ethylbenzene, toluene and *m*-xylene) (Haddad et al., 2001). This approach is similar to the one proposed by the same group for calculating the biological hazard index for chemical mixtures to be used in biological monitoring of worker exposure (Haddad et al., 1999). The interaction based hazard index for systemic toxicant mixtures was calculated from tissue dose levels in a similar way as the hazard index:

$$HI_I = \sum_{i=1}^{n} \frac{TMi}{TRi} \qquad (24)$$

where TR_i and TM_i are estimates of tissue dose levels derived from PBTK models. TR_i is the tissue dose levels calculated (by PBTK models) based on guideline values of individual compounds in the mixture (in this case they used threshold limit values; but as the background equation just requires the "acceptable level" ADI or RfD may also be used). TM_i is the estimated tissue dose levels of each compound in the mixture during human exposure calculated in mixture PBTK models which take interactions into account.

The same group of scientists suggested a similar approach for mixtures of carcinogenic compounds in that they revised the following equation for calculation of the carcinogenic risk related to mixture exposure (CRM):

$$CRM = \sum_{i=1}^{n} (E \times q^*_i) \qquad (25)$$

where q^*_i is the carcinogenic potential of compound i expressed as risk per unit dose and E is the exposure.

Rewriting this equation gives

$$CRM = \sum_{i=1}^{n} (TM_i \times q^*_{tt}\ i) \qquad (26)$$

where $q^*_{tt}i$ is the tissue dose based unit risk for each carcinogenic compound in the mixture and this level is estimated in PBTK models for the individual compounds in the mixture. TM_i is defined above. By using TM_i in the calculation of CRM interactions are taken into account as it describes the target tissue dose of the compounds in the mixture.

17.4 INTERACTION THRESHOLDS

El-Masri and co-workers have studied the different modes of inhibition mechanism between trichloroethylene (TCE) and 1,1-dichloroethylene (DCE) at different doses administered to

rats and examined the presence of an interaction threshold between the two compounds in a gas uptake experiment (El-Masri et al., 1996).

A PBTK model was developed to simulate this experiment. At first they examined the different modes of inhibition interactions i.e. whether the interaction between the two compounds could be described by competitive, non-competitive or uncompetitive equations in the PBTK model. They examined the gas uptake in rats exposed to various concentrations of TCE and/or DCE. The simulations of this experiment showed that the competitive inhibition interaction was the best description of the results from the experiment.

In order to predict the range at which the interaction threshold would be found, mathematical descriptions of the percentage of available enzyme sites occupied by one chemical in the absence and presence of the other was inserted in the PBTK model. For a range of concentrations of both TCE and DCE they performed simulation calculating the percentage of enzyme sites occupied by each compound. The results were plotted in curves showing the percentage of enzyme sites occupied by one of the compounds in the absence and presence of the other compound as a function of the concentration of the first compound. The curves for both compounds showed that the two lowest concentrations of the second compound did not deviate from the absence of the second compound. This means that at a concentration range of 100 ppm or less DCE and TCE did not competitively inhibit each other's metabolism. Finally, this interaction threshold was verified experimentally by determining the gas uptake of rats exposed to 2000 ppm of one chemical and the other chemical was set to 100 ppm in one experiment and 50 ppm in another (El-Masri et al., 1996).

This experiment illustrates how interaction threshold can be estimated using a PBTK model. Another example is explained in chapter 18 describing a model for the two organophosphorus pesticides chlorpyrifos and parathion developed by (El-Masri et al., 2004).

18 PBTK/TD MODELS ON PESTICIDES

PBTK models have been developed for decades especially in the area of pharmacology. In the area of toxicology and risk assessment the model development started in the mid 1980ies with work on volatile compounds. PBTK models describing dietary or gavage administration have been more rarely published than models using inhalation exposure. A literature search was performed in 2009 and an alert was set up in The National Center for Biotechnology Information (NCBI). This has up till now resulted in about 40 papers describing PBTK models on single pesticide exposure by dietary or gavage administration in rodents or humans and only two describing mixtures of pesticides.

An overview of these PBTK/TD models build for single pesticides in rodents or humans are shown in Appendix I as well as a table on the two PBTK/TD models built for mixtures of pesticides. In the following the two models on pesticide mixtures will be described.

A PBTK model for the two organophosphorus pesticides chlorpyrifos and parathion and their metabolites chlorpyrifos-oxon and paraoxon, respectively, were developed by El-Masri and co-workers in order to simulate the interaction threshold for the joint toxicity of the two

pesticides in rats (El-Masri et al., 2004). A schematic overview of the model is shown in Figure 17. At first a model for each of the parent compounds was developed in order to estimate the blood concentrations of their metabolites. Second the output from these models i.e. the concentrations of metabolites in blood were linked to a sub-model describing the kinetic of acetylcholinesterase. That is, the model consists of four sub-models for the compounds incl. metabolites and one model describing acetylcholinesterase kinetics. The models for the two parent compounds were linked with their respective metabolites via the liver: the metabolites produced act as a sink for the parent compounds. The overall model describes the interactions between the pesticides at the P450 enzymatic bio-activation site and at the acetylcholinesterase binding sites (El-Masri et al., 2004).

The interaction between chlorpyrifos and parathion was described by equations for competitive inhibition (see equations in Table 5). The authors assumed that the hydrolysis of the metabolites would not undergo interaction mechanisms.

They simulated the plasma acetylcholinesterase activity for oral doses from 0.08 to 0.1 mg/kg and plotted the area under the acetylcholinesterase activity-time curve as a function of the oral dose. They calculated the response addition (algebraic addition of the response from single compound exposures of parathion and chlorpyrifos) and compared this with the model prediction of the effect from the mixture (El-Masri et al., 2004). It is not clear why they calculated response addition for the two similar acting compounds.

El-Masri assumed that the interaction threshold is equal to the dose where the above calculated response addition were equal to the model simulation of the response from the mixture. They concluded that the interaction threshold was at an oral dose of 0.08 mg/kg of each compound. Above this threshold they concluded that antagonism by enzymatic competitive inhibition is the mode of interaction (El-Masri et al., 2004).

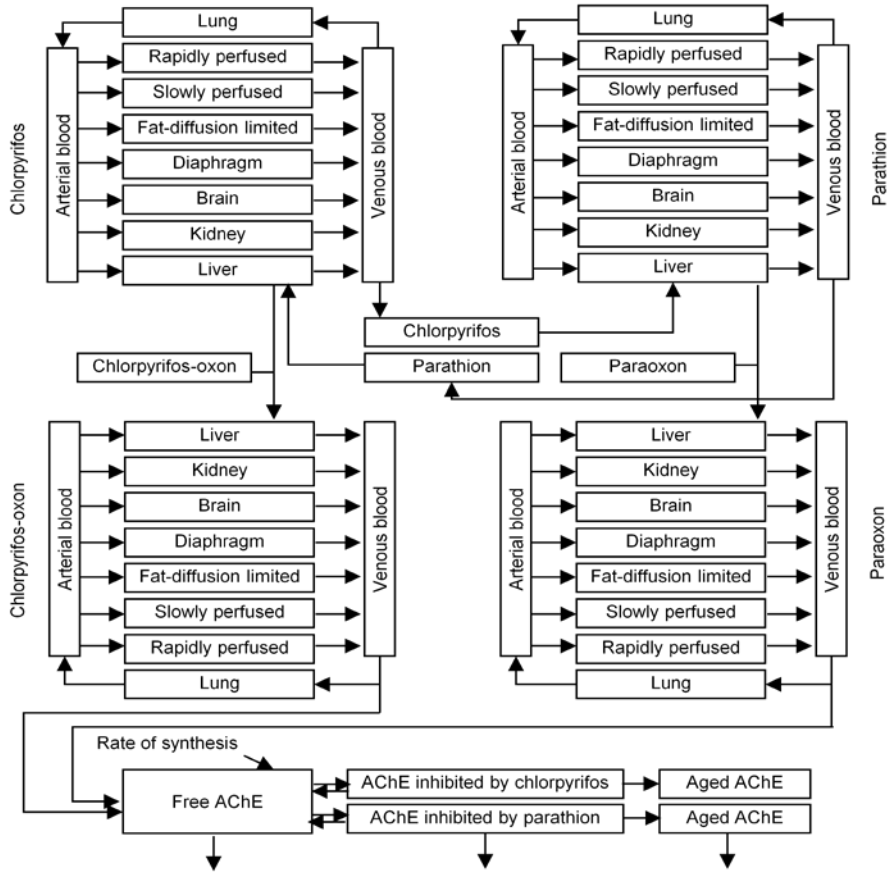

Figure 17: Schematic overview of a PBTK model for the two pesticides chlorpyrifos and parathion and their metabolites chlorpyrifos-oxon and paraoxon, respectively. The model consists of five sub-models, one for each parent compound and metabolite, as well as one sub-model describing the kinetic of acetylcholinesterase linked to the two sub-models for the metabolites. Adapted from (El-Masri et al., 2004).

Timchalk and Poet developed a binary PBPK/PD model for the two organophosphorus pesticides chlorpyrifos and diazinon as well as their oxon metabolites (Timchalk and Poet, 2008). The model describes tissue dosimetry as well as esterase (acetylcholine-, butyrylcholinesterase and carboxylesterase) inhibition in rats after oral (gavage and dietary) and dermal exposure. The basic structure was similar to the one developed by El-Masri and co-workers and described above.

It was anticipated that chlorpyrifos and diazinon due to similar pharmacokinetics, pharmacodynamics and mode of action could interact at a number of metabolic steps ("oral absorption, CYP450 mediated activation/detoxification, PON-1 detoxification, protein binding and blood/tissue cholinesterase (ChE) binding/inhibition"), see Table 6. The model was developed based on previously published models for the individual insecticides (published in (Timchalk et al., 2002b) (Poet et al., 2004)) and the model was evaluated against data from a study on rats performed earlier (published in (Timchalk et al., 2005)).

Table 6. Hypothesised interactions of organophosphates at different metabolic steps as well as the response interactions. Table adopted from (Timchalk, 2010).

Parameters	Importance	Type of chemical interaction	Implications
CYP450 mixed-function oxidase metabolism	Metabolic activation/detoxification of parent compound	Substrate (parent compound) competition for enzyme	Changes in oxon concentrations
Reversible plasma-protein binding	Systemic transport of parent compound	Substrate (parent compound) competition for available protein binding sites	Increased levels of "free" parent chemical available for metabolism
A-esterase metabolism	Important metabolic step responsible for detoxification	Substrate (oxon) competition for enzyme	Changes in oxon concentrations
AChE binding/inhibition	Toxicological response	Substrates (oxon) combine to increase inhibition of AChE	Increased toxicity due to additive response

The metabolic CYP450 interaction of chlorpyrifos and diazinon to oxon and chlorpyrifos to 3,5,6-trichloro-2-pyridinol were described as non-competitive whereas the metabolism of diazinon to 2-isopropyl-methyl-6-hydroxypyrimidine was described as competitive based on *in vitro* experiments (see equations in Table 5). The B-esterase metabolism was described as dose additive while no interactions were assumed for the hydrolysis of oxon (PON-1).

Experimentally they found that at high doses there might have been a competition between chlorpyrifos and diazinon for CYP450 metabolism. However, at environmental relevant exposures the authors conclude that interactions will most likely be negligible and the pharmacokinetics at that level are expected to be linear and the inhibition of cholinesterase dose-additive.

In the rat study chlorpyrifos was found to be more potent than diazinon *in vivo*. This corresponds with the findings *in vitro* where chlorpyrifos was found to be more readily metabolised to its oxon metabolite than diazinon and thereby to a larger extent metabolised to the actual substrate for A- and B-esterase.

The authors conclude that the model simulations were consistent with the experimental data. They showed a dose- and time-dependent inhibition of the cholinesterase activity in brain, red blood cells (RBC) and plasma. The extent of inhibition followed plasma > RBC > brain for both chlorpyrifos and diazinon.

19 ORGANOPHOSPHATES: MECHANISM OF ACTION AND BIOTRANSFORMATION

Organophosphates are widely used as insecticides in the food production and residues are often found in food. These compounds are esters of phosphoric acid and their primary toxicological effect is associated with the inhibition of acetylcholinesterase activity in both central and peripheral nerve tissues.

Earlier work on combined action of pesticides in food revealed that organophosphates are well-studied (Reffstrup, 2002). As mentioned in chapter 9, U.S. EPA and Food Standard Agency in United Kingdom have performed cumulative risk assessment of this group of pesticides. The amount of data available for this group of pesticides makes it suitable as a

starting point in PBTK/TD modelling. Therefore, one of the organophosphates, chlorpyrifos, was chosen for PBTK/TD modelling in the present thesis.

The mechanism behind the inhibition of acetylcholinesterase and other cholinestrases by organophosphates and the similar acting carbamates is described in the following as is the biotransformation of organophosphates.

19.1 FUNCTION AND INHIBITION OF CHOLINESTERASE

In the body afferent neurons carry signals from the peripheral nerve endings into the central nervous system (CNS) whereas efferent neurons carry signals from CNS to muscles or gland cells. Interneurons connect the afferent and efferent neurons in CNS, see Figure 18. Interneurons account for 99 percent of all neurons. The efferent division of the peripheral nervous system is subdivided into the somatic and autonomic nervous system. Neurons of the somatic nervous system stimulate skeletal muscle whereas the autonomic neurons innervate smooth and cardiac muscle, glands and the neurons that form the enteric nervous system.

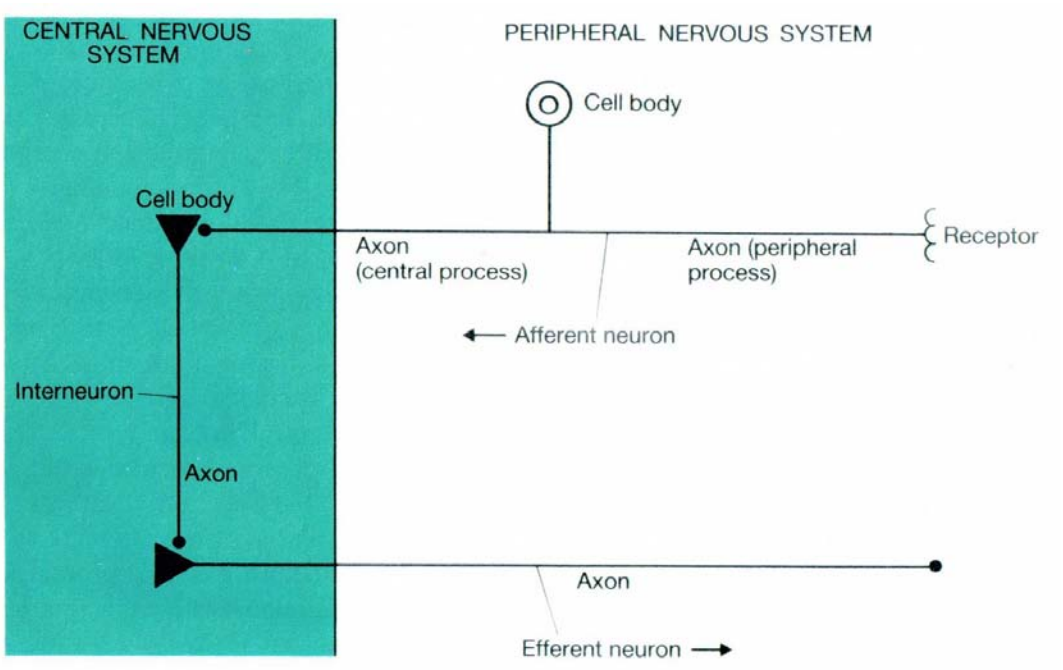

Figure 18: Schematic representation of the location of afferent neurons, efferent neurons as well as interneurons. The direction of transmission of neural activity is indicated with arrows. The cell body and the long peripheral process of the axon are outside the CNS whereas the relatively short central process enters the brain or spinal cord. The dendrites are not shown in the figure. Figure from (Vander et al., 1990).

The autonomic nervous system is further divided in the parasympathetic and sympathetic division. The main neurotransmitter responsible for the stimulation of the parasympathetic system is acetylcholine (Vander et al., 1990).

Figure 19 shows an overview of the peripheral nervous system.

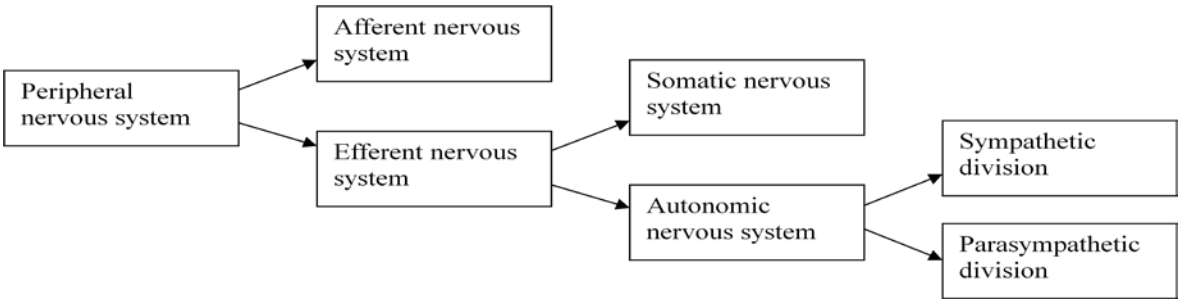

Figure 19: Overview of the peripheral nervous system (Vander et al., 1990).

19.1.1 ACETYLCHOLINE AND ACETYLCHOLINESTERASE

Acetylcholine is the major neurotransmitter in the efferent division of the peripheral / parasympathetic nervous system. It is synthesised from choline and acetyl coenzyme A in the cytoplasm of synaptic terminals and then stored in synaptic vesicles. Fibres that release acetylcholine are called cholinergic fibres.

Acetylcholine is released from the presynaptic axon terminal into the synaptic cleft followed by a binding to the receptors on the postsynaptic membrane, see Figure 20. Both the esteratic and the anionic site of acetylcholine will bind to acetylcholinesterase as shown in Figure 21.

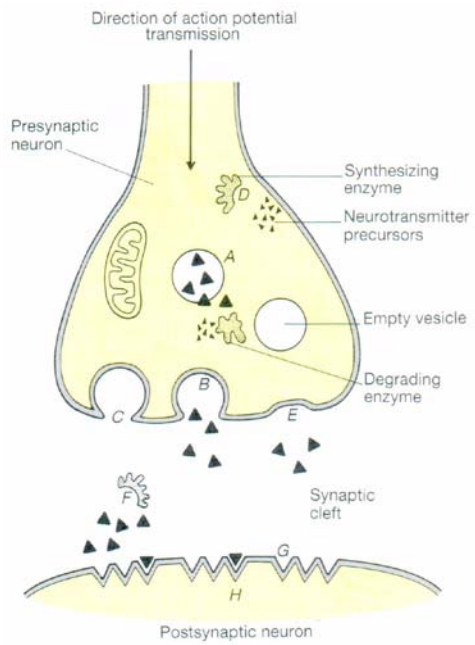

Figure 20: Action of chemicals at synapses. "(A) Increase leakage of neurotransmitter from vesicle to cytoplasm, exposing it to enzyme breakdown, (B) increase transmitter release, (C) block transmitter release, (D) inhibit transmitter synthesis, (E) block transmitter reuptake, (F) block enzymes that metabolize transmitter, (G) bind to receptor to block (antagonist) or mimic (agonist) transmitter action, (H) inhibit or facilitate second-messenger activity" (Vander et al., 1990).

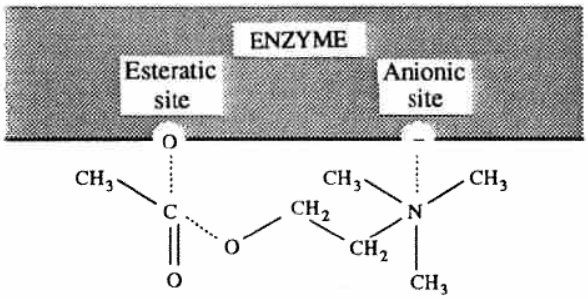

Figure 21. Reaction of acetylcholine with acetylcholinesterase. Figure from (Hayes and Laws, 1991).

The concentration of acetylcholine at the postsynaptic membrane is reduced by diffusion away from the receptors and thereby the receptor activation will stop. When acetylcholine is released from the receptors it will be decomposed to choline by acetylcholinesterase which is located on the pre- and postsynaptic membranes and this will also decrease the concentration of acetylcholine (Vander et al., 1990). The decomposition of acetylcholine by acetylcholinesterase happens almost instantly and therefore under normal conditions there is no accumulation of the ester. The rapid destruction of acetylcholine accounts for the brevity and unity of each normal propagated impulse (Hayes and Laws, 1991). Choline is actively transported back into the axon terminals where it is re-used to synthesize acetylcholine.

In addition to its presence in synapses acetylcholinesterase is also present in the outer membrane of RBC and to a lesser extent in plasma. However, its physiological functions in blood are unknown (Lotti, 2010).

19.1.2 INHIBITION OF ACETHYLCHOLINESTRASE

Organophosphates in the body can be hydrolysed by A-esterases and B-esterases. A-esterases hydrolyse these esters to products that are inactive as inhibitors for cholinesterase and in most cases these products are of low toxicity. Contrary to this, hydrolysis of organophosphates by B-esterases, including cholinesterases, causes an inhibition of cholinesterase, as seen in the following.

Some of the organophosphates are thiophosphates which are desulphurated by cytochrome P450 enzymes (CYP450, which is one of the most important groups of xenobiotic metabolising enzymes) in the body resulting in oxons ($(RO)_2P(O)OX$) which are the actual substrate for A- and B-esterases.

Organophosphate oxons, $(RO)_2P(O)OX$, attack the active site in the acetylcholinesterase protein, EOH, namely a serine hydroxyl group. This results in a temporary intermediate complex that partially hydrolyzes resulting in the loss of the X-substituent group. The reaction is progressive and the amount of reaction (i.e. inhibition) increases over time. It involves two molecules, namely the enzyme and the inhibitor; therefore the process is called bimolecular (Hayes and Laws, 1991; O'Brien, 1967).

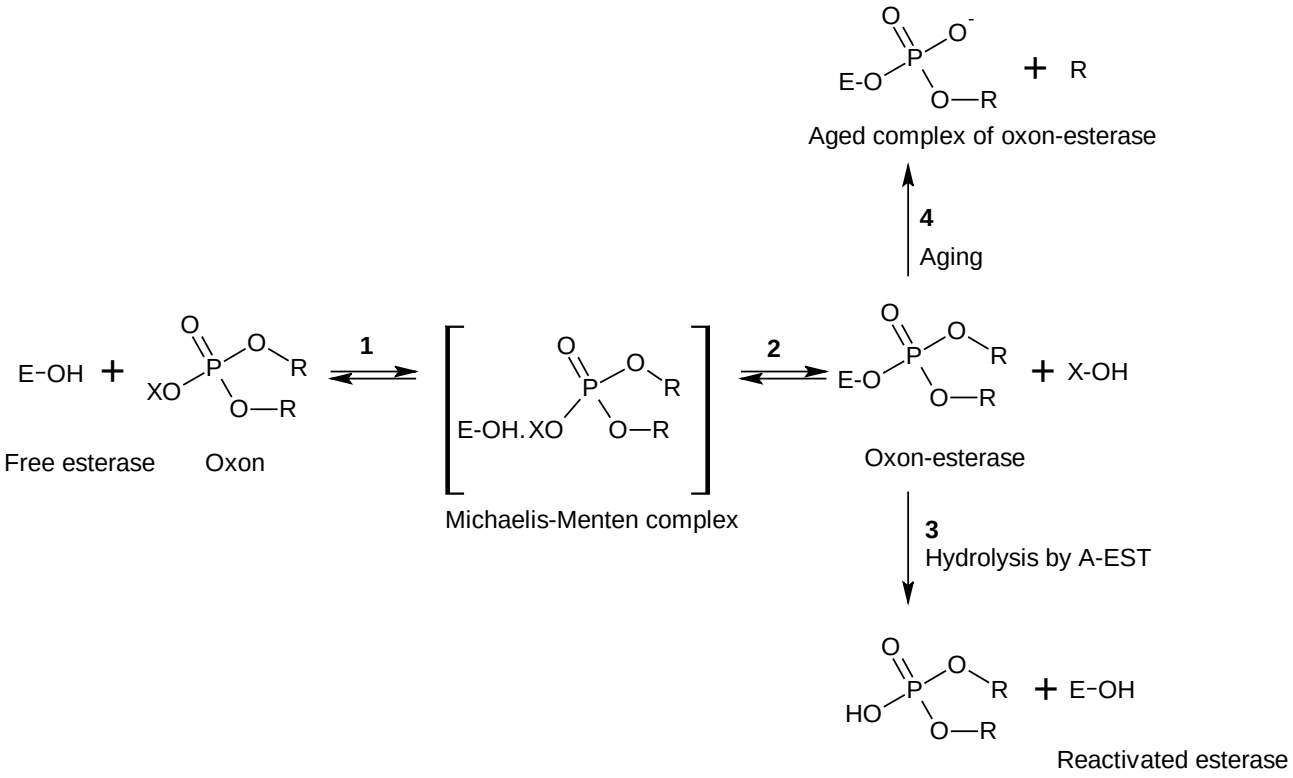

Figure 22. Interaction of an organophosphate with an esterase (e.g. acetylcholinesterase). In step 1 an enzyme-inhibitor complex is formed followed by the formation of oxon-esterase, step 2. Step 3 is the hydrolysis of the phosphorylated ester, i.e. a reactivation process (releases esterase) and step 4 is the aging process. Figure modified from (Lotti, 2010).

The reaction of paraoxon with acetylcholinesterase is shown in Figure 23 which is another way of showing how an organophosphate is bound to esterase i.e. the first step in Figure 22. Paraoxon and most other organophosphorus pesticides only react with acetylcholinesterase at its esteratic site and not its anionic site because of lack of a positive charge in the acidic group, see the reaction between acetylcholine and acetylcholinesterase in Figure 21 for comparison. The phosphorus esters are bound more strongly to the esteratic site of acetylcholinesterase than the carbonyl group in acetylcholine is to the same esteratic site. Therefore, breakage of the bound between a phosphorus ester and enzyme (step 3) takes much longer time (hr) compared to breakage of the acetylcholine-enzyme bound (μseconds) (Hayes and Laws, 1991; Klaassen, 1996).

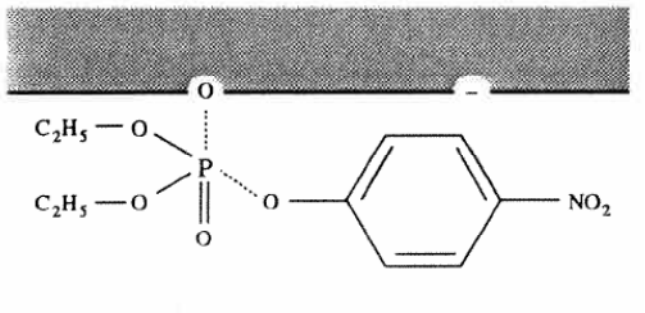

Figure 23. Reaction of paraoxon with acetylcholinesterase. Figure from (Hayes and Laws, 1991)

The phosphorylated enzyme is inhibited because its active site is occupied and therefore incapable of carrying out its normal function. When the enzyme is inhibited it causes accumulation of acetylcholine. The ion channels in the presynaptic terminal remain open and the depolarization is maintained causing that the membrane cannot generate an action potential. For many organophosphates the breakage between the ester and the esterase is very slow and the toxicity will persist until acetylcholinesterase is re-synthesised in sufficient quantities to efficiently decompose the excess acetylcholine (Hayes and Laws, 1991; Klaassen, 1996).

The reaction in step 2 in Figure 22 is the hydrolysis of the phosphorylated ester by A-esterase (e.g. paraoxonase, PON-1) resulting in reactivation of the esterase and release of a dialkylester.

Reaction 4 in Figure 22 is a process where the stability of the phosphorylated enzyme is enhanced by the loss of one of the alkyl groups (R-group). This process is called the aging-process. Aging is defined as the development of an inability to be reactivated (O'Brien, 1967). The formation of aged compounds decreases the possibility of regeneration. The portion of oxon-esterase that can be regenerated decreases exponentially (a first order reaction) with time at a given temperature (Klaassen, 1996). The rate of the aging-process depends on the enzyme involved and on the attached phosphoryl residue. For example in humans the rate of the aging-process for a particular dialkoxy phosphate is 5-10 times faster for plasma cholinesterase than for RBC cholinesterase. The aging process for both enzymes is most rapidly with isopropoxy phosphate. The rates of aging of acetylcholinesterase in mammals will increase in the order: diethyl < diisopropyl ≥ dimethyl < isopropyl-methyl (Hayes and Laws, 1991).

A good correlation has been seen between signs of poisoning and the degree of inhibition of acetylcholinesterase in RBC. However, since acute poisoning requires prompt treatment, a measurement of inhibition of acetylcholinesterase in RBC is only used as a confirmation of a diagnosis of acute organophosphorus poisoning (Lotti, 2010).

19.1.3 SYNTHESIS OF NEW ACETYLCHOLINESTERASE

If acetylcholinesterase is inhibited irreversible, synthesis of new acetylcholinesterase is the only way to re-establish the activity. New acetylcholinesterase in the blood is produced in erythropoietic cells of the bone marrow and the plasma enzyme is synthesized in the liver and brain acetylcholinesterase is synthesized within the nerve cell body (Hayes and Laws, 1991).

19.1.4 INHIBITION OF ACETYLCHOLINESTERASE BY CARBAMATES

Another group of insecticides that inhibit acetylcholinesterases are carbamates. They inhibit acetylcholinesterase in a similar manner as organophosphates:

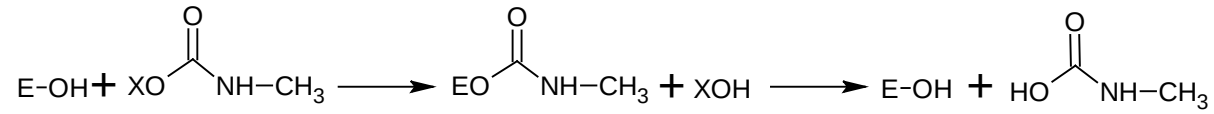

The main difference between the processes for organophosphates and carbamates is the rate at which the reactivation takes place (determined by a regeneration rate constant). For organophosphates the rate is extremely low which is why the process is considered as irreversible (even though it is not totally irreversible). However, for carbamates the reactivation is sufficiently rapid to be considered as reversible and the turnover rates are low (Klaassen, 1996; Krieger, 2010).

19.1.5 EFFECTS OF ACETYLCHOLINESTERASE INHIBITION

Respiratory failure is the most important clinical sign of severe poisoning by organophosphates. Symptoms of a mild poisoning are variable and no clear-cut signs have been recognised. The symptoms and signs depend on the chemical, the dose, and the time from exposure to observation (Lotti, 2010).

According to Hayes and Laws a minimal excess of acetylcholine compared to the normal level causes "(a) excessive activity of the parasympathetic system (miosis, sweating, profuse secretions in the upper respiratory tract, abdominal cramps and discomfort in the chest from overactivity of smooth muscle, and nausea, vomiting, and diarrhea); (b) central nervous system effects (headache, giddiness, and nervousness); and (c) overreactivity of the voluntary muscles (fasciculations)." (Hayes and Laws, 1991) A higher accumulation of acetylcholine increases the parasympathetic and central nervous system symptoms but it causes noticeable weakness of the muscles (Hayes and Laws, 1991). This is due to the previously described depolarization at the presynaptic membrane causing that the membrane cannot generate an action potential – and this further results in a deficient ability of the muscle to contract in response to nerve stimulation resulting in skeletal-muscle paralysis and death from asphyxiation (deficient supply of oxygen to the body) (Vander et al., 1990).

Respiratory failure and consequent death after intake of organophosphorus pesticides is typically caused by excessive secretion of mucus in the respiratory tract, bronchoconstriction,

weakness of the muscles of respiration or failure of the respiratory center (Hayes and Laws, 1991).

19.1.6 BUTYRYLCHOLINESTRASE AND CARBOXYLESTERASE

Butyrylcholinesterase and carboxylesterase can also bind organophosphates irreversibly (1:1 ratio) and these esterases are thereby being inactivated. The binding is without an adverse effect and therefore is considered as a detoxification pathway since it reduces the amount of organophosphate or oxon available to inhibit acetylcholinesterase (Timchalk, 2010). According to Chambers and co-workers this process is not considered as a metabolising step because of the irreversibility, leading to a stoichiometric destruction of one organophosphate (or oxon) molecule per serine esterase molecule (i.e. the active site in the acetylcholinesterase protein, EOH) and thereby inhibiting the esterase for a long time. However, these processes are resulting in the same product produced in dearylation and hydrolysis reactions (Chambers et al., 2010).

Butyrylcholinesterase has different substrate specificity than acetylcholinesterase as it hydrolyses butyrylcholine. Measurement of the inhibition of plasma butyrylcholinesterase is a valuable indication of exposure to organophosphates but since the physiological function of butyrylcholinesterase is unknown such an inhibition does not necessarily indicate that the exposure is poisonous (Lotti, 2010).

In human serum butyrylcholinesterase is the main cholinesterase (>99 %) and therefore it is the primary defence against chlorpyrifos (CPF) (Testai et al., 2010).

19.2 BIOTRANSFORMATION OF ORGANOPHOSPHORUS PESTICIDES

Organophosphorus pesticides in the body can be hydrolysed by A-esterases to products that are inactive as inhibitors of cholinesterase and in most cases the products are of low toxicity. The organophosphorus pesticides can also be split by transferases (glutathione S-alkyltransferase and glutathione S-aryltransferase) producing gluthathione conjugates, see Figure 24.

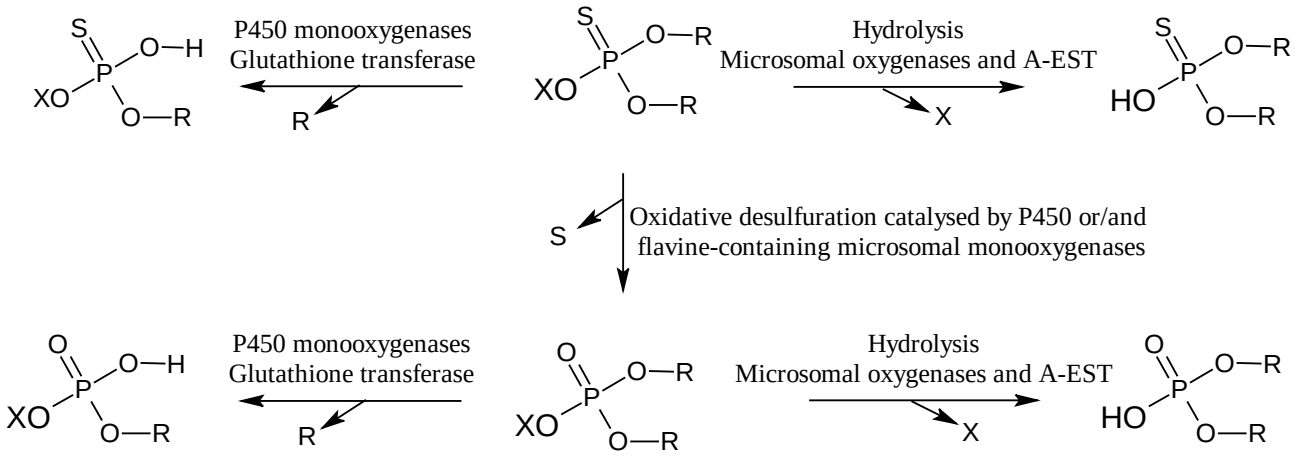

Figure 24: General scheme of biotransformation of dialkylphosphorothionate pesticides. Figure modified from (Spencer et al., 2000).

The desulphuration of the phosphorthionate to an oxon can be mediated by either CYP450 enzymes or by flavin monooxygenases (FMOs, which are capable of oxidizing N, P or S occurring in xenobiotics) (Chambers et al., 2010).

The hydrolysis reactions are catalysed by A-esterase (phosphotriesterases) (Chambers et al., 2010).

The organophosphate malathion has a lower toxicity in mammals than other organophosphate because carboxylesterases perform an important catalytic hydrolysis of the carboxylic acid esters in malathion resulting in a detoxification. The hydrolysis to acid-groups occur more readily than the CYP-mediated desulphuration, leading to an effective detoxification (Chambers et al., 2010).

Phase 2 (conjugation) reactions frequently take place and will make the organophosphates more water soluble allowing the metabolites to be readily excreted. Hydrophilic conjugates like sulphate and glucuronide conjugates catalysed by sulphotranferases and glucuronosyl transferases can occur. These metabolites are not inhibitors of cholinesterase and in that sense this pathway leads to detoxification (Chambers et al., 2010).

The parent organophosphate and the oxon are well distributed in the body and due to extensive metabolism they are rarely excreted in the urine (Timchalk, 2010).

20 CHLORPYRIFOS – BIOTRANSFORMATION AND INHIBITION OF CHOLINESTERASE

Chlorpyrifos does not directly inhibit acetylcholinesterase. First it must be metabolised to the corresponding oxygen analogue (an oxon). In the body chlorpyrifos will be desulphurated by CYP450 primarily in the liver resulting in chlorpyrifos-oxon which is the actual substrate for A- and B-esterase. Extrahepatic metabolism has also been reported in other tissues, including brain (Timchalk, 2010). For example chlorpyrifos is mainly metabolized in the liver, but metabolism in brain and intestine has also been reported (Testai et al., 2010).

Detoxification of chlorpyrifos can happen in different ways:

- dearylation of chlorpyrifos to 3,5,6-trichloro-2-pyridinol (TCP) and diethylthiophosphate mediated by CYP450 (detoxification pathway D1 in Figure 25)
- hydrolysis of chlorpyrifos-oxon to TCP and diethylphosphate mediated by A-esterases (paraoxonases, PON-1) (detoxification pathway D2 in Figure 25)
- hydrolysis of chlorpyrifos-oxon by the B-esterases butyrylcholinesterase and carboxylesterase – this binding detoxifies the oxon, however, the B-esterase become stoichiometrically inhibited (detoxification pathway D3 in Figure 25).
- conjugation of chlorpyrifos-oxon by glutathione-S-transferases with reduced glutathione (GSH) (detoxification pathway D4 in Figure 25). This pathway is not included in the PBTK model
- conjugation of TCP by glucuronyl-transferases and sulphotransferases resulting in the corresponding glucuronide and sulphate conjugates (detoxification pathway D5 in Figure 25) .

(Testai et al., 2010; Timchalk et al., 2002b; Timchalk et al., 2007b; Timchalk, 2010)

Pathway D1 and D2 in Figure 25 are the main detoxification pathways for chlorpyrifos. TCP, but also diethylthiophosphate, diethylphosphate, GSH conjugates, sulphates and glucuronides are excreted in the urine. Chlorpyrifos is not found in the urine. In the PBTK model TCP is functioning as a marker of detoxification.

The ratio of activation to detoxification can differ by species, gender and age (Timchalk, 2010), however this is not taken into account in the present model.

The half-life for elimination of chlorpyrifos from various organs is between 10 and 16 hr, however, elimination from fat is estimated to be 62 hr (Testai et al., 2010).

The hydrolysis of chlorpyrifos-oxon by the B-esterases butyrylcholinesterase and carboxylesterase shown as detoxification pathway D3 in Figure 25 is resulting in the same metabolites (TCP and diethylphosphate) as pathway D2 (Chambers et al., 2010). Therefore, sometimes the reaction scheme for the model are simplified by using only one arrow to describe these two pathways, even though they are handled differently in the model.

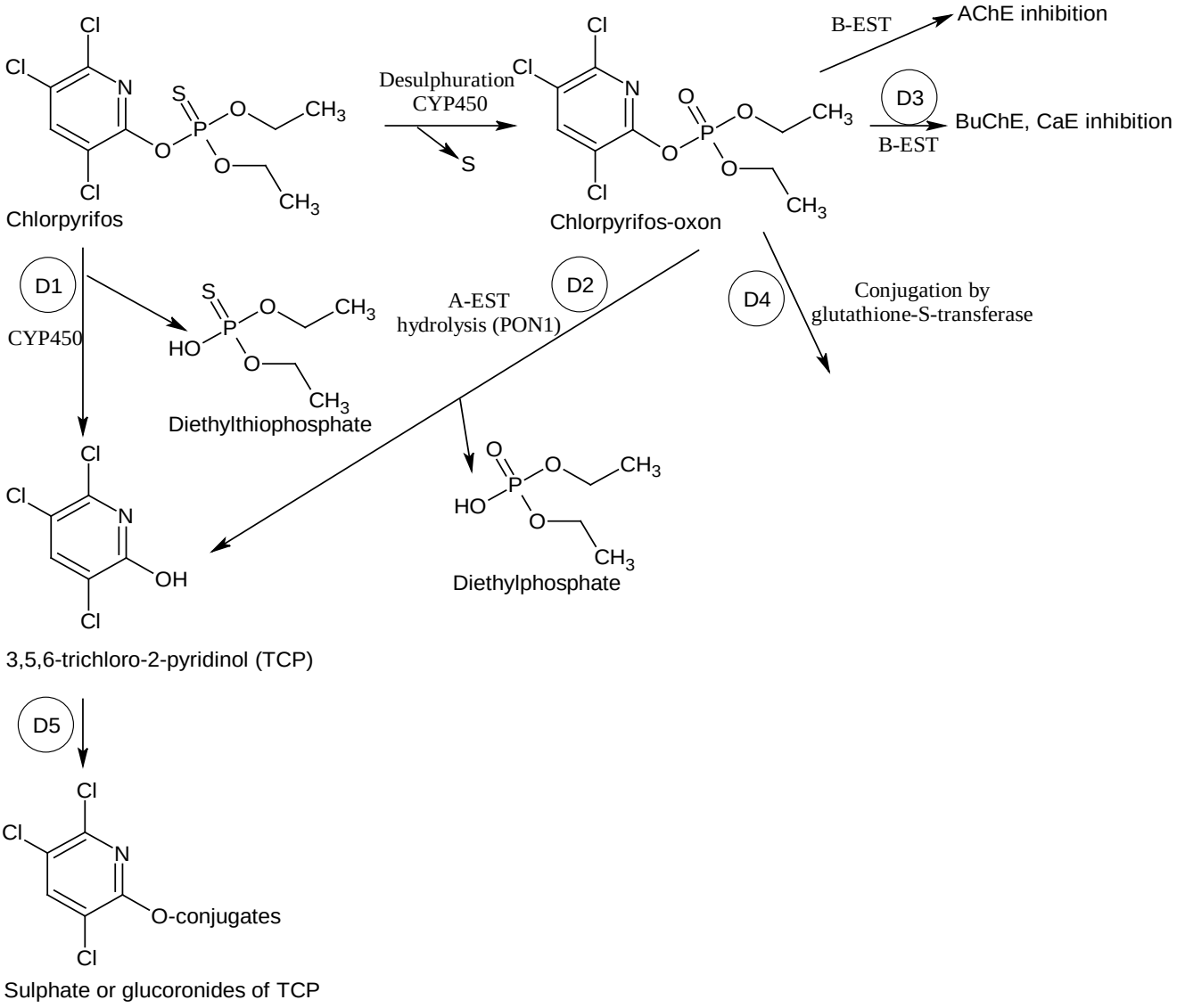

Figure 25: Metabolic scheme for chlorpyrifos. D1-D5 denotes detoxification pathways as explained in the text. AChE: acetylcholinesterase, BuChE: butyrylcholinesterase, CaE: carboxylesterase.

Interaction of chlorpyrifos-oxon with acetylcholinesterase is shown in Figure 26. This bimolecular process is described by a bimolecular inhibition rate constant, Ki, and the reactivation of free esterase is described by the rate constant Kr, and Ka is the aging rate constant. The bimolecular inhibition rate constant is an indicator of inhibitory potency as it describes the affinity of the oxon for B-esterase as well as the phosphorylation of the complex between cholinesterase and organophosphate, i.e. step 1 and 2 in Figure 22.

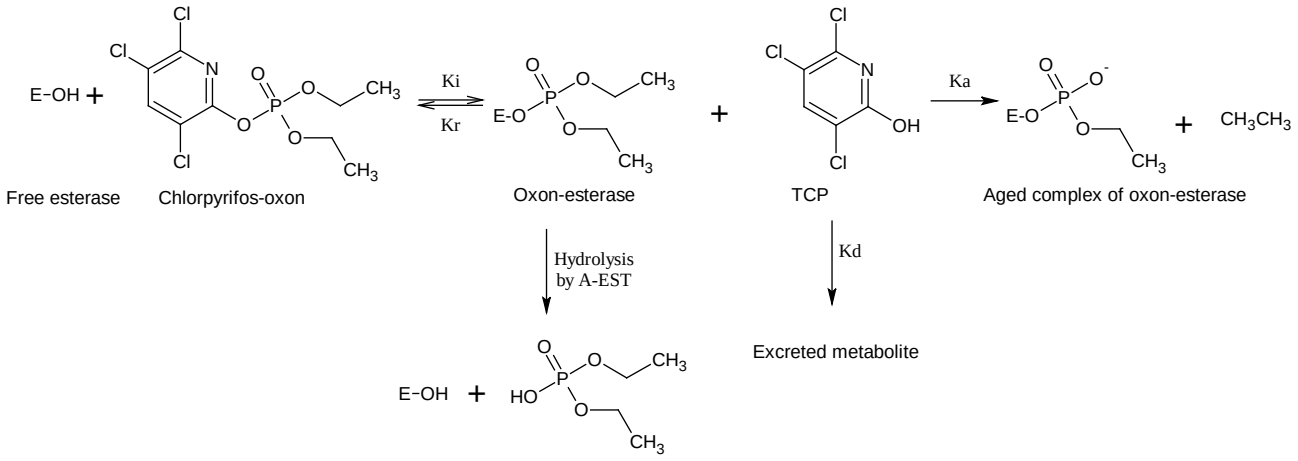

Figure 26: Inhibition of cholinesterase by chlorpyrifos-oxon. For simplicity the formation of the Michaelis-Menten complex (step 1 in Figure 22) is omitted.

21 DESCRIPTION OF THE PBTK/TD MODEL FOR CHLORPYRIFOS IN RATS

The PBTK/TD model for chlorpyrifos describes the disposition of the parent compound and the two metabolites chlorpyrifos-oxon and TCP in rats and humans as well as the inhibition of acetylcholinesterase by chlorpyrifos-oxon. The present model is build based on the model made by Timchalk and co-workers published in (Timchalk et al., 2002b). The original model contained three routes of administration namely dietary, gavage, and dermal. In the present model dermal exposure is omitted (and so are the skin compartment) because the present project only aims at developing models for use in risk assessment of chemical substances in food i.e. only oral intake is relevant. This is the primary modification in the structure compared to the model by Timchalk and co-workers, however, the major changes are to be found in the parameter values which will be explained in section 21.2 and discussed in chapter 24.

The metabolic scheme for chlorpyrifos is shown in Figure 27 and the structure of the PBTK/TD model is shown in Figure 28.

The present model constists of eight compartments: liver, brain, diaphragm, fat, rapid perfused tissues, slowly perfused tissues and blood (arterial and venous). Experiments have shown that there can be significant differences between arterial and venous blood concentrations of diisopropylfluorophosphate (DFP) (Gearhart et al., 1994). It is believed that the same accounts for chlorpyrifos therefore separate compartments for arterial and venous blood were introduced in the model by Timchalk and co-workers.

The model on diisopropylfluorophosphate developed by Gearhart and co-workers included a kidney-compartment (Gearhart et al., 1990). It was not explained why this compartment was not included in the model by Timchalk et al. (2002b). Instead of a kidney-compartment a compartment describing the appearance of metabolite TCP and its urinary excretion was included. Lu and co-workers developed a child-specific PBTK model based on the model in

(Timchalk et al., 2002b) extending the TCP compartment describing the urinary excretion with a physiologic description in order to be able to incorporate known differences between children and adults (Lu et al., 2010). However, in the present model the excretion will be described similar to the work done by Timchalk et al. (2002b).

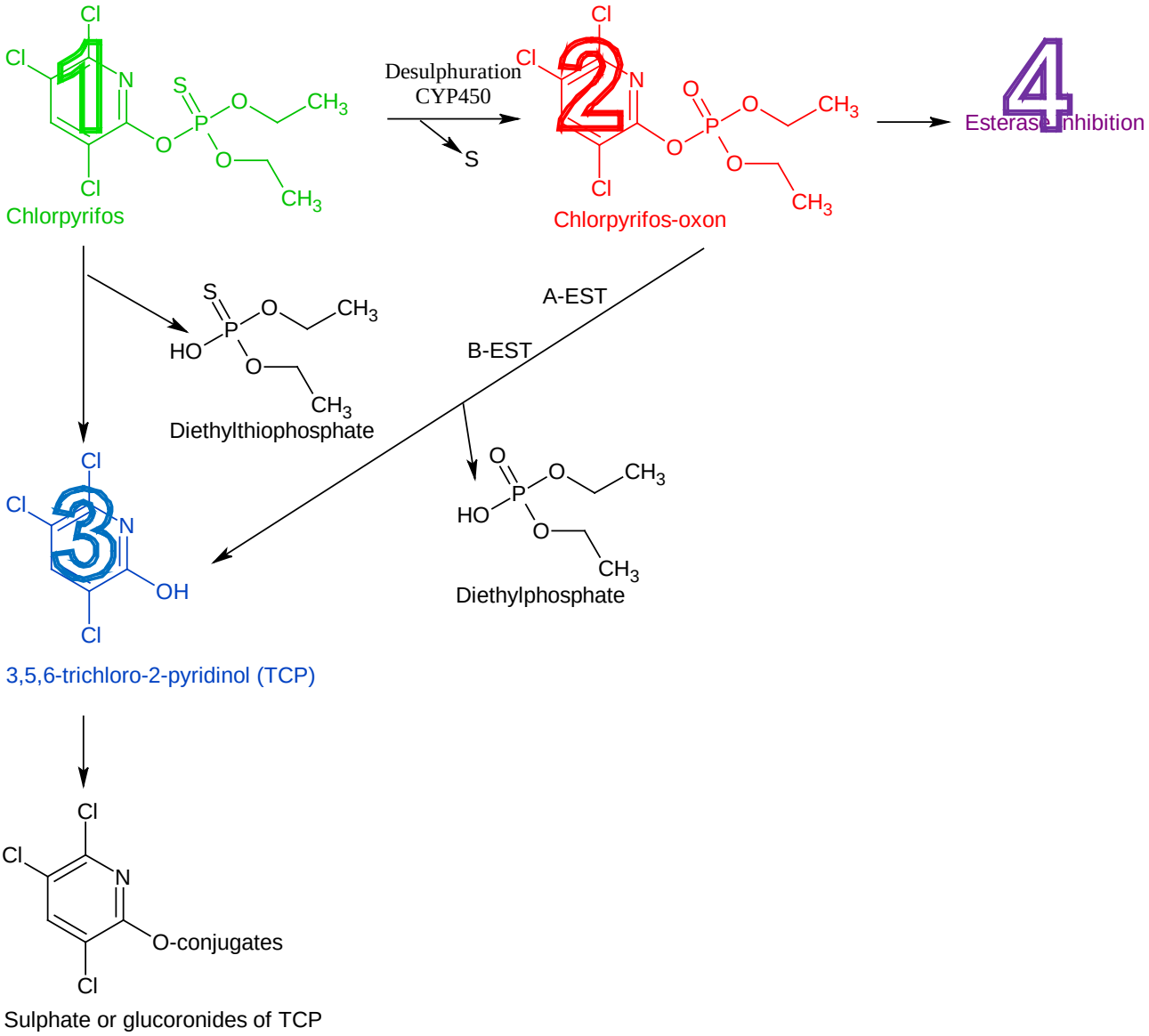

Figure 27: Metabolism of chlorpyrifos in rats and humans. The numbers and colours refer to Figure 28.

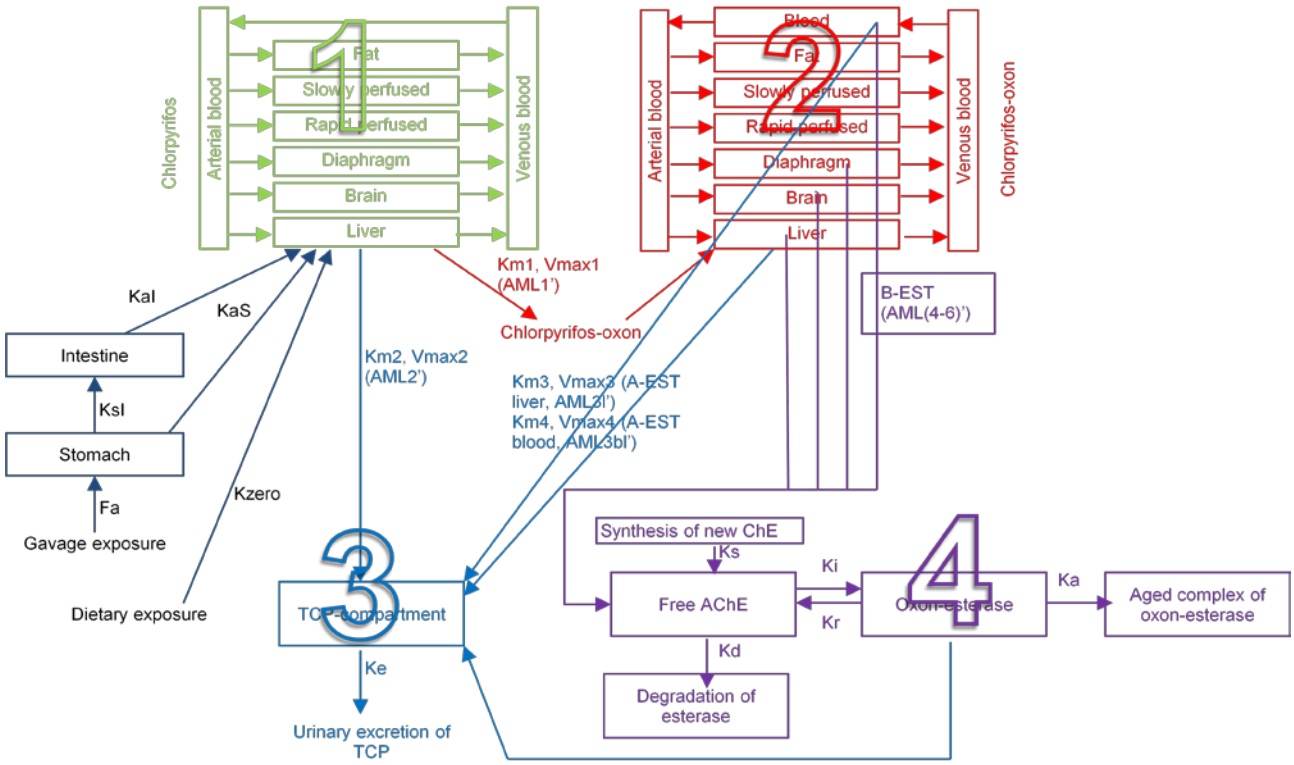

Figure 28: PBTK/TD model to describe the disposition of chlorpyrifos, chlorpyrifos-oxon and TCP in rats and humans as well as the inhibition of acetylcholinesterase. The colours and number 1-3 refer to the metabolism of chlorpyrifos as shown in Figure 27 and number 4 refers to inhibition of acetylcholinesterase as described in Figure 26.

21.1 MODEL CODE

The overall equations in the model will be outlined below. The model equations are described in the following order: absorption of chlorpyrifos after dietary and gavage exposure, distribution of chlorpyrifos and chlorpyrifos-oxon in the compartments, metabolism of chlorpyrifos to chlorpyrifos-oxon by CYP450, metabolism of chlorpyrifos-oxon to TCP by A-esterase (PON-1) as well as inhibition of B-esterase s by chlorpyrifos-oxon which in the case of acetylcholinesterase leads to toxicity and in the case of butyrylcholinesterase and carboxylesterase leads to detoxification.

As mentioned before the present model is a re-building and modification of the model presented in (Timchalk et al., 2002b), and the model code was made by inspiration from (Timchalk et al., 2007b). The latter paper presented an age-dependent PBTK/TD model on chlorpyrifos including the model code developed in the SimuSolv and adapted to asclXtreme for sensitivity analysis.

The model code presented in this thesis is written in Berkeley Madonna and a list of abbreviations used in the model can be seen in Appendix II. The abbreviations used in the following are based on the two publications by Timchalk and co-workers (2002b and 2007b)

and they may sometimes differ from those used in the theoretical chapters 13-17. The parameters used in the equations will be described in section 21.2.

Concerning the mathematical notation in the text a differential equation du/dt will be written as du'.

21.1.1 INPUT TO THE MODEL

As mentioned before (and seen in Figure 28) the present model contains two oral routes of administration namely dietary and by gavage. Under specific exposure situations where contribution from both dietary and gavage exposure appears the total exposure or input to the liver will be the sum of each of the routes (see equation 7)

Dietary exposure

The dietary exposure, Dietexp, is expressed as a constant zero-order rate over a 12-hr interval to describe 12 hr eating followed by 12 hr rest. In Berkeley Madonna a function named MOD was used for that. The MOD-function makes the program repeat the function periodically meaning that the input will last for 12 hr and then the input will be 0 for the next 12 hr:

$$\text{Dietexp} = \text{IF MOD(TIME, 24)} <= 12 \text{ THEN kzero ELSE 0} \quad (\mu\text{mol/hr}) \quad (1)$$

where kzero is the zero-order uptake rate (µmol/hr) during 12 hr consumption in a 24 hr interval and is calculated from the dietary administration of chlorpyrifos, Diet (µmol/day) and the fractional absorption, Fa:

$$\text{kzero} = \text{Diet} * \text{Fa} / (12\ \text{hr/day}) \quad (\mu\text{mol/hr}) \quad (2)$$

The fractional absorption expresses how much of the compound will be absorbed after intake. The dietary administration of chlorpyrifos is calculated from the oral administration (Oral_adm, mg/kg bw/day) taking body weight (BW, kg) and molecular weight of chlorpyrifos (Mc, mg/µmol) into account:

$$\text{Diet} = \text{Oral\_adm} * \text{BW} / \text{Mc} \quad (\mu\text{mol/day}) \quad (3)$$

Gavage exposure

The gavage administration of the organophosphate in the model is described as a two-compartment uptake model, see Figure 28. The two compartments are stomach (Stom) and intestine (Intes) and uptake and transfer between the two are described by first-order rate equations. At time zero the total gavage dose of chlorpyrifos is delivered in the stomach. Disappearance of chlorpyrifos from the stomach will depend on the absorption rate constant for the stomach (KaS, hr^{-1}) (i.e. from the stomach to the liver) as well as the rate constant for transfer between the stomach and the intestine (KsI, hr^{-1}). In other words the rate of change in the amount of chlorpyrifos in stomach (Stom') is the rate of change in the amount leaving the stomach to the liver and to the intestine:

$$\text{Stom}' = -\text{KaS} * \text{Stom} - \text{KsI} * \text{Stom} \quad (\mu\text{mol/hr}) \quad (4)$$

When solving this differential equation the initial value of the amount in the stomach (Stom) is the gavage exposure (converted to µmol).

The rate of change in the amount of chlorpyrifos in the intestine (Intes') is the amount of compound entering the intestine from the stomach minus the amount absorbed from the intestine into the liver:

$$Intes' = KsI*Stom - KaI*Intes \quad (\mu mol/hr) \quad (5)$$

where KaI (hr^{-1}) is the rate constant for absorption of chlorpyrifos from the intestine to the liver and Intes is the amount of chlorpyrifos in the intestine.

The rate of oral absorption (Oral_abs', µmol/hr) (input to the liver-compartment) from gavage exposure is equal to the sum of absorption rates from stomach and intestine:

$$Oral\_abs'=KaS*Stom+KaI*Intes \quad (\mu mol/hr) \quad (6)$$

Total exposure

The rate of total input to liver from diet and gavage (Input_l', µmol/hr) is calculated from:

$$Input\_l'=Oral\_abs'+Dietexp \quad (\mu mol/hr) \quad (7)$$

Normally only one of the two methods of oral administration is used. In this case the input from the other will be zero.

Repeated bolus exposure

In some experiments chlorpyrifos is given to the test species for example once a day for a certain time period. In order to simulate this repeated exposure scenario (Repeat_exp, µmol/hr) the following equation was used:

$$Repeat\_exp=PULSE(dose,0,R)*SQUAREPULSE(0,repeated) \quad (\mu mol/hr) \quad (8)$$

PULSE(dose,0,R) is a pulse-function in Berkeley Madonna describing a pulse with the volume of size "dose" (see equation (9)) giving the first pulse at time 0 and repeated with the dosing interval R (e.g. 24 hr in case of a daily dosage).

The second part of equation (8) is another pulse-function called the square pulse. The height of this pulse is 1 and in equation (8) it is starting at time 0 and lasting for duration "repeated" (in hr).

"dose" is the repeated dose of chlorpyrifos calculated from the exposure (dose_in, mg/kg bw/day) similarly to equations (2) and (3):

$$dose=(dose\_in)*BW*Fa/Mc \quad (\mu mol/day) \quad (9)$$

In this scenario equation (7) for rate of total input to liver (Input_l', µmol/hr) is extended with the input from repeated bolus exposure:

$$Input\_l'=Oral\_abs'+Dietexp+Repeat\_exp \quad (\mu mol/hr) \quad (10)$$

Simulation of repeated bolus exposure was not included in (Timchalk et al., 2002b), but as the present model was used to simulate experiments with this kind of dosing scenario (see section 23.3) it was included.

21.1.2 DISTRIBUTION

Phosphothionate pesticides such as chlorpyrifos are generally well distributed in tissue throughout the body. The parent phosphothionate or oxon is not excreted due to extensive metabolism (Timchalk, 2010).

After absorption chlorpyrifos enters the bloodstream and in the model (see Figure 28) the amount of absorbed chlorpyrifos is added directly to the liver compartment (first-pass effect). A major part of the chlorpyrifos (and chlorpyrifos-oxon) will be bound to plasma proteins but only free chlorpyrifos is metabolised in the liver to the active metabolite chlorpyrifos-oxon or to the detoxification product TCP. Only free chlorpyrifos and free chlorpyrifos-oxon are assumed to be capable of entering the other tissue compartments. This distribution is shown in Figure 29. The binding of the pesticide to proteins are expected to be so rapid that equilibrium is established within milliseconds (Rowland and Tozer, 1995; Timchalk et al., 2002b). In the model the concentration of chlorpyrifos and chlorpyrifos-oxon are multiplied by a factor for plasma protein binding (FBc and FBco for chlorpyrifos and chlorpyrifos-oxon, respectively) to calculate the concentration of free compound entering the other tissues. This is further described later.

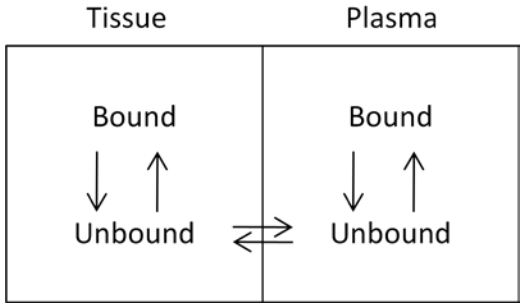

Figure 29: distribution of the compound in the body is dependent on the binding to plasma proteins and in the tissue compartments. Only non-bound compound is capable of entering the tissue compartments. Figure modified from (Rowland and Tozer, 1995).

Distribution in compartments

For each tissue compartment t (i.e. liver, brain, diaphragm, rapid perfused tissues, slowly perfused tissues, and fat) a mass balance differential equations were included describing the concentration of chlorpyrifos in venous blood leaving the tissues.

The rate of change in chlorpyrifos concentration in tissues that does not form chlorpyrifos-oxon (all tissues except the liver) is described by the blood flow rate to the tissue times the difference between the concentrations of the free compound in arterial blood entering the tissues (CA_free, (µmol/l) and venous blood leaving the tissue t (CVt_free, µmol/l):

$$Ct' = Qt/Vt*(CA\_free-CVt\_free) \quad (\mu mol/l/hr) \quad (11)$$

where Qt (l/hr) and Vt (l) is the blood flow and volume of the relevant tissue t, respectively. CA_free is calculated from equation (22). The concentration of free chlorpyrifos in venous blood leaving tissue t is calculated as:

$$CVt\_free=Ct/PCtc \quad (\mu mol/l) \quad (12)$$

where Ct (µmol/l) is determined from the above differential equation and PCtc (unitless) is the tissue:blood partition coefficient for chlorpyrifos.

Chlorpyrifos-oxon in compartments

Similar equations for each compartment are included in the model to describe the distribution of chlorpyrifos-oxon as well. However, the concentration of chlorpyrifos-oxon in liver, brain, diaphragm and blood compartments are influenced by binding to (inhibition) and metabolism performed by B-esterase as described in section 21.1.4.

Chlorpyrifos in the liver compartment

The distribution in the liver is calculated as described above. However, the equations are slightly expanded taking metabolism into account. This is explained later in section 21.1.3.

Chlorpyrifos in the blood compartment

The concentration of chlorpyrifos in blood (Cbl, µmol/l) is calculated from the following differential equation which is similar to the equation for Ct' (equation 11). However, in the blood-compartment the input is the sum of concentration of chlorpyrifos draining from all other tissues, CV, minus the concentration in arterial blood, CA. The rate of change in concentration of chlorpyrifos in blood (Cbl', µmol/l/hr) is:

$$Cbl'=QC/Vbl*(CV-CA) \quad (\mu mol/l/hr) \quad (13)$$

where QC (l/hr) is the cardiac output and Vbl (l) is the volume of blood. Total concentration of chlorpyrifos in venous blood, CV (µmol/l) is the sum of free (CV_free, µmol/l) and bound (Cbl_bound, µmol/l) chlorpyrifos in blood:

$$CV=CV\_free+Cbl\_bound \quad (\mu mol/hr) \quad (14)$$

How to determine CV_free is shown in equation (20). The concentration of bound chlorpyrifos in blood (µmol/l) is calculated from the blood concentration (Cbl, µmol/l) using a factor for plasma protein binding, FBc (%):

$$Cbl\_bound=Cbl*FBc/100 \quad (\mu mol/l) \quad (15)$$

The total concentration of chlorpyrifos in mixed venous blood (CV, µmol/l), should be calculated from the following differential equation describing the rate of change in venous blood (CV'):

$$CV'*V=\sum(Qi*CVi)-QC*CV \quad (\mu mol/hr) \quad (16)$$

(Johanson, 1997). The right hand side is the sum of the individual flows (Qi, l/hr) times the individual concentrations in venous blood (CVi, µmol/l) leaving the tissue minus the product of cardiac output and the concentration in mixed venous blood.

The sum of the individual flows is equal to the cardiac output. However, it is assumed that steady-state is almost immediately reached in mixed venous blood which in mathematical terms can be written as CV'*V=0. Inserting this into equation (16) and rearranging:

$$0=\sum(Qi*CVi)-QC*CV \quad (\mu mol/hr) \quad (17)$$

$$\sum(Qi*CVi)=QC*CV \quad (\mu mol/hr) \quad (18)$$

Then the total concentration of free chlorpyrifos in mixed venous blood from tissues (µmol/l) is:

$$CV=(\sum(Qi*CVi))/QC \quad (\mu mol/l) \quad (19)$$

The assumption that the steady-state is almost immediately reached in mixed venous blood is used in most PBPK models (Johanson, 1997). In the present model the equation for CV_free (µmol/l) becomes:

$$CV\_free=(CVf*Qf+CVs*Qs+CVr*Qr+CVdi*Qdi+CVbr*Qbr+CVl*Ql)/QC \quad (20)$$

which is the sum of the individual flows times the individual concentrations in venous blood leaving each tissue and then divided by the cardiac output. f=fat, s=slowly perfused, r=rapidly perfused, di=diaphragm, br= brain and l=liver.

Concentration of chlorpyrifos in arterial blood (CA µmol/l) is calculated as the concentration of chlorpyrifos in blood divided by the partition coefficient for chlorpyrifos (which is actually 1):

$$CA=Cbl/PCbl \quad (\mu mol/l) \quad (21)$$

This means that in the model the concentration in arterial blood is equal to the concentration in blood.

The concentration of free chlorpyrifos in arterial blood (CA_free, µmol/l) is determined as the concentration in arterial blood times 1 minus the fraction of bound chlorpyrifos (FBc, %):

$$CA\_free=CA*(1-FBc/100) \quad (\mu mol/l) \quad (22)$$

21.1.3 METABOLISM BY CYP450 AND A-ESTERASE

CYP450 metabolism of chlorpyrifos to chlorpyrifos-oxon

The main metabolic activation as well as detoxification of chlorpyrifos occurs in the liver (Timchalk, 2010). The metabolism of free chlorpyrifos to chlorpyrifos-oxon and to TCP by CYP450 in liver is described as saturable enzymatic processes and modelled with Michaelis-Menten equation which was described in chapter 13. The rate of change in the amount of free chlorpyrifos (µmol/hr) is calculated from:

$$AML1'=(Vmax1*Cl)/(Km1+Cl) \quad (\mu mol/hr) \quad (23)$$

for chlorpyrifos to chlorpyrifos-oxon, and

$$AML2' = (Vmax2 * Cl)/(Km2 + Cl) \quad (\mu mol/hr) \quad (24)$$

for chlorpyrifos to TCP.

Vmax1 and Km1 are the maximum velocity (µmol/h) and Michaelis-Menten constant (µmol/l) for metabolism of chlorpyrifos to chlorpyrifos-oxon. Vmax2 and Km2 are the maximum velocity (µmol/h) and Michaelis-Menten constant (µmol/l) for metabolism of chlorpyrifos to TCP. Cl is the concentration of chlorpyrifos in liver (µmol/l).

The rate of change in concentration of chlorpyrifos in liver (Cl', µmol/l/hr) is calculated as the difference between the concentration in arterial and venous blood plus the rate of intake from dietary and/or gavage exposure minus the sum of rate of change in concentration of free chlorpyrifos metabolised to chlorpyrifos-oxon and TCP:

$$Cl' = (Ql * (CA\_free - CVl) + Input\_l' - AML1' - AML2')/Vl \quad (\mu mol/l/hr) \quad (25)$$

where Vl is the volume of the liver and the concentration of free chlorpyrifos in venous blood draining the liver, CVl, (µmol/l) is calculated as described for CVt_free in equation (12).

The maximum velocity for the two metabolism processes (Vmax1 and Vmax2, µmol/hr), were obtained from VmaxC1 and VmaxC2 (µmol/hr/kg) by allometric scaling to the body weight (BW, kg) as described by El-Masri and co-workers:

$$Vmax = VmaxC * BW^{0.7} \quad (\mu mol/hr) \quad (26)$$

(El-Masri et al., 1996).

The 0.7 in the above equation from El-Masri et al. is also used as exponent in the present model as no figure were presented in (Timchalk et al., 2002b). Different exponents have been used in the literature varying from 0.67 to 0.75 (U.S.EPA, 2006a). These scaling functions have been determined by measuring body weight and metabolic rate of different species (adult animal) covering a broad size range. Plotting these data on a double logarithmic scale give a straight line from which the exponent can be estimated as the slope of the curve (Travis and Hattemer-Frey, 1990).

A-esterase metabolism of chlorpyrifos-oxon to TCP

The hydrolysis of chlorpyrifos-oxon by PON-1 in liver and blood (step D2 in Figure 25) is also described by Michaelis-Menten equation. The rate of this A-esterase metabolism (µmol/hr) of chlorpyrifos-oxon to TCP in liver (AML3l', µmol/hr) and blood (AML3bl', µmol/hr) is calculated by the following two equations:

$$AML3l' = (Vmax3 * Clo)/(Km3 + Clo) \quad (\mu mol/hr) \quad (27)$$

$$AML3bl' = (Vmax4 * Cblo)/(Km4 + Cblo) \quad (\mu mol/hr) \quad (28)$$

where Vmax3 and Vmax4 are the maximum velocity for metabolism (µmol/h) of chlorpyrifos-oxon to TCP in liver and blood respectively, and Km3 and Km4 are the Michaelis-Menten constants (µmol/l) for metabolism to TCP. Clo and Cblo are the concentration of chlorpyrifos-oxon in liver and blood (µmol/l), respectively.

21.1.4 METABOLISM BY B-ESTERASES

B-esterases are described in four compartments in the model namely liver, brain, diaphragm and blood (plasma and RBC). The choice of compartments for exhibiting B-esterase activity is only explained by Timchalk et al. for RBC: they point out that RBC acetylcholinesterase inhibition is an important biomarker for exposure to e.g. chlorpyrifos (Timchalk et al., 2002b).

This assumption is supported by a study performed by Chen and co-workers. They found that inhibition of acetylcholinesterase in RBC is an important biomarker of organophosphorus pesticide exposure since RBC acetylcholinesterase is 12- to 14-fold more sensitive as indicator of chlorpyrifos exposure than acetylcholinesterase inhibition in e.g. brain (Chen et al., 1999).

Gearhart and co-workers pointed out that blood acetylcholinesterase is a useful indication of acetylcholinesterase activity in less accessible organs and blood is an important site of diisopropylfluorophosphate metabolism (Gearhart et al., 1994). The FAO/WHO Joint Meeting on Pesticide Residues (JMPR) has concluded that in the absence of data on brain acetylcholinesterase activity, measurements of acetylcholinesterase activity in RBC would better display toxicity than plasma acetylcholinesterase activity (IPCS, 1990).

Nostrandt et al. examined the inhibition of acetylcholinesterase by chlorpyrifos in different tissues after gavage administration of 0, 10, 30, 60 and 100 mg/kg to rats. They found the following order of potency of the inhibition: blood (whole blood, RBC, plasma) >> heart > retina ≈ brain ≈ liver > diaphragm > quadriceps (Nostrandt et al., 1997). Based on this study it seems reasonably to include B-esterase for blood (incl. RBC), brain, liver and diaphragm in the model. However, it is not obvious why heart is not included in the model by (Timchalk et al., 2002b).

Chlorpyrifos-oxon in liver, brain, diaphragm and blood

The set of equations describing the changes in the four compartments with B-esterase activity (liver, brain, diaphragm and blood) will be exemplified by the liver in the following.

The rate of change in amount of chlorpyrifos-oxon in liver (µmol/h) is the sum of the change in chlorpyrifos-oxon amount in liver (Cao_free – CVlo_free) and chlorpyrifos-oxon that have been formed by metabolism of chlorpyrifos by CYP450 (AML1') minus the amount of chlorpyrifos-oxon metabolised by A-esterase to TCP (AML3l') or metabolised by B-esterases (AML4', AML5' and AML6'). The rate of change in concentration of chlorpyrifos-oxon in liver (µmol/l/h) is then calculated as the rate of change in amount of chlorpyrifos-oxon in liver divided by the liver volume (Vl, l):

$$Clo'=(Ql*(CAo\_free-CVlo\_free)+AML1'-AML3l'-(AML4'+AML5'+AML6'))/Vl \quad (\mu mol/l/hr) \quad (29)$$

The concentration of free chlorpyrifos-oxon in arterial blood, CAo_free (µmol/l) and the concentration of free chlorpyrifos-oxon in venous blood draining the liver (CVlo, µmol/l), are calculated in a similar way as CA_free and CVt_free in equation (22) and (12) respectively using chlorpyrifos-oxon relevant parameters and concentrations. AML1' and AML3l' are described in equations (23) and (27).

The rate of metabolism of chlorpyrifos-oxon to TCP by acetylcholinesterase (µmol/hr) in the four relevant compartments are described by second order processes as a product of the amount of esterase binding sites in tissue t, AAChEt (µmol/hr), the bimolecular inhibition rate constant (Ki (µmol*hr)$^{-1}$), and the concentration of chlorpyrifos-oxon in tissue t (Cto, µmol/l):

AML4t'=AAChEt*Ki*Cto (µmol/hr) (30)

The rate of change of acetylcholinesterase (AAChEt, µmol/hr) in tissue t is calculated by solving equation (33) for each of the four tissues (liver, brain, diaphragm and blood). Cto for brain and diaphragm is calculated from equations similar to equation (29) omitting AML1' (only relevant in liver) and AML3l' (only relevant in liver and blood).

The rate of metabolism by butyrylcholinesterase (AML5t') and carboxylesterase (AML6t') are calculated for the four compartments similarly to equation (30).

B-esterase inhibition in the liver, brain, diaphragm and blood compartment:
In the following the equations concerning acetylcholinesterase is outlined, see Figure 30. A similar set of equations are included for butyrylcholinesterase and carboxylesterase, see model code Appendix II.

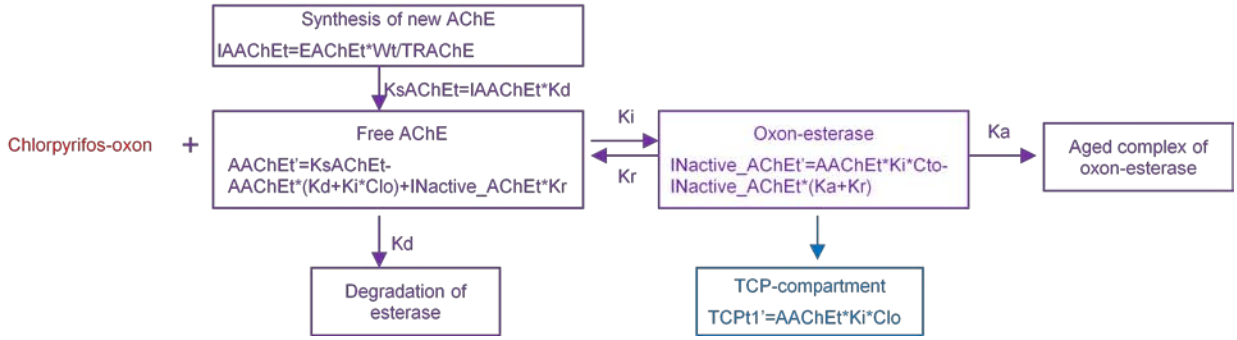

Figure 30. An extract of Figure 28 showing the compartments in which B-esterase activity is described and the differential equations describing the esterase activity. The equations are written for acetylcholinesterase but similar ones are used to describe butyrylcholinesterase and carboxylesterase in brain, liver, diaphragm and blood.

The following equations are included in the model for the four compartments for which B-esterase inhibition is taken into account and specific parameters are used for each tissue.

The synthesis rate for acetylcholinesterase in tissue t (KsAChEt, µmol/hr) is described as a zero order process calculated as the product of the initial amount of acetylcholinesterase binding sites (IAAChEt, µmol) and the enzyme degradation rate (Kd, h^{-1}):

KsAChEt=IAAChEt*Kd (µmol/hr) (31)

The initial amount of acetylcholinesterase binding sites is calculated from the enzyme turnover rate (TRAChE, enzyme hydrolysed/hr), and enzyme activity (EAChEt, µmol/kg tissue/hr) for the specific tissue:

IAAChEt=EAChEt*Wt/TRAChE (µmol) (32)

where Wt is the weight of the specific tissue t (kg).

The rate of change of amount acetylcholinesterase in tissue t, AAChEt' (µmol/hr) is calculated as the enzyme synthesis (KsAChEt) minus the degradation and loss of enzyme due to oxon-bound acetylcholinesterase plus the reactivation of inactive enzyme:

$$AAChEt' = KsAChEt - AAChEt*(Kd+Ki*Cto) + INactive\_AChEt*Kr \quad (\mu mol/hr) \quad (33)$$

where Kr is the reactivation rate constant (hr^{-1}). The initial amount of acetylcholinesterase binding sites, IAAChEt (equation (32)) is the initial value when solving this differential equation.

INactive_AChEt (µmol) in equation (33) is the amount of acetylcholinesterase inactivated (inhibited) due to phosphorylation. The rate of change in amount of inactivated acetylcholinesterase, INactive_AChEt' (µmol/hr) is calculated as the difference between the rate of change in amount of acetylcholinesterase bound to oxon (described as a second-order process) and the rate of change in amount of acetylcholinesterase which is no longer bound as oxon-esterase due to either reactivation or aging (first-order processes):

$$INactive\_AChEt' = AAChEt*Ki*Cto - INactive\_AChEt*(Ka+Kr) \quad (\mu mol/hr) \quad (34)$$

The percentage of inhibited acetylcholinesterase in tissue t, Inhib_AChEt, is calculated as the proportion of the amount of available acetylcholinesterase and the initial amount of acetylcholinesterase binding sites:

$$Inhib\_AChEt = AAChEt*100/IAAChEt \quad (\mu mol) \quad (35)$$

A similar set of equations are included for both butyrylcholinesterase and carboxylesterase for the brain, diaphragm, liver and plasma. The total B-esterase inhibition in tissue t (B_EST_total_t, µmol) can be calculated as the sum of amount of inhibited acetylcholinesterase (AAChEt), butyrylcholinesterase (ABuChEt) and carboxylesterase (ACaEt):

$$B\_EST\_total\_t = AAChEt + ABuChEt + ACaEt \quad (\mu mol) \quad (36)$$

Then the total B-EST inhibition in each tissue can be calculated as percentage of the initial inhibition of esterase by acetylcholinesterase (IAAChEt), butyrylcholinesterase (IABuChEt) and carboxylesterase (IACaEt):

$$Inhib\_tot\_t = B\_EST\_total\_t*100/(IAAChEt+IABuChEt+IACaEt) \quad (\%) \quad (37)$$

The total cholinesterase inhibition in tissue t can be calculated from:

$$Inhib\_ChEt\_total = (AAChEt+ABuChEt)*100/(IAAChEt+IABuChEt) \quad (\%) \quad (38)$$

21.1.5 ELIMINATION AS TCP

The formation of TCP due to the phosphorylation of acetylcholinesterase is calculated in equation (30). As seen in Figure 28 input to the TCP compartment origin from chlorpyrifos in liver (AML2'), chlorpyrifos-oxon in liver (AML3l') and blood (AML3bl') as well as from the

metabolism of chlorpyrifos-oxon by B-esterases (AML4t', AML5t', AML6t'). The rate of change in the total TCP formation is calculated as:

$$TCP\_form' = AML2' + AML3bl' + AML3l' + \sum AML4t' + \sum AML5t' + \sum AML6t' \quad (\mu mol/hr) \quad (40)$$

To describe the TCP-compartment the urinary excretion should also be taken into account. TCP is 100 % excreted via the urine. The rate of urinary excretion of TCP (TCPexc', µmol/hr) is described as:

$$TCPexc' = ATCP * Ke \quad (\mu mol/hr) \quad (41)$$

where Ke is the first order elimination rate constant (hr^{-1}). The amount of TCP (ATCP, µmol) is calculated by solving the following equation describing the rate of change in the amount of TCP (ATCP', µmol/hr):

$$ATCP' = TCP\_form' - TCPexc' \quad (\mu mol/hr) \quad (42)$$

TCP_form' is the rate of change in the amount of TCP formed from all sources (i.e. CYP450, A-EST, B-EST) and TCPexc' is the rate of change in the amount of TCP eliminated urinary.

The concentration of TCP in blood (CTCPbl, µmol/l) is calculated as the amount of TCP divided by the volume of distribution (Vd, l):

$$CTCPbl = ATCP / Vd \quad (\mu mol/l) \quad (43)$$

The volume of distribution is not a measurable volume. It represents that volume in which a compound will distribute in the body depending on several physicochemical properties. It relates the plasma concentration with the amount of compound in the body during the elimination phase (Rowland and Tozer, 1995).

21.1.6 MASS BALANCE CHECK

The total mass (µmol) of chlorpyrifos (total_massCPF), chlorpyrifos-oxon (total_massOxon) and TCP (total_massTCP) are calculated as:

$$total\_massCPF = Input\_l + \sum Ct_i * Vt_i \quad (\mu mol) \quad (44)$$

where Ct_i is the concentration of chlorpyrifos in tissue i and Vt_i is the volume of each tissue i in the model (fat, slowly perfused tissues, rapidly perfused tissues, diaphragm, brain and blood).

$$total\_massOxon = \sum Ct_io * Vt_io \quad (\mu mol) \quad (45)$$

where Ct_io is the concentration of chlorpyrifos-oxon in tissue i and Vt_i is the volume of each tissue i in the model.

$$total\_massTCP = ATCP + TCPexc \quad (\mu mol) \quad (46)$$

Total amount of chlorpyrifos delivered in the experiment should equal the amount calculated by the code. This means that the equation below for TOTAL (which is the total amount of metabolites delivered to tissues or excreted) should equal total_massCPF.

$$TOTAL=total\_massOxon+total\_massTCP \quad (\mu mol) \quad (47)$$

21.2 PARAMETERS

This section contains a critical evaluation of the parameters in (Timchalk et al., 2002b) which are used in the model. The origins of the parameters will be described to the extent it has been possible to track them.

The following species specific and chemical specific parameters are used in the model for chlorpyrifos:

- Species specific parameters: body weights, tissue weights, tissue volumes, cardiac output, and tissue flow rates.
- Chemical specific parameters: molecular weights, partition coefficients, plasma protein binding, fractional absorption, Michaelis-Menten constants, maximum velocity of metabolic reactions, bimolecular inhibition rate, reactivation rate, aging time, volume of distribution, first order elimination rate constant, enzyme turnover rates, enzyme activity, and enzyme degradation rate.

An overview of the parameters and their origins, assumptions and deviations from (Timchalk et al., 2002b) are shown in Table 7 and the values of the parameters used in the present model on rat are shown in Table 8.

Table 7. Overview of parameters used in the PBTK/TD model for chlorpyrifos in rats.

Parameter abbreviation	**Parameter**	**Estimated / measured/ calculated/ fitted**	**Source**	**Assumptions /comments**	**Deviations from the model by (Timchalk et al., 2002b)**
KaS	Absorption in stomach (hr^{-1})	Fitted by Timchalk et al.	(Timchalk et al., 2002b)		
KaI	Absorption in intestine (hr^{-1})	Fitted by Timchalk et al.	(Timchalk et al., 2002b)		
KsI	Transfer stomach-intestine (hr^{-1})	Fitted by Timchalk et al.	(Timchalk et al., 2002b)		
Fa	Fractional absorption (%)	"Unpublished data"	(Timchalk et al., 2002b)	Timchalk et al. have stated 0.80 % for rats and 0.72 % for humans. For humans Nolan et al. (1984) has stated 72 %, and therefore it seems as the data should have been presented as 80 % (and 72 % for humans).	
BW	Body weight (kg)				
Mc	Molecular weight of CPF (mg/µmol)	Calculated			
PEbl, PEbr, PEdi, PEf, PEl, PEr, PEs	Tissue weight as percentage of body weight (%)		(Gearhart et al., 1990; Gearhart et al., 1994)	Tissue volume is equal to tissue weight (1:1). Weight of blood is equal	Timchalk et al. / present model: PEbr=1.2 / 1.16

Parameter abbreviation	Parameter	Estimated / measured/ calculated/ fitted	Source	Assumptions /comments	Deviations from the model by (Timchalk et al., 2002b)
				to weight of venous (PEv) and arterial (PEa) blood: PEbl=PEv+PEa. Weight of slowly perfused tissues, PEs, is from (Gearhart et al., 1994)	PEr=4 / 3.88 PEs=78 / 68.66 PEdi=0.03 / 0.3
Vbrc, Vlc, Vrc, Vfc, Vsc, Vdic, Vvc, Vac, Vblc	Tissue volumes as percentage of body weight (%)		(Gearhart et al., 1990; Gearhart et al., 1994)	Tissue volume is equal to tissue weight (1:1). Volume of blood is equal to volume of venous and arterial blood: Vblc=Vvc+Vac. Vsc is from (Gearhart et al., 1994)	Timchalk et al. / present model: Vbrc=1.2 / 1.16 Vrc=4 / 3.88 Vsc=78 / 68.66 Vdic=0.03 / 0.3
QC	Cardiac output (l/hr)	Calculated	(Andersen et al., 1987)		
Qbrc, Qdi, Qfc, Qlc, Qrc, Qsc	Blood flow in organ as percentage of cardiac output (%)		(Gearhart et al., 1990)	In the present model Q for rapidly perfused tissues(Qrc) is equal to the published values for Q richly perfused + kidney given by (Gearhart et al., 1990)	Timchalk et al / present model: Qrc=42.6 / 47.96 Qsc=14 / 14.4
PCbrc, PCdic, PCfc, PClc, PCrc, PCsc, PCbl, PCbro, PCdio, PCfo, PClo, PCro, PCso, PCblo,	Partition coefficient of CPF and CPF-oxon	Calculated by Timchalk et al. based on *in vitro* data	(Timchalk et al., 2002b)	Measured data not reported, therefore data not checked	
FBc, FBo	Plasma protein binding of CPF and CPF-oxon	Measured by Sultatos et al.: 97 % CPF were reversible bound to blood.	(Sultatos et al., 1984; Timchalk et al., 2002b)	Timchalk et al. assumed that binding for CPF-oxon is slightly higher than for CPF (98%)	
Km1	Michaelis-Menten constant for desulfuration of CPF to CPF-oxon (μM)	Measured	(Ma and Chambers, 1994)	Data for female rats. Timchalk et al. used Km1=2.86 referring to Ma and Chambers but this value is not reported in that publication.	Timchalk et al. used Km1=2.86. In present model Km1=3.23 (data for female rats – as Timchalk et al. selected for Km2)
VmaxC1	Maximum velocity of CPF desulfuration to CPF-oxon in liver microsomes (μmol/hr/kg)	Measured by Ma and Chambers. Re-calculated by Timchalk et al.	(Ma and Chambers, 1994; Timchalk et al., 2002b)	Calculation could not be verified (see text)	
Vmax1	Maximum velocity of CPF desulfuration to CPF-oxon in liver microsomes (μmol/hr)	Calculated from VmaxC1	(El-Masri et al., 1996)		
Km2	Michaelis-Menten constant for dearylation of CPF to TCP (μM)	Measured	(Ma and Chambers, 1994; Timchalk et al., 2002b)	Data for female rats	Timchalk et al. used Km2=24. In present model Km2=24.3 as given by Ma and Chambers
VmaxC2	Maximum velocity of CPF dearylation to TCP in liver microsomes (μmol/hr/kg)	Measured by Ma and Chambers. Re-calculated by Timchalk et al.	(Ma and Chambers, 1994)	Calculation could not be verified (see text)	
Vmax2	Maximum velocity of CPF	Calculated from VmaxC1: Vmax1=VmaxC1*BW^0.7	(El-Masri et al., 1996)		

Parameter abbreviation	Parameter	Estimated / measured/ calculated/ fitted	Source	Assumptions /comments	Deviations from the model by (Timchalk et al., 2002b)
	dearylation to TCP in liver microsomes (µmol/hr)				
TRAChE, TRBuChE, TRCaE	Enzyme turnover rate of AChE, BuChE and CaE (enzyme hydrolysed/hr)	Data from literature – Timchalk et al. refers to Maxwell et al. (1987). Maxwell et al. refers to literature values: AChE: measured for DFP (Wang and Murphy, 1982) OK BuChE: measured for DFP (Main et al., 1972) not OK (see comments) CaE: (Ikeda et al., 1977) No value for enzyme turnover rate found	(Main et al., 1972; Maxwell et al., 1987; Wang and Murphy, 1982)	Assumed that turnover rate is the same for CPF and DFP. Concerning BuChE: Timchalk et al and Maxwell et al have used the turnover rate for acetylthiocholine ($6.10*10^4$ min^{-1}) instead of that for BuChE ($1.71*10^5$ min^{-1}) measured by Main et al. Unclear origin of the value for CaE	Timchalk et al. used TRBuChE= $3.66*10^6$. In the present model, TRBuChE = $1.71*10^5$ min^{-1} = $1.03*10^7$ h^{-1} as measured by Main et al.
EAChEbr, EAChEdi, EAChEp, EBuChEbr, EBuChEdi, EBuChEl, EBuChEp, ECaEbr, ECaEdi, ECaEl, ECaEp	Enzyme activity (µmol/kg tissue/hr)	EAChEt, ECaEt and EChEt_total measured by Maxwell et al., converted from (µmol/min/g tissue) to (µmol/hr/kg tissue). EBuChEt= EChEt_total – EAChEt	(Maxwell et al., 1987)		Timchalk et al. used ECaEbr=$6*10^3$ µmol/kg tissue/hr. In present model ECaEbr=$6*10^4$ µmol/kg tissue/hr which corresponds to the data in (Maxwell et al., 1987).
Kd1-Kd13	Enzyme degradation rate (hr^{-1})	Kd for AChE was determined for DFP in plasma and brain by Gearhart et al. from literature data. These two values are used for other tissues as well as for BuChE RBC AChE: estimated by Timchalk et al. from RBC life-span. For CaE: estimated for each tissue by fitting model to data from literature – by Timchalk et al.	(Gearhart et al., 1990; Timchalk et al., 2002b)	Assumed that Kd for DFP is the same for CPF. It is not clear how Timchalk et al. decided to disperse the two measured Kd-values to the other organs.	
Ki1-Ki13	Bimolecular inhibition rate (1/(µM*hr))	For AChE and BuChE: fitting model to experimental data. For RBC AChE: fitted to data from literature. For CaE: estimated based on ratio of Ki for AChE and CaE from (Gearhart et al., 1990). (Timchalk et al., 2002b)	(Gearhart et al., 1990; Timchalk et al., 2002b)	For AChE and BuChE: assume same Ki for all tissues (except RBC)	
Kr1-Kr13	Reactivation rate (hr^{-1})	Measured in brain for AChE by Carr and Chambers. This value used for all relevant compartments as well as for BuChE and CaE (Timchalk et al., 2002b). AChE RBC: measurement and fitting performed by (Timchalk et al., 2002b).	(Carr and Chambers, 1996; Timchalk et al., 2002b)	Reactivation rate is the same for AChE, BuChE and CaE – and in all compartments (except AChE RBC)	In present model Kr1-4 = 0.01403 hr^{-1} as measured by (Carr and Chambers, 1996). Timchalk et al. wrote Kr1-4 = 0.0143 hr^{-1} but this must be a typing error
Ka1-Ka13	Aging rate (hr^{-1})	Measured in brain for AChE by Carr and Chambers. Ka for BuChE and CaE: set equal to Ka for AChE	(Carr and Chambers, 1996)	Rate of aging is the same for AChE, BuChE and CaE – and in all compartments	

Parameter abbreviation	Parameter	Estimated / measured/ calculated/ fitted	Source	Assumptions /comments	Deviations from the model by (Timchalk et al., 2002b)
		(Timchalk et al., 2002b)			
Km3	Michaelis-Menten constant for CPF-oxon -> TCP in liver (µM)	1) Calculated by Mortensen et al. from experiment 2) Km3 optimized in (Timchalk et al., 2007b)	1) (Mortensen et al., 1996) 2) (Timchalk et al., 2007b)	Km3 was changed in present model due to wrong output of the model (see section 21.2.1)	Timchalk et al. / present model: 240 / 577 µM
Vmax3	Maximum velocity of CPF–oxon hydrolysed to TCP in liver (µmol/hr)	1) Vmax3 is calculated by Mortensen et al. from experimental data 2) Vmax3 changed in (Timchalk et al., 2007b)	1) (El-Masri et al., 1996; Mortensen et al., 1996) 2) (Timchalk et al., 2007b)	Vmax3 was changed in present model due to wrong output of the model (see section 21.2.1)	Timchalk et al. / present model: VmaxC3 = 74421 / 38002 µmol/hr
Km4	Michaelis-Menten constant for CPF-oxon -> TCP in blood (µM)	1) Calculated by Mortensen et al. from experimental data 2) Km4 optimized in (Timchalk et al., 2007b)	1)(Mortensen et al., 1996) 2) (Timchalk et al., 2007b)	Km4 was changed in present model due to wrong output of the model (see section 21.2.1)	Timchalk et al. / present model: 250 / 464 µM
Vmax4	Maximum velocity of CPF–oxon hydrolysed to TCP in blood (µmol/hr)	1) Vmax4 is calculated by Mortensen et al. from experimental data 2) Vmax4 changed in (Timchalk et al., 2007b)	1) (El-Masri et al., 1996; Mortensen et al., 1996) 2) (Timchalk et al., 2007b)	Vmax4 was changed in present model due to wrong output of the model (see section 21.2.1)	Timchalk et al. / present model: VmaxC4 = 57003 / 40377 µmol/hr
Vd	Volume of distribution (l)	Calculated based on "unpublished data"	(Timchalk et al., 2002b)		
Ke	1. order elimination rate constant (hr^{-1})	Calculated based on "unpublished data"	(Timchalk et al., 2002b)		

Kas, Kal, KsI (l/hr)

These constants are estimated by Timchalk et al. (2002b) by fitting the model to experimental data for inhibition of plasma cholinesterase in F344 rats administered chlorpyrifos by gavage exposure at dose levels between 0.5 and 100 mg/kg bw (Timchalk et al., 2002b).

Fractional absorption (%)

Nolan et al. have stated that the fractional absorption of chlorpyrifos, Fa, is 72 % for humans (Nolan et al., 1984). This level of fractional absorption is in accordance with other published data: Up to 90 % chlorpyrifos were absorbed in rats within 72 h, and 70 % in humans within 96 h (JMPR, 2000). Timchalk et al. stated that Fa was 0.80 % for rats and 0.72 % for humans. It should have been presented as 80 % and 72 %.

Body weight (kg)

Timchalk et al. have not directly stated the size of body weight used in their model. They used a cardiac output of 5.4 l/h referring to the calculation-method presented by Andersen and co-workers (1987) (see below in the section: "Cardiac output") and this indicates a body weight of 250 g for rats. Therefore, in the present model for rats 0.25 kg is used.

Tissue weight as percentage of body weight and tissue volumes as percentage of body weight (%)

It is anticipated that tissue weight and tissue volumes are the same i.e. 1 litre weighs 1 kg. Unit density (litre=kg) is a generally used assumption and it seems reasonable since the typical range is from 0.9 kg/l for fat to 1.06 kg/l for muscle (U.S.EPA, 2006a).

Timchalk and co-workers refer to (Gearhart et al., 1990) for the data on rats, however some of the values deviates from the ones given in that paper:

- Brain, Vbrc=1.2 % (Timchalk et al., 2002b) and 1.16 % (Gearhart et al., 1990): difference due to round off (1.16 % used in present model)
- Rapidly perfused tissues, Vrc=4 % (Timchalk et al., 2002b) and 2 % (Gearhart et al., 1990): difference probably due to: Vrc = richly perfused + kidney + lung = 2+0.73+1.15 = 3.88 %, as kidney and lung is not included in the model. (3.88 % used in present model)
- Slowly perfused tissues, Vsc=78 % (Timchalk et al., 2002b)/ 74.7(Gearhart et al., 1990) (concerning value used in present model, see below)

The total weight of tissues is 100.23 and 99.74 % of body weight, respectively, using the datasets in (Timchalk et al., 2002b) and in (Gearhart et al., 1990). This seems a bit odd since e.g. weight of skeleton is not included. Therefore, the dataset given by Gearhart and co-workers in 1994 seems more realistic since the total weight of tissues is 90.73 % of the body weight leaving about 10 % to other tissues and the skeleton. Bones have been reported to constitute 5-7 % of the body weight for rats (Brown et al., 1997). The difference in the values of total weight of tissues is due to differences in the value for the tissue weight for slowly perfused tissues. Timchalk et al. (2002b) and Gearhart et al. (1990) used 78 % and 74.7 %, respectively wheras Gearhart et al. (1994) reported 68.66 %. The value of 68.66 % is used in the present model for weight of the slowly perfused tissues.

The tissue weight as percentage of body weight for diaphragm was given for rats to be 0.3 % in (Gearhart et al., 1990) but 0.03 % in (Gearhart et al., 1994). For mice 0.3 % was given in both references (and also for humans in (Gearhart et al., 1994)). Therefore, the value of 0.03 % is considered to be a typing error in the Gearhart et al. paper from 1994. In the present model the value of 0.3 % was used.

Cardiac output (l/hr)

Andersen and co-workers (Andersen et al., 1987) have calculated the cardiac output (QC) by the following equation:

$QC=15\ l/h/kg*(BW)^{0.74} = 15\ l/h/kg*(0.25\ kg)^{0.74} = 5.4\ l/h$

Blood flow in organ as percentage of cardiac output (%)

According to Timchalk and co-workers (2002b) they used data on blood flow in organs (Qt) presented by (Gearhart et al., 1990), however there are certain discrepancies:

Timchalk et al. (2002b) used Qrc=42.6 % for blood flow as percentage of cardiac output in rapidly perfused tissues. However, Gearhart and co-workers (1990) stated 27.96 % for rapidly perfused tissues. It might be that Timchalk et al. added the value for blood flow in kidney (20.0 %), however this would give a Qrc=47.96 %. The difference may be due to their incorporation of a skin-compartment with blood flow set to 5.8 % (however, this would give Qrc=(47.96-5.8)% = 42.16 %). No data for blood flow in skin is given by Gearhart et al., and no reference indicated by Timchalk et al.

In the present model blood flow for rapidly perfused tissues is equal to the published value of blood flow for rapidly perfused tissues plus kidney, both values given by (Gearhart et al., 1990), i.e. Qrc=(27.96+20)%=47.96 %.

Timchalk et al. (2002b) used Qs=14 % for slowly perfused tissues. In the present model Qs=14.4 % (value from (Gearhart et al., 1990)).

The sum of organ blood flows used in the model is 99.96 %, which is acceptable.

Partition coefficient of chlorpyrifos and chlorpyrifos-oxon
The partition coefficients of chlorpyrifos and chlorpyrifos-oxon are calculated by Timchalk and co-workers based on *in vitro* data (Timchalk et al., 2002b).

Plasma protein binding of chlorpyrifos and chlorpyrifos-oxon (%)
Timchalk and co-workers used the value for plasma protein binding for chlorpyrifos (FBc = 97 %) measured by Sultatos and co-workers (Sultatos et al., 1984). They assumed that plasma protein binding for chlorpyrifos-oxon was slightly higher than for chlorpyrifos (Timchalk et al., 2002b), and therefore set to FBo = 98 %.

Michaelis-Menten constant for desulfuration (CPF -> CPF-oxon), Km1 (µM)
The Michaelis-Menten constant for the desulfuration process was measured by (Ma and Chambers, 1994). Timchalk et al. used Km1 = 2.86 µmol/l, however this value is not given in the publication by Ma and Chambers. In the present model Km1 = 3.23 µmol/l as measured by Ma and Chambers for female rats is used. The selected Km1-value is for females because the value for Km2 given by Timchalk et al. was for females as well.

Maximum velocity of metabolism, VmaxC1 and Vmax1 (µmol/hr/kg and µmol/hr)
Timchalk et al. (2002b) refer to (Ma and Chambers, 1994) concerning the data on VmaxC1 but they did not explain how they performed the calculation of Vmax to the right unit. Ma and Chambers have measured Vmax *in vitro* as nmol product formed/min/g wet weight equivalent of liver microsomes and VmaxC1 is given by Timchalk et al. in the unit µmol/hr/kg.

El-Masri et al. (1996) have shown how such data can be re-calculated. First step is to calculate a constant, f, expressing the amount of total protein in a liver:

$$f = \frac{mg\_microsomal\_protein}{nmol\_P450} * \frac{nmol\_P450}{g\_wet\_liver} * wet\_whole\_liver\_weight$$

using the following data:

- cytochrome P-450 content in liver tissue: 33.8 nmol P450/g wet liver (Igari et al., 1982)
- cytochrome P-450 content in liver microsomes: 0.695 nmol P450/mg microsomal protein (Igari et al., 1982)
- the actual wet weight of liver which in the present model is: Wl = PEl*BW/100 = 4 %* 0.25 kg/100 = 10 g wet liver (Timchalk et al., 2002b)

Insertion of these data gives:

$$f = \frac{mg\_microsomal\_protein}{0.695 nmol\_P450} * \frac{33.8 nmol\_P450}{g\_wet\_liver} * 10 wet\_whole\_liver\_weight = 486 mg\_protein$$

The second step is to calculate VmaxC:

$$V\max C = \frac{f * V\max\_measured}{body\_weight}$$

Ma and Chambers (1994) have measured the following values for Vmax1:

Male: 6.32 nmol product formed/min/g wet weight equivalent of liver microsomes

Female: 3.25 nmol product formed/min/g wet weight equivalent of liver microsomes

Calculation of VmaxC1 for male rats gives:

$$V\max C1 = \frac{486 mg\_protein * 6.32 nmol/min/g\_protein}{0.250 kg} * 10^{-3} g/mg * 10^{-3} \mu mol/nmol * 60 min/h$$

$$= 0.737 \mu mol/h/kg\_bw$$

Calculation of VmaxC1 for female rats gives:

$$V\max C1 = \frac{486 mg\_protein * 3.25 nmol/min/g\_protein}{0.250 kg} * 10^{-3} g/mg * 10^{-3} \mu mol/nmol * 60 min/h$$

$$= 0.379 \mu mol/h/kg\_bw$$

These results are not in accordance with the value of 80 µmol/h/kg bw calculated by Timchalk et al. (2002b). The calculations were also performed with different values of liver and body weight but it was not possible to verify the values given by Timchalk et al.

It was decided to use the values from Timchalk et al. (2002b) on VmaxC1 even though the data could not be verified.

In the model Vmax1 is the parameter used in the equations. This is calculated from VmaxC1 using equation (26).

Michaelis-Menten constant for dearylation (CPF -> TCP), Km2 (µM)

Michaelis-Menten constant for the dearylation process was measured by Ma and Chambers (Ma and Chambers, 1994). They found that Km2 was 15.6 ± 3.5 µM for males and 24.3 ± 8.1 µM for females. Timchalk and co-workers used Km2 = 24 µM with no explanation of choice of sex. Km2 = 24.3 µM is used in the present model.

Maximum velocity of metabolism, VmaxC2 and Vmax2 (µmol/hr/kg and µmol/hr)

Timchalk et al. refer to Ma and Chambers (1994) concerning the data on VmaxC2 but it has not been possible to figure out how they made the calculation. The calculations described for VmaxC1 were also performed for VmaxC2 but the results were not in accordance with the value calculated by Timchalk et al. It was decided to use the values from Timchalk et al. on VmaxC2 even though the data could not be verified.

In the model Vmax2 is the parameter used in the equations. This is calculated from VmaxC2 using equation (26).

Enzyme turnover rates for esterases (enzyme hydrolysed/hr)
Timchalk et al. (2002b) used (Maxwell et al., 1987) as reference for the enzyme turnover rates. However, Maxwell and co-workers used values from the literature:

- For acetylcholinesterase: $1.17*10^7 h^{-1}$ (Wang and Murphy, 1982), value verified in the literature.
- For butyrylcholinesterase: $1.71*10^5$ min^{-1} ($=1.03*10^7 h^{-1}$) (Main et al., 1972). Timchalk et al. and Maxwell et al. have used the turnover rate for acetylthiocholine ($6.10*10^4$ $min^{-1}=3.66*10^6 h^{-1}$) instead of that for butyrylcholinesterase measured by (Main et al., 1972). However, this may be a mistake. In the present model, TRBuChE = $1.71*10^5$ min^{-1} as measured by Main et al. was used.
- As reference for the value of carboxylesterase Maxwell and co-workers used (Ikeda et al., 1977). However it has not been possible to find the enzyme turnover rate in that paper. Therefore, it was not possible to verify the value used by Timchalk et al. However, the value was used in the present model.

Enzyme activity (µmol/kg tissue/hr)
Activity of acetylcholinesterase, total cholinesterase and carboxylesterase in control rat tissues were measured by Maxwell et al. (1987). Butyrylcholinesterase activity was calculated from these data as: butyrylcholinesterase = total cholinesterase – acetylcholinesterase. The activities in the paper by Maxwell et al. were given in (µmol/min/g tissue) and then converted to (µmol/hr/kg tissue) by Timchalk et al. (2002b) (i.e. multiplication with a factor: 60 min/h $*10^3$g/kg)

The values given by Timchalk et al. are in accordance with Maxwell et al. except for one case: for the enzyme activity of carboxylesterase in brain. Timchalk et al. used $6*10^3$ µmol/kg tissue/hr instead of $6*10^4$ µmol/kg tissue/hr. The value $6*10^4$ µmol/kg tissue/hr corresponds with the data in Maxwell et al. 1987 and was therefore used in the present model.

Enzyme degradation rate, Kd (hr^{-1})
The degradation rate for acetylcholinesterase was determined in plasma and brain for diisopropylfluorophosphate from literature data (Gearhart et al., 1990). Assuming that the degradation rate is the same for chlorpyrifos, the same levels were used for chlorpyrifos in the model for all tissues as well as for butyrylcholinesterase (Timchalk et al., 2002b). It is not clear on what basis Timchalk et al. decided to disperse the two measured Kd-values to the other organs. The same values for Kd was used in the present model

The degradation rate for acetylcholinesterase in RBC was estimated by Timchalk et al. based on RBC life-span.

The degradation rate for carboxylesterase in all tissues were found by Timchalk et al. by fitting to data from literature (Timchalk et al., 2002b).

Bimolecular inhibition rate, Ki (1/(µM*hr))
Timchalk and co-workers (2002b) determined the bimolecular inhibition rate for acetylcholinesterase and butyrylcholinesterase by fitting the model to experimental data. It is unclear from paper whether data on plasma or brain were used. They found that using *in vitro* data of Ki for acetylcholinesterase and butyrylcholinesterase in plasma (values found in literature) caused overestimation of the inhibition of both B-esterases in plasma *in vivo*. Therefore, they reduced the values of Ki to better describe the *in vivo* data (Timchalk et al., 2002b).

The bimolecular inhibition rate for RBC acetylcholinesterase was estimated by fitting the model to data from literature (Timchalk et al., 2002b).

The bimolecular inhibition rate for carboxylesterase for each tissue were estimated based on ratio of Ki for acetylcholinesterase and carboxylesterase using data from Gearhart et al. (1990) and Timchalk et al. (2002b):

$$\text{Ki\_CaE} = \frac{\text{Ki\_CaE\_from\_Gearhart}}{\text{Ki\_AChE\_from\_Gearhart}} * \text{Ki\_AChE\_from\_Timchalk}$$

$$= \frac{1.10(\mu M/h)^{-1}}{14.16(\mu M/h)^{-1}} * 243(\mu M/h)^{-1} = 18.9(\mu M/h)^{-1} \cong 20(\mu M/h)^{-1}$$

Reactivation rate, Kr (hr^{-1})
The reactivation rate for acetylcholinesterase was determined in rat brains by Carr and Chambers (1996). Data were not available for butyrylcholinesterase and carboxylesterase, therefore the reactivation rate for these were set equal to Kr for acetylcholinesterase (Timchalk et al., 2002b). Timchalk et al. wrote Kr1-4 = $0.0143 hr^{-1}$ but this must be a typing error since Carr and Chambers measured Kr1-4 = 0.01403 hr^{-1} (Carr and Chambers, 1996). This latter value was used in the present model.

The acetylcholinesterase was measured in RBC by Timchalk and co-workers. The reactivation rate for RBC was determined by fitting to experimental data and set to 0.04 hr^{-1} (Timchalk et al., 2002b).

Aging rate, Ka (hr^{-1})
The aging rate was measured for chlorpyrifos-oxon interaction with acetylcholinesterase in rat brains by Carr and Chambers (Carr and Chambers, 1996). Ka for butyrylcholinesterase and carboxylesterase were not available and were therefore set equal to the rate measured for acetylcholinesterase (Timchalk et al., 2002b)

Michaelis-Menten constants for CPF-oxon -> TCP in liver, Km3 (µM), and for CPF-oxon -> TCP in blood, Km4 (µM)
The Km values were calculated based on kinetic analysis for chlorpyrifos performed by Mortensen et al. (Mortensen et al., 1996). These values were used in Timchalk et al. (2002b). The parameters were optimized by (Timchalk et al., 2007b), and since the value of Km3, Vmax3, Km4 and Vmax4 from (Timchalk et al., 2007b) resulted in the best model output compared with the experimental data presented in (Timchalk et al., 2002b) it was decided to use the values from (Timchalk et al., 2007b). This topic is further explained in section 21.2.1.

VmaxC3 and Vmax3 for liver (µmol/hr/kg)
Mortensen et al. performed kinetic analysis for chlorpyrifos. Based on these data they calculated the velocity of chlorpyrifos-oxon hydrolysed to TCP in liver, Vmax3, to 47 µmol/min/mL or gram tissue (Mortensen et al., 1996). Recalculating the unit:

$$Vmax3 = 47\ \mu mol/min/mL\ tissue * 60\ min/hr * 10\ mL\ tissue = 28200\ \mu mol/hr$$

where the volume of a rat liver was calculated from the organ volume as percentage of body weight:

$$Vl = Vlc*BW/100 = 4\ \% * 0.25\ kg/100 = 10\ mL$$

Timchalk et al. used VmaxC3 = 74421 µmol/hr/kg. This can be recalculated to Vmax3 by equation (26):

$$Vmax3 = VmaxC3 * BW^{0.7} = 74421\ \mu mol/hr/kg * 0.25\ kg^{0.7} = 28200\ \mu mol/hr$$

These calculations show agreement between the data in (Mortensen et al., 1996) and in (Timchalk et al., 2002b). In a newer paper by Timchalk and co-workers (Timchalk et al., 2007b) another value of Vmax3 were used, eventhough the reference was also made to (Mortensen et al., 1996). There is no explanation in the reference by Timchalk and co-workers (2007b) concerning this discrepancy. Irrespective the discrepancy it was decided to use the parameter-value for VmaxC3 (as well as Km3, VmaxC4 and Km4) from (Timchalk et al., 2007b) since it resulted in the best model output compared with the experimental data presented in (Timchalk et al., 2002b). This topic is further explained in section 21.2.1.

VmaxC4 and Vmax4 for blood (µmol/hr/kg)
As for Vmax3 Mortensen et al. calculated the velocity of chlorpyrifos-oxon hydrolysed to TCP in blood, Vmax4, to 24 µmol/min/mL or gram tissue (Mortensen et al., 1996). Recalculation in the same way as for Vmax3 gives Vmax4 = 21600 µmol/hr (Vmax4 = 24 µmol/min/mL tissue * 60 min/hr * 15 mL tissue = 21600 µmol/hr, where Vbl = Vblc*BW/100 = 6 % * 0.25 kg/100 = 15 mL). This corresponds with VmaxC4 = 57003 µmol/hr/kg (Vmax4 = 57003 µmol/hr/kg * 0.25 $kg^{0.7}$ = 21600 µmol/hr).

These calculations show agreement between the data in (Mortensen et al., 1996) and in (Timchalk et al., 2002b). However, as described for Vmax3 (and in section 21.2.1) Timchalk and co-workers (2007b) presented other values for the metabolic rate constants in a more recent paper (Timchalk et al., 2007b), and these values resulted in better model output compared with the experimental data presented in (Timchalk et al., 2002b). Therefore, it was decided to use the metabolic rate constants (incl. Vmax4) from (Timchalk et al., 2007b).

Volume of distribution, Vd (l)
Volume of distribution was calculated by Timchalk et al. from unpublished data (Timchalk et al., 2002b).

1. order elimination constant, Ke (hr^{-1})
The first order elimination constant was calculated by Timchalk et al. from unpublished data (Timchalk et al., 2002b).

Table 8. Parameter values used in the rat and human models for chlorpyrifos and chlorpyrifos-oxon

Parameter	Abbreviation	Rat	Human
Absorption in stomach (hr^{-1})	KaS	0.01	0.01
Absorption in intestine (hr^{-1})	KaI	0.5	0.5
Transfer stomach-intestine (hr^{-1})	KsI	0.5	0.5
Fractional absorption (%)	Fa	0.8	0.72
Body weight (kg)	BW	0.25	70
Molecular weight of CPF (mg/μmol)	Mc	0.35	0.35
Weight of brain as percentage of body weight (%)	PEbr	1.16	2
Weight of liver as percentage of body weight (%)	PEl	4	2.57
Weight of rapidly perfused tissue as percentage of body weight (%)	PEr	3.88	5.48
Weight of fat as percentage of body weight (%)	PEf	7	21.42
Weight of slowly perfused tissue as percentage of body weight (%)	PEs	68.66	43.71
Weight of diaphragm as percentage of body weight (%)	PEdi	0.3	0.3
Weight of blood as percentage of body weight (%)	PEbl	6	7.7
Cardiac output (l/hr)	QC	5.4	347.9
Blood flow in brain as percentage of cardiac output (%)	Qbrc	3	11.4
Blood flow in diaphragm as percentage of cardiac output (%)	Qdic	0.6	0.6
Blood flow in fat as percentage of cardiac output (%)	Qfc	9	5.2
Blood flow in liver as percentage of cardiac output (%)	Qlc	25	22.7
Blood flow in rapidly perfused tissue as percentage of cardiac output (%)	Qrc	47.96	39.6
Blood flow in slowly perfused tissue as percentage of cardiac output (%)	Qsc	14.4	20.5
Volume of brain as percentage of body weight (%)	Vbrc	1.16	2.14
Volume of liver as percentage of body weight (%)	Vlc	4	2.57
Volume of rapidly perfused tissue as percentage of body weight (%)	Vrc	3.88	5.48
Volume of fat as percentage of body weight (%)	Vfc	7	21.42
Volume of slowly perfused tissue as percentage of body weight (%)	Vsc	68.66	43.71
Volume of diaphragm as percentage of body weight (%)	Vdic	0.3	0.3
Volume of venous blood as percentage of body weight (%)	Vvc	4	5.7
Volume of arterial blood as percentage of body weight (%)	Vac	2	2
Volume of blood as percentage of body weight (%)	Vblc	6	7.7
Blood:brain partition coefficient for chlorpyrifos	PCbrc	33	33
Blood:diaphragm partition coefficient for chlorpyrifos	PCdic	6	6
Blood:fat partition coefficient for chlorpyrifos	PCfc	435	435
Blood:liver partition coefficient for chlorpyrifos	PClc	22	22
Blood:rapidly perfused partition coefficient for chlorpyrifos	PCrc	10	10
Blood:slowly perfused partition coefficient for chlorpyrifos	PCsc	6	6
Blood:blood partition coefficient for chlorpyrifos	PCbl	1	1
Plasma protein binding of chlorpyrifos	FBc	97	97
Michaelis-Menten constant for desulfuration (μM)	Km1	3.23	3.23
Velocity of CPF desulfuration to CPF-oxon in liver microsomes (μmol/hr/kg)	VmaxC1	80	80
Michaelis-Menten constant for dearylation (μM)	Km2	24.3	24.3
Velocity of CPF dearylation to TCP in liver microsomes(μmol/hr/kg)	VmaxC2	273	273
Blood:brain partition coefficient for chlorpyrifos-oxon	PCbro	26	26
Blood:diaphragm partition coefficient for chlorpyrifos-oxon	PCdio	4.9	4.9
Blood:fat partition coefficient for chlorpyrifos-oxon	PCfo	342	342
Blood:liver partition coefficient for chlorpyrifos-oxon	PClo	17	17
Blood:rapidly perfused partition coefficient for chlorpyrifos-oxon	PCro	8.1	8.1
Blood:slowly perfused partition coefficient for chlorpyrifos-oxon	PCso	4.9	4.9
Blood:blood partition coefficient for chlorpyrifos-oxon	PCblo	1	1
Enzyme turnover rate of AChE (enzyme hydrolysed/hr)	TRAChE	$1.17*10^7$	$1.17*10^7$
Enzyme turnover rate of BuChE (enzyme hydrolysed/hr)	TRBuChE	$1.03*10^7$	$1.03*10^7$
Enzyme turnover rate of CaE (enzyme hydrolysed/hr)	TRCaE	109000	109000
Enzyme activity, brain AChE (μmol/kg tissue/hr)	EAChEbr	440000	440000
Enzyme activity, diaphragm AChE (μmol/kg tissue/hr)	EAChEdi	77400	77400
Enzyme activity, liver AChE (μmol/kg tissue/hr)	EAChEl	10200	10200
Enzyme activity, plasma (in human: RBC) AChE (μmol/kg tissue/hr)	EAChEp	13200	EAChErbc 13200
Enzyme activity, brain BuChE (μmol/kg tissue/hr)	EBuChEbr	46800	46800
Enzyme activity, diaphragm BuChE (μmol/kg tissue/hr)	EBuChEdi	26400	26400
Enzyme activity, liver BuChE (μmol/kg tissue/hr)	EBuChEl	30000	30000
Enzyme activity, plasma BuChE (μmol/kg tissue/hr)	EBuChEp	15600	$1.73*10^6$
Enzyme activity, brain CaE (μmol/kg tissue/hr)	ECaEbr	60000	6000
Enzyme activity, diaphragm CaE (μmol/kg tissue/hr)	ECaEdi	318000	318000
Enzyme activity, liver CaE (μmol/kg tissue/hr)	ECaEl	$1.94*10^6$	$1.94*10^6$
Enzyme activity, plasma CaE (μmol/kg tissue/hr)	ECaEp	456000	456000
Enzyme degradation rate, brain, AChE (hr^{-1})	Kd1	0.01	0.01
Enzyme degradation rate, diaphragm AChE (hr^{-1})	Kd2	0.01	0.01
Enzyme degradation rate, liver AChE (hr^{-1})	Kd3	0.1	0.1
Enzyme degradation rate, plasma AChE (hr^{-1})	Kd4	0.1	-
Enzyme degradation rate, RBC AChE (hr^{-1})	Kd5	0.008	$8*10^{-4}$
Enzyme degradation rate brain BuChE (hr^{-1})	Kd6	0.01	0.01
Enzyme degradation rate, diaphragm BuChE (hr^{-1})	Kd7	0.01	0.01
Enzyme degradation rate, liver BuChE (hr^{-1})	Kd8	0.1	0.1
Enzyme degradation rate, plasma BuChE (hr^{-1})	Kd9	0.1	0.0042
Enzyme degradation rate, brain CaE (hr^{-1})	Kd10	$7.54*10^{-4}$	$7.54*10^{-4}$
Enzyme degradation rate, diaphragm CaE (hr^{-1})	Kd11	0.001	0.001
Enzyme degradation rate, liver CaE (hr^{-1})	Kd12	0.001	0.001
Enzyme degradation rate, plasma CaE (hr^{-1})	Kd13	0.0033	0.0033
Bimolecular inhibition rate, all tissues, AChE (1/(μM*hr))	Ki1	243	243
Bimolecular inhibition rate, RBC AChE (1/(μM*hr))	Ki5	100	100
Bimolecular inhibition rate, all tissues BuChE (1/(μM*hr))	Ki6	2000	2000
Bimolecular inhibition rate, brain CaE (1/(μM*hr))	Ki10	20	20

Parameter	Abbreviation	Rat	Human
Bimolecular inhibition rate, diaphragm CaE (1/(μM*hr))	Ki11	20	20
Bimolecular inhibition rate, liver CaE (1/(μM*hr))	Ki12	20	20
Bimolecular inhibition rate, plasma CaE (1/(μM*hr))	Ki13	20	20
Reactivation rate (hr^{-1}), AChE	Kr1	0.01403	0.01403
Reactivation rate (hr^{-1}), RBC AChE	Kr5	0.04	0.04
Reactivation rate (hr^{-1}), BuChE	Kr6	0.01403	$1.43*10^{-3}$
Reactivation rate (hr^{-1}), CaE	Kr10	0.01403	0.01403
Aging rate (hr^{-1}), AChE	Ka1	0.0113	0.0113
Aging rate (hr^{-1}), BuChE	Ka6	0.0113	0.0113
Aging rate (hr^{-1}), CaE	Ka10	0.0113	0.0113

Parameter	Abbreviation	Rat	Human
Michaelis-Menten constant for CPF-oxon -> TCP in liver (μM)	Km3	577	577
Velocity of CPF–oxon hydrolysed to TCP in liver (μmol/hr/kg)	VmaxC3	38002	38002
Michaelis-Menten constant for CPF-oxon -> TCP in blood (μM)	Km4	464	464
Velocity of CPF–oxon hydrolysed to TCP in blood (μmol/hr/kg)	VmaxC4	40377	40377
Volume of distribution (l)	Vd	35	35
1. order elimination rate constant (hr^{-1})	Ke	0.017	0.017
Plasma protein binding of chlorpyrifos-oxon	FBo	98	98

21.2.1 PROBLEMS WITH THE METABOLIC PARAMETERS ON CHLORPYRIFOS-OXON

The toxicodynamic part of the model caused the most problems in developing the model in this project. The toxicokinetic part was fairly straight forward but when running the toxicodynamic part describing the metabolism by B-esterases the model output (e.g. the percentage of inhibition of acetylcholinesterase in a tissue) did not look like the graphs presented in (Timchalk et al., 2002b). The efforts done to solve this problem are illustrated in this section. When not otherwise stated the figures are model output from the present project.

Simulations of the inhibition of acetylcholinesterase using the parameter-values from (Timchalk et al., 2002b) showed levels of inhibition much lower than expected from that paper and from other references. As an example, simulation of inhibition of acetylcholinesterase in rat brain after exposure to chlorpyrifos at 5-100 mg/kg bw is shown in Figure 31A – to be compared with that of Timchalk et al. (2002b) in Figure 32.

When zooming in on the curve in Figure 31A (zoom not shown) it was seen that the shape of the curve was the same as in Figure 32 meaning that the equations were correct and the difference must be due to some of the parameters.

A: 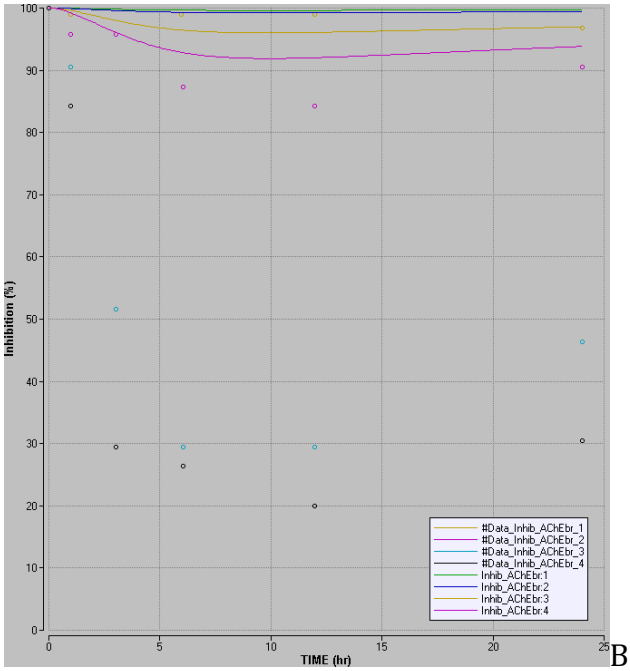

B: 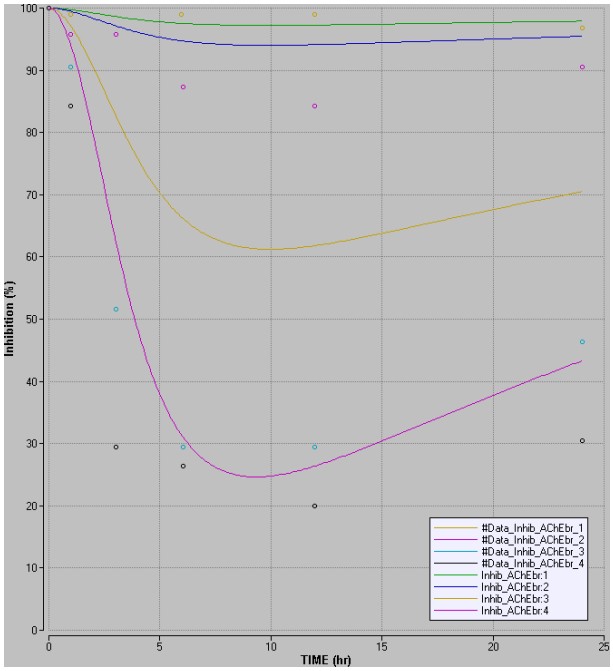

Figure 31. Inhibition (shown as % of control) of acetylcholinesterase in rat brain by chlorpyrifos. Curves are model simulations for gavage doses: 5 (Inhib_AChEbr:1), 10 (Inhib_AChEbr:2), 50 (Inhib_AChEbr:3) and 100 (Inhib_AChEbr:4) mg/kg. Data points (Data_Inhib_AChEbr) are experimental data from (Timchalk et al., 2002b), doses as for the curves, except that Data_Inhib_AChEbr:1 is 0-5 mg/kg. Values of VmaxC3, Km3, VmaxC4 and Km4 (see Table 9) from A: (Timchalk et al., 2002b) and B: (Timchalk et al., 2007b). Please note that there is no agreement between colours of data points and the corresponding simulation curves at the various concentrations in the figure.

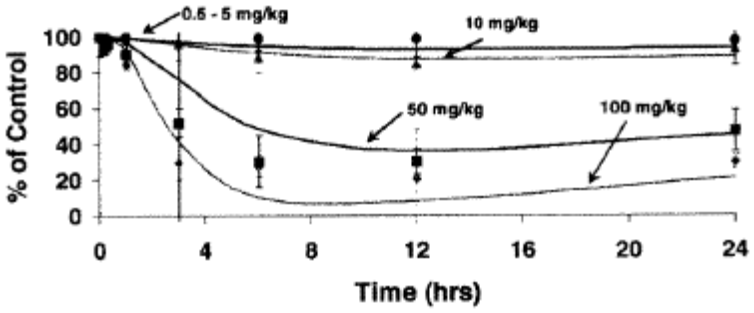

Figure 32. Inhibition of brain acetylcholinesterase in rats administered chlorpyrifos by gavage at the following dose levels: 0.5-5 (filled circle), 10 (filled triangle), 50 (filled square) and 100 mg/kg (filled diamond). Lines show the PBTK simulations and data points show the experimental data. Figure from (Timchalk et al., 2002b).

The model code and parameters were examined closely and it was deduced that the problem in the model was related to the low chlorpyrifos-oxon concentration in blood leaving the liver resulting in too low tissue concentrations in all other compartments (except liver) to execute

a visible effect on acetylcholinesterase inhibition. This means that the metabolism described in the model could be too fast to allow chlorpyrifos-oxon to distribute to the other compartments. Therefore, the metabolic rate constants Km3, VmaxC3, Km4 and VmaxC4 were examined more closely. In the more recent paper by Timchalk and co-workers (2007b) values of these parameters were used that differed from the values given in Timchalk et al. (2002b), see Table 9. In both papers reference was made to (Mortensen et al., 1996) for the VmaxC-values. The Michaelis-Menten constants Km3 and Km4 were "optimized" in (Timchalk et al., 2007b) and therefore changed compared to (Timchalk et al., 2002b).

Table 9. Values of VmaxC3, Km3, VmaxC4 and Km4 from (Timchalk et al., 2002b) and (Timchalk et al., 2007b). In both papers reference were made to Mortensen et al. for the VmaxC-values.

Parameter	**(Timchalk et al., 2002b)**	**(Timchalk et al., 2007b)**
Km3 (µmol/l), liver	240[1)]	577[2)]
VmaxC3 (µmol/h/kg), liver	74421[1)]	38002[1)]
Km4 (µmol/l), blood	250[1)]	464[2)]
VmaxC4 (µmol/h/kg), blood	57003[1)]	40377[1)]

[1)] "Fixed". Calculated by (Mortensen et al., 1996)

[2)] "Optimized parameter". Optimization performed by (Timchalk et al., 2007b)

When using the Timchalk et al. (2007) set of parameters from Table 9, keeping all the other parameters unchanged the model presented a picture (see Figure 31B) much more similar to Timchalk et al. (2002b), Figure 32.

The difference of the model predictions when using the two sets of parameters in Table 9 are also illustrated in Figure 33. The figure shows simulation of the inhibition of brain acetylcholinesterase (Figure 33A) and plasma cholinesterase (which is the sum of acetyl- and butyrylcholinesterase) (Figure 33B) in rats administered by gavage with chlorpyrifos at 100 mg/kg bw using VmaxC3, Km3, VmaxC4 and Km4 from the two references (Timchalk et al., 2002b) and (Timchalk et al., 2007b).

A: 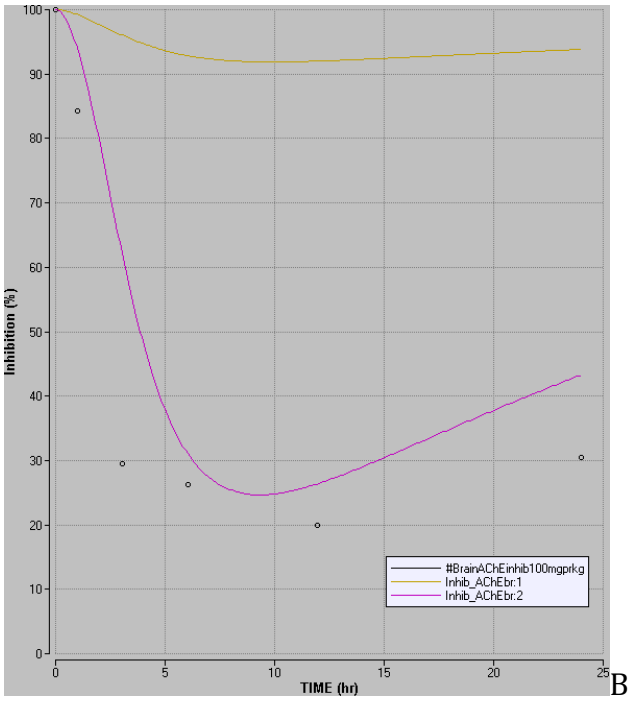

B: 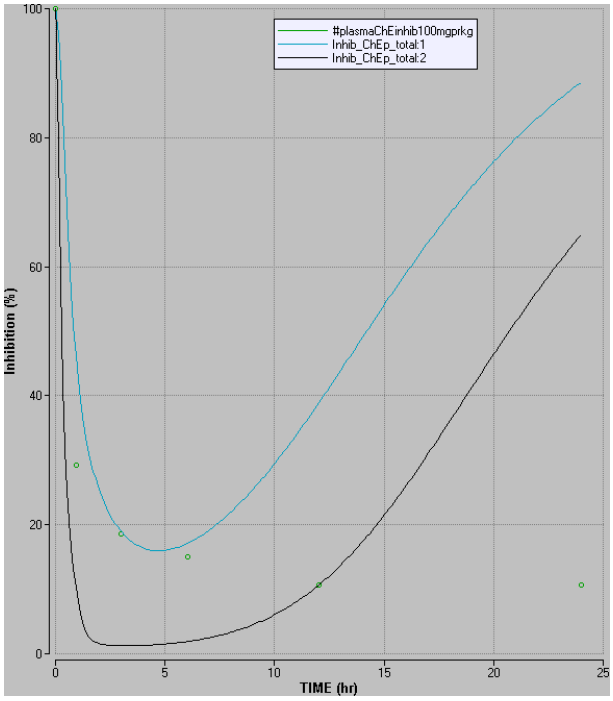

Figure 33. A: Model prediction of inhibition of brain acetylcholinesterase (shown as % of control) after a gavage dose of 100 mg/kg bw. Simulation using VmaxC3, Km3, VmaxC4 and Km4 values from (Timchalk et al., 2002b) (Inhib_AChEbr:1, yellow curve) and from (Timchalk et al., 2007b) (Inhib_AChEbr:2, red curve). B: Model prediction of inhibition of plasma cholinesterase (sum of acetyl- and butyrylcholinesterase) by chlorpyrifos (shown as % of control) after a gavage dose of 100 mg/kg bw. Simulation using VmaxC3, Km3, VmaxC4 and Km4 values from (Timchalk et al., 2002b) (Inhib_ChEp_total:1, blue curve) and from (Timchalk et al., 2007b) (Inhib_ChEp_total:2, black curve).
Data points in both figures are experimental data from (Timchalk et al., 2002b).

In Figure 34 the plasma cholinesterase inhibition (sum of acetyl- and butyrylcholinesterase) is shown. The same graphs presented by Timchalk et al. (2002b) are shown in Figure 35. The curves are very similar. However, it seems as the recovery of cholinesterase activity in Figure 34 is faster than in the simulations in Figure 35 presented by Timchalk et al. (2002b).

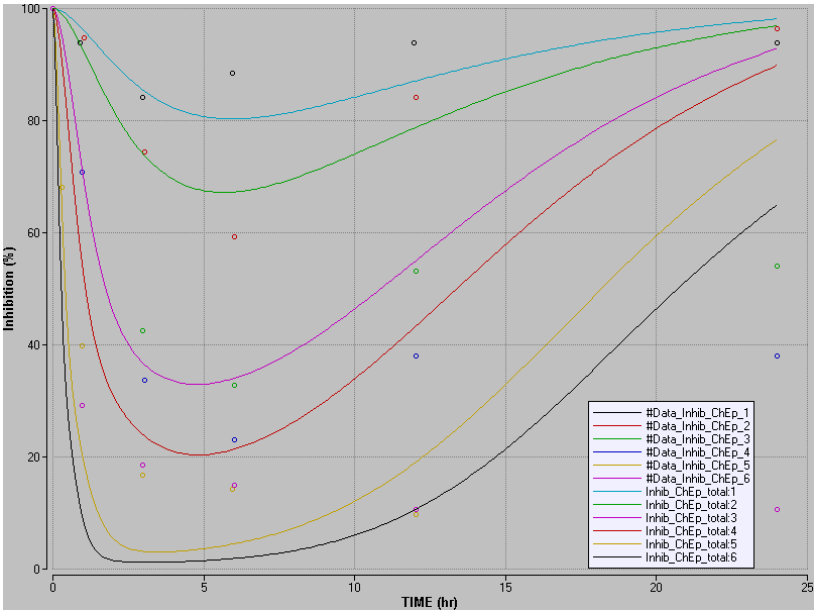

Figure 34. PBTK prediction of cholinesterase (sum of acetylcholine- and butyrylcholinesterase) inhibition in plasma (shown as % of control) after gavage doses: 0.5, 1, 5, 10, 50 and 100 mg/kg (Inhib_ChEp_total:1-6). Values of VmaxC3, Km3, VmaxC4 and Km4 were from (Timchalk et al., 2007b). Data points (Data_Inhib_ChEp_1-6) are experimental data from (Timchalk et al., 2002b). Please note that there is no agreement between colours of data points and the corresponding simulation curves at the various concentrations in the figure.

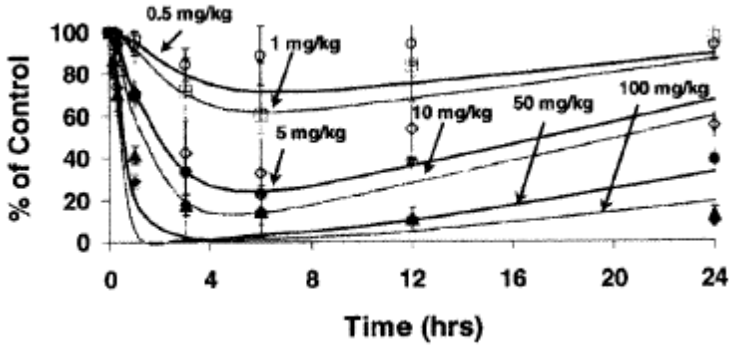

Figure 35. Inhibition of plasma cholinesterase in F344 rats administered chlorpyrifos by gavage at the following dose levels: 0.5 (open circle), 1 (open square), 5 (open diamond), 10 (filled circle), 50 (filled triangle) and 100 mg/kg (filled diamond). Lines show the PBTK simulations and data points show the experimental data. Figure from (Timchalk et al., 2002b)

The re-calculation of the Vmax data from (Mortensen et al., 1996) was shown in the previous section. That re-calculation supported the values for Vmax3 and Vmax4 that Timchalk and co-workers used in (Timchalk et al., 2002b). In (Timchalk et al., 2007b) they also referred to Mortensen et al. (1996). However, the values for Vmax3 and Vmax4 were different and thereby not in agreement with Mortensen et al. (1996). There is no explanation in the reference concerning this discrepancy. The simulations of acetylcholinesterase inhibition

using the parameters from 2007 were not quite the same as the ones shown in (Timchalk et al., 2002b) but they resulted in curves which were more similar to the curves shown in (Timchalk et al., 2002b) than simulations using values from the 2002 paper.

Irrespective of the discrepancy it was decided to use the parameter-values for VmaxC3, Km3, VmaxC4 and Km4 from Timchalk et al. (2007b) since they resulted in the best model output compared with the experimental data presented in Timchalk et al. (2002b).

22 DESCRIPTION OF THE PBTK/TD MODEL FOR CHLORPYRIFOS IN HUMANS

A set of parameters for a PBTK/TD model for chlorpyrifos in humans was presented by Timchalk and co-workers (2002b). The PBTK/TD model for humans was included in the present project in order to perform extrapolations from animals to humans as an important part of the risk assessment.

There is one major difference between the two models: acetylcholinesterase activity in plasma is not included in the model for humans. Timchalk and co-workers stated that human plasma do not contain acetylcholinesterase (with reference to (Ecobichon and Comeau, 1973)) but only butyrylcholine- and carboxylesterase (Timchalk et al., 2002b). This assumption is supported by (Testai et al., 2010) stating that >99 % of the human serum cholinesterase is butyrylcholinesterase. Therefore, the present model for humans is developed in the same way as was done by Timchalk et al. (2002b).

The species specific (physiological) parameters were changed from rats to humans. These includes weight (and volume) of tissue as percentage of body weight. The fractional absorption was also changed in the human model.

The enzyme activity for butyrylcholinesterase in plasma was decreased and the degradation rate and reactivation rate for butyrylcholinesterase was decreased (Timchalk et al., 2002b). The level of cholinesterase activity was supposed to be similar in rats and humans. In order to compensate for the lack of acetylcholinesterase the amount of butyrylcholinesterase in plasma was increased.

The enzyme degradation rate for acetylcholinesterase in RBC was lowered compared to the rat model (Timchalk et al., 2002b).

Table 10 shows the parameters that have been changed in the human model compared to the rat model in order to make a model that can describe the toxicokinetic and toxicodynamic in humans exposed to chlorpyrifos.

The values of parameters used in the present model on humans are shown in Table 8.

Table 10. Overview of those parameters that are changed in the PBTK/TD model for chlorpyrifos in humans compared to rats.

Parameter abbreviation	Parameter	Estimated / measured/ calculated/ fitted	Source	Assumptions /comments	Deviations from the model by (Timchalk et al., 2002b)
Fa	Fractional absorption (%)	Measured	(Nolan et al., 1984; Timchalk et al., 2002b)	Timchalk et al. have stated 0.72 % for humans. For humans Nolan et al. (1984) have stated 72 %, and therefore it seems as the data should have been presented as 72 %	
BW	Body weight (kg)			Calculated from the same equation as used to calculate QC (see below)	
PEbl, PEdi, PEf, PEl, PEr, PEs	Tissue weight as percentage of body weight (%)	Values form literature reported by Brown et al. (not all consistent with the values reported by (Timchalk et al., 2002b), see text). Tissue weights for diaphragm and blood were taken from Gearhart et al.	(Brown et al., 1997; Gearhart et al., 1994)	Tissue volume is equal to tissue weight (1:1). Volume of blood is equal to volume of venous and arterial blood: Vblc=Vvc+Vac.	Timchalk et al./present model: PEl: 3 / 2.57; PEr: 4 / 5.48; PEf: 21 / 21.42; PEs: 63 / 43.71; PEdi: 0.03 / 0.3; PEbl: 7 / 7.7.
Vlc, Vrc, Vfc, Vsc, Vdic, Vvc, Vac, Vblc	Tissue volumes as percentage of body weight (%)	Values form literature reported by Brown et al. (not all consistent with the values reported by (Timchalk et al., 2002b), see text). Tissue volumes for diaphragm and blood were taken from Gearhart et al.	(Brown et al., 1997; Gearhart et al., 1994)	Tissue volume is equal to tissue weight (1:1). Volume of blood is equal to volume of venous and arterial blood: Vblc=Vvc+Vac.	Timchalk et al./present model: Vlc: 3 / 2.57; Vrc: 4 / 5.48; Vfc: 21 / 21.42; Vsc: 63 / 43.71; Vdic: 0.03 / 0.3; Vblc: 7 / 7.7
QC	Cardiac output (l/hr)	Calculated from QC=15 l/h*(BW)^0.74 where BW=70kg	(Andersen et al., 1987)		
Qdic, Qrc, Qsc	Blood flow in diaphragm, rapidly and slowly perfused tissues as percentage of cardiac output (%)	Qdic (diaphragm) from (Gearhart et al., 1994). Q for rapidly perfused tissues, Qrc, calculated as sum of Q for heart, kidneys and hepatoportal system using data from (Brown et al., 1997). Q for slowly perfused tissues, Qsc, is calculated as 100-(sum of all other Qic)	(Brown et al., 1997; Gearhart et al., 1994)		Timchalk et al / present model: Qrc=40 / 39.6 Qsc=14 / 20.5
EAChErbc, EBuChEp	Enzyme activity for AChE in RBC, and BuChE in plasma (µmol/kg tissue/hr)	Value for EAChE in plasma used for EAChErbc. EBuChEp was optimised (together with reactivation rate for BuChE, Kr6) by Timchalk et al. by fitting to experimental data	(Timchalk et al., 2002b)	Present model: it was assumed that enzyme activity for AChE in humans RBC was equal to enzyme activity for AChE in plasma in rat. Uncertain whether Timchalk et al. did the same	See comments
Kd5, Kd9	Enzyme degradation rate for AChE in RBC and BuChE in plasma (hr^{-1})	Kd5 for RBC AChE: estimated by Timchalk et al. from RBC life-span. Kd9 for BuChE in plasma fitted by Timchalk et al. to data from literature	(Timchalk et al., 2002b)		
Kr6	Reactivation rate for BuChE (hr^{-1})	Kr6 was optimised (together with enzyme activity for BuChE in plasma) by Timchalk et al. by fitting to experimental data	(Timchalk et al., 2002b)		

Fractional absorption (%)
Nolan et al. have stated that the fractional absorption for chlorpyrifos, Fa, is 72 % for humans (Nolan et al., 1984). Timchalk et al. (2002b) stated that Fa was 0.72 % for humans, however, it should have been presented as 72 %.

Body weight (kg)
Timchalk et al. (2002b) did not directly state the size of body weight used in their model. They used a cardiac output of 347.9 l/h referring to the calculation-method presented by Andersen and co-workers (1987) (see below in the section: "Cardiac output") and this indicates a body weight of 70 kg for humans, which therefore was used in the present model for humans.

Tissue weight as percentage of body weight and tissue volumes as percentage of body weight (%)
The weight of tissues presented (Timchalk et al., 2002b) were taken from (Brown et al., 1997). However, several discrepancies were observed:

- The weight of slowly perfused tissues were calculated as the sum of muscle and skin using data from (Brown et al., 1997), PEs=40+3.71=43.71 %. Timchalk and co-workers stated 63%.
- The weight of rapidly perfused tissues was calculated as the sum of several organs (adrenals + gastrointestinal tract + stomach + small intestine + large intestine + heart + kidneys + lungs + pancreas + spleen + thyroid = 0.02 + 1.71 + 0.21 + 0.91 + 0.53 + 0.47 + 0.44 + 0.76 + 0.14 + 0.26 + 0.03 = 5.48 %) using data from Brown et al. (1997). Timchalk and co-workers used 4 %. The sum calculated above (5.48 %) was used in the present model.
- Brown et al. did not give a value for diaphragm and blood, therefore Timchalk and co-workers must have used another source. In the present model the value 0.3 % for diaphragm from (Gearhart et al., 1994) was used. The weight of blood for use in the present model were calculated as the sum of the weight of arterial and venous blood (=2+5.7=7.7 %) from (Gearhart et al., 1994). Timchalk and co-workers stated 0.03 % for diaphragm and 7 % for blood.

There are consistency between the values for weight of liver and fat given in (Brown et al., 1997) and (Timchalk et al., 2002b) and the differences are due to rounding off.

The sum of all weight of tissues gives 83.18 %. This leaves 16.8 % to bones, which is consistent with the 14.29 % stated by Brown and co-workers.

Cardiac output (l/hr)
Andersen and co-workers (Andersen et al., 1987) have calculated the cardiac output (QC) by the following equation:

$QC=15\ l/h/kg*(BW)^{0.74} = 15\ l/h/kg*(70\ kg)^{0.74} = 347.9\ l/h$

Blood flow in organ as percentage of cardiac output (%)
Timchalk and co-workers (2002b) stated that the blood flow in organs were taken from (Brown et al., 1997), however, the value for blood flow in diaphragm, Qdi, is not given by

(Brown et al., 1997). In the present model the value (0.3%) is taken from (Gearhart et al., 1994) whereas Timchalk et al. used 0.03 %.

Blood flow in rapidly perfused tissues, Qrc, was calculated as the sum of the blood flow for heart, kidneys and hepatoportal system using data from (Brown et al., 1997): Qrc=4+17.5+18.1=39.6% which is in good agreement with the 40% used in (Timchalk et al., 2002b).

Blood flow in slowly perfused tissues, Qsc, is supposed to account for blood flow in the rest of the body, i.e. Qsc=100-(sum of all other Qic)=20.5 %. This value was used in present model. Timchalk and co-workers used Qsc =14 % but they also had a separate value for blood flow in skin (5.8%), meaning that their total Qsc=19.8 % (i.e. almost the same value).

Enzyme activity for acetylcholinesterase in RBC and butyrylcholinesterase in plasma (µmol/kg tissue/hr)

As the acetylcholinesterase activity in plasma was assumed to be almost equal to zero and therefore was omitted in the model the amount of butyrylcholinesterase in plasma was increased in the model since the level of cholinesterase were supposed to be unchanged compared to the rat. This was done by increasing the enzyme activity for butyrylcholinesterase in plasma, and decreasing the degradation rate and the reactivation rate for butyrylcholinesterase as described above (Timchalk et al., 2002b).

Concerning the determination of the enzyme activity for butyrylcholinesterase in plasma there are inconsistencies between text and table in Timchalk et al. (2002b). In the text they explain that the enzyme activity for butyrylcholinesterase in plasma (together with the reactivation rate for butyrylcholinesterase, Kr6) was optimised against experimental data for butyrylcholinesterase inhibition in plasma. However, in the table with parameters they refer to a figure showing data on plasma concentrations of chlorpyrifos and TCP.

The enzyme activity for acetylcholinesterase in RBC was not stated by Timchalk et al. (2002b). This parameter should be used for calculation of the amount of esterase binding sites in RBC. It was not explained what value they used. In the present rat model, enzyme activity for acetylcholinesterase in RBC was set equal to enzyme activity for acetylcholinesterase in plasma. The same could not be done in the model for humans due to the lack of acetylcholinesterase in plasma. As no figure for enzyme activity for acetylcholinesterase in human plasma was available the value for acetylcholinesterase in rat plasma was used in the present model. However, it is negotiable whether this is biologically plausible.

Enzyme degradation rate for acetylcholinesterase in RBC and butyrylcholinesterase in plasma, Kd5 and Kd9 (hr^{-1})

The enzyme degradation rate for acetylcholinesterase in RBC, Kd5, was estimated by Timchalk et al. from the RBC life-span (Timchalk et al., 2002b).

Timchalk et al. estimated enzyme degradation rate for butyrylcholinesterase in plasma, Kd9, by fitting to experimental data from literature (Timchalk et al., 2002b).

Reactivation rate for butyrylcholinesterase, Kr6 (hr^{-1})
The reactivation rate for butyrylcholinesterase, Kr6, was optimised together with enzyme activity for butyrylcholinesterase in plasma by fitting to experimental data from a human study (Timchalk et al., 2002b).

Volume of distribution, Vd (l)
Volume of distribution was calculated by Timchalk et al. from data from literature (Timchalk et al., 2002b).

1. order elimination constant, Ke (hr^{-1})
The first order elimination constant was calculated by Timchalk et al. from data from literature (Timchalk et al., 2002b).

23 RESULTS FROM PBTK/TD MODELLING

In this section simulations performed in the present models will be compared with simulations and experimental data presented in (Timchalk et al., 2002b). This was done in order to evaluate the applicability of the model.

Subsequently it will be shown how a NOAEL for chlorpyrifos in rats and humans can be estimated from simulations in the two PBTK/TD models.

When not otherwise stated the figures are model output from the present project (all curves are on grey background).

Method for numerical integration
There are five numerical integration methods available in Berkeley Madonna. These are Euler' Method, Runge-Kutta 2, Runge-Kutta 4, Auto-stepwise and Rosenbrock (stiff). Berkeley Madonna uses Runge-Kutta 4 by default, however using this method in the present model resulted in an error message concerning "Floating-point exception(s): invalid overflow". This problem is described by so-called stiffness which can be solved by using the Rosenbrock (stiff) method in Berkeley Madonna (Yang and Lu, 2007). The maximum step-size was decreased in the rat model (decreased from 1 to 0.1) in order to make the curves smoother.

23.1 COMPARISON OF THE RAT MODEL WITH RESULTS FROM TIMCHALK ET AL.

In the following simulations of the concentrations of chlorpyrifos and chlorpyrifos-oxon in blood, inhibition of acetylcholinesterase in brain and inhibition of cholinesterase (acetylcholinesterase + butyrylcholinesterase) in plasma will be compared with experimental data as well as simulations by Timchalk and co-workers from (Timchalk et al., 2002b).

Concentration of chlorpyrifos and chlorpyrifos-oxon in blood
Simulations of the blood concentrations of chlorpyrifos after exposure to various dose levels are shown in Figure 36. The concentrations ranged from $4.6*10^{-2}$ to 1.4 μM.

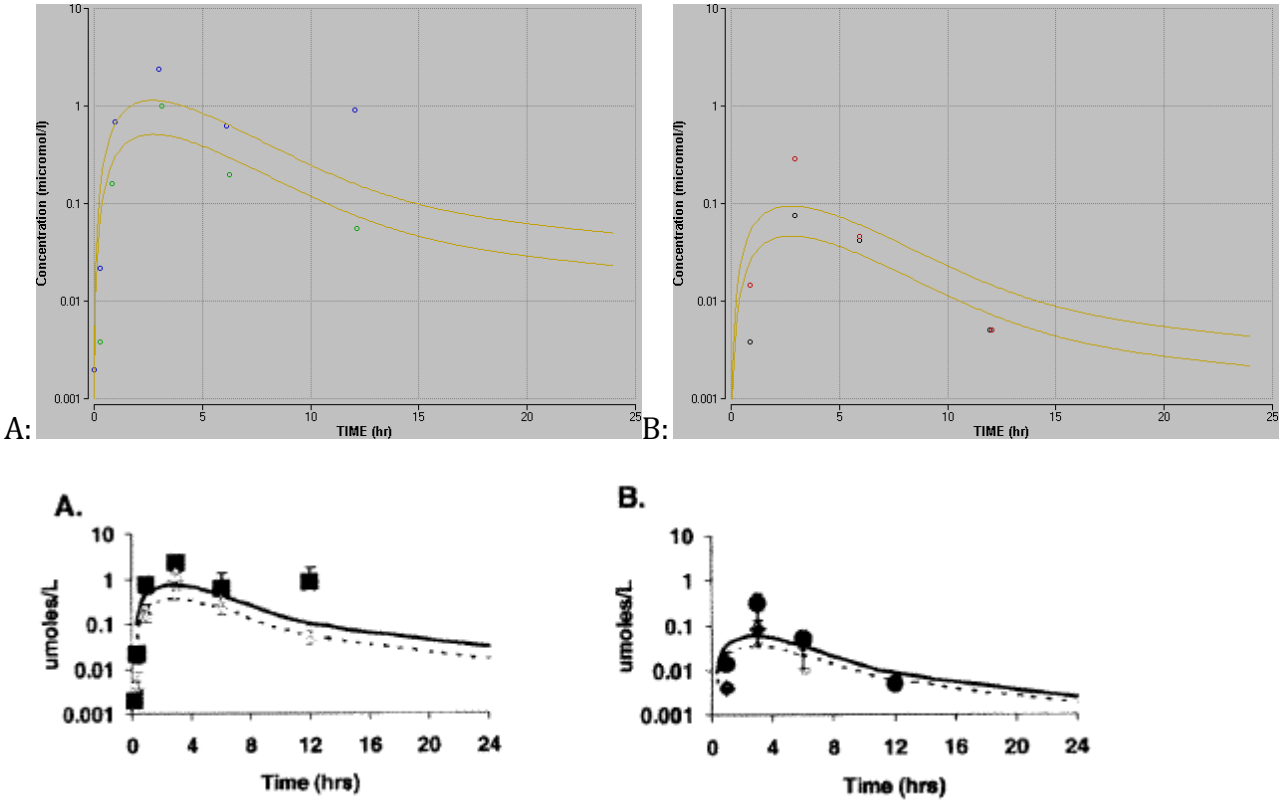

Figure 36. Concentration of chlorpyrifos in blood after gavage exposure of various dose levels. Upper figure is simulations from present project / lower figure from (Timchalk et al., 2002b). A: 50 (green/triangle) and 100 (blue/square) mg/kg bw/day and B: 5 (black/diamond) and 10 (red/circle) mg/kg bw/day. Data points in all figures are experimental data from (Timchalk et al., 2002b) and lines are simulations.

Visual inspection of the graphs shows good agreement between the simulations from the present project, data points as well as the simulations performed by Timchalk and co-workers. However, both models underestimate the peak value (maximum concentration) at all doses.

The concentrations of chlorpyrifos-oxon in blood (Figure 37) ranged from $6.8*10^{-4}$ to $1.9*10^{-2}$ µM. These concentrations are about 100 times less that the concentration of chlorpyrifos in blood. Timchalk and co-workers stated that the measured concentrations of chlorpyrifos-oxon in blood were in the range of $2*10^{-3}$ to $7*10^{-3}$ µM. Their simulations resulted in slightly higher concentrations for chlorpyrifos-oxon: $3*10^{-3}$ to $3.6*10^{-2}$ µM. Although not exactly similar the concentration levels simulated in the two models as well as the experimental data are comparative. The simulation curves also have the same shape as the curves for chlorpyrifos oxon-concentration presented in (Timchalk et al., 2007b).

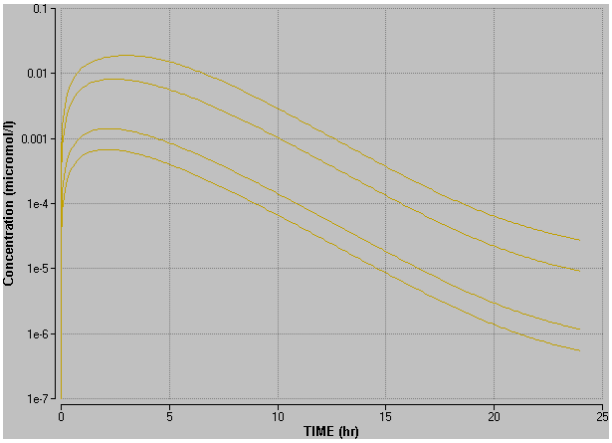

Figure 37. Simulation of chlorpyrifos-oxon concentration in blood after gavage exposure at (from bottom to top) 5, 10, 50, 100 mg/kg bw/day.

Inhibition of acetylcholinesterase

Figure 31B and 34 in the previous chapter show simulations of inhibition of acetylcholinesterase in brain and cholinesterase (acetylcholine- and butyrylcholinesterase) in plasma, respectively. These simulations should be compared with the experimental data as well as the simulations performed by Timchalk and co-workers shown in Figure 32 and 35.

The simulated curves of acetylcholinesterase inhibition in brain over time showed the same overall pattern as the experimental results. However, at some doses the inhibition was underestimated (10, 50 and 100 mg/kg bw/day), at 5 mg/kg bw/day a minor overestimation was seen but below 5 mg/kg/day the prediction was good.

Concerning the simulation of the sum of acetyl- and butyrylcholinesterase inhibition in plasma the results were not clear-cut (see Figure 34). At the two lowest doses (0.5 and 1 mg/kg bw/day) the simulations were good compared to the experimental data. At 5 and 10 mg/kg bw/day the estimation was good for the first 12 hr but after that the model underestimated the inhibition. At the two highest doses (50 and 100 mg/kg bw/day) the model overestimated the inhibition during the first 11-12 hr (actually, at 100 mg/kg bw/day the simulated curve goes straight through the data point at 12 hr), and thereafter the inhibition was underestimated.

For doses from 10-100 mg/kg bw the curves for inhibition of acetylcholinesterase in brain and plasma from 12-24 hr are far above the experimental data and it seems as the model overestimates the regeneration of cholinesterase.

Maximum plasma cholinesterase

Figure 38 shows the inhibition of acetylcholinesterase, butyrylcholinesterase and total cholinesterase (sum of acetylcholinesterase and butyrylcholinesterase) in plasma over a broad range of dose levels. The simulation in the present model results in a delayed increase in inhibition of cholinesterase compared to (Timchalk et al., 2002b). However, the overall course of the curves is consistent with the simulations performed by Timchalk and co-workers.

A: 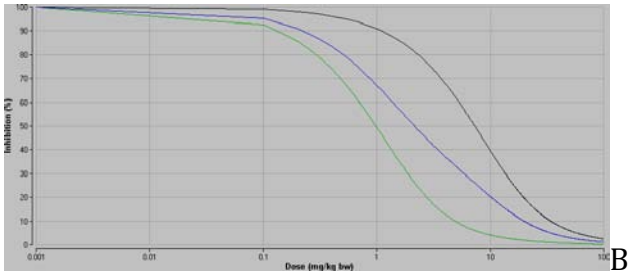 B: 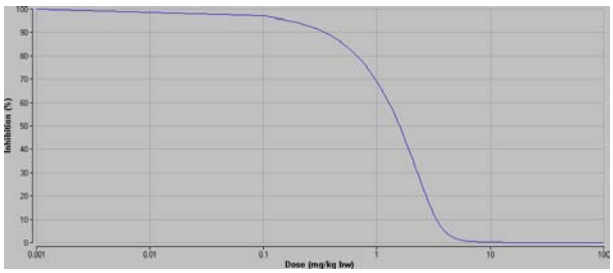

C: 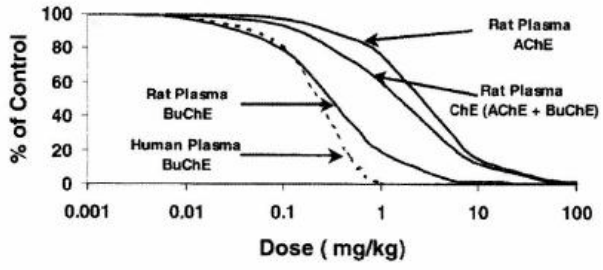

Figure 38. Dose response curves performed as parameter plots (1000 runs). A: simulated inhibition (% of control) of plasma acetylcholinesterase (black), butyrylcholinesterase (green) and total cholinesterase (sum of acetylcholinesterase and butyrylcholinesterase; blue curve) in rats after a single gavage dose in the range of 0.001-100 mg/kg bw. B: simulated inhibition of butyrylcholinesterase in humans after a single gavage dose in the range of 0.001-100 mg/kg bw. C: Simulated inhibition of the acetylcholine- and butyrylesterases in rats and humans in the range of 0.001-100 mg/kg bw. Figure from (Timchalk et al., 2002b).

Extent of inhibition

Gearhart et al. (1990) experimentally found (based on the sizes of the bimolecular rate constants) that the extent of inhibition of the three esterases were in the following order: butyrylcholinesterase >> acetylcholinesterase > carboxylesterase. The same result was found in the present model after a single gavage dose of 50 mg/kg bw/day.

Concerning the extent of inhibition in the different compartments, Timchalk et al. (2002b) found the following order: plasma > RBC≥ brain . This is similar to the finding in the present model: plasma ≥ RBC > brain.

Mass balance check

There is an overlay between simulated curves of the mass of chlorpyrifos and of the sum of the mass of TCP and chlorpyrifos-oxon meaning that the overall mass balance in the model is alright. There is only a slight difference between the curves for chlorpyrifos and for TCP (and this difference is accounted for by chlorpyrifos-oxon) demonstrating that the amount of free chlorpyrifos-oxon very quickly disappears in the model.

Conclusion on the comparisons

The results from the present model are in good agreement with the experimental data and the simulations performed by Timchalk et al. (2002b) especially concerning concentrations of chlorpyrifos and chlorpyrifos-oxon in blood.

The simulations of acetylcholinesterase in brain and cholinesterase in plasma are reasonably comparative with the experimental data as well as the simulations performed by Timchalk and co-workers (2002b). However, there is a tendency of underestimation, especially at higher doses and the recovery after inhibition also seems to be too fast compared with the experimental data.

23.2 COMPARISON OF THE HUMAN MODEL WITH RESULTS FROM TIMCHALK ET AL.

As for the rat model, simulations were made in order to compare the results with the experimental data and simulations in (Timchalk et al., 2002b). In the following examples of these simulations will be shown.

Concentration of chlorpyrifos in blood after poisoning

Figure 39A shows a time series of chlorpyrifos concentration in serum in a 25-year-old male after drinking a concentrated formulation of chlorpyrifos. Timchalk et al. found that it was possible to use the model to find the dose (180 mg/kg bw) resulting in the acute toxicological responses. In the present project concentrations of chlorpyrifos in blood were simulated (single bolus dose) for various dose values. The simulations showed that a smaller dose (140 mg/kg bw) would fit the data better by the present model, see Figure 39B.

A: 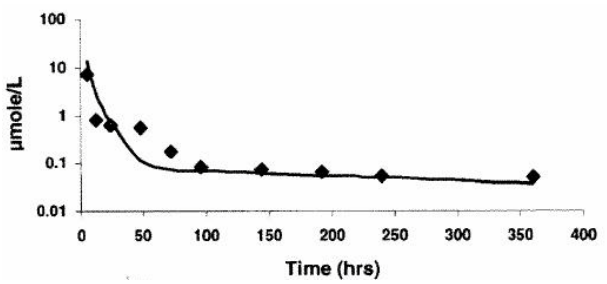

B: 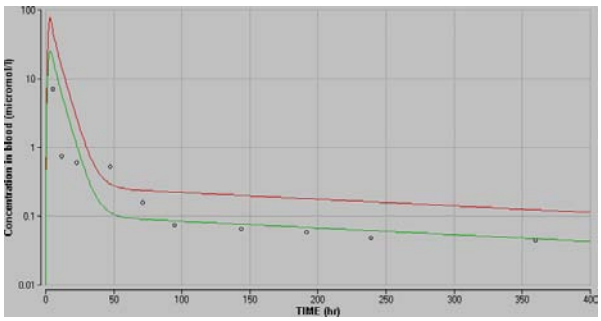

Figure 39. A: Chlorpyrifos in serum from a single poisoned victim that originally ingested a commercial product containing chlorpyrifos. Timchalk simulated that the dose was: 180 mg/kg bw/day. B: Simulation in the present model of chlorpyrifos in blood: 180 (red) and 140 (green) mg/kg bw/day. Data points are measured in victim, as reported by (Timchalk et al., 2002b)

Plasma concentration of TCP

Five volunteers were administered a single dose of 1 or 2 mg chlorpyrifos/kg bw and inhibition of acetylcholinesterase in plasma was measured. Experimental data on concentrations of TCP in plasma as well as simulation of this scenario is shown in Figure 40.

A: 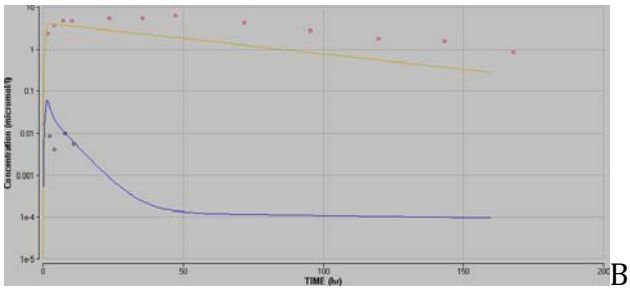 B: 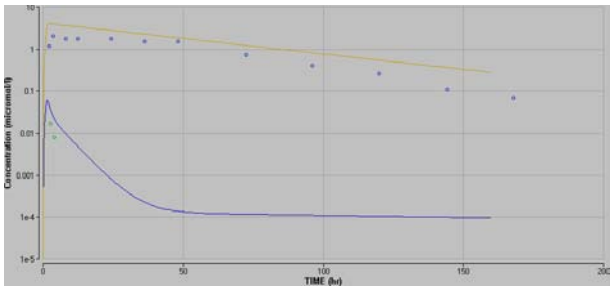

C: 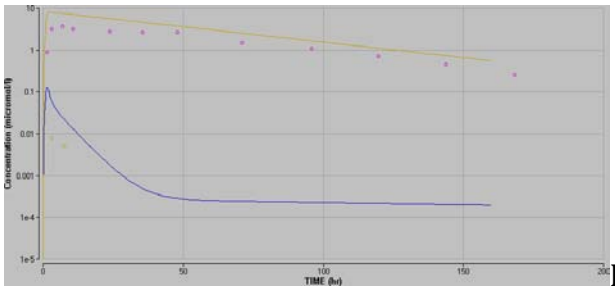 D: 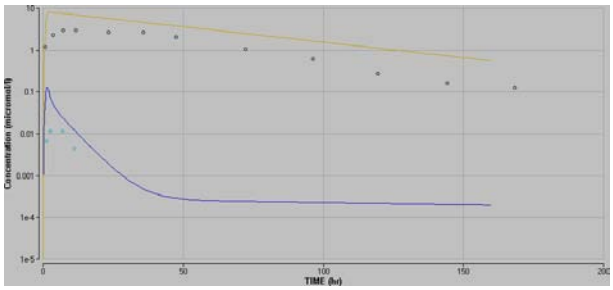

E: 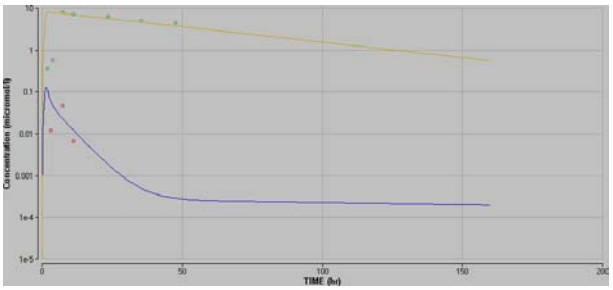

Figure 40. Concentrations of chlorpyrifos (lower curves and data points) and TCP (upper curves and data points) in plasma of volunteers after a single dose of chlorpyrifos at 1 mg/kg bw (A and B) or 2 mg/kg bw (C, D and E). Data points are experimental data from (Timchalk et al., 2002b) for human volunteers receiving a single oral dose. Simulations were performed as a single bolus dose.

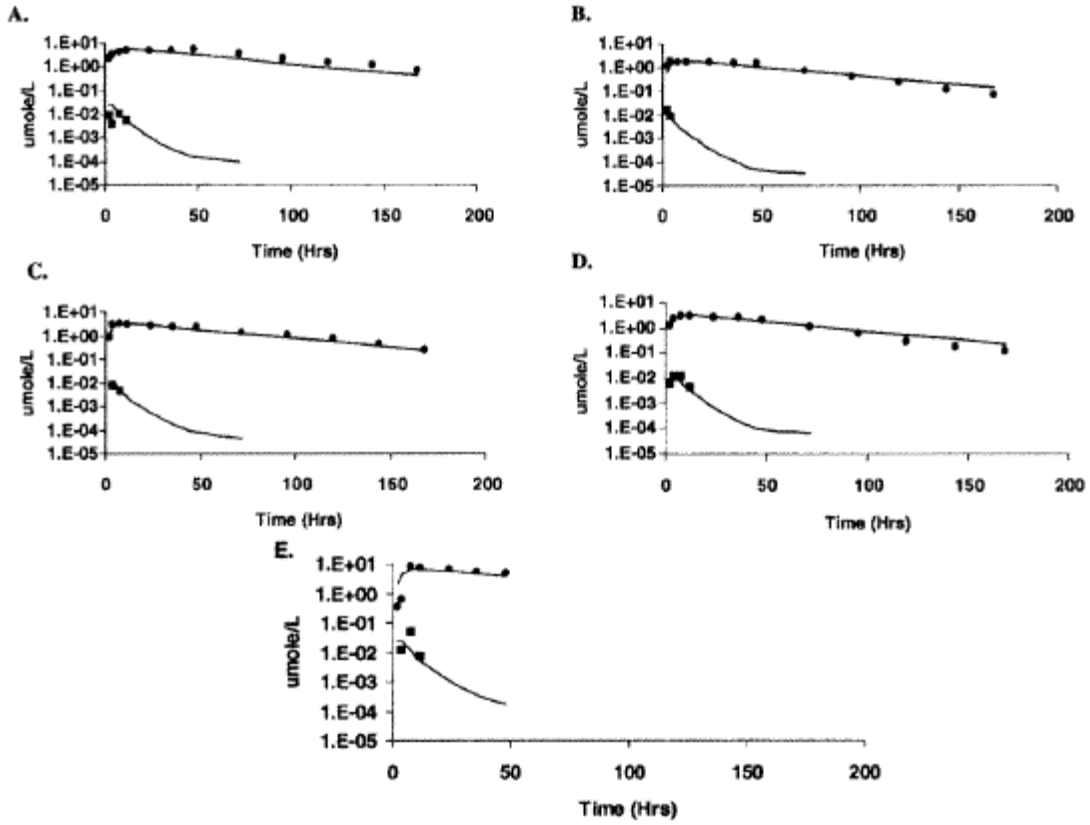

Figure 41. Experimental (data points) and model simulations (lines) of plasma concentrations of TCP (upper curves and data points) and chlorpyrifos (lower curves and data points) from five volunteers (A-E) after receiving a single dose of chlorpyrifos. A and B: 1 mg/kg bw. C, D and E: 2 mg/kg bw. Figure from (Timchalk et al., 2002b).

Comparison of experimental data and simulations in Figure 40 shows that the present model is making a good prediction for volunteer E. For volunteer A (1 mg/kg bw) the chlorpyrifos concentration was underestimated but in all other simulations the concentration of chlorpyrifos and TCP were overestimated. The overestimation of volunteer C and D was about a factor 2: simulation of 1 mg/kg bw in the model would better had described the experimental data of these two volunteers exposed to 2 mg/kg bw.

The simulations performed by Timchalk and co-workers (Figure 41) fitted the experimental data very well.

Inhibition of acetylcholinesterase in RBC

In the same study as described above inhibition of acetylcholinesterase in RBC were measured. The inhibition of acetylcholinesterase in RBC was close to zero. Timchalk and co-workers found that the slight inhibition found in the volunteers was only due to inhibition in volunteer E, see Figure 42.

Simulation of acetylcholinesterase inhibition in RBC in Figure 42A was about 3 % i.e. in good agreement with the results from (Timchalk et al., 2002b).

A: 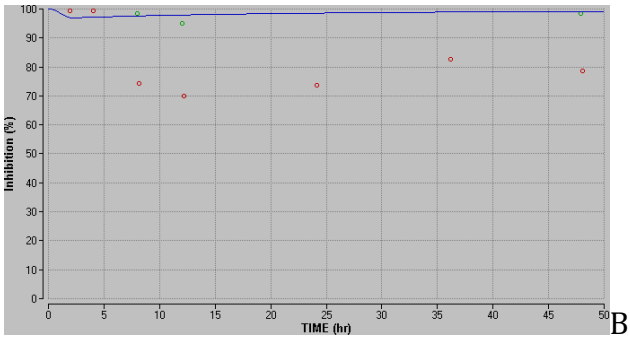

B: 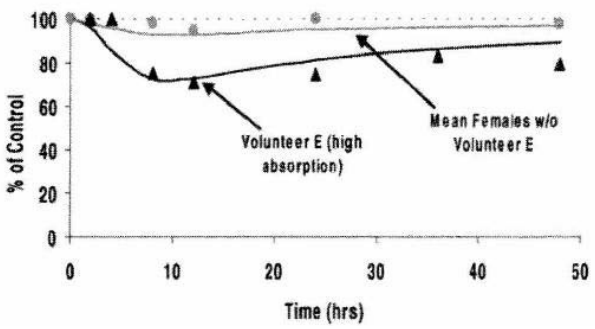

Figure 42. Inhibition of acetylcholinesterase (shown as % of control) in human RBC after an oral dose of 2 mg CPF/kg bw. A: Simulation by the present model (blue line) as single bolus dose. Green data points are mean of six females and red data points are volunteer E. Experimental data from (Timchalk et al., 2002b) (equal to the ones shown in B). B: Figure from (Timchalk et al., 2002b).

Concentration in blood of TCP

The blood concentration of TCP was simulated at 0.5 mg/kg bw given as a single bolus dose in humans, see Figure 43A. The present model failed to simulate the peak value of the TCP concentration in blood but the simulation was comparative with the experimental data from 20 hr. Figure 43B (upper curve) shows the same results from (Timchalk et al., 2002b). It is difficult to see from the figure whether their model also fails to simulate the peak concentration but it seems as the curve fits the data points slightly better.

A: 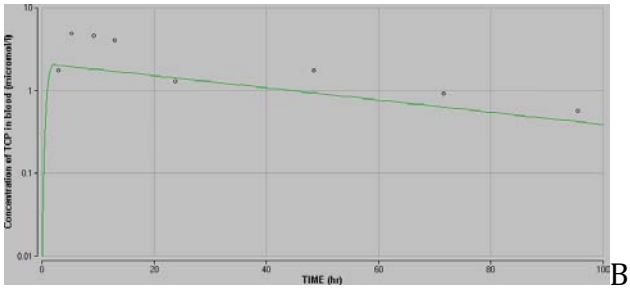

B: 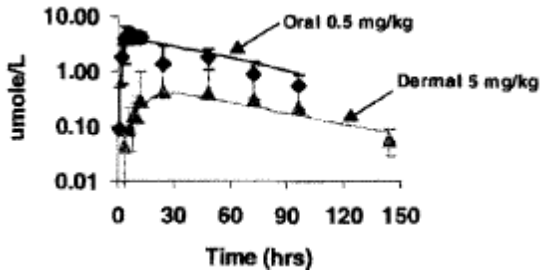

Figure 43. Blood concentrations (log scale) of TCP in human volunteers administered an oral dose of 0.5 mg/kg bw. A: Simulation by the present model performed as a single bolus dose (line), data points are experimental data as reported by Timchalk et al. B: Simulation and experimental data from (Timchalk et al., 2002b) (The lower curve on the graph is the concentration of TCP after a dermal dose of 5 mg/kg bw).

Extent of inhibition

The extent of inhibition of the three esterases in brain, plasma and RBC were found to be in the following order: butyrylcholinesterase >> acetylcholinesterase > carboxylesterase, i.e. the same order as in the rat model.

Concerning the extent of inhibition in the different compartments, the cholinesterase was inhibited in the following order of compartments: plasma BuChE > RBC AChE >> brain AChE.

Mass balance check
The mass balance was checked and found to be satisfying in the same way as for the rat model.

Conclusion on the comparisons
The results from the present model are in good agreement with the simulations performed by Timchalk et al. (2002b). The concentrations of chlorpyrifos and TCP in blood were described within a factor of 2 of the experimental data. There is a tendency that the model overestimates the concentration compared to the experimental data as well as the simulations performed by Timchalk and co-workers.

Only one simulation was performed to describe inhibition of acetylcholinesterase activity in RBC of humans. This simulation was performed at a low dose of chlorpyrifos. The result was comparable with the experimental data.

23.3 USE OF THE PBTK/TD MODELS

The process of estimating a NOAEL for chlorpyrifos in the developed PBTK/TD models for rats and humans including extrapolation between the species will be described in the following.

23.3.1 ESTIMATION OF NOAEL'S FOR CHLORPYRIFOS BY THE PBTK/TD MODEL

The FAO/WHO Joint Meeting on Pesticide Residues (JMPR) has established an acceptable daily intake (ADI) for chlorpyrifos of 0.01 mg/kg bw on the basis of a NOAEL of 1 mg/kg bw/day for inhibition of acetylcholinesterase in brain in studies in mice, rats and dogs (100-fold safety factor) and a NOAEL of 0.1 mg/kg bw/day for inhibition of acetylcholinesterase in RBC in humans (10-fold safety factor) (JMPR, 2000). In this chapter focus will be on three studies: two of the long-term rat studies and one study in humans.

Simulation of the scenarios in these three studies will be shown including evaluation of the NOAELs used by JMPR. Further it will be shown how to derive a NOAEL from the rat model and make extrapolation to humans. However, first it will briefly be described how to interpret the results of acetylcholinesterase inhibition in animals and humans.

23.3.1.1 INTERPRETATION OF CHOLINESTERASE INHIBITION

The primary end-points of concern in toxicological studies on compounds that inhibit acetylcholinesterase are inhibition of brain acetylcholinesterase activity and clinical signs (JMPR, 1999). JMPR also considers RBC acetylcholinesterase inhibition to be an adverse effect as it can be used as a biomarker of acetylcholinesterase activity in nerve synapses. However, the esterase activity in brain is of greater value in risk assessment than data on acetylcholinesterase inhibition in RBC. Acetylcholinesterase in RBC is not playing a role in the cholinergic transmission, however, the cholinesterase in RBC and in nervous system are considered biochemically identical (IPCS, 1990; JMPR, 1999).

Plasma cholinesterase is not regarded to play any role in cholinergic transmission and is not considered toxicologically relevant (IPCS, 1990).

JMPR considered that use of inhibition of acetylcholinesterase in RBC as a surrogate for peripheral target tissue effects is justified for acute exposures resulting in greater acetylcholinesterase inhibition in RBC than in the brain when data on inhibition of acetylcholinesterase activity in periferal target tissues are not available. They point out that in repeated-dose studies the acetylcholinesterase inhibition in RBC might overestimate the inhibition in peripheral tissues because the resynthesis of acetylcholinesterase in RBC is lower than in the nervous system. Therefore, they recommended in these cases to compare dose-response curves for inhibition of acetylcholinesterase in RBC and brain and the occurrence of clinical signs (JMPR, 1999).

Butyrylcholinesterase inhibition in plasma is not considered to be a sign of an adverse toxicological effect. But it is a useful tool for monitoring occupational exposure as it can be used as a biomarker (JMPR, 1999).

There are certain uncertainties in the measurement of inhibition of cholinestearase activity: timing of sampling, sample storage conditions (*ex-vivo* reactivation of cholinesterase inhibited by organophosphorus pesticides have been identified), conditions of the assay (especially important for cholinesterase activity in RBC because the resyntesis rate is smaller than in the nervous system) (JMPR, 1999).

JMPR considered that statistically significant inhibition of acetylcholinesterase above 20 % represent a clear toxicological effect. When a statistically significant inhibition of less than 20 % or statistically insignificant inhibition above 20 % is observed, a more detailed analysis of the data is necessesary (JMPR, 1999).

23.3.1.2 NO-EFFECT LEVEL IN RATS – RAT STUDY 1

One of the studies JMPR used for establishing the ADI for chlorpyrifos was a 2-year study in which groups of rats (25 male and 25 female per group) were given chlorpyrifos in the diet at doses of 0, 0.01, 0.03, 0.1, 1 or 3 mg/kg bw/day. In the following this study will be referred to as study 1. Cholinesterase activities in plasma and erythrocytes and were measured in 5-7 rats at 1 week, 1, 3, 6, 9, 12, 18 months and 2 year, and brain cholinesterase activities at 6 and 12 months and 2 year.

Plasma cholinesterase activity was significantly inhibited at 3 mg/kg bw: 20-40 % in males and 55-74 % in females. At 1 mg/kg bw the activity was less severely inhibited at the first months of dosing but from 6 months and onwards the activity was significantly inhibited by 18-38 % in males and 50-69 % in females (JMPR, 2000).

At 1 and 3 mg/kg bw/day the *erythrocyte (RBC) cholinesterase* activity was inhibited by 13-90 % and 60-100 %, respectively, and little effect were found at the lower doses. The *brain cholinesterase* activity was also significantly inhibited by 30-53 % after treatment at 3 mg/kg bw/day and to a lesser degree (3-16 %) at 1 mg/kg bw/day. Full restoration of cholinesterase activity was seen (JMPR, 2000).

The NOAEL for inhibition of cholinesterase activity in plasma and erythrocytes was 0.1 mg/kg bw/day based on significant inhibition at 1 mg/kg bw/day and the NOAEL for inhibition of acetylcholinesterase activity in brain was 1 mg/kg bw/day based on the significant inhibition at 3 mg/kg bw/day (JMPR, 2000).

Using the developed PBTK/TD model in the present model simulations of inhibition of acetylcholinesterase in rats at the dosage regimen in study 1 were performed as daily oral administration during 12 hr for a two year period (= 17520 hr).

Simulation of acetylcholinesterase inhibition in brain

In Figure 44 is shown the simulation of inhibition of acetylcholinesterase in rat brain after repeated dietary intake at the dosage regimen in the rat study 1 (0.01, 0.03, 0.1, 1 and 3 mg/kg bw/day for two years (17520 hr)). Acetylcholinesterase inhibition at the doses corresponding to the NOAEL (1 mg/kg bw/day) and lowest observed adverse effect level (LOAEL: 3 mg/kg bw/day) was around 1 % and 3-5 %, respectively. These levels of inhibition are lower than found in study 1: 3-16 % inhibition at 1 mg/kg bw/day and 30-53 % at 3 mg/kg bw/day (JMPR, 2000). The corresponding concentrations are shown in Table 11.

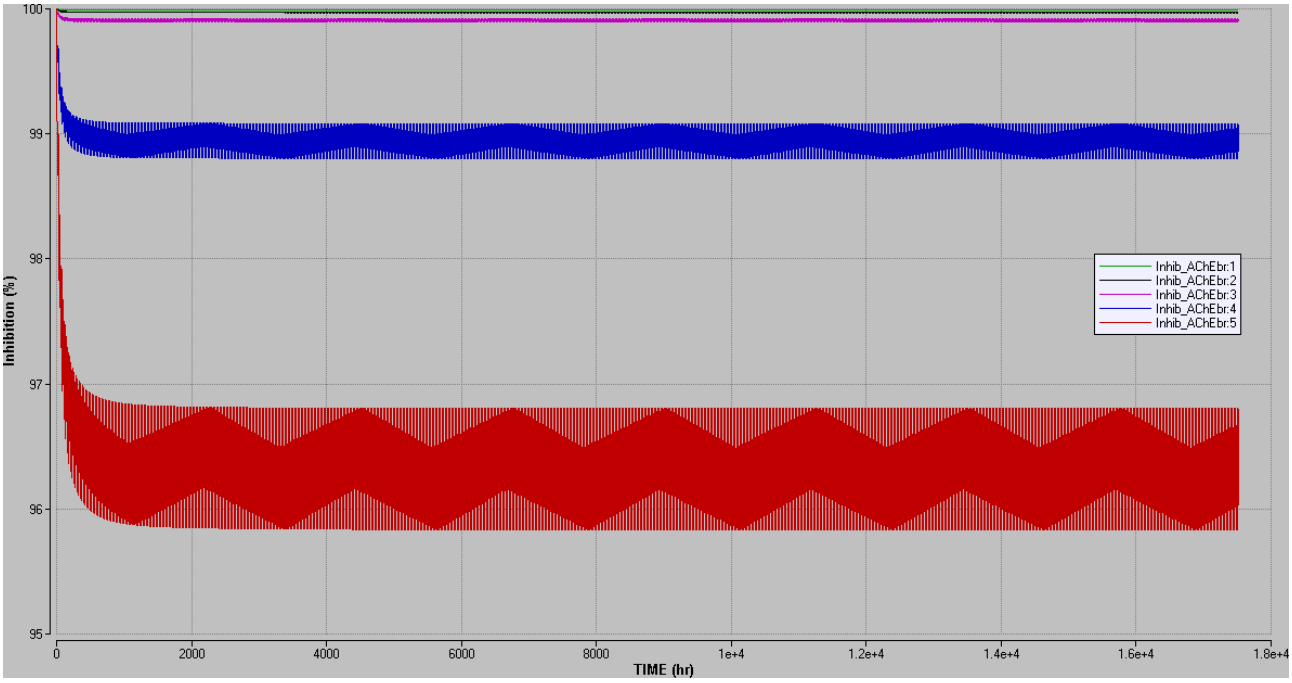

Figure 44. Simulation of inhibition of brain acetylcholinesterase (shown as % of control) in rats after repeated dietary intake of 0.01 (green), 0.03 (black), 0.1 (pink), 1 (blue) and 3 (red) mg/kg bw/day for two years (17520 hr). Please note that the y-axis is from 95 to 100 %.

Simulation of acetylcholinesterase inhibition in RBC

The inhibition of the acetylcholinesterase activity in RBC was greater than in brain, see Figure 45. At 1 mg/kg bw/day and 3 mg/kg bw/day the inhibition were 4-9 % and 16-24 %, respectively (whereas 13-90 % and 60-100 % respectively, in experiment). As for the acethylcholinesterase inhibition in brain these levels of inhibition are lower than found in study 1 (NOAEL for acetylcholinesterase inhibition in RBC was 0.1 mg/kg bw/day).

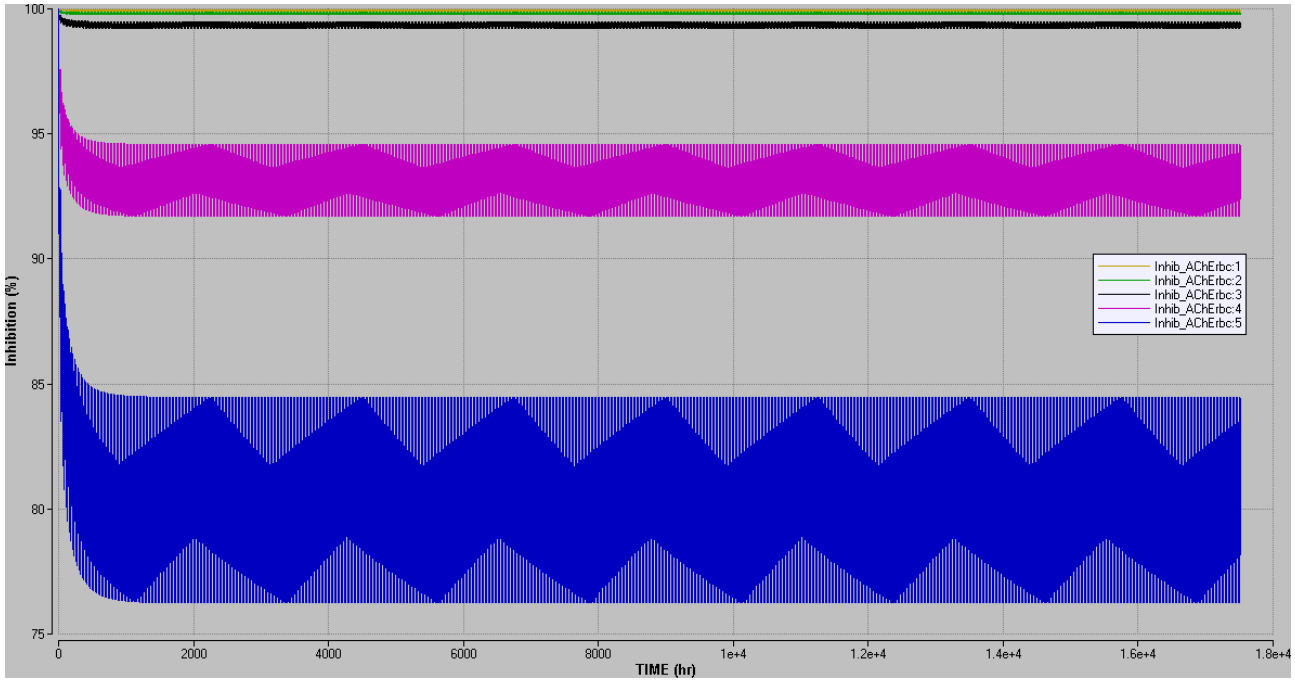

Figure 45. Simulation of inhibition of RBC acetylcholinesterase (shown as % of control) in rats after repeated dietary intake of 0.01 (yellow), 0.03 (green), 0.1 (black), 1 (pink) and 3 (blue) mg/kg bw/day for two years (17520 hr). Please note that the y-axis is from 75 to 100%.

Brain and red blood cell acetylcholinesterase

In Figure 44 and 45 the acetylcholinesterase inhibition is increased during the first dosages before a steady state level is reached. However, in all scenarios steady state is reached after 400 hr.

It seems as the model underestimates the acetylcholinesterase inhibition for both brain and RBC. As mentioned earlier JMPR considers that a 20 % inhibition of acetylcholinesterase represents a clear toxicological effect. Based on this assumption simulations were made in order to find the dose that corresponded to about 20 % inhibition. By using the feature "parameter plot" in Berkeley Madonna it is possible to get at plot of the result from each run as a single point on the graph over a range of parameter values. In this specific case the variable parameter is the dose administered orally (Oral_adm). In order to determine the dose corresponding to about 20 % inhibition of acetylcholinesterase, a parameter plot was performed using the "minimum" inhibition of acetylcholinesterase on the Y-axis. This is the lowest data points of the amplitudes seen in graphs like Figure 44 and 45, i.e. the maximum inhibition of acetylcholinesterase at the actual dose. The corresponding maximal concentrations of chlorpyrifos in blood was also calculated and plotted in the parameter plot.

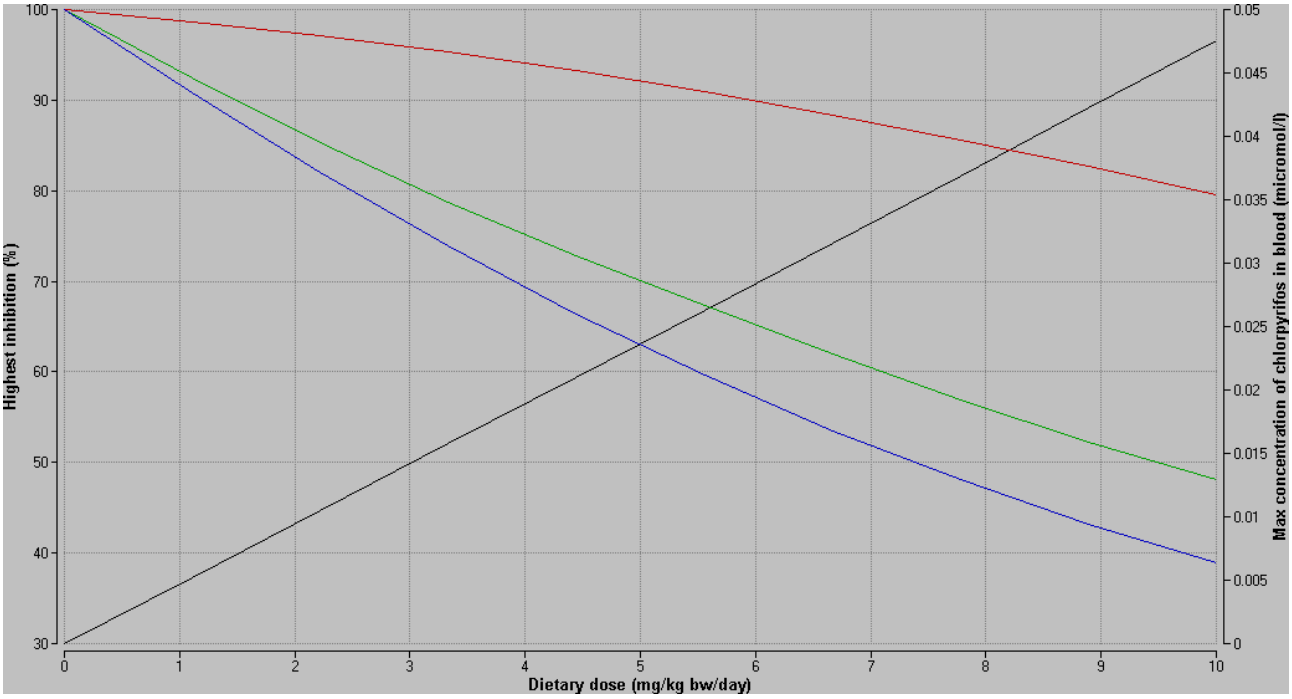

Figure 46. Parameter plot (10 runs). Simulation of the maximal inhibition of acetylcholinesterase (shown as % of control) in brain (red), RBC (blue) and plasma (green) as well as the maximal concentrations of chlorpyrifos in blood (black line, right Y-axis) in rats at various dietary dose-levels in the range from 0 to 10 mg/kg bw/day.

From the parameter plot is seen that the NOAEL for brain acetylcholinesterase activity (i.e. the dose corresponding to 20 % inhibition on the graph) would be between 9 and 10 mg/kg bw/day and for RBC the dose would be between 2 and 3 mg/kg bw/day.

Simulations of two years exposure to these doses showed that the NOAEL for brain acetylcholinesterase activity would be 9 mg/kg bw/day resulting in 13-18 % inhibition. For RBC the NOAEL was 2 mg/kg bw/day resulting in 10-17 % inhibition. The corresponding blood and brain concentrations of chlorpyrifos can be seen in Table 12.

Table 11. The results from the simulations of acetylcholinesterase inhibtion in brain and RBC after 2 years of exposure in rats (red) and humans (black). The three dose levels correspond to the NOAEL and LOAEL values found in study 1. All simulations were made as daily oral administration during 12 hr followed by 12 hr rest.

Dose (mg/kg bw/day)	Rats Inhibition AChE in brain (%)	Humans Inhibition AChE in brain (%)	Rats Inhibition AChE in RBC (%)	Humans Inhibition AChE in RBC (%)	Rats Concentration of CPF in blood and brain (µM)	Humans Concentration of CPF in blood and brain (µM)
0.1 (JMPR NOAEL for RBC in rat)	<1	<1	1	1-2	Up to 0.00047	Up to 0.0021
1 (JMPR NOAEL for brain in rat)	1	<1	4-9	38-40	Up to 0.0047	Up to 0.022
3 (JMPR LOAEL in brain in rat)	3-5	3-5	16-24	72-75	Up to 0.014	Up to 0.065

Table 12. The results from the simulations of acetylcholinesterase inhibition in brain and RBC after 2 years of exposure to rats (red) and humans (black). The dosage levels simulated are estimated as NOAEL from Figure 46 and 47 for rats and humans, respectively. The upper two lines are dose-levels determined as NOAEL values in the model in rats and the results of the extrapolation to humans. The two lines below are NOAEL values determined based on a parameter plot performed in the human model (see section 23.3.1.3). All simulations are made as daily oral administration (during 12 hr).

Dose (mg/kg bw/day)	Rats Inhibition AChE in brain (%)	Humans Inhibition AChE in brain (%)	Rats Inhibition AChE in RBC (%)	Humans Inhibition AChE in RBC (%)	Rats Concentration of CPF in blood and brain (µM)	Humans Concentration of CPF in blood and brain (µM)
2	2-3	1-3	10-17 (NOAEL in simulation)	60-64	Up to 0.0095	Up to 0.043
9	13-18 (NOAEL in simulation)	25-33	37-58	92-96	Up to 0.043	Up to 0.20
0.5	-	<1	-	18-19 (NOAEL in simulation)	-	Up to 0.011
7	-	14-19 (NOAEL in simulation)	-	89-93	-	Up to 0.15

Inhibition of plasma acetylcholinesterase

As mentioned before, the experimental result reported by JMPR for study 1 indicated a tendency of increased plasma acetylcholinesterase activity over time in that the activity at 1 mg/kg bw/day was low during the first six months but increased from six months and onwards to a level of 18-38 % in males and 50-69 % in females (JMPR, 2000). Such a course was not found in the model. In the simulation the first couple of dosages resulted in a slightly higher inhibition of plasma acetylcholinesterase than the subsequent dosages but a steady state level was reached after about 120 hr.

As seen in the parameter plot, Figure 46, a dosage of 3 mg/kg bw/day would result in about 20 % inhibition of acetylcholinesterase in plasma. The same result was achieved in the 2-year simulations: a dosage of 3 mg/kg bw/day resulted in an inhibition of up to 20 % with a high amplitude as the activity was in the range of 80-101 %. Comparing this with the experimental result (20-40 % in males and 55-74 % in females) showed that the model also underestimated the acetylcholinesterase inhibition in plasma but not as much as the inhibition of acetylcholinesterase in brain and RBC. However, model simulation of a single gavage dose of chlorpyrifos at 3 mg/kg bw showed an inhibition of acetylcholinesterase in plasma of 25 % indicating that the model might be better for prediction of dosages over a shorter time period.

As plasma is not regarded to be relevant in the cholinergic transmission (IPCS, 1990) it was decided not to make simulations of this endpoint in the following.

23.3.1.3 EXTRAPOLATION FROM RATS TO HUMANS

In order to find a NOAEL for chlorpyrifos in humans the results from the rat model were extrapolated by using the model for humans. Simulations were made for the dose-levels corresponding to the NOAEL found in study 1 (Table 11). The simulations were made as oral doses over a period of 2 years similar to the simulations in the rat model. Results from the simulations are shown in Table 11.

The simulated inhibition of acetylcholinesterase in brain was the same in both rats and humans at these dose levels, however, the simulated inhibition of acetylcholinesterase in RBC is much higher in humans than in rats. This is due to a lower degradation rate for acetylcholinesterase in RBC in rats.

In order to establish a NOAEL in humans a parameter plot were made in the human model (Figure 47) in the same way as described above for the rat model.

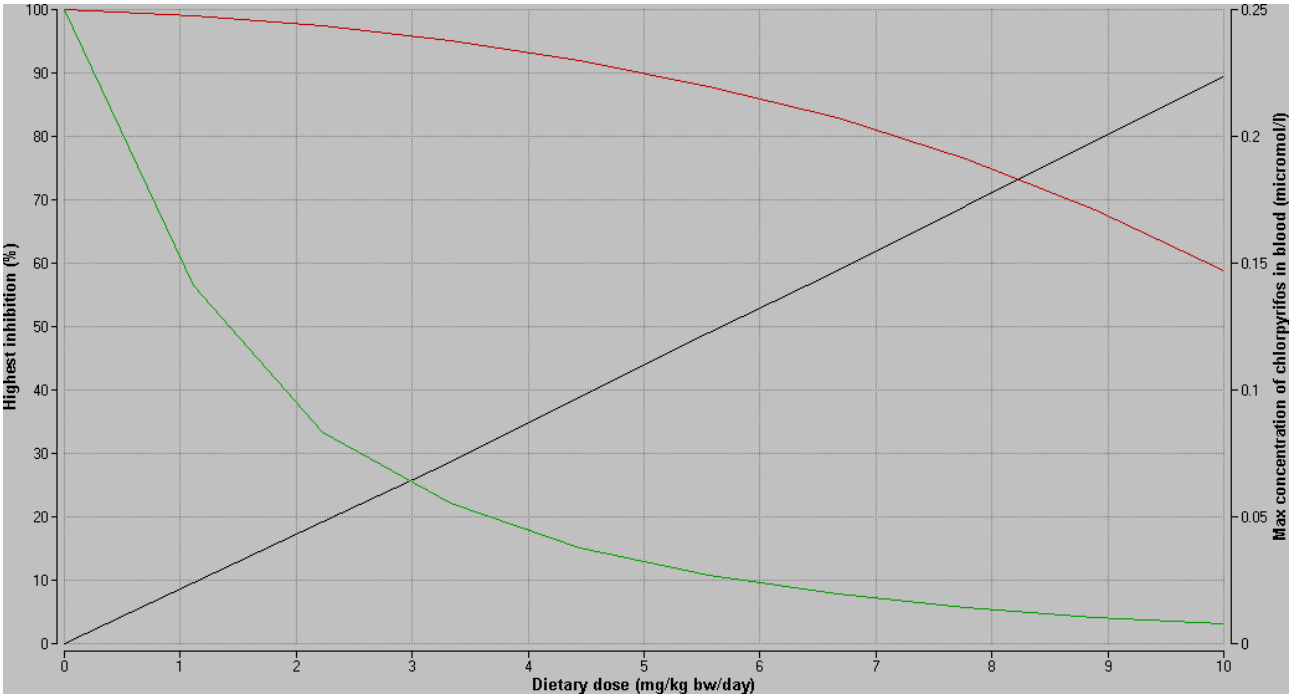

Figure 47. Parameter plot (10 runs). Simulation of the maximal inhibition of acetylcholinesterase (shown as % of control) in brain (red) and RBC (green) as well as the maximal concentrations of chlorpyrifos in blood (black line, right Y-axis) in humans at various dietary dose-levels in the range from 0 to 10 mg/kg bw/day.

From Figure 47 a 20 % inhibition of acetylcholinesterase in brain (i.e. the NOAEL) was found to occur after around 7 mg/kg bw/day and for RBC around 0.5 mg/kg bw/day. Simulations were made for acetylcholinesterase activity in human brain and red blood cell as well as chlorpyrifos concentration in blood and brain for these dose ranges. The simulations (and choosing a value with only one digit) confirmed these NOAELs. The inhibition of acetylcholinesterase and the chlorpyrifos concentration in blood are shown in Table 12.

The parameter plots of acetylcholinesterase activity in RBC in Figure 47 (human) shows a much steeper curve than in Figure 46 (rat). This illustrates the higher acetylcholinesterase inhibition in human RBC compared to rats.

23.3.1.4 NO-EFFECT LEVEL IN RATS – RAT STUDY 2

In another long-term study used by JMPR for establishing ADI, rats (60 males and 60 females per group) were given a diet containing chlorpyrifos at 0, 0.05, 0.1, 1 or 10 mg/kg bw/day for 2 year. This study will be referred to in the following as study 2. Cholinesterase activities in

plasma and erythrocytes were measured in ten rats of each sex per group at 6, 12, 18 and 24 months. At 12 and 24 month acetylcholinesterase activity was measured in half-brain samples examined at necropsies (JMPR, 2000).

At 10 mg/kg bw/day cholinesterase activities were inhibited in plasma (56-87 %), erythrocyte (20-40 %) and brain (57-61 %). At 1 mg/kg bw/day the inhibition in plasma was 39-71 % in males and 60-87 % in females; in erythrocytes it was 20-40 % in males and ≤22 % in females, and the activity of cholinesterase was not affected in brain. Doses of 0.05 and 0.1 mg/kg bw/day did not result in any treatment-related effects.

The NOAEL for inhibition of cholinesterase activity in erythrocytes was 0.1 mg/kg bw/day based on > 20 % or statistically significant inhibition at 1 mg/kg bw/day. The NOAEL for brain cholinesterase activity was 1 mg/kg bw/day based on the inhibition observed at 10 mg/kg bw/day (JMPR, 2000).

Simulation of the inhibition of acetylcholinesterase in brain, RBC and plasma as well as chlorpyrifos concentration in blood after a dosage regimen as described from study 2 is shown in Table 13 together with the experimental results.

Table 13. Experimental results (black) (JMPR, 2000) and results from the simulation of rat study 2 (blue). Dose levels at 0.1, 1 and 10 mg/kg bw/day, simulation for one year.

Dose (mg/kg bw/day)	**Rat Inhibition AChE in brain (%)**	**Rat Inhibition AChE in RBC (%)**	**Rat Inhibition AChE in plasma (%)**	**Rat Concentration in blood (µM)**
10, experiment	57-61	20-40	56-87	Not analysed
10, simulation	16-21	40-61	52 (amplitude: 48-106 % activity)	Up to 0.048
1, experiment (JMPR NOAEL for brain)	Not affected	Males: 20-40 Females ≤22	Males: 39-71 Females: 60-87	Not analysed
1, simulation	1-2	5-9	6-7	Up to 0.0047
0.1, experiment (JMPR NOAEL for RBC)	Not affected	Not affected	Not affected	Not analysed
0.1, simulation	<1	<1	<1	Up to $4.7*10^{-4}$

The model underestimated the inhibition of acetylcholinesterase, especially in brain. A small underestimation was seen of the inhibition of acetylcholinesterase in RBC and plasma. However, at the highest dose the inhibition of acetylcholinesterase in RBC was overestimated.

The deviation within and between the experimental results from rat study 1 and 2 are high, especially in the level of acetylcholinesterase inhibition in brain: 13-90 % in study 1 and 20-40 % in study 2. For study 2 the measured values of acetylcholinesterase activity were given in (JMPR, 2000). For comparison Figure 48 shows results from model simulations together with experimental data for this study scenario. The experimental data consist of one time series for males and one for females. These data points are plotted jointly in Figure 48. The PBTK/TD model is developed without any considerations concerning sex and the parameters were not selected to account for possible differences in sensitivity between the sexes.

A: 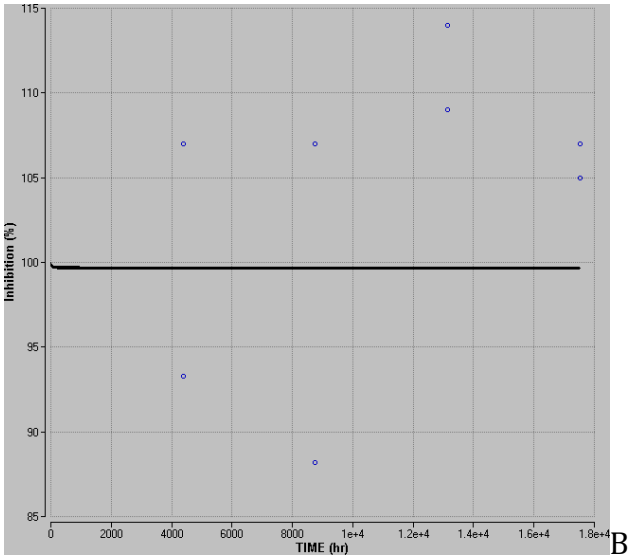

B: 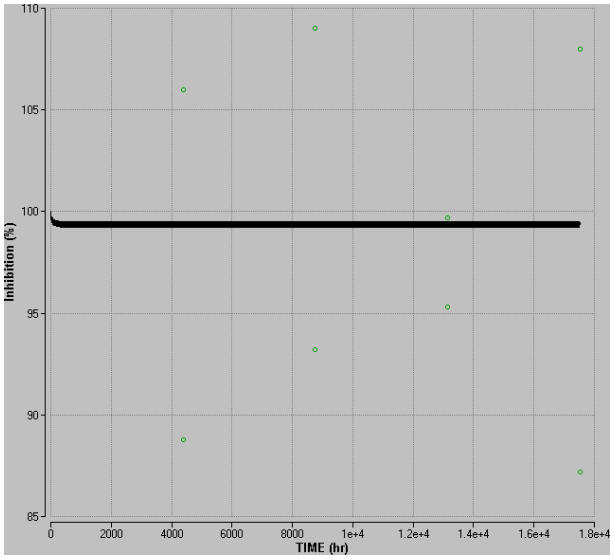

C: 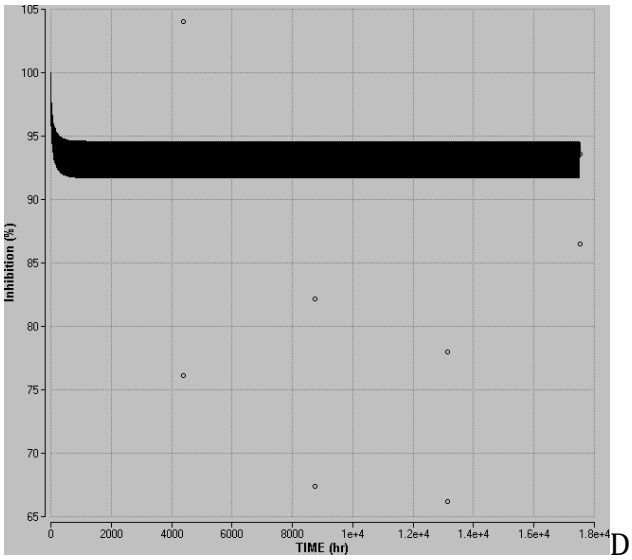

D: 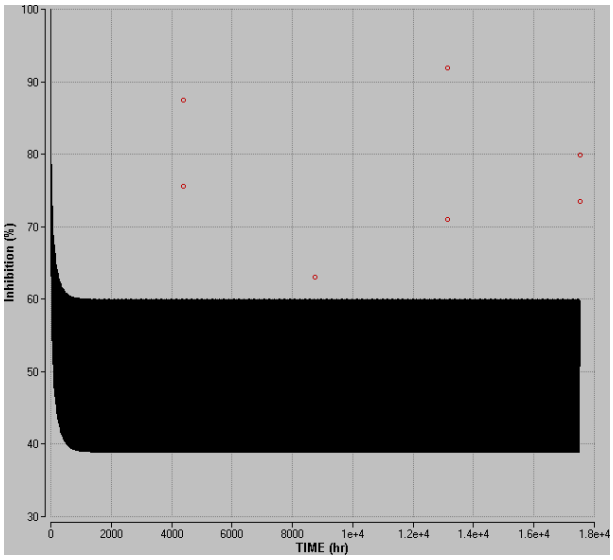

Figure 48. Inhibition of acetylcholinesterase (shown as % of control) in RBC in rats after doses at 0.05 (A), 0.1 (B), 1 (C) and 10 (D) mg/kg bw/day during two years. Curves are model simulations and data points are experimental values (for both males and females) as given in (JMPR, 2000). The width of the curves is due to fluctuations between night and day (eating and not eating periods). At 10 mg/kg bw/day one of data point are hidden behind the curve: 59.5 % at 8760 hr.

The variation of the experimental data is wide which is clearly seen from Figure 48. For the two lowest doses, the simulation lies within the range of the data points. At 1 mg/kg bw/day the model underestimates the inhibition whereas at 10 mg/kg bw/day the inhibition is overestimated.

23.3.1.5 NO-EFFECT LEVEL IN HUMANS

The ADI of 0.01 mg/kg bw for chlorpyrifos was also established based on a NOAEL of 0.1 mg/kg bw/day (highest dose tested) for inhibition of red blood cell acetylcholinesterase

activity found in a study on humans (10-fold safety factor). Groups of four healthy males received tablets with 0, 0.014, 0.03 or 0.1 mg CPF/kg bw/day for 48, 27, 20 and 9 days, respectively, with breakfast. A 70 % inhibition of plasma cholinesterase activity was measured and "runny nose, blurred vision and a feeling of faintness" were reported on day 9 in one of the men dosed with 0.1 mg/kg/day. Also "marked" inhibition of plasma cholinesterase activity was seen in the other men in this dosage group (JMPR, 2000).

No inhibition of erythrocytes cholinesterase or other treatment-related effects were seen in any of the men. At 0.03 mg/kg bw/day, more than 20 % inhibition of mean plasma cholinesterase was seen on days 16-20 of treatment. A 20 % inhibition of plasma cholinesterase was seen on day 13 at 0.014 mg/kg bw/day but no inhibition was seen on day 20 to 27. However, the statistically analysis only showed significant inhibition of mean plasma cholinesterase activity at 0.1 mg/kg bw/day (JMPR, 1973; JMPR, 2000).

Simulation of the NOAEL-study in humans described by JMPR

In the simulation scenario based on the two rat studies repeated dosage is simulated as an uptake through 12 hr followed by 12 hr sleep. In simulating the human study described above this is not the optimum conditions as the subjects in the experiment were given a tablet containing chlorpyrifos with breakfast for 9 to 27 days i.e. the exposure is more like a bolus dose. In order to simulate this scenario, another equation was introduced in the model, as described in section 21.1.1 (look for "Repeated bolus exposure"). The simulation of the experiment is shown in Figure 49. The inhibition of acetylcholinesterase in both brain and RBC were very small in the model simulation (below 0.1 and 0.4 %, respectively) as well as in the experiment.

A: 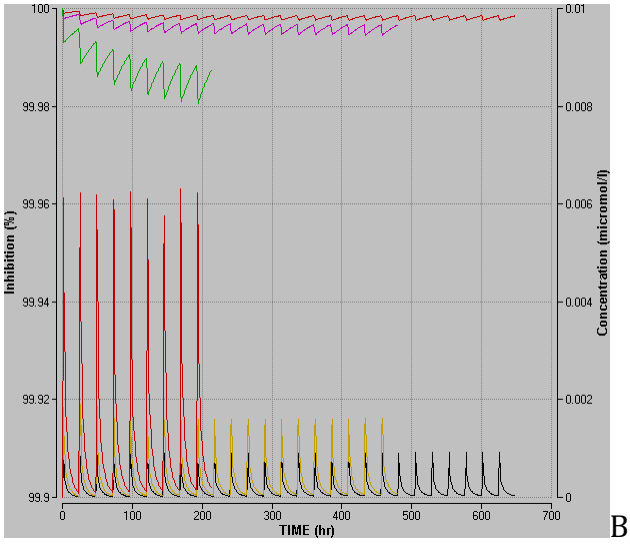

B: 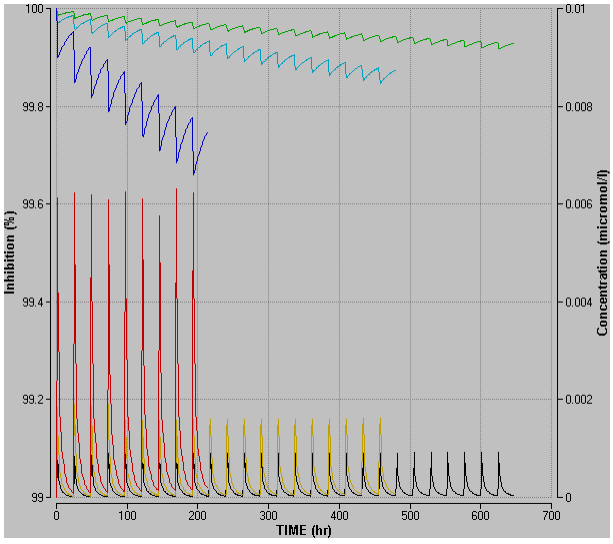

Figure 49. Simulation of brain and RBC acetylcholinesterase inhibition (shown as % of control) as well as concentration of chlorpyrifos in blood in humans after a daily bolus dose of 0.014, 0.03 or 0.1 mg CPF/kg bw/day for 27, 20 and 9 days, respectively. Lower part of the figures shows concentration of chlorpyrifos in blood (right Y-axes in both graphs) after dosage at 0.014 (black), 0.03 (yellow) or 0.1 (red) mg CPF/kg bw/day. A: Inhibition of acetylcholinesterase in brain 0.014 (red), 0.03 (pink) and 0.1 (green), B: Inhibition of

acetylcholinesterase in RBC 0.014 (green), 0.03 (turquoise) and 0.1 (blue). Please note that the inhibition of acetylcholinesterase in both graphs is very low.

Results of the simulations of inhibition of acetylcholinesterase in brain and RBC were the same whether the simulations were made as repeated bolus dose or as daily oral administration during 12 hr intervals. The only difference was the amplitude of the curves with the bolus dose scenario (not surprisingly) giving the highest fluctuations in the curves.

As explained earlier (in "Description of the PBTK/TD model for chlorpyrifos in humans") acetylcholinesterase activity for plasma was not incorporated in the model. Therefore, it is not possible to simulate this. However, it is possible to simulate the inhibition of butyrylcholinesterase in plasma, see Figure 50.

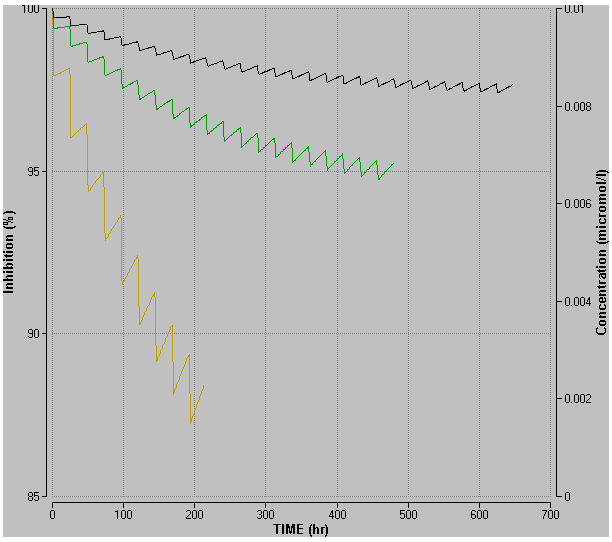

Figure 50. Simulation of plasma butyrylcholinesterase inhibition (shown as % of control) in humans after a daily bolus dose of 0.014 (black), 0.03 (green) or 0.1 (yellow) mg CPF/kg bw/day for 27, 20 and 9 days, respectively.

Comparison of the simulation with the experimental data reported by (JMPR, 2000) shows a large underestimation in the model. Butyrylcholinesterase activity is inhibited by 28 % in the model compared with up to 70 % for the experimental data at the highest dose. At 0.03 mg/kg bw/day the inhibition was simulated to be 13 % but it was more than 20 % in the study. At the lowest dose the inhibition increased to 6 % after 27 days but in the study a 20 % inhibition was found on day 13 and no inhibition on day 27.

24 DISCUSSION ON PBTK/TD MODELS

One of the objectives of this Ph.D.-project was to establish PBTK/TD models in order to improve methods for risk assessment of mixtures of chemicals. However, during the work it became obvious that the development of the model was more complicated than expected. Therefore, the focus changed to a critical examination of the PBTK/TD model on chlorpyrifos published by Timchalk et al. (2002b). This work revealed many problems and pitfalls especially concerning the parameters which will be discussed in section 24.1.

The other objective was to examine the applicability of PBTK/TD models in risk assessment of mixtures. However, it was not possible to develop new PBTK/TD models describing mixtures within the timeframe of the project. The advantages and disadvantages of their use in risk assessment will, however, be presented and discussed in section 24.2.

When a model is used in risk assessment it is very important to know the quality of the parameters used, including the justification of their use. This includes a comprehensive documentation of the modelling in order to make it possible for risk assessors to assess the quality of the model and for other scientists to reproduce the model. These requirements will be reviewed in section 24.3.

24.1 DISCUSSION OF THE MODELS FOR CHLORPYRIFOS IN RATS AND HUMANS IN THIS THESIS

It is clear from this thesis that it is not straightforward to reproduce a model published in literature. The model for chlorpyrifos was chosen because the publication seemed good at first sight – in fact it seemed to be one of the best described models available on pesticides. However, the work on re-building the model clearly showed that the authors of such publications should report their results in much more detail in order to enable colleagues to reproduce their work and e.g. evaluate part of it for further developing the model.

The development of the toxicodynamic part of the model (description of e.g. inhibition of acetylcholinesterase) was the most problematic. The difficulties arose due to problems with the values of some of the metabolic parameters (maximum velocity and Michaelis-Menten constants) because these parameters had a huge impact on the outcome of the toxicodynamic model. Figure 34 showing the simulated concentration of chlorpyrifos in blood could be made early on in this project whereas the PBTD part (which was dependent on the metabolic description) of the model caused a lot of trouble due to uncertainties in and unclear descriptions of the selection of appropriate parameters for the model.

In addition, several of the parameters used were absent in the literature and not determined by Timchalk and co-workers (2002b) in relation to their model development. Therefore, various assumptions had to be made in order to fill in the data gaps. Other parameters were not clearly defined and documented by Timchalk et al. Some of these parameters are discussed in this section focussing on the metabolic parameters.

A change in some of the parameters may result in outcome of the present model more similar to the experimental data. However, such a change needs to be biologically justified. The

justifications for changing the reactivation rate, degradation rate and bimolecular inhibition constants in the description of acetylcholinesterase will be discussed in section 24.1.2.

The usefulness of the present models for estimating a NOAEL for rats and humans will be discussed. Further, the overall outcome from the process of model development and the following visual evaluation of the models will be discussed followed by some concluding remarks on these models.

24.1.1 PROBLEMS WITH PARAMETERS

Many assumptions were made during the development of the PBTK/TD models not least in the selection of parameters. Some parameters are missing in the literature making it necessary e.g. to estimate them and to use data for other compounds than the actual compound. For example some parameters (e.g. enzyme turnover rates and degradation rate) were assumed to be equal for chlorpyrifos and diisopropylfluorophosphate.

Due to lack of data on chlorpyrifos-oxon the plasma protein binding for this compound was assumed to be slightly higher than for chlorpyrifos. Other parameters like the bimolecular inhibition rate, aging rate and reactivation rate were assumed to be the same for two or all three B-esterases due to lack of data on all esterases. However, it was not evaluated by Timchalk et al. (2002b) whether these assumptions were appropriate.

Some of the parameters were insufficient. In such cases it is very important to document and justify the choice of alternative parameters to fill in the data gaps. However, this was not always done in Timchalk et al. (2002b) making it difficult to to assess the assumptions.

Other parameters were cited wrongly from the original literature e.g. enzyme turnover time for butyrylcholinesterase, enzyme activity for carboxylesterase in brain and the reactivation rates for acetylcholinesterase, butyrylcholinesterase and carboxylesterase.

Some of the parameter values for tissue weights, tissue volume and blood flow for tissues given in Timchalk et al. (2002b) were not consistent with the data found in original literature. A set of standardized physiological parameters would make it easier to choose such parameter values for the PBTK modelling.

Evaluation of the models developed in the present project was performed by comparing model predictions with experimental data as well as with model predictions from Timchalk et al. (2002b) – by visual inspection. It was clear that the metabolic parameters had substantial impact on the outcome of the model. However, their origins were not clearly defined and documented.

Knaak and co-workers have compiled physicochemical and biological data for development of PBTK models describing organophosphorus pesticides (Knaak et al., 2004). Parameter values from this compilation will be used in the following for comparison with the values used in the present model.

Km1, Km2, VmaxC and VmaxC2

The values of the Michaelis-Menten constants for desulfuration (chlorpyrifos to chlorpyrifos-oxon, Km1) differed by a factor 6 in (Knaak et al., 2004). The lowest value (1.11 µM) was measured for males by (Ma and Chambers, 1994). The value used in the present model is from the same paper, selecting the value for the female rat which was three times higher (3.23 µM). Ma and Chambers found a 10-fold difference between the Km-value for the desulfuration process between their experiment and literature values from (Ma and Chambers, 1994; Sultatos et al., 1984).

It was not possible to verify the values for maximum velocities for the metabolism of chlorpyrifos to chlorpyrifos-oxon and to TCP (VmaxC1 and VmaxC2) presented by (Timchalk et al., 2002b). Knaak et al. found values of VmaxC1 for chlorpyrifos in literature varying by about a factor of 8 (from 10.2 to 76.9 µmol/hr/kg bw) (Knaak et al., 2004). Compared to this, the value used in Timchalk et al (2002b) and the present model (80 µmol/hr/kg bw) is high.

The Km1 and VmaxC1 used in a present model results in a high intrinsic clearance (extraction ratio) for the desulfuration: VmaxC1/Km1=80/3.23≈25. This is twice as much as the other values of intrinsic clearance calculated by Knaak et al. (9.2 and 12.6) for the two set of reference values they showed (Knaak et al., 2004).

The Km1 and VmaxC1 values were from a study performed by Ma and Chambers (Ma and Chambers, 1994). These authors made a new study where they found that the desulfuration of chlorpyrifos was biphasic and therefore described by two Km1 and VmaxC1 values (Ma and Chambers, 1995). This result was not incorporated in the present model but it may probably improve the model to do it.

The variance in the values collected for the Michaelis-Menten constant for dearylation (chlorpyrifos to TCP, Km2) is of a factor 5 (4.8 to 24.3 µM) with the highest value used in the present model (Knaak et al., 2004; Ma and Chambers, 1994). The maximum velocity chosen by Timchalk and co-workers (2002b) for this process was also high: 273 µmol/hr/kg bw compared with the range from 34 to 161.6 µmol/hr/kg bw in other papers as referred in (Knaak et al., 2004).

The intrinsic clearance calculated based on data for the dearylation was in the range of 2.4 to 33.7 (Knaak et al., 2004). The intrinsic clearance calculated using data from Timchalk et al. (2002b) was 11.4.

It seems as if there is a variance between the males and females in values for the Michaelis-Menten constant and maximum velocity of metabolism for both desulfuration and dearylation. However, it is beyond the scope of this project to elucidate this.

Km3, Km4, VmaxC3 and VmaxC4

The problems with these parameters were shown in section 21.2. It was not possible to verify the values for the maximum velocities and Michaelis-Menten constants for the metabolism of chlorpyrifos-oxon to TCP in liver and blood (VmaxC3, Km3 and VmaxC4, Km4, respectively) presented by Timchalk and co-workers (2007b). Furthermore, it was not explained why the parameters were changed compared to their previous model (Timchalk et al., 2007b).

The biochemical parameters (Michaelis-Menten constants, Km3, Km4) were determined by fitting the model to data from *in vivo* studies. The values used in the present model were fitted by Timchalk and co-workers in (Timchalk et al., 2007b). Such data are dependent on the model structure and the other parameters used in that model. Therefore, U.S. EPA points out that caution should be taken in using such data in other models with a different structure or parameter values (U.S.EPA, 2006a).

Km3 values given by Knaak et al. (2004) varied by a factor 7.7 (200 and 1530 µM) but VmaxC3 varied by a factor of about 2300 (40.5 and 92109 µmol/hr/kg bw). Km3 and VmaxC3 from (Timchalk et al., 2007b) used in the present model were both within these ranges (Km3=577 µM and VmaxC3=38002 µmol/hr/kg bw). Concerning the lower values for Km3 and VmaxC3, Knaak et al. refers to Mortensen et al. (1996). The low value of VmaxC3 seems strange compared to VmaxC3 calculated in the present thesis from data in Mortensen et al. (1996): VmaxC3=74421 µmol/hr/kg bw. The lower value of Km3 (40.5 µM) in Knaak et al. (2004) is also given with reference to Mortensen et al. (1996). However, Mortensen et al. states Km3=47 µM.

The parameter values used in (Timchalk et al., 2007b) and in the present model resulted in an extraction ratio of: VmaxC3/Km3=38002/577=66 which is of the same size as given in Knaak et al. (0.2 to 60) (Knaak et al., 2004). The values for VmaxC3 and Km3 in (Timchalk et al., 2002b) resulted in a much higher ratio (310).

The Michaelis-Menten constant for the hydrolysis of chlorpyrifos-oxon to TCP in blood, Km4, deviated by a factor 2.7 between rats and humans (200 µM for rats and 75 µM for humans) (Knaak et al., 2004). The value for the rat was at the same level as used by Timchalk and co-workers (250 µM) (Timchalk et al., 2002b) but in the present model and in (Timchalk et al., 2007b) a 2.3 higher value was used (464 µM).

The maximum velocity for the hydrolysis of chlorpyrifos-oxon to TCP in blood, VmaxC4, was stated to be 27.5 µmol/hr/kg bw for rats and 4.4 µmol/hr/kg bw measured in human blood (Knaak et al., 2004). These values are order of magnitudes lower than given in (Timchalk et al., 2002b) and (Timchalk et al., 2007b): 57003 and 40377 µmol/hr/kg bw, respectively.

Like the data for Km3 and VmaxC3 there ought to be a mix-up of units for VmaxC4. The VmaxC4-value of 27.5 is given with reference to (Mortensen et al., 1996) and should be comparable with the 57003 µmol/hr/kg bw, see section 21.2.

The Km4 and VmaxC4 for rat and human blood given in (Knaak et al., 2004) resulted in extraction ratios of the same magnitude (0.138 and 0.058 respectively), whereas the values used in (Timchalk et al., 2002b) resulted in a much higher value (228). The values used in the present model (and in (Timchalk et al., 2007b)) gave an extraction ratio of: VmaxC4/Km4=40377/464=87.

An updated version of the model by Timchalk et al.

A search in Web of Science showed that the paper by Timchalk et al. (2002b) had been cited 89 times and these citations include model development based on this paper. It has not been elucidated whether the developers of these new models (or extensions/improvement of the

model) have realised the problems with the original paper. Timchalk and co-workers have published several papers in which they present further work based on this paper – one example is their paper from 2007b, which also have been used in the present thesis. In 2010 they presented an updated version of their model from 2002 (Timchalk et al., 2010).

The new model is structurally equal to the old one but it was extended with equations describing CYP450 metabolism of chlorpyrifos to chlorpyrifos-oxon in the brain compartment. The metabolic parameters Km1, VmaxC1, Km2, VmaxC2, Km3 and Km4 are changed giving reference to (Poet et al., 2003), but with no explanation of the calculations. Concerning the parameters VmaxC3 and VmaxC4 these were changed to the values used in (Timchalk et al., 2007a).

Changing these parameters (Km1, VmaxC1, Km2, VmaxC2, Km3 and Km4) in the present model resulted primarily in a change in chlorpyrifos concentration in blood (higher) and the inhibition of brain acetylcholinesterase (lower).

Partition coefficients, blood flow in tissues and the TCP parameters (volume of distribution and elimination rate constant) were also changed in the toxicokinetic part of the model.

With respect to the parameters used in the toxicodynamic part (parameters describing the inhibition of esterases by chlorpyrifos-oxon), there are more discrepancies between the values in the parameter-table in (Timchalk et al., 2010) and the accompanying model code than between the parameters used in their model in 2002 and in 2010.

Timchalk and co-workers did not explain why the changes were made.

Metabolic constants, conclusion

The magnitude of the Michaelis-Menten constants and maximum velocities has substantial impact on the outcome of the model. El-Masri and co-workers developed a PBTK/TD model for chlorpyrifos and parathion and their metabolites (see chapter 18). In developing this model they found, that the most sensitive parameters were the Michaelis-Menten constant (Km) and maximal velocity (Vmax) as well as the binding and dissociation constants of free and bound acetylcholinesterase for both compounds (i.e. a small change in these parameters would result in a significant change in the model outcome) (El-Masri et al., 2004).

For parathion Knaak and co-workers have pointed out that “the variation in Vmax and Km is most likely due to differences in the number of active CYPs in harvested microsomes and their specific content” (Knaak et al., 2004). This most likely also accounts for chlorpyrifos.

As described above several discrepancies are observed between the studies on these metabolic parameters (Michaelis-Menten constants and maximum velocities) and they have high impact on the outcome of the model. VmaxC1, VmaxC2 (both from (Timchalk et al., 2002b)), Km4 and Vmax4 (both from (Timchalk et al., 2007b)) used in the present model are all beyond the range of values compiled from the literature by Knaak and co-workers (2004). Furthermore, the origin of these values is unclear. Therefore, it is uncertain whether there is a biological evidence for these values. There is a glaring need for further studies in order to better determine these parameters.

24.1.2 JUSTIFICATION FOR CHANGES IN RATE CONSTANTS DESCRIBING ESTERASE?

The simulations of inhibition of acetylcholinesterase in the different compartments in the present model were not in total agreement with the simulations by Timchalk and co-workers (2002b). The introduced change in the metabolic parameters, VmaxC3, VmaxC4, Km3 and Km4 resulted in more similar predictions compared to their simulations and the experimental data. However, still the results are not identical. The observed deviations may also be explained by differences in software and the method of numerical integration. However, this has not been examined further.

Simulations of the inhibition of brain acetylcholinesterase and plasma cholinesterase in the present rat model resulted in curves with too high steepness after the initial inhibition (i.e. from about 12 hr). The curves are far above the experimental data for doses from 10 to 100 mg/kg bw (compare the data points at 24 hr and the simulation curves in Figure 31B and 34). This means that the model overestimates the recovery of cholinesterase. It is seen from Figure 30 that this overestimation must be due to one or more of the following three possibilities: 1) a too high reactivation rate (Kr), 2) a too high degradation of esterase (Kd) or 3) that the bimolecular inhibition constant (Ki) is too low.

The bimolecular inhibition constant (Ki) determines the size of inhibition (i.e. to what extent the inhibition will be) but it also changes the recovery-part of the curve. The reactivation rate (Kr) together with the degradation of esterase (Kd) determine the steepness of the recovery-part of the curve. The smaller the more flat the curve will be.

Decrease in the reactivation rate for acetylcholinesterase in brain and plasma (Kr1) or for acetylcholinesterase in RBC (Kr5) give a lower slope of the increasing part of the curve. An increase in the bimolecular inhibition rate also results in a curve of acetylcholinesterase inhibition which is more similar to the experimental data for brain and RBC. However, for plasma a change in Kr1 (decrease) and Ki1 (increase) will still result in overestimation of the experimental data. The enzyme degradation rate, Kd affects the ability of esterase-curves to regenerate after decreased activity (after the inhibition). A smaller Kd (Kd1-Kd5) gives a slower recovery of acetylcholinesterase. Simultaneous changes of reactivation rate (decrease) or degradation rate (decrease) and bimolecular inhibition rate (increase) can change the curves to fit the data even better. However, there is not necessarily biological evidence for such changes in parameters.

A higher value of Ki1 (for acetylcholinesterase) may be supported by the results from other authors who measured values twice as high as the value in (Timchalk et al., 2002b) (243 $\mu M^{-1}hr^{-1}$): 558 $\mu M^{-1}hr^{-1}$ (Amitai et al., 1998) and 450 $\mu M^{-1}hr^{-1}$ (Carr and Chambers, 1996). The values for the Ki used in the present model were estimated by Timchalk et al. (2002b) by fitting the model to experimental data. It was unclear from the paper whether data on plasma or brain were used. Their initial values of Ki for acetylcholinesterase and butyrylcholinesterase in plasma and acetylcholinesterase in RBC were *in vitro* data taken from Amitai et al. (1998). They found that the model overestimated the inhibition of both B-esterases in plasma *in vivo* and therefore Timchalk and co-workers reduced the values of Ki to better describe the *in vivo* data. Inserting the values for Ki stated by Amitai et al. in the present

model resulted in some improvement of the esterase inhibition curves but in overestimation in some and no changes in others. Hence, such a change did not solve the problem with the fast recovery of esterase.

Timchalk et al. assumed that acetylcholinesterase, butyrylcholinesterase and carboxylesterase could be described by the same reactivation rate, Kr, and in all compartments (except acetylcholinesterase in RBC) (Timchalk et al., 2002b). Kousba et al. measured an *in vitro* determined rat salivary butyrylcholinesterase reactivation rate of 0.07 hr^{-1} which was similar to a Kr for paraoxon found in the literature (Kousba et al., 2003). This is a factor of 5 higher than the value used in the present model and in (Timchalk et al., 2002b) (0.01403 hr^{-1}). In another study Kr for acetylcholinesterase in rat brains were determined to 0.084-0.087 hr^{-1} (Kousba et al., 2004) which is a factor 6 higher than the value used in the present model. This indicates that a lowering of Kr may not be biologically plausible.

The enzyme degradation rate, Kd, was determined for acetylcholinesterase bound to diisopropylfluorophosphate in plasma and brain and it was assumed to be equal to Kd for acetylcholinesterase and butyrylcholinesterase for chlorpyrifos and also equal to Kd in liver and diaphragm (Timchalk et al., 2002b). It is not clear on what basis Timchalk et al. decided to disperse the two measured Kd-values to the other tissues. Kd for acetylcholinesterase and butyrylcholinesterase was set equal in brain and diaphragm, and ten times higher in liver and plasma. The biological argumentation of this assumption was not explained by Timchalk et al. (2002b).

24.1.3 SPECIAL CONDITIONS CONCERNING THE HUMAN MODEL

Almost all data from the rat model were used in the human model as well. That is, the ADME as well as most of the description of the B-esterase activity are assumed to be the same in rats and humans. This assumption may need to be investigated further.

Acetylcholinesterase in plasma was omitted from the human model because this esterase is only present in minor amount in plasma. Timchalk and co-workers adjusted the parameters describing butyrylcholinesterase in plasma in order to let butyrylcholinesterase compensate for the lack of acetylcholinesterase in this compartment. The biological reasoning of these changes in parameters was not explained.

In the present model it was assumed that the enzyme activity of acetylcholinesterase in human RBC was equal to enzyme activity of acetylcholinesterase in plasma in rat. It was not explained whether Timchalk et al. (2002b) did the same. From the data given by Timchalk et al. it seems like the only possible way, they could have done it. However, the biological evidence of this has not been examined.

24.1.4 USEFULNESS OF THE DEVELOPED MODELS IN THIS THESIS FOR ESTIMATING NOAEL

The PBTK/TD models for rats and humans developed in the present thesis were used for estimating NOAELs for chlorpyrifos in rats and humans, see section 23.3.1. The results from these simulations will be discussed in the following.

Brain acetylcholinesterase
The simulations showed that a dosage of 9 mg/kg bw/day in rats resulted in about 20 % inhibition of acetylcholinesterase in brain, i.e. this is the NOAEL for this endpoint. The corresponding chlorpyrifos concentration in blood was up to 0.043 µM, see Table 12. In the human model this blood concentration was achieved after a dose of 2 mg/kg bw/day resulting in only 1-3 % acetylcholinesterase inhibition in brain. In the human model an about 4.5 times higher chlorpyrifos concentration in blood (up to 0.15 µM) was necessary to give about 20 % inhibition of brain acetylcholinesterase. The 20 % inhibition occurred after an external dose (7 mg/kg bw/day) similar to the NOAEL in rats (9 mg/kg bw/day).

This shows that the there is a difference between humans and rats in how high internal dose a certain exposure will cause. However, there is a good correlation between the dosage and the inhibition of brain acetylcholinesterase in rats and humans i.e. the species are evenly sensitive in relation to this end point in relation to exposure (even though different internal doses are achieved from the same dosage level in the two species).

RBC acetylcholinesterase
For inhibition of acetylcholinesterase in RBC the relationship between internal dose and effect from the rat and the human model is more comparable, see Table 12. A dose of 2 mg/kg bw/day results in an inhibition in RBC acetylcholinesterase of 10-17 % in rats (i.e. NOAEL in simulation) and a chlorpyrifos blood concentration of up to 0.0095 µM. In the human model this blood concentration level (up to 0.011 µM) also results in about 20 % inhibition of RBC acetylcholinesterase, however, after a dose of 0.5 mg/kg bw/day.

In the human model the enzyme degradation rate for acetylcholinesterase in RBC was lowered compared to the rat model (Timchalk et al., 2002b). This change in the parameter-value might be the reason why the simulations result in a better correlation between internal dose and inhibition of RBC acetylcholinesterase than for brain acetylcholinesterase in the model.

Short-term versus long-term simulations
As mentioned in section 23.3.1.2, model simulation in the rat model of a single gavage dose of chlorpyrifos at 3 mg/kg bw showed an inhibition of acetylcholinesterase in plasma of 25 % which is higher than the level of inhibition after 2 years repeated dosage (up to 20 %). This indicates that the rat model might be better for prediction of dosages over a shorter time period. This impression is supported by the results from the comparisons of predictions from the present model with the experimental data as described in sections 23.1 and 23.2. The inhibition of plasma acetylcholinesterase in rats simulated over a shorter timeframe was reasonably comparative with the experimental data, especially at low doses (below 5 mg/kg bw/day). Nevertheless, underestimation was seen especially from 12 hr i.e. the prediction of the recovery of acetylcholinesterase was too fast. When the recovery in the present model is too fast it prevents accumulation of inhibited acetylcholinesterase and leading to an underestimation of the inhibition after simulation of long-term exposure in the model.

24.1.5 POSSIBLE EXPLANATIONS FOR DEVIATIONS FROM THE EXPERIMENTAL DATA

It is at present discussed whether metabolites of organophosphorus compounds formed in the environment e.g. in food may influence the amount measured in the human body (Lu et al., 2010). The underestimation of the TCP concentrations in the human model (Figure 40 and 43) may be explained by the existence of external formed TCP that would increase the concentrations measured in the experiments. However, the predicted concentrations of chlorpyrifos were also lower than the measured concentrations. Therefore, this explanation does not account for the total deviation from the experimental data.

Timchalk and co-workers (2002b) suggested that an overestimation in the model at environmentally relevant doses may be due to the lack of incorporation of metabolism in the intestine. The model only takes metabolism in the liver into consideration, however, CYP450 and PON1 metabolism has also been observed in the intestine. Especially at low doses this first-pass metabolism may remove chlorpyrifos-oxon from the circulation. Therefore, a description of metabolism in the intestine should be incorporated in the model (Poet et al., 2003). From the simulations presented in (Timchalk et al., 2002b) and in the present thesis there is no indication that overestimation should be the major problem with the models. In the present model only a minor overestimation of inhibition of brain acetylcholinesterase was seen at low doses (5 mg/kg bw/day; < 5 mg/kg/day: no overestimation). For plasma acetylcholinesterase inhibition the predictions were good at low doses.

24.1.6 CONCLUSION ON THE OUTCOME OF THE MODELLING

The present model was not able to perform simulations identical to the ones performed by Timchalk and co-workers (2002b), however, the shape of the curves were similar at low doses and over short timeframes (12 hr). Simulations during longer timeframes resulted in a too fast recovery of acetylcholinesterase compared to the experimental data. An underestimation of acetylcholinesterase inhibition was also seen in (Timchalk et al., 2002b) but not to the same extent. It will require further work to elucidate what causes these differences.

The simulations performed for estimating NOAELs indicate species differences in the inhibition of acetylcholinesterase in brain and RBC in relation to the chlorpyrifos blood concentration and dosage. In the model the human are more sensitive than the rat when it comes to inhibition of RBC acetylcholinesterase in relation to the exposure. However, in humans a lower dosage level (exposure) results in this internal dose. When it comes to inhibition of brain acetylcholinesterase the simulations show that the same dose level gives rise to the same degree of inhibition in rats and humans (i.e. the species are equally sensitive in relation to this end point), but the internal dose has to be 4.5 times higher in humans than in rats to result in the same response.

The simulations show that the present model underestimates the risk in many cases. The NOAEL for inhibition of RBC acetylcholinesterase was predicted to be 5 to 20 times higher in humans and rats, respectively, compared to the NOAELs established for this endpoint based on experimental studies. For the inhibition of brain acetylcholinesterase the NOAEL was predicted 9 times higher than was found in the rat study. A NOAEL established based on

experimental data will of course also contain uncertainties e.g. due to interspecies variations (see Figure 48) and by the selection of doses and dose-spacing in the study.

The model for rats was able to make good predictions of the concentrations of chlorpyrifos and chlorpyrifos-oxon in blood. The model for humans predicted the concentrations of chlorpyrifos and chlorpyrifos-oxon within a factor of 2 of the experimental data which is a relatively good prediction. This suggests that the toxicokinetic part of the model is more in line with the experimental data, whereas, the simulations of esterase inhibition suggest that the toxicodynamic part of the model need to be improved. A model that underestimates the risk is not appropriate in the risk assessment.

Overall, the work in re-building/developing and using these two PBTK/TD models for chlorpyrifos show that it is extremely important to carefully select the parameters to be used in a PBTK model. Further, the documentation and reasoning of the model structure, parameters and equations are of great importance in order to make a robust model and to enable other scientists to reproduce the model. This will be discussed further more broadly in the following section.

24.2 ADVANTAGES/DISADVANTAGES OF PBTK MODELS AND THEIR USE IN RISK ASSESSMENT

Application of PBTK/TD models to risk assessment has certain advantages and disadvantages.

The obtainable advantages are:

- The models can predict tissue concentrations and true toxicokinetic parameter values under a variety of conditions and thereby make the risk assessment more biologically realistic
- Mechanistic information on interactions can be incorporated and interaction threshold determined
- Decreased need for e.g. *in vivo* studies in the risk assessment
- Possible to make interspecies, high-dose to low-dose, route-to-route and exposure scenario extrapolations. In this way the risk assessor can simulate various scenarios including scenarios which cannot be studied experimentally
- Models for subpopulations such as children may help the risk assessor determine whether special care should be taken for such groups
- The use of uncertainty factors will be more scientifically based e.g. justifying a decrease in the uncertainty factor from the normally used default factor of 100.

The disadvantages are:

- Require extensive physiological, biochemical and physicochemical parameter-related data. No internationally accepted reference values exist
- Requires extensive documentation including justifications for the choices made in the model development

- Parameters especially for humans are sometimes difficult to obtain because not all data are measurable
- Mathematically complex compared to other calculations used in risk assessment.

The advantages and disadvantages will be discussed in the following.

Parameters

The importance of keeping the statement "The model is only as good as the input parameters" (Krishnan and Andersen, 2010) in mind has been clearly elucidated in this thesis. It is of paramount importance to make use of good and well defined parameters in the modelling.

It has been found that metabolic rate constant values for carbon tetrachloride in rats estimated from PBTK models were sensitive not only to compound specific partition coefficients (for blood and fat) but also to the physiological parameters fat volume and blood flow in fat, liver and slowly perfused tissues. Therefore, an accurate characterization of values for physiological parameters is also important for the establishment of metabolic rate constants from a PBTK model (Brown et al., 1997). This will probably also be relevant for other compounds like e.g. pesticides.

It is necessary to establish internationally acceptable reference values for physiological and anatomical parameters such as tissue weights and blood flows. Significant work has already been done in making reference values for use in PBTK modelling (Brown et al., 1997; Davies and Morris, 1993; Thompson et al., 2009; U.S.EPA, 1988a; U.S.EPA, 2009). However, there is still no consensus on these data.

With respect to biochemical parameters especially metabolic parameters such as Vmax and Km a standardized experimental method for deriving these parameters is important. A clear method for normalising these data is also crucial in order to make it possible to use the data in PBTK models.

Tissue dose

The classical practice of estimating risk assumes that the toxic effect is related to the administered dose. In the application of a PBTK model in risk assessment it is assumed that the toxic effect of a chemical in the target tissue can be related in some way to the dose of the chemical in the tissue. In other words it is assumed that except for toxicodynamic differences between animal species equivalent tissue dose will result in similar responses regardless of species, exposure route, or experimental regimen (Clewell, 2010; Travis and Hattemer-Frey, 1990).

Use of PBTK models in the risk assessment will provide knowledge about the connection between exposure and internal dose taking absorption, distribution, metabolism and elimination into account and this will form a biological more realistic basis for the risk assessment.

A validated PBTK model can be used to derive NOAELs in the way described in this thesis. However, at present this model as it is presented, is not yet reliable i.e. sufficiently robust for this use.

Extrapolations
In the area of risk assessment including cumulative risk assessment, the ability to make interspecies extrapolation is of great value. As seen in this thesis an extrapolation from rats to humans is performed primarily by changing the parameters for the model, not the equations. In this process it is important to consider possible differences between the species e.g. as in the present model the lack of acetylcholinesterase in plasma in humans. The parameters are sometimes difficult to obtain in humans since not all data are measurable. In such cases *in vitro* assays, *in vivo* rodent data or data estimated by QSAR might help.

Experiments are normally performed at high doses compared to the exposure from the levels found in food. Therefore, high-dose to low-dose extrapolation is an important feature in the risk assessment making it possible to simulate scenarios at dose levels relevant for e.g. intake of pesticides as residues in food.

For future use of the model the probability of changing the route of exposure might be useful. For the time being the model can simulate dietary and gavage exposure. Both exposure routes can be simulated as single or repeated exposures. These different scenarios have been demonstrated in this thesis. If it becomes necessary to take dermal exposure into account (e.g. from occupational use) a few equations could be inserted in order to simulate this exposure route.

Interactions
Several methods to describe interactions in PBTK models have been presented in this thesis. Metabolic inhibition is the most frequently seen type of interaction in PBTK models and equations describing competitive, non-competitive and uncompetitive interactions have been proposed.

Unfortunately, it was not possible to test these methods in this project. Development of a PBTK/TD model for diisopropylfluorophosphate based on a model developed by Gearhart and co-workers (Gearhart et al., 1990; Gearhart et al., 1994) was initiated. The plan was to combine the models for chlorpyrifos and diisopropylfluorophosphate and simulate a combined intake of these two compounds via food. Because the work with the chlorpyrifos-model took much longer time than expected, the model for a mixture of the two organophosphates with similar mechanism of action is not finished and will not be included in this thesis.

Subpopulations
The National Institute for Public Health and the Environment in the Netherlands (RIVM) have made an overview of data concerning differences between children and adults with respect to exposure, toxicokinetic and toxicodynamic (Wolterink et al., 2002). There are a lot of physiological and toxicokinetic difference between children and adults which may result in different internal doses. However, it is not possible to make an overall prediction of the different processes. For example, a compound that is more extensively absorbed may be less metabolised to a toxic metabolite or excreted more rapidly. RIVM recommends to use PBTK modelling to get more insight in these differences (Wolterink et al., 2002)

Large differences in toxicodynamics between children and adults have been observed especially during early development. Generally, children are supposed to be more sensitive to effects of toxic chemicals than adults. These effects will in principal be identified in the reproduction and developmental neurotoxicity studies which are normally performed for pesticides. However, the critical windows in development of rodents and humans are not always the same and therefore care should be taken with respect to route and level of exposure in order to make it possible to extrapolate between species (Wolterink et al., 2002).

PBTK models can be developed for subpopulations such as infants and children. Initial work has already been done in this direction, e.g. the age-dependent model for chlorpyrifos in pre-weanling rats which indicated that the neonatal rats were quantitatively more sensitive than adults to high dose acute effects (Timchalk et al., 2007b). Based on the model by Timchalk et al. (2002b) Lu and co-workers developed a model for children with focus on the urinary excretion of the chlorpyrifos-metabolite TCP using data for 3-6 years old children (Lu et al., 2010).

Law of Parsimony

Woodruff and co-workers examined the difference between a five-compartment PBTK model, a three-compartment PBTK model and a non-physiological compartment model of benzene toxicokinetic. Each model was fitted to four sets of experimental data (three sets of *in vivo* experiments and one hypothetical) using Monte Carlo simulations to take the variability of the parameters into account. They found a larger difference between the predictions by the same model fitted to different data sets than between the predictions from the three models, i.e. the three-compartment (with two thirds the number of parameters and two differential equations less) and the five-compartment PBTK model produced the same predictions. Therefore, they recommend using a reduced model. A large number of parameters can cause a large variability. However, the authors found that despite the number of parameters in the PBTK models these models did not produce much more variability than the non-physiological compartment model. The variability of the predictions was more affected on the type of data than the type of model and the number of parameters (Woodruff et al., 1992).

Their results are in line with the Law of Parsimony. As mentioned earlier large numbers of compartments in a model are not necessarily equal to accuracy and usefulness of the model (Krishnan and Andersen, 2001; Yang and Lu, 2007). The International Programme on Chemical Safety has suggested to develop simple PBTK models for preliminary assessments while more complex PBTK model may be relevant for compounds for which the margin between exposure and effect is small (IPCS, 2010).

Uncertainty factors

An uncertainty factor of 100 has been used as a default in risk assessment for more than 50 years. This standard uncertainty factor includes a factor of 10 for intraspecies uncertainties and a factor of 10 for interspecies uncertainties. It has been suggested to further divide these 10-fold factors to allow incorporation of e.g. toxicokinetic differences and thereby replace or minimize the relevant part of the overall default uncertainty factor. The 10-fold uncertainty factor for interspecies differences was suggested to be divided in $10^{0.6}$ (4) and $10^{0.4}$ (2.5) for uncertainties in toxicokinetics and toxicodynamics, respectively. The intraspecies uncertainty

factor was suggested to be subdivided in the square root of 10 for uncertainties in both toxicokinetics and toxicodynamics (Dorne and Renwick, 2005; IPCS, 2005).

This concept was tried in a model for isopropanol. Gentry and co-workers developed a PBTK model for isopropanol for use in risk assessment. They stated that the uncertainty factor by using this PBTK model can be decreased from 100 to 30. They divided both 10-fold uncertainty factors in the square root of 10. They assumed that the use of their PBTK model in risk assessment decreased the uncertainties in toxicokinetic differences between species. Therefore, the uncertainty by using their model was decreased to a square root of 10 (i.e. ≈ 3). The total uncertainty factor applied for this model was therefore 3*10=30 (Gentry et al., 2002a).

However, concerning models developed and presented in this thesis it seems as when it comes to inhibition of acetylcholinesterase an uncertainty factor of 10 for interspecies differences would be appropriate.

Uncertainties and model evaluation

There are no formal guidelines or guidance on how to validate PBTK models but it is a developing area. For the application of PBTK models in risk assessment the focus should be on the purpose-specific evaluation rather than generic validation. This means that aspects relating to the biological basis of the model structure and parameters are just as important as the comparison of model simulations with toxicokinetic data and dose metrics. This should be supplemented with analysis of variability, uncertainty and sensitivity (IPCS, 2010; Krishnan and Andersen, 2010).

When a PBTK model does not adequately describe the behaviour of the system this may be due to:

1) mistakes in the structure of the model i.e. the model does not describe the system adequately
2) incorrect level of detail in the structure (e.g. incorrect lumping of important compartments) which may not be consistent with the type of experimental data
3) wrong mathematical description of the relationship between the compartments
4) uncertainties in the extrapolations which means that the new scenario simulated deviates from the application domain for which the model was developed and tested
5) uncertainties in the parameter values as a result of:
    a. limitations in the precision and accuracy of measurements resulting in random errors
    b. systematic biases
    c. an indirectly measured parameter used instead of a parameter that was not measurable directly
    d. no data to support the parameters
    e. uncertainties in the experimental data used to determine parameters by fit of the model

    (Isukapalli et al., 2010; Krishnan and Andersen, 2010).

In vitro assays and QSAR

Efforts in using *in vitro* data as input to the PBTK models describing *in vivo* data would be valuable. However, Loizou and co-workers states that some examples in the scientific literature showed limitation of models to predict *in vivo* data using metabolic parameters estimated from *in vitro* studies (Loizou et al., 2008).

There is a need for improving the scientific basis for making extrapolations from well studied chemicals to compounds with limited information. An example is metabolites of pesticides formed in plants before consumption. The range of toxicological studies required for placing a pesticide on the market does not to the same extent include studies on their metabolites compared to the parent compound. Therefore, limited information on the toxicological properties of these compounds is available.

QSAR could be used to derive chemical specific parameters such as Km, Vmax and partition coefficients. Use of QSAR in deriving parameters for PBTK modelling may accelerate screening applications in risk assessment for compounds such as the pesticide metabolites that have not undergone extensive toxicity testing (Andersen, 1995).

These kinds of extrapolations if successful could decrease the need for additional studies including the use of experimental animal studies.

24.3 REQUIREMENTS OF DOCUMENTATION OF A PBTK MODEL

Andersen et al. has provided a good suggestion on how to document and present PBTK models in publications (Andersen et al., 1995). They stated that a manuscript describing a PBTK model should include sufficient information about the model in order to make it possible for an experienced modeller to reproduce the structure of the model. Table 14 shows the necessary information to be presented in the manuscript.

Table 14. A list on how to document a model in publications. Adapted from (Andersen et al., 1995).

Characteristics of a good modeling paper:
1. Clear presentation of all equations
2. Computer program made available on request
3. Clear definition of all variables/parameters
4. Clear definition of units to ensure proper dimensions
5. Definition of criteria to evaluate predictions or fits
6. Time, species, and exposure domain where model is valid
7. Hypothesis testing and model discrimination as necessary

A workshop held on good modelling practice (International Workshop on the Development of GMP for PBPK Models in Greece on April 27–29, 2007) recommended to prepare a standard, brief model description summary which should be readable for all risk assessors and then a more detailed model documentation for specialists published separately. The summary should include:

1. “Introduction including problem formulation (applicability of model).

2. A text description of the model (species, routes, etc) with schematic diagram, and an overview of the information and data supporting the model structure.
3. Metabolic pathways for the chemical and an overview of the supporting information and data.
4. Relationship to mode of action including dose metric predictions and supporting information.
5. Distributional predictions of model outputs and their implications (e.g., Monte Carlo simulation of human variability).
6. Overview of uncertainty and sensitivity analyses.
7. Source of complete information (e.g., citation)" (Loizou et al., 2008).

Additionally, model documentation and supporting information such as calculations done to convert published scientific information into the form used in the model should be accessible e.g. via the internet (Loizou et al., 2008).

These recommendations are in line with the methodology described by the International Programme on Chemical Safety (IPCS, 2010).

25 FUTURE PERSPECTIVES

Overall, development of PBTK models for the most common chemical mixtures of concern to be used routinely would be of great value in future risk assessments. However, PBTK modelling is data demanding and resource intensive and this should be counterbalanced by the increased accuracy and scientifically basis assessed using them. Therefore, in the near future they will only be used for higher tier assessment.

Validation of the models and development of principles and guidance for good modelling practice (Loizou et al., 2008) as well as statistical research to support model assumptions is needed. Teuschler has specified the statistical research to "include testing for similar shapes of component dose–response curves, determining whether additivity assumptions are applicable or not for describing mixture risk, and using algorithms to form groups of similar components or similar mixtures" (Teuschler, 2007).

In addition, developments in the area of toxicogenomics have also been suggested as a way of increasing our knowledge of mechanism of toxicity in order to better understand and improve the approaches for risk assessment of combined actions of chemicals (Andersen and Krewski, 2009; El-Masri, 2007; Groten et al., 2001).

PBTK modelling using Bayesian Markov Chain Monte Carlo calculations of the parameters is a developing field which is expected to provide more robust parameters.

Looking into the crystal ball an integration of PBTK modelling with the biochemical reaction network will be a forthcoming tool in handling very complex mixtures of chemicals. Such a computer simulation platform will provide a possibility for modelling biological systems from the whole body down to the molecular interaction level.

The methods integrating PBTK with either Bayesian Markov Chain Monte Carlo calculations or the biochemical reaction network will be described shortly in two separate sections in the following.

25.1 USE OF BAYESIAN ANALYSIS USING MARKOV CHAIN MONTE CARLO CALCULATIONS

It has been debated whether effort should be put in developing parameters based on key sensitive datasets to be used for evaluating the predictive ability for PBTK models or whether it would be better to make use of all data as training-sets and in that way parameterise the model. Bayesian analysis using Markov Chain Monte Carlo calculations is being used for this purpose (Krishnan et al., 2010). In the Bayesian analysis a priori knowledge of physiological, anatomical and physiochemical parameters can be summarized as prior distributions. The prior knowledge on parameters can be obtained from the scientific literature, *in vitro* experiments or from fitting previous data values. In the Bayesian analysis the prior distributions of parameter values will be combined with the data likelihood to yield posterior parameter distributions instead of single data point estimates. When Bayesian analysis is coupled to Markov Chain Monte Carlo simulations the model can assess distributions for population parameters (Bois, 2000; Jonsson et al., 2001).

In the area of PBTK modelling of pesticides an example of a PBTK model using Bayesian Markov Chain Monte Carlo calculations of the parameters was performed by Nong and co-workers (Nong et al., 2008). The model was developed for the carbamate carbaryl based on the models on diisopropylfluorophosphate and parathion previously published by Gearhart and co-workers (Gearhart et al., 1990) describing the metabolism as well as the inhibition of cholinesterase. Some of the prior estimates for the parameters used in the model were obtained by fitting with mean experimental values from rat studies while the Markov Chain Monte Carlo calculations made use of the individual measurements from the experiments. The posterior parameter distributions estimated by the present Bayesian analysis was assessed to be more robust as it takes the physiological and experimental variability for the kinetics and the inhibition response of carbaryl into account. Distributions of the model output were generated by conducting a Monte Carlo simulation based on the mean and standard deviations of the marginal posterior distributions for the parameters from Markov Chain Monte Carlo analysis (Nong et al., 2008).

25.2 BIOCHEMICAL REACTION NETWORK

An integration of PBTK models and biochemical reaction networks has been predicted to be a forthcoming important tool to be used for handling very complex chemical mixtures (Yang and Lu, 2007).

The reaction network tool was originally developed in the chemical and petroleum engineering field for prediction of the amounts of reactants, intermediates and products as a function of time for a series of coupled chemical reactions. In the area of toxicology of chemical mixtures this method has been modified in order to examine biochemical reaction

networks associated with the toxicological processes in an organism after exposure to toxic chemicals. This is done by considering the individual processes in the oil refinery equivalent to the organs in the body even though the mechanisms in organs are more complicated. By doing so, the already developed modelling tool can be used in toxicology. The input to the model database is information such as chemical structures, chemical properties and chemical reaction mechanisms. When the model have been fed with enough information, it is supposed to accurately predict the metabolic pathways (i.e. biochemical reaction networks) showing the interconnections between the metabolites and the concentrations of the compounds in the mixture over time. The output from such a model can be coupled to a PBTK model to give a more complete picture of the risk (Yang and Lu, 2007). Klein and co-workers have described the linking of biochemical reaction networks with PBTK models in more details. They point out: "The recent explosive growth of genomics, proteomics, and related bioinformatics in the biomedical field again parallel the availability of analytical and IT technologies to chemical engineering. A logical question is whether biologically based modelling can be advanced to the biochemical reaction network level by using proven chemical engineering modeling technology" (Klein et al., 2002).

26 CONCLUSION

The overall objectives of this Ph.D. project were to evaluate the existing knowledge on methods for risk assessment of combined actions of chemicals, establish PBTK models in order to improve methods for risk assessment of mixtures of chemicals and to examine the applicability of PBTK models in risk assessment of mixtures.

Of the various approaches for risk assessment of mixtures of chemicals discussed, the whole mixture approaches would be the ideal choice for assessment of e.g. pesticide residues in food. However, they are normally not applicable since they require a large number of experimental data that are rarely available. This leaves the single compound approaches as the more realistic ones.

In the risk assessment of multiple residues of pesticides in food, the individual compounds will be considered for possible candidates in one (or more) cumulative assessment groups. When adequate data are available, a common mechanism group should be established. The cumulative risk assessment of this group will then be performed assuming simple similar action using preferably the point of departure index, but in practice the hazard index based on a health based guidance value i.e. ADI/RfD might normally be sufficient. In some cases a refinement may be required i.e. using the NOAEL as point of departure for a relevant and critical toxicological effect different from the effect on which the cumulative assessment group is based.

Where more than one common mechanism group based on simple similar actions are identified, they should be assessed separately as indicated above. In addition, the potential for interactions between the groups (or single compounds) have to be considered. If interactions between the groups (or compounds) can be ruled out, simple dissimilar action can be anticipated, and the effect of the mixture should be assessed by response addition. However, it is a common perception that at very low doses of dissimilar acting compounds (where none of

the compounds in the mixture have any toxic effect) no adverse effect of the mixture will be anticipated as well.

In many cases it can be predicted that evaluators will tend to use very pragmatic approaches, such as assuming that all compounds in the mixture show simple similar actions, and thus use the hazard index or point of departure index, as such evaluations would be more convincing if lack of interaction between the compounds at the actual dose level had been demonstrated.

Therefore, a crucial point in the assessment is whether there is interaction or no interaction between the compounds in the mixture. Although interactions among chemicals at high doses are well-known, there is currently no single simple approach to judge upon potential interactions at the low doses that humans are exposed to from pesticide residues in food. For this purpose, PBTK models in the future could be useful as a tool to assess combined tissue doses and to help predict potential interactions including thresholds for such effects.

The use of PBTK modelling in the risk assessment of mixtures is an upcoming field involving challenges. PBTK models are complex and should of course only be used when it is considered essential. If reliable models are developed they can provide better knowledge and understanding of the effects of mixtures in the organism and provide improved information on tissue dose levels and variations between species and within a population. Moreover, scientifically supportable results in the risk assessment of mixtures of pesticides would help the risk managers in making more reliable decisions.

If the PBTK models are expanded by a toxicodynamic part, the model could be even better and make it possible to identify deviations from additivity at the toxicodynamic level. However, this area is still in its infancy and it will probably be better to put more effort into improving the toxicokinetic part especially by establishing internationally acceptable reference values for various parameters before extending the model with a toxicodynamic part.

The work in this thesis clearly emphasizes the importance of a higher degree of transparency in relation to the developed models. The documentation should include considerations concerning the model structure and equations as well of the choice of parameters and their origin. The parameter values should of course by correctly cited in the published papers. Without such documentation it is not possible for other scientists to reproduce, evaluate and further develop the models. The credibility of the PBTK models is crucial for a spreading of their use in risk assessment.

There is at present a lack of adequate data for use in the PBTK models. Further studies are needed in order to extend the database of parameters but it will not be realistic to perform studies to determine all parameters for all chemicals. Therefore, development of a model will also involve assumptions. It is important that these assumptions are reasonable and biologically based. Further, these assumptions should be documented.

PBTK models have a potential as an important tool in the risk assessment, but there is still a lack of acceptance of their use by the regulatory agencies. As shown in this thesis the development of PBTK models requires a lot of knowledge and not at least data and it is quite time consuming to compile. However, this problem is maybe not the main point in the lack of

acceptance of the use of these models. It is more likely that the PBTK model is perceived as a black box to many toxicologists. As this thesis has shown there is a glaring need for transparency in the modelling both concerning the parameters and the model structure. A clear description of the model as well as a consensus on the criteria for model evaluation would most likely increase the chances of a broad acceptance of the use of PBTK models.

This Ph.D.-project constitutes the initial work on implementing PBTK/TD models in the risk assessment of combined toxic action of chemical substances in food at the DTU National Food Institute. The work has revealed some major problems and pitfalls in the developing process. However if reliable, these models will provide knowledge of the relationship between internal concentration of the chemical and the observed toxic effects and this knowledge will reduce the uncertainty in the risk assessment. Therefore, the work will continue implementing these models as a helpful tool in the future risk assessment.

27 REFERENCES

Advisory Committee on Hazardous Substances, 2007. Chemical mixtures: a framework for assessing risks. Liu, Q. (Ed.). Version 6.

Amitai, G., Moorad, D., Adani, R., Doctor, B.P., 1998. Inhibition of acetylcholinesterase and butyrylcholinesterase by chlorpyrifos-oxon. Biochem. Pharmacol. 56 (3), 293-299.

Andersen, M.E., Clewell III, H.J., Frederick, C.B., 1995. Applying simulation modeling to problems in toxicology and risk assessment - a short perspective. Toxicol. Appl. Pharmacol. 133, 181-187.

Andersen, M.E., 2003. Toxicokinetic modeling and its applications in chemical risk assessment. Toxicol. Lett. 138 (1-2), 9-27.

Andersen, M.E., 1995. Development of physiologically based pharmacokinetic and physiologically based pharmacodynamic models for applications in toxicology and risk assessment. Toxicol. Lett. 79 (1-3), 35-44.

Andersen, M.E., Clewell III, H.J., Gargas, M.L., Smith, F.A., Reitz, R.H., 1987. Physiologically based pharmacokinetics and the risk assessment process for methylene chloride. Toxicol. Appl. Pharmacol. 87, 185-205.

Andersen, M.E., Krewski, D., 2009. Toxicity testing in the 21st century: bringing the vision to life. Toxicol. Sci. 107 (2), 324-330.

Andersen, M.E., Krishnan, K., 2010. Quantitative Modeling in Toxicology: An Introduction. In: Andersen, M.E., Krishnan, K. (Eds.), Quantitative Modeling in Toxicology. John Wiley & Sons, Ltd, West Sussex, United Kingdom, pp. 3-18.

ATSDR, 2001. Guidance for the preparation of an interaction profile. Pohl, H., Hansen, H., Wilbur, S., Odin, M., Ingerman, L., Bosch, S., McClure, P., Coleman, J. (Eds.). U.S. Department of Health and Human Services. Public Health Service. Agency for Toxic Substances and Disease Registry. Division of Toxicology.

ATSDR, 2004. Guidance manual for the assessment of joint toxic action of chemical mixtures. Wilbur, S., Hansen, H., Pohl, H., Colman, J., Stiteler, W. (Eds.). U.S. Department of Health and Human Services. Public Health Service. Agency for Toxic Substances and Disease Registry. Division of Toxicology.

Balci, O., 1997. Verification, validation and accreditation of simulation models. In: Andradóttir, S., Healy, K.J., Withers, D.H., Nelson, B.L. (Eds.), Proceedings of the 1997 Winter Simulation Conference. pp. 135-141.

Barlow, S., Renwick, A.G., Kleiner, J., Bridges, J.W., Busk, L., Dybing, E., Edler, L., Eisenbrand, G., Fink-Gremmels, J., Knaap, A., Kroes, R., Liem, D., Muller, D.J., Page, S., Rolland, V., Schlatter, J., Tritscher, A., Tueting, W., Wurtzen, G., 2006. Risk assessment of substances that are both genotoxic and carcinogenic report of an international conference organized by EFSA and WHO with support of ILSI Europe. Food Chem. Toxicol. 44 (10), 1636-1650.

Belfiore, C.J., 2005. Pesticides and persistent organic polluntants (POPs). In: Reddy, M.B., Yang, R.S.H., Clewell III, H.J., Andersen, M.E. (Eds.), Physiologically based pharmacokinetic modeling. Science and applications. John Wiley & Sons, Inc., New Jersey, pp. 169-205.

Belfiore, C.J., Yang, R.S., Chubb, L.S., Lohitnavy, M., Lohitnavy, O.S., Andersen, M.E., 2007. Hepatic sequestration of chlordecone and hexafluoroacetone evaluated by pharmacokinetic modeling. Toxicology 234 (1-2), 59-72.

Berenbaum, M.C., 1989. What is synergy? Pharmacol. Rev. 41, 93-141.

Bliss, C.I., 1939. The toxicity of poisons applied jointly. Ann. App. Biol. 26, 585-615.

Bois, F.Y., 2000. Statistical analysis of Fisher et al. PBPK model of trichloroethylene kinetics. Environ Health Perspect. 108 Suppl 2, 275-282.

Boon, P.E., van Klaveren, J.D., 2003. Cumulative exposure to acetylcholinesterase inhibiting compounds in the Dutch population and young children. Toxic equivalency approach with acephate and phosmet as index compounds. RIKILT - Institute of Food Safety. 2003.003.

Borgert, C.J., Price, B., Wells, C.S., Glenn, S., 2001. Evaluating chemical interaction studies for mixture risk assessment. Hum. Ecol. Risk Assess. 7 (2), 259-306.

Borgert, C.J., Quill, T.F., McCarty, L.S., Mason, A.M., 2004. Can mode of action predict mixture toxicity for risk assessment? Toxicol. Appl. Pharmacol. 201 (2), 85-96.

Bosgra, S., van der Voet, H., Boon, P.E., Slob, W., 2009. An integrated probabilistic framework for cumulative risk assessment of common mechanism chemicals in food: An example with organophosphorus pesticids. Regul. Toxicol. Pharmacol. 54, 124-133.

Botham, P., Chambers, J., Kenyon, E., Matthews, H.B.S., Sultatos, L., Van Pelt, C., Zeise, L., Faustman, E., Mileson, B., 1999. Report of the toxicology breakout group (BOG). In: Mileson, B.E., Faustman, E., Olin, S., Ryan, P.B., Ferenc, S., Burke, T. (Eds.), A framework for cumulative risk assessment. International Life Sciences Institute, pp. 5-23.

Bouchard, M., Gosselin, N.H., Brunet, R.C., Samuel, O., Dumoulin, M.J., Carrier, G., 2003. A toxicokinetic model of malathion and its metabolites as a tool to assess human exposure and risk through measurements of urinary biomarkers. Toxicol Sci. 73 (1), 182-194.

Brown, R.P., Delp, M.D., Lindstedt, S.L., Rhomberg, L.R., Beliles, R.P., 1997. Physiological parameter values for physiologically based pharmacokinetic models. Toxicol Ind. Health 13 (4), 407-484.

Bungay, P.M., Dedrick, R.L., Matthews, H.B., 1981. Enteric transport of chlordecone (Kepone) in the rat. J. Pharmacokinet. Biopharm. 9 (3), 309-341.

Campbell, J.L., Krishnan, K., Clewell, H.J.I., Andersen, M.E., 2010. Modeling kinetic interactions of chemical mixtures. In: Mumtaz, M. (Ed.), Principles and practice of mixtures toxicology. Wiley-VCH, Weinheim, pp. 125-158.

Carr, R.L., Chambers, J.E., 1996. Kinetic analysis of the in vitro inhibition, aging, and reactivation of brain acetylcholinesterase from rat and channel catfish by paraoxon and chlorpyrifos-oxon. Toxicol. Appl. Pharmacol. 139 (2), 365-373.

Cassee, F.R., Groten, J.P., van Bladeren, P.J., Feron, V.J., 1998. Toxicological evaluation and risk assessment of chemical mixtures. Crit. Rev. Toxicol. 28 (1), 73-101.

Chambers, J.E., Meek, E.C., Chambers, H.W., 2010. The Metabolism of Organophosphorus Insecticides. In: Krieger, R., Doull, J., Hemmen, J., Hodgson, E., Maibach, H., Reiter, L., Ritter, L., Ross, J., Slikker, W. (Eds.), Hayes' Handbook of Pesticides. Academic Press, Elsevier Inc., pp. 1399-1407.

Chan, M.P., Morisawa, S., Nakayama, A., Kawamoto, Y., Sugimoto, M., Yoneda, M., 2006. A physiologically based pharmacokinetic model for endosulfan in the male Sprague-Dawley rats. Environ Toxicol. 21 (5), 464-478.

Chen, W.L., Sheets, J.J., Nolan, R.J., Mattsson, J.L., 1999. Human red blood cell acetylcholinesterase inhibition as the appropriate and conservative surrogate endpoint for establishing chlorpyrifos reference dose. Regul. Toxicol. Pharmacol. 29 (1), 15-22.

Chiu, W.A., Barton, H.A., Dewoskin, R.S., Schlosser, P., Thompson, C.M., Sonawane, B., Lipscomb, J.C., Krishnan, K., 2007. Evaluation of physiologically based pharmacokinetic models for use in risk assessment. J. Appl. Toxicol. 27 (3), 218-237.

Christensen, H.B., Petersen, A., Poulsen, M.E., Grossmann, A., Holm, M., 2006. Pesticide residues in food 2005 - results from the Danish pesticide survey [Pesticidrester i fødevarer 2005 - resultater fra den danske pesticidkontrol]. Report in Danish. Danish Veterinary and Food Administration. FødevareRapport 2006:23.

Clewell, H.J.I., 2010. Application of Physiologically Based Pharmacokinetic Modeling in Health Risk Assessment. In: Andersen, M.E., Krishnan, K. (Eds.), Quantitative Modeling in Toxicology. John Wiley & Sons, Ltd, West Sussex, United Kingdom, pp. 399-428.

Clewell, R.A., Clewell, H.J., III, 2008. Development and specification of physiologically based pharmacokinetic models for use in risk assessment. Regul. Toxicol. Pharmacol. 50 (1), 129-143.

Committee on Toxicity, 2002. Risk assessment of mixtures of pesticides and similar substances. Chairman: Professor Hughes, I., Chairman of the Working Group on Risk Assessment of Pesticides and similar substances: Professor Woods, H.F. (Eds.). Committee on Toxicity of Chemicals in Food, Consumer Products and the Environment. FSA/0691/0902.

Conolly, R.B., 2001. Biologically motivated quantitative models and the mixture toxicity problem. Toxicol. Sci. 63 (1), 1-2.

Davies, B., Morris, T., 1993. Physiological parameters in laboratory animals and humans. Pharm. Res. 10 (7), 1093-1095.

Dejongh, J., Blaauboer, B.J., 1997. Simulation of lindane kinetics in rats. Toxicology 122 (1-2), 1-9.

Dennison, J.E., Andersen, M.E., Clewell, H.J., Yang, R.S., 2004. Development of a physiologically based pharmacokinetic model for volatile fractions of gasoline using chemical lumping analysis. Environ. Sci. Technol. 38 (21), 5674-5681.

Dennison, J.E., Andersen, M.E., Yang, R.S., 2003. Characterization of the pharmacokinetics of gasoline using PBPK modeling with a complex mixtures chemical lumping approach. Inhal. Toxicol. 15 (10), 961-986.

DeWoskin, R.S., Thompson, C.M., 2008. Renal clearance parameters for PBPK model analysis of early lifestage differences in the disposition of environmental toxicants. Regul. Toxicol. Pharmacol. 51 (1), 66-86.

Dorne, J.L., Renwick, A.G., 2005. The refinement of uncertainty/safety factors in risk assessment by the incorporation of data on toxicokinetic variability in humans. Toxicol Sci. 86 (1), 20-26.

Durkin, P., Hertzberg, R., Diamond, G., 2004. Application of PBPK model for 2,4-D to estimates of risk in backpack applicators. Environ. Toxicol. Pharmacol. 16, 73-91.

Ecobichon, D.J., Comeau, A.M., 1973. Pseudocholinesterases of mammalian plasma: physicochemical properties and organophosphate inhibition in eleven species. Toxicol Appl. Pharmacol. 24 (1), 92-100.

EFSA, 2006. Conclusion regarding the peer review of the pesticide risk assessment of the active substance malathion. Finalised 13 January 2006. EFSA Scientific Report. 63. pp. 1-86.

EFSA, 2007. EFSA scientific colloquium. 28-29 November 2006 - Parma, Italy. Summary report. Cumulative risk assessment of pesticides to human health: the way forward.

EFSA, 2008. Scientific opinion of the Panel on Plant Protection Products and their Residues (PPR Panel) on a request from the EFSA evaluate the suitability of existing methodologies and, if appropriate, the identification of new approaches to assess cumulative and synergistic risks from pesticides to human health with a view to set MRLs for those pesticides in the frame of Regulation (EC) 396/2005. (Question N° EFSA-Q-2006-160). The EFSA Journal. 704. pp. 1-84.

EFSA, 2009. Panel on Plant Protection Products and their Residues (PPR Panel). Scientific Opinion on risk assessment for a selected group of pesticides from the triazole group to test possible methodologies to assess cumulative effects from exposure throughout food from these pesticides on human health on request of EFSA. The EFSA Journal. 7 (9), 1167.

El-Masri, H.A., 2007. Experimental and mathematical modeling methods for the investigation of toxicological interactions. Toxicol. Appl. Pharmacol. 223 (2), 148-154.

El-Masri, H.A., Moiz, M., Mumtaz, M.L., Yushak, L., 2004. Application of physiologically-based pharmacokinetic modeling to investigate the toxicological interaction between chlorpyrifos and parathion in the rat. Environ. Toxicol. Pharmacol. 16, 57-71.

El-Masri, H.A., Tessari, J.D., Yang, R.S., 1996. Exploration of an interaction threshold for the joint toxicity of trichloroethylene and 1,1-dichloroethylene: utilization of a PBPK model. Arch Toxicol. 70 (9), 527-539.

Emond, C., Charbonneau, M., Krishnan, K., 2005. Physiologically based modeling of the accumulation in plasma and tissue lipids of a mixture of PCB congeners in female Sprague-Dawley rats. J. Toxicol. Environ Health A 68 (16), 1393-1412.

European Parliament and Council, 2005. Regulation (EC) No. 396/2005 of the Europealn Parliament and of the Council of 23 February 2005 on maximum residue levels of pesticides in or on food and feed of plant and animal origin and amending Council Directive 91/414/EEC. Official Journal of the European Union L70, 1-16.

Feron, V.J., Groten, J.P., Jonker, D., Cassee, F.R., van Bladeren, P.J., 1995a. Toxicology of chemical mixtures: challenges for today and the future. Toxicology 105 (2-3), 415-427.

Feron, V.J., Groten, J.P., van Zorge, J.A., Cassee, F.R., Jonker, D., van Bladeren, P.J., 1995b. Toxicity studies in rats of simple mixtures of chemicals with the same or different target organs. Toxicol. Lett. 82-83, 505-512.

Feron, V.J., van Vliet, P.W., Notten, W.R.F., 2004. Exposure to combinations of substances: a system for assessing health risks. Environ. Toxicol. Pharmacol. 18, 215-222.

Food Standards Agency, 2005. A critique of the United States Environmental Protection Agency's (US EPA) grouping of insecticidal organophosphates and N-methyl carbamates into common mechanism groups. http://www.food.gov.uk/multimedia/pdfs/papercmg.pdf.

Gearhart, J.M., Jepson, G.W., Clewell, H.J., III, Andersen, M.E., Conolly, R.B., 1990. Physiologically based pharmacokinetic and pharmacodynamic model for the inhibition of acetylcholinesterase by diisopropylfluorophosphate. Toxicol Appl. Pharmacol. 106 (2), 295-310.

Gearhart, J.M., Jepson, G.W., Clewell, H.J., Andersen, M.E., Conolly, R.B., 1994. Physiologically based pharmacokinetic model for the inhibition of acetylcholinesterase by organophosphate esters. Environ Health Perspect. 102 Suppl 11, 51-60.

Gentry, P.R., Covington, T.R., Andersen, M.E., Clewell, H.J., III, 2002a. Application of a physiologically based pharmacokinetic model for isopropanol in the derivation of a reference dose and reference concentration. Regul. Toxicol. Pharmacol. 36 (1), 51-68.

Gentry, P.R., Hack, C.E., Haber, L., Maier, A., Clewell, H.J., III, 2002b. An approach for the quantitative consideration of genetic polymorphism data in chemical risk assessment: examples with warfarin and parathion. Toxicol. Sci. 70 (1), 120-139.

Godin, S.J., DeVito, M.J., Hughes, M.F., Ross, D.G., Scollon, E.J., Starr, J.M., Setzer, R.W., Conolly, R.B., Tornero-Velez, R., 2010. Physiologically based pharmacokinetic modeling of deltamethrin: development of a rat and human diffusion-limited model. Toxicol Sci. 115 (2), 330-343.

Groten, J.P., Feron, V.J., Suhnel, J., 2001. Toxicology of simple and complex mixtures. Trends Pharmacol. Sci. 22 (6), 316-322.

Groten, J.P., Schoen, E.D., van Bladeren, P.J., Kuper, C.F., van Zorge, J.A., Feron, V.J., 1997. Subacute toxicity of a mixture of nine chemicals in rats: detecting interactive effects with a fractionated two-level factorial design. Fundam. Appl. Toxicol. 36 (1), 15-29.

Haddad, S., Beliveau, M., Tardif, R., Krishnan, K., 2001. A PBPK modeling-based approach to account for interactions in the health risk assessment of chemical mixtures. Toxicol. Sci. 63 (1), 125-131.

Haddad, S., Charest-Tardif, G., Krishnan, K., 2000. Physiologically based modeling of the maximal effect of metabolic interactions on the kinetics of components of complex chemical mixtures. J. Toxicol. Environ Health A 61 (3), 209-223.

Haddad, S., Tardif, R., Boyd, J., Krishnan, K., 2010. Physiologically Based Modeling of Pharmacokinetic Interactions in Chemical Mixtures. In: Andersen, M.E., Krishnan, K. (Eds.), Quantitative Modeling in Toxicology. John Wiley & Sons, Ltd, West Sussex, United Kingdom, pp. 83-105.

Haddad, S., Tardif, R., Viau, C., Krishnan, K., 1999. A modeling approach to account for toxicokinetic interactions in the calculation of biological hazard index for chemical mixtures. Toxicol. Lett. 108 (2-3), 303-308.

Hayes, W.J., Laws, E.R.Jr., 1991. Handbook of Pesticide Toxicology. Academic Press, Inc..

Health Council of the Netherlands, 2002. Exposure to combinations of substances: a system for assessing health risks. Health Council of the Netherlands. 2002/05.

Igari, Y., Sugiyama, Y., Awazu, S., Hanano, M., 1982. Comparative physiologically based pharmacokinetics of hexobarbital, phenobarbital and thiopental in the rat. J. Pharmacokinet. Biopharm. 10 (1), 53-75.

Ikeda, T., Tsuda, S., Shirasu, Y., 1992. Pharmacokinetic analysis of protection by an organophosphorus insecticide, chlorfenvinphos, against the toxicity of its succeeding dosage in rats. Fundam. Appl. Toxicol 18 (2), 299-306.

Ikeda, Y., Okamura, K., Fujii, S., 1977. Purification and characterization of rat liver microsomal monoacylglycerol lipase in comparison to the other esterases. Biochim. Biophys. Acta 488 (1), 128-139.

IPCS, 1990. Principles for the Toxicological Assessment of Pesticide Residues in Food. World Health Organization. Environmental Health Criteria 104.

IPCS, 2005. Chemical-specific adjusment factors for interspecies differences and human variability: guidance document for use of data in dose/concentration-response assessment. World Health Organization. Harmonization project document no. 2. pp. 1-96.

IPCS, 2009a. Assessment of combined exposures to multiple chemicals: Report of a WHO/IPCS international workshop on aggregate/cumulative risk assessment. Meek, M.E., Boobis, A.R., Heinemeyer, G., Kleiner, J., Lund, B.-O., Olin, S., Pavittranon, S., Rodriguez, C., Van Raaij, M., Vickers, C., Waight-Sharma, N., Vermeire, T., Dellaro, V., Dewhurst, I., Tritscher, A., Mangelsdorf, I., Teuschler, L., De Rosa, C., Mumtaz, M., Larsen, J.C. (Eds.). World Health Organization. Harmonization Project Document 7.

IPCS, 2009b. Principles and methods for the risk assessment of chemicals in food. World Health Organization. Environmental Health Criteria 240.

IPCS, 2010. Characterization and Application of Physiologically Based Pharmacokinetic Models in Risk Assessment. World Health Organization. Harmonization Project Document 9.

Isukapalli, S.S., Spendiff, M., Georgopoulos, P.G., Krishnan, K., 2010. Uncertainty, variability, and sensitivity analyses in simulation models. In: Andersen, M.E., Krishnan, K. (Eds.), Quantitative Modeling in Toxicology. John Wiley & Sons, Ltd, West Sussex, United Kingdom, pp. 429-458.

Jensen, A.F., Petersen, A., Granby, K., 2003. Cumulative risk assessment of the intake of organophosphorus and carbamate pesticides in the Danish diet. Food Add. Contam. 20 (8), 776-785.

JMPR, 1973. Evaluations of some pesticide residues in food. WHO Pesticide Residues Series, No. 2. WHO, Geneva.

JMPR, 1993. Pesticide residues in food - 1992. Evaluations. Part II - Toxicology. Joint FAO / WHO Meeting on Pesticide Residues. Rome 21-30 September 1992. WHO, Geneva. WHO/PCS/93.34.

JMPR, 1998. Pesticide residues in food - 1997. Evaluations. Part II - Toxicological and Environmental. Joint FAO / WHO Meeting on Pesticide Residues. Lyon 22 September - 1 October 1997. WHO, Geneva. WHO/PCS/98.6.

JMPR, 1999. Pesticide residues in food - 1998. Report 1998. Report of the Joint Meeting of the FAO Panel of Experts on Pesticide Residues in Food and the Environment and the WHO Core Assessment Group on Pesticide Residues. Rome, Italy, 21 - 30 September 1998. WHO, Rome. FAO plant production and protection paper 148.

JMPR, 2000. Pesticide residues in food - 1999. Evaluations. Part II - Toxicological. Joint FAO / WHO Meeting on Pesticide Residues. Rome 20 - 29 September 1999. WHO, Geneva. WHO/PCS/00.4.

JMPR, 2004. Pesticide residues in food - 2003. Evaluations. Part II - Toxicological. Joint FAO / WHO Meeting on Pesticide Residues. Geneva 15 - 24 September 2003. WHO, Geneva. WHO/PCS/04.1.

Johanson, G., 1997. Toxicokinetics: Modeling Disposition. In: Sipes, I.G., Gandolf, A.J., McQueen, C.A. (Eds.), Comprehensive Toxicology. Volume 1. General Principles. Elsevier, Oxford, pp. 167-188.

Johns, D.O., Owens, E.O., Thompson, C.M., Sonawane, B., Hattis, D., Krishnan, K., 2010. Physiological Parameters and Databases for PBPK Modeling. In: Andersen, M.E., Krishnan, K. (Eds.), Quantitative Modeling in Toxicology. John Wiley & Sons, Ltd, West Sussex, United Kingdom, pp. 107-134.

Jonker, D., Woutersen, R.A., Feron, V.J., 1996. Toxicity of mixtures of nephrotoxicants with similar or dissimilar mode of action. Food Chem. Toxicol. 34 (11-12), 1075-1082.

Jonker, D., Woutersen, R.A., van Bladeren, P.J., Til, H.P., Feron, V.J., 1990. 4-week oral toxicity study of a combination of eight chemicals in rats: comparison with the toxicity of the individual compounds. Food Chem. Toxicol. 28 (9), 623-631.

Jonker, D., Woutersen, R.A., van Bladeren, P.J., Til, H.P., Feron, V.J., 1993. Subacute (4-wk) oral toxicity of a combination of four nephrotoxins in rats: comparison with the toxicity of the individual compounds. Food Chem. Toxicol. 31 (2), 125-136.

Jonsson, F., Bois, F.Y., Johanson, G., 2001. Assessing the reliability of PBPK models using data from methyl chloride-exposed, non-conjugating human subjects. Arch Toxicol. 75 (4), 189-199.

Kedderis, G.L., 1997. Toxicokinetics: biotransformation of toxicants. In: Sipes, I.G., Gandolf, A.J., McQueen, C.A. (Eds.), Comprehensive Toxicology. Volume 1. General Principles. Elsevier, Oxford, pp. 135-148.

Kim, C.S., Binienda, Z., Sandberg, J.A., 1996. Construction of a physiologically based pharmacokinetic model for 2,4-dichlorophenoxyacetic acid dosimetry in the developing rabbit brain. Toxicol. Appl. Pharmacol. 136 (2), 250-259.

Kim, C.S., Gargas, M.L., Andersen, M.E., 1994. Pharmacokinetic modeling of 2,4-dichlorophenoxyacetic acid (2,4-D) in rat and in rabbit brain following single dose administration. Toxicol Lett. 74 (3), 189-201.

Kim, C.S., Slikker, W., Jr., Binienda, Z., Gargas, M.L., Andersen, M.E., 1995. Development of a physiologically based pharmacokinetic model for 2,4-dichlorophenoxyacetic acid dosimetry in discrete areas of the rabbit brain. Neurotoxicol. Teratol. 17 (2), 111-120.

Kim, K.B., Anand, S.S., Kim, H.J., White, C.A., Bruckner, J.V., 2008. Toxicokinetics and tissue distribution of deltamethrin in adult Sprague-Dawley rats. Toxicol. Sci. 101 (2), 197-205.

Klaassen, C.D., 1996. Casarett and Doull's Toxicology. The Basic Science of Poisons. McGraw-Hill Inc..

Klein, M.T., Hou, G., Quann, R.J., Wei, W., Liao, K.H., Yang, R.S., Campain, J.A., Mazurek, M.A., Broadbelt, L.J., 2002. BioMOL: a computer-assisted biological modeling tool for complex chemical mixtures and biological processes at the molecular level. Environ Health Perspect. 110 Suppl 6, 1025-1029.

Knaak, J.B., Dary, C.C., Power, F., Thompson, C.B., Blancato, J.N., 2004. Physicochemical and biological data for the development of predictive organophosphorus pesticide QSARs and PBPK/PD models for human risk assessment. Crit Rev. Toxicol. 34 (2), 143-207.

Könemann, W.H., Pieters, M.N., 1996. Confusions of concepts in mixture toxicology. Food Chem. Toxicol. 34 (11-12), 1025-1031.

Kousba, A.A., Poet, T.S., Timchalk, C., 2003. Characterization of the in vitro kinetic interaction of chlorpyrifos-oxon with rat salivary cholinesterase: a potential biomonitoring matrix. Toxicology 188 (2-3), 219-232.

Kousba, A.A., Sultatos, L.G., Poet, T.S., Timchalk, C., 2004. Comparison of chlorpyrifos-oxon and paraoxon acetylcholinesterase inhibition dynamics: potential role of a peripheral binding site. Toxicol Sci. 80 (2), 239-248.

Krieger, R., 2010. Hayes' Handbook of Pesticides. Academic Press, Elsevier Inc..

Krishnan, K., Paterson, J., Williams, D.T., 1997. Health risk assessment of drinking water contaminants in Canada: The applicability of mixture risk assessment methods. Regul. Toxicol. Pharmacol. 26 (2), 179-187.

Krishnan, K., Andersen, M.E., Clewell III, H.J., Yang, R.S.H., 1994. Physiologically based pharmacokinetic modeling of chemical mixtures. In: Yang, R.S.H. (Ed.), Toxicology of Chemical Mixtures. Academic Press, New York, pp. 399-437.

Krishnan, K., Andersen, M.E., 2001. Physiologically based pharmacokinetic modeling in toxicology. In: Hayes, A.W. (Ed.), Principles and methods of toxicology. Taylor & Francis, Philadelphia, pp. 193-241.

Krishnan, K., Andersen, M.E., 2010. Evaluation of Quantitative Models in Toxicology: Progress and Challenges. In: Andersen, M.E., Krishnan, K. (Eds.), Quantitative Modeling in Toxicology. John Wiley & Sons, Ltd, West Sussex, United Kingdom, pp. 459-475.

Krishnan, K., Haddad, S., Béliveau, M., Tardif, R., 2002. Physiological modeling and extrapolation of pharmacokinetic interactions from binary to more complex chemical mixtures. Environ Health Perspect. 110 (Suppl 6), 989-994.

Krishnan, K., Loizou, G.D., Spendiff, M., Lipscomb, J.C., Andersen, M.E., 2010. PBPK Modeling: A Primer. In: Andersen, M.E., Krishnan, K. (Eds.), Quantitative Modeling in Toxicology. John Wiley & Sons, Ltd, West Sussex, United Kingdom, pp. 21-58.

Larsen, J.C., Binderup, M.-L., Dalgaard, M., Dragsted, L.O., Hossaini, A., Ladefoged, O., Lam, H.R., Madsen, C., Meyer, O., Rasmussen, E.S., Reffstrup, T.K., Søborg, I., Vinggaard, A.M., Østergård, G., 2003. Combined actions and interactions of chemicals in mixtures. The toxicological effects of exposure to mixtures of industrial and environmental chemicals. Larsen, J.C. (Ed.). Danish Veterinary and Food Administration. FødevareRapport. 12.

Lindstrom, F.T., Gillett, J.W., Rodecap, S.E., 1976. Distribution of HEOD (dieldrin) in mammals: III. Transport-transfer. Arch Environ Contam Toxicol 4 (3), 257-288.

Lindstrom, F.T., Gillett, J.W., Rodecap, S.E., 1975. Distribution of HEOD (dieldrin) in mammals: II. some applications of the preliminary model. Arch Environ Contam Toxicol 3 (2), 166-182.

Lindstrom, F.T., Gillett, J.W., Rodecap, S.E., 1974. Distribution of HEOD (dieldrin) in mammals. I. Preliminary model. Arch Environ Contam Toxicol 2 (1), 9-42.

Loizou, G., Spendiff, M., Barton, H.A., Bessems, J., Bois, F.Y., d'Yvoire, M.B., Buist, H., Clewell, H.J., III, Meek, B., Gundert-Remy, U., Goerlitz, G., Schmitt, W., 2008. Development of good modelling practice for physiologically based pharmacokinetic models for use in risk assessment: the first steps. Regul. Toxicol. Pharmacol. 50 (3), 400-411.

Lotti, M., 2010. Clinical Toxicology of Anticholinesterase Agents in Humans. In: Krieger, R., Doull, J., Hemmen, J., Hodgson, E., Maibach, H., Reiter, L., Ritter, L., Ross, J., Slikker, W. (Eds.), Hayes' Handbook of Pesticides. Academic Press, Elsevier Inc., pp. 1543-1589.

Lu, C., Holbrook, C.M., Andres, L.M., 2010. The implications of using a physiologically based pharmacokinetic (PBPK) model for pesticide risk assessment. Environ Health Perspect. 118 (1), 125-130.

Lu, Y., Lohitnavy, M., Reddy, M.B., Lohitnavy, O., Ashley, A., Yang, R.S., 2006. An updated physiologically based pharmacokinetic model for hexachlorobenzene: incorporation of pathophysiological states following partial hepatectomy and hexachlorobenzene treatment. Toxicol. Sci. 91 (1), 29-41.

Luijk, R., Schalk, S., Muilerman, H., 2000. Have we lost our heads? Neurotoxin residues harmful to the developing brains of our children. Consumentenbond and Stichting Natuur en Milieu, The Netherlands.

Lutz, R.J., Dedrick, R.L., Matthews, H.B., Eling, T.E., Anderson, M.W., 1977. A preliminary pharmacokinetic model for several chlorinated biphenyls in the rat. Drug Metab Dispos. 5 (4), 386-396.

Ma, T., Chambers, J.E., 1995. A kinetic analysis of hepatic microsomal activation of parathion and chlorpyrifos in control and phenobarbital-treated rats. J. Biochem. Toxicol 10 (2), 63-68.

Ma, T., Chambers, J.E., 1994. Kinetic parameters of desulfuration and dearylation of parathion and chlorpyrifos by rat liver microsomes. Food Chem. Toxicol. 32 (8), 763-767.

Main, A.R., Tarkan, E., Aull, J.L., Soucie, W.G., 1972. Purification of horse serum cholinesterase by preparative polyacrylamide gel electrophoresis. J. Biol. Chem. 247 (2), 566-571.

Maxwell, D.M., Lenz, D.E., Groff, W.A., Kaminskis, A., Froehlich, H.L., 1987. The effects of blood flow and detoxification on in vivo cholinesterase inhibition by soman in rats. Toxicol. Appl. Pharmacol. 88 (1), 66-76.

Maxwell, D.M., Vlahacos, C.P., Lenz, D.E., 1988. A pharmacodynamic model for soman in the rat. Toxicol. Lett. 43 (1-3), 175-188.

McCarty, L.S., Borgert, C.J., 2006. Review of the toxicity of chemical mixtures: Theory, policy, and regulatory practice. Regul. Toxicol. Pharmacol. 45, 119-143.

McMullin, T.S., Hanneman, W.H., Cranmer, B.K., Tessari, J.D., Andersen, M.E., 2007. Oral absorption and oxidative metabolism of atrazine in rats evaluated by physiological modeling approaches. Toxicology 240 (1-2), 1-14.

Mileson, B.E., Chambers, J.E., Chen, W.L., Dettbarn, W., Ehrich, M., Eldefrawi, A.T., Gaylor, D.W., Hamernik, K., Hodgson, E., Karczmar, A.G., Padilla, S., Pope, C.N., Richardson, R.J., Saunders, D.R., Sheets, L.P., Sultatos, L.G., Wallace, K.B., 1998. Common mechanism of toxicity: a case study of organophosphorus pesticides. Toxicol. Sci. 41 (1), 8-20.

Mileson, B.E., Faustman, E., Olin, S., Ryan, P.B., Ferenc, S., Burke, T., 1999. A framework for cumulative risk assessment. Mileson, B.E., Faustman, E., Olin, S., Ryan, P.B., Ferenc, S., Burke, T. (Eds.). International Life Sciences Institute. An ILSI Risk Science Institute Workshop Report. pp. 1-55.

Mirfazaelian, A., Kim, K.B., Anand, S.S., Kim, H.J., Tornero-Velez, R., Bruckner, J.V., Fisher, J.W., 2006. Development of a physiologically based pharmacokinetic model for deltamethrin in the adult male Sprague-Dawley rat. Toxicol. Sci. 93 (2), 432-442.

Mortensen, S.R., Chanda, S.M., Hooper, M.J., Padilla, S., 1996. Maturational differences in chlorpyrifos-oxonase activity may contribute to age-related sensitivity to chlorpyrifos. J. Biochem. Toxicol. 11 (6), 279-287.

Müller, A.K., Bosgra, S., Boon, P.E., van der Voet, H., Nielsen, E., Ladefoged, O., 2009. Probabilistic cumulative risk assesment of anti-androgenic pesticides in food. Food Chem. Toxicol. Accepted.

Mumtaz, M.M., 1995. Risk assessment of chemical mixtures from a public health perspective. Toxicol. Lett. 82-83, 527-532.

Mumtaz, M.M., De Rosa, C.T., Groten, J., Feron, V.J., Hansen, H., Durkin, P.R., 1998. Estimation of toxicity of chemical mixtures through modeling of chemical interactions. Environ. Health Perspect. 106 Suppl. 6, 1353-1360.

Mumtaz, M.M., Durkin, P.R., 1992. A weight-of-evidence approach for assessing interactions in chemical mixtures. Toxicol. Ind. Health 8 (6), 377-406.

National Research Council, 1993. Pesticides in the diets of infants and children. National Academy Press, Washington, D.C.

National Research Council, 1989. Drinking water and health, volume 9: selected issues in risk assessment. National Academy Press, Washington, D.C.

National Research Council, 1987. Drinking water and health. Volume 8: Pharmacokinetics in risk assessment. National Academy Press. Volume 8.

National Research Council, 2007. Toxicity testing in the twenty-first century: A vision and a strategy. Krewski, D.c.o.C.o.T.a.A.o.E.A. (Ed.). National Academy Press.

Nestorov, I., 2003. Whole body pharmacokinetic models. Clin. Pharmacokinet. 42 (10), 883-908.

Nolan, R.J., Rick, D.L., Freshour, N.L., Saunders, J.H., 1984. Chlorpyrifos: pharmacokinetics in human volunteers. Toxicol Appl. Pharmacol. 73 (1), 8-15.

Nong, A., Tan, Y.M., Krolski, M.E., Wang, J., Lunchick, C., Conolly, R.B., Clewell, H.J., III, 2008. Bayesian calibration of a physiologically based pharmacokinetic/pharmacodynamic model of carbaryl cholinesterase inhibition. J. Toxicol. Environ Health A 71 (20), 1363-1381.

Norwegian Scientific Committee for Food Safety, 2008. Combined toxic effects of multiple chemical exposures. Alexander, J., Hetland, R.B., Vikse, R., Dybing, E., Eriksen, G.S., Farstad, W., Jenssen, B.M., Paulsen, J.E., Skåre, J.U., Steffensen, I.-L., Øvrebø, S. (Eds.). Vitenskapskomiteen for Mattrygghet / Norwegian Scientific Committee for Food Safety. Report 1.

Nostrandt, A.C., Padilla, S., Moser, V.C., 1997. The relationship of oral chlorpyrifos effects on behavior, cholinesterase inhibition, and muscarinic receptor density in rat. Pharmacol. Biochem. Behav. 58 (1), 15-23.

O'Brien, R.D., 1967. Insecticides. Action and Metabolism. Academic Press Inc., New York and London.

OECD, 2010. OECD guideline for the testing of chemicals. Toxicokinetics. Organisation for Economic Co-operation and Development. TG 417. pp. 1-20.

Pelekis, M., Emond, C., 2009. Physiological modeling and derivation of the rat to human toxicokinetic uncertainty factor for the carbamate pesticide aldicarb. Environ. Toxicol. Pharmacol. 28, 179-191.

Poet, T.S., Kousba, A.A., Dennison, S.L., Timchalk, C., 2004. Physiologically based pharmacokinetic/pharmacodynamic model for the organophosphorus pesticide diazinon. Neurotoxicology 25 (6), 1013-1030.

Poet, T.S., Wu, H., Kousba, A.A., Timchalk, C., 2003. In vitro rat hepatic and intestinal metabolism of the organophosphate pesticides chlorpyrifos and diazinon. Toxicol Sci. 72 (2), 193-200.

Price, K., Krishnan, K., 2011. An integrated QSAR-PBPK modelling approach for predicting the inhalation toxicokinetics of mixtures of volatile organic chemicals in the rat. SAR QSAR. Environ. Res. 22 (1-2), 107-128.

Ramsey, J.C., Andersen, M.E., 1984. A physiologically based description of the inhalation pharmacokinetics of styrene in rats and humans. Toxicol. Appl. Pharmacol. 73 (1), 159-175.

Reffstrup, T.K., 2002. Combined actions of pesticides in food. Danish Veterinary Food Administration. FødevareRapport. 19.

Rowland, M., Balant, L., Peck, C., 2004. Physiologically based pharmacokinetics in drug development and regulatory science: a workshop report (Georgetown University, Washington, DC, May 29-30, 2002). AAPS. PharmSci. 6 (1), 1-12.

Rowland, M., Tozer, T.N., 1995. Clinical Pharmcokinetics. Concepts and Applications. Lippincott Williams & Wilkins, Philadelphia.

Safe, S., 1990. Polychlorinated Biphenyls (PCBs), Dibenzo-p-Dioxins (PCDDs), Dibenzofurans (PCDFs), and Related Compounds: Environmental and Mechanistic Considerations Which Support the Development of Toxic Equivalency Factors (TEFs). Crit. Rev. Toxicol. 21 (1), 51-88.

Safe, S.H., 1998. Hazard and risk assessment of chemical mixtures using the toxic equivalency factor approach. Environ. Health Perspect. 106 (Supplement 4), 1051-1058.

Seed, J., Brown, R.P., Olin, S.S., Foran, J.A., 1995. Chemical mixtures: current risk assessment methodologies and future directions. Regul. Toxicol. Pharmacol. 22, 76-94.

Simmons, J.E., 1996. Application of physiologically based pharmacokinetic modelling to combination toxicology. Food Chem. Toxicol. 34 (11-12), 1067-1073.

Slikker, W., Jr., Andersen, M.E., Bogdanffy, M.S., Bus, J.S., Cohen, S.D., Conolly, R.B., David, R.M., Doerrer, N.G., Dorman, D.C., Gaylor, D.W., Hattis, D., Rogers, J.M., Woodrow, S.R., Swenberg, J.A., Wallace, K., 2004. Dose-dependent transitions in mechanisms of toxicity. Toxicol. Appl. Pharmacol. 201 (3), 203-225.

Smith, J.N., Campbell, J.A., Busby-Hjerpe, A.L., Lee, S., Poet, T.S., Barr, D.B., Timchalk, C., 2009. Comparative chlorpyrifos pharmacokinetics via multiple routes of exposure and vehicles of administration in the adult rat. Toxicology 261 (1-2), 47-58.

Spencer, P.S., Schaumburg, H.H., Ludolph, A.C., 2000. Experimental and Clinical Neurotoxicology. Oxford University Press.

Sultatos, L.G., Shao, M., Murphy, S.D., 1984. The role of hepatic biotransformation in mediating the acute toxicity of the phosphorothionate insecticide chlorpyrifos. Toxicol. Appl. Pharmacol. 73 (1), 60-68.

Svendsgaard, D.J., Greco, W.R., 1995. Session summary: experimental designs, analyses and quantitative models. Toxicology 105 (2-3), 157-160.

Svendsgaard, D.J., Hertzberg, R.C., 1994. Statistical methods for the toxicological evaluation of the additivity assumption as used in the environmental protection agency chemical mixture risk assessment guidelines. In: Yang, R.S.H. (Ed.), Toxicology of Chemical Mixtures. Academic Press, New York, pp. 599-642.

Testai, E., Buratti, F.M., Consiglio, E.D., 2010. Chlorpyrifos. In: Krieger, R., Doull, J., Hemmen, J., Hodgson, E., Maibach, H., Reiter, L., Ritter, L., Ross, J., Slikker, W. (Eds.), Hayes' Handbook of Pesticides. Academic Press, Elsevier Inc., pp. 1505-1526.

Teuschler, L.K., 2007. Deciding which chemical mixtures risk assessment methods work best for what mixtures. Toxicol. Appl. Pharmacol. 223 (2), 139-147.

Thompson, C.M., Johns, D.O., Sonawane, B., Barton, H.A., Hattis, D., Tardif, R., Krishnan, K., 2009. Database for physiologically based pharmacokinetic (PBPK) modeling: physiological data for healthy and health-impaired elderly. J. Toxicol Environ. Health B Crit Rev. 12 (1), 1-24.

Timchalk, C., 2010. Organophosphorus Insecticide Pharmacokinetics. In: Krieger, R., Doull, J., Hemmen, J., Hodgson, E., Maibach, H., Reiter, L., Ritter, L., Ross, J., Slikker, W. (Eds.), Hayes' Handbook of Pesticides. Academic Press, Elsevier Inc., pp. 1410-1433.

Timchalk, C., Campbell, J.A., Liu, G., Lin, Y., Kousba, A.A., 2007a. Development of a non-invasive biomonitoring approach to determine exposure to the organophosphorus insecticide chlorpyrifos in rat saliva. Toxicol. Appl. Pharmacol. 219, 217-225.

Timchalk, C., Hinderliter, P.M., Poet, T.S., 2010. Modeling cholinesterase inhibition. In: Andersen, M.E., Krishnan, K. (Eds.), Quantitative Modeling in Toxicology. John Wiley & Sons, Ltd, West Sussex, United Kingdom, pp. 137-165.

Timchalk, C., Kousba, A., Poet, T.S., 2002a. Monte Carlo analysis of the human chlorpyrifos-oxonase (PON1) polymorphism using a physiologically based pharmacokinetic and pharmacodynamic (PBPK/PD) model. Toxicol. Lett. 135 (1-2), 51-59.

Timchalk, C., Kousba, A.A., Poet, T.S., 2007b. An age-dependent physiologically based pharmacokinetic/pharmacodynamic model for the organophosphorus insecticide chlorpyrifos in the preweanling rat. Toxicol. Sci. 98 (2), 348-365.

Timchalk, C., Nolan, R.J., Mendrala, A.L., Dittenber, D.A., Brzak, K.A., Mattsson, J.L., 2002b. A Physiologically based pharmacokinetic and pharmacodynamic (PBPK/PD) model for the organophosphate insecticide chlorpyrifos in rats and humans. Toxicol. Sci. 66 (1), 34-53.

Timchalk, C., Poet, T.S., 2008. Development of a physiologically based pharmacokinetic and pharmacodynamic model to determine dosimetry and cholinesterase inhibition for a binary mixture of chlorpyrifos and diazinon in the rat. Neurotoxicology 29 (3), 428-443.

Timchalk, C., Poet, T.S., Hinman, M.N., Busby, A.L., Kousba, A.A., 2005. Pharmacokinetic and pharmacodynamic interaction for a binary mixture of chlorpyrifos and diazinon in the rat. Toxicol. Appl. Pharmacol. 205 (1), 31-42.

Travis, C.C., Hattemer-Frey, H.A., 1990. Pharmacokinetics and its application to risk assessment. In: Saxena, J. (Ed.), Hazard Assessment of chemicals: Volume 7. Hemisphere Publishing Corporation, pp. 39-82.

U.S.EPA, 1986. Guidance for health risk assessment of chemical mixtures. Federal Register 51(185). Risk Assessment Forum, U.S. Environmental Protection Agency, Washington, DC. EPA/630/R-98/002. pp. 34014-34025.

U.S.EPA, 1988a. Reference physiological parameters in pharmacokinetic modeling. Arms, A.D., Travis, C.C. (Eds.). EPA/600/S6-88-004.

U.S.EPA, 1988b. Technical support document on risk assessment of chemical mixtures. U.S. Environmental Protection Agency, Environmental Criteria and Assessment Office, Cincinnati. EPA/600/8-90/064.

U.S.EPA, 1989a. Interim Procedures for Estimating Risks Associated with Exposures to Mixtures of Chlorinated Dibenzo-P-Dioxins and-Dibenzofurans (CDDs and CDFs) and 1989 Update. U.S. Environmental Protection Agency, Risk Assessment Forum, Washington DC. EPA/625/3-89/016 (NTIS PB90145756).

U.S.EPA, 1989b. Risk assessment. Guidance for Superfund, volume 1, human health evaluation manual (Part A). Interim final. Risk Assessment Forum, U.S. Environmental Protection Agency, Washington, DC. EPA/540/1-89-002.

U.S.EPA, 1999a. Guidance for identifying pesticide chemicals and other substances that have a common mechanism of toxicity. Docket Number: OPP-00542. (Acessed 29-1-1999a).

U.S.EPA, 1999b. Guidance for performing aggregate exposure and risk assessments. Office of Pesticide Programs, U.S. Environmental Protection Agency. Item: 6043.

U.S.EPA, 2000. Supplementary guidance for conducting health risk assessment of chemical mixtures. U.S. Environmental Protection Agency. Risk Assessment Forum Technical Panel. Office of EPA/630/R-00/002.

U.S.EPA, 2002. Guidance on cumulative risk assessment of pesticide chemicals that have a common mechanism of toxicity. Office of Pesticide Programs. U.S. Environmental Protection Agency. Washington, D.C. 20460.

U.S.EPA, 2003. Developing relative potency factors for pesticide mixtures: biostatistical analyses of joint dose-response. National Center for Environmental Assessment. Office of Research and Development. U.S. Environmental Protection Agency. Cincinnati, OH 45268. EPA/600/R-03/052.

U.S.EPA, 2005. Guidelines for Carcinogen Risk Assessment. Risk Assessment Forum, U.S. Environmental Protection Agency. EPA/630/P-03/001FMarch 2005.

U.S.EPA, 2006a. Approaches for the Application of Physiologically Based Pharmacokinetic (PBPK) Models and Supporting Data in Risk Assessment. Barton, H., Chiu, W., DeWoskin, R., Foureman, G., Krishnan, K., Lipscomb, J., Schlosser, P., Sonawane, B., Thompson, C. (Eds.). National Center for Environmental Assessment. Office of Research and Development. U.S. Environmental Protection Agency, Washington, DC. EPA/600/R-05/043F.

U.S.EPA, 2006b. Cumulative risk from chloroacetanilide pesticides. U.S. Environmental Protection Agency Office of Pesticide Programs Health Effects Division.

U.S.EPA, 2006c. Organophosphorus cumulative risk assessment 2006 update. U.S. Environmental Protection Agency Office of Pesticide Programs.

U.S.EPA, 2006d. Triazine cumulative risk assessment. U.S. Environmental Protection Agency Office of Pesticide Programs Health Effects Division.

U.S.EPA, 2007. Revised *N*-methyl carbamate cumulative risk assessment. U.S. Environmental Protection Agency Office of Pesticide Programs.

U.S.EPA, 2009. Physiological Infomation Database (PID). http://cfpub.epa.gov/ncea/risk/recordisplay.cfm?deid=202847.

United States of America in Congress, 1996. Food quality protection act of 1996. Public Law. 104-170. pp. 1489-1538.

Van den Berg, M., Birnbaum, L., Bosveld, A.T.C., Brunström, B., Cook, P., Feeley, M., Giesy, J.P., Hanberg, A., Hasegawa, R., Kennedy, S.W., Kubiak, T., Larsen, J.C., van Leuwen, F.X.R., Liem, D., Nolt, C., Peterson, R.E., Poellinger, L., Safe, S., Shrenk, D., Tillitt, D., Tysklind, M., Younes, M., Wærn, F., Zacharewski, T., 1998. Toxic Equivalency Factors (TEFs) for PCBs, PCDDs, PCDFs for Humans and Wildlife. Environ. Health Perspect. 106, 775-792.

Van den Berg, M., Birnbaum, L.S., Denison, M., De, V.M., Farland, W., Feeley, M., Fiedler, H., Hakansson, H., Hanberg, A., Haws, L., Rose, M., Safe, S., Schrenk, D., Tohyama, C., Tritscher, A., Tuomisto, J., Tysklind, M., Walker, N., Peterson, R.E., 2006. The 2005 World Health Organization reevaluation of human and Mammalian toxic equivalency factors for dioxins and dioxin-like compounds. Toxicol. Sci. 93 (2), 223-241.

Vander, A.J., Sherman, J.H., Luciano, D.S., 1990. Human Physiology. The Mechanisms of Body Function. McGraw-Hill, Inc..

Wang, C., Murphy, S.D., 1982. The role of non-critical binding proteins in the sensitivity of acetylcholinesterase from different species to diisopropyl fluorophosphate (DFP), in vitro. Life Sci. 31 (2), 139-149.

Wilkinson, C.F., Christoph, G.R., Julien, E., Kelley, J.M., Kronenberg, J., McCarthy, J., Reiss, R., 2000. Assessing the risks of exposures to multiple chemicals with a common mechanism of toxicity: how to cumulate? Regul. Toxicol. Pharmacol. 31 (1), 30-43.

Wolterink, G., Piersma, A.H., van Engelen, J.G.M., 2002. Risk assessment of chemicals: what about children? RIVM. RIVM report. 613340005/2002. pp. 1-29.

Woodruff, T.J., Bois, F.Y., Auslander, D., Spear, R.C., 1992. Structure and parameterization of pharmacokinetic models: their impact on model predictions. Risk Anal. 12 (2), 189-201.

Yang, R.S.H., Lu, Y., 2007. The application of physiologically based pharmacokinetic (PBPK) modeling to risk assessment. In: Robson, M.G., Toscano, W. (Eds.), Risk assessment for environmental health. John Wiley & Sons, San Francisco, pp. 85-120.

Yesair, D.W., Feder, P.I., Chin, A.E., Naber, S.J., Kuiper-Goodman, T., Scott, C.S., Robinson, P.E., 1986. Development, evaluation and use of a pharmacokinetic model for hexachlorobenzene. IARC Sci. Publ. (77), 297-318.

Zhang, X., Tsang, A.M., Okino, M.S., Power, F.W., Knaak, J.B., Harrison, L.S., Dary, C.C., 2007. A physiologically based pharmacokinetic/pharmacodynamic model for carbofuran in Sprague-Dawley rats using the exposure-related dose estimating model. Toxicol. Sci. 100 (2), 345-359.

APPENDIX I

OVERVIEW OF PBTK/TD MODELS ON A SINGLE PESTICIDE

Substances	Species	Route of administration	Purpose of model simulation. Model structure	Computer program used	Model developed	Reference
2,4-D (chlorophenoxy herbicide)	Humans: worker exposure	Skin. Studies: rats: i.v. or oral. Humans: single oral dose. (Data from literature)	PK in rats and humans. Tissue binding, binding to plasma, high-dose inhibition of urinary excretion. Simple representation of the inhibitory effects of 2,4-D on renal excretory transport. Provides basis for comparing concentration of 2,4-D in plasma in experimental mammals and humans.		Own model	(Durkin et al., 2004)
2,4-D (chlorophenoxy herbicide)	Rats, rabbits	Rats: i.v. or oral; rabbit: i.p.	Concentration in plasma, brain. Kinetics in central nervous system. Model consisted of brain, body, venous and arterial compartments	SimuSolv	Own model	(Kim et al., 1994)
2,4-D (chlorophenoxy herbicide)	Rabbits	i.p., i.v.	Dosimetry in discrete areas of the brain, blood	SimuSolv	Own model	(Kim et al., 1995)
2,4-D (chlorophenoxy herbicide)	Rabbits	I.v. or i.p.	Dosimetry in developing rabbit brain. Model consisted of brain, body and venous and arterial compartments for the mother linked to the fetus by placenta	SimuSolv	Own model	(Kim et al., 1996)
2,4-D (chlorophenoxy herbicide)	Rats	I.v., s.c.	Concentration in blood and 6 brain regions. 6 compartments + 6 brain regions	SimuSolv	Based on (Kim et al., 1994; Kim et al., 1995)	(Kim et al., 2001
Aldicarb (carbamate)	Rats, humans	Oral, i.v.	AChE inhibition. Objective: determine the interspecies toxicokinetic uncertainty factor. Lungs, brain, liver, stomach, kidney, fat, rest of body, venous and arterial blood	ACSL	Own model	(Pelekis and Emond, 2009)
Atrazine -> 3 metabolites (triazine)	Rats	Oral	Time courses of individual chlorotriazines after dosing with atrazine. Absorption and oxidative metabolism. Liver, lumped body compartment, (gut) for each metabolite – linked together	Berkeley Madonna	Own model	(McMullin et al., 2007)
Atrazine and metabolites (triazine)	Rats	Oral	Time courses of total chlorotriazine after dosing with atrazine. Blood, body, brain compartment	ACSL	Own model	(McMuillin et al 2003
Carbaryl (carbamate)-> metabolites	Rats	I.v., oral, gavage	Tissue concentrations. Subsequently predict ChE inhibition in brain, blood. Markov Chain Monte Carlo calibration of model parameters. 5 compartments, 3 linked models	ACSL	Own model	(Nong et al., 2008)
Carbofuran (carbamate) -> 16 metabolites	Rats	Oral	Tissue dosimetry + PD (blood and brain AChE). 12 compartments + portal, venous, arterial blood	ERDEM PBPK/PD (Exposure-Related Dose Estimating	Own model	(Zhang et al., 2007)

Substances	Species	Route of administration	Purpose of model simulation. Model structure	Computer program used	Model developed	Reference
				Model)		
Chlordecone (Kepone)	Rats	I.v., oral	Enteric transport. A whole body PBPK model with detailed description of GI tract		Own model	(Bungay et al., 1981)
Chlordecone, mirex, hexafluoroacetone	Rats, rhesus monkeys	Oral, inhalation or s.c.	Differences in liver and fat partitioning. 5 compartments (chlordecone, mirex), hexafluoroacetone: 6 compartments (extra compartment: ventilatory uptake and elimination from alveoli)	ACSL	Own model	(Belfiore et al., 2007)
Chlorofenvinfos (OP)	Rats	Oral, i.v.	Effect of chlorofenvinfos pretreatment of chlorofenvinfos concentrations in plasma and liver as well as changes in parameters. Model consisted of slowly and rapidly equilibrating tissues, liver and gut compartments	MULTI	Own model	(Ikeda et al., 1992)
Chlorpyrifos (OP) -> chlorpyrifos-oxon, TCP	Rats	Acute and chronic oral and dermal	PK/PD model modified to account for altered lipid-tissue partition coefficients and major physiological and biochemical changes of pregnancy. Target tissue dosimetry, plasma protein binding of chlorpyrifos and oxon + dynamic response (esterase inhibition)	AcslXtreme v2.4	Based on (Timchalk and Poet, 2008) (Timchalk et al., 2002b; Timchalk et al., 2007b; Timchalk et al., 2005)	(Lowe et al 2009
Chlorpyrifos (OP) -> TCP	Humans - children 3-6 years	Oral, inhalation	Urinary excretion of TCP (the metabolite description was expanded compared to original model in order to simulate differences at different life stages)	ERDEM (Exposure-Related Dose Estimating Model)	Based on (Timchalk et al., 2002b)	(Lu et al., 2010)
Chlorpyrifos (OP) -> chlorpyrifos-oxon, TCP	Rats	Dietary, gavage, dermal	Tissue dosimetry + PD (inhibition of AChE, BuChE, CaE) in preweanling and adult rats. Model from Timchalk et al., (2002b) were modified by incorporating age-dependent PBPK/PD	SimuSolv	Based on (Timchalk et al., 2002b)	(Timchalk et al., 2007b)
Chlorpyrifos (OP) -> chlorpyrifos-oxon, TCP	Humans	Dermal, oral, gavage	"Impact of CPF-oxonase status on the theoretical concentration of CPF-oxon in the human brain." "The impact of the human CPF-oxonase metabolic polymorphism on CPF metabolism and detoxification was evaluated using Monte Carlo analysis"	SimuSolv	Based on (Timchalk et al., 2002b)	(Timchalk et al., 2002a)
Chlorpyrifos (OP) -> chlorpyrifos-oxon, TCP	Rats	Gavage	Incorporation of a compartment in the existing model to describe the time-course of TCP concentration in blood and saliva	SimuSolv	Based on (Timchalk et al., 2002b)	(Timchalk et al., 2007a)
Chlorpyrifos (OP) -> chlorpyrisfos-oxon, TCP	Rats, humans	Dermal, dietary, gavage	Tissue dosimetry. PD: inhibition of AChE, BuChE, CaE	SimuSolv	Own model	(Timchalk et al., 2002b)
Chlorpyrifos (OP) -> chlorpyrisfos-oxon, TCP	Rats	Gavage, i.v., s.c. (one or more exposure route)	Concentration in blood, brain, plasma, urine, fat. Chlorpyrifos more extensively metabolised after oral administration than after i.v. or s.c. exposure		Based on (Timchalk et al., 2002b)	(Smith et al., 2009)
Deltamethrin (pyrethroid)	Rats,	Oral, i.v.	Absorption in gastrointestinal tract excluding saturable	AcslXtreme	Based on	(Godin et al., 2010)

Substances	Species	Route of administration	Purpose of model simulation. Model structure	Computer program used	Model developed	Reference
	humans		absorption process (unlike Mirfazaelian et al.)		(Mirfazaelian et al., 2006)	
Deltamethrin (pyrethroid)	Rats	Po, i.v., oral. (Data from (Kim et al., 2008))	Cytochrome P-450 mediated metabolism in liver, CaE-mediated metabolism in plasma in liver. Dosimetry in the central nervous system - tissue concentration in plasma blood, brain, fat, muscle. 7 compartments	AcslXtreme v1.3.2	Own model	(Mirfazaelian et al., 2006)
Diazinon (OP) -> diazinon-oxon and 2-isopropyl-4-methyl-6-hydroxypyrimidine (IMHP)	Rats, humans	Dermal, oral (gavage, dietary)	Concentration of the compounds in plasma and urinary elimination of IMHP. Inhibition of AChE and BuChE	SimuSolv	Based on (Timchalk et al., 2002b; Timchalk et al., 2002a)	(Poet et al., 2004)
Dieldrin (chlorinated hydrocarbon insecticides)	Rats, humans	Mammals	Tissue concentration especially adipose and lipid-phase in blood. Based upon lipid-phase transport and transfer to tissue lipids. 8 tissues characterised by blood lipid flows and tissue lipid masses		Own model	(Lindstrom et al., 1975; Lindstrom et al., 1976; Lindstrom et al., 1974)
Diisopropylfluorophosphate (OP)	Rats, mice	I.v., s.c.	Inhibition of AChE in brain, liver, kidney, rapidly perfused tissues, venous and arterial blood. 9 compartments + blood	ACSL	Model structure based on (Ramsey and Andersen, 1984)	(Gearhart et al., 1990)
Diisopropylfluorophosphate (OP). Model adapted for parathion and its metabolite paraoxon	Rats, mice, humans	Inhalation, i.v. injection	Simulate PK data from mice and rats. Inhibition of AChE in brain, liver, kidney, rapidly perfused tissues, venous and arterial blood. 9 compartments + blood	ACSL	Own model	(Gearhart et al., 1994)
Endosulfan (chlorinated hydrocarbon insecticides) and metabolites	Rats	Oral, single dose	Tissue concentration: liver, kidney, brain, testes, blood. 9 compartment model based on PK data. Model verified by data from experiments in literature	Microsoft Visual Basic 6.3	Model structure based on (Ramsey and Andersen, 1984)	(Chan et al., 2006)
Hexachlorobenzene (aromatic hydrocarbon, fungicide)	Male rats	Oral, i.v.	Blood is divided in plasma and RBC. RBC binding. Elimination process of HCB from plasma to GI. Compartment: plasma, RBC, liver, fat, slowly and rapidly perfused tissue, GI lumen	ACSL	Own model	(Lu et al., 2006)
Hexachlorobenzene (aromatic hydrocarbon, fungicide)	Rats (growing), humans (growing)	Oral, intubation	ADME in growing rats and humans. 8-9 compartments		Own model	(Yesair et al., 1986)
Lindane (chlorinated hydrocarbon insecticides)	Rats	Oral or i.p.	Concentration in blood, brain, fat, muscle. 5 compartment model based on PK data. Model verified by data from literature	ACSL	Model structure based on (Lutz et al., 1977)	(Dejongh and Blaauboer, 1997)
Malathion (OP)	Humans	Dermal	ADME. Simulate the urinary excretion of metabolites		Own model	Dong et al, 1994 as

Substances	Species	Route of administration	Purpose of model simulation. Model structure	Computer program used	Model developed	Reference
						cited in (Belfiore, 2005)
Malathion (OP)	Humans	Dermal	ADME. Simulate the urinary excretion of metabolites		Own model	Rabovsky and Brown, 1993 as cited in (Belfiore, 2005)
Malathion + 4 metabolites (OP)	humans	I.v, oral, dermal	Tissue concentration + urinary excretion. From NOAEL it predicts corresponding biological reference values	MathCad	Own model	(Bouchard et al., 2003)
p,p'-DDE (a Persistent metabolite of p,p'-DDT)	Rats	For gestation: oral. For dam/pup: milk	Tissue dosimetry. How maternal exposure to DDE affects perinatal sexual development *in utero* or in early postnatal period. Models for gestation, dam and pup	SimuSolv	Based on O'Flaherty et al 1992	(You et al 1999
Parathion (OP)	*In vitro*	Mice	Parameters determined *in vitro* were used in model to predict tissue levels of parathion measured after i.v. dosing		Own model	Sultatos et al, 1990 as cited in (Belfiore, 2005)
Parathion (OP), (also model for warfarin)		I.v., s.c.	Incorporate information on polymorphism into analysis of toxicokinetic variability. Metabolism of parathion to paraoxon. Inhibition of AChE, BuChE, CaE. 8 compartments for parathion and for paraoxon. Authors conclude that "combining PBTK modeling with Monte Carlo analysis provides a powerful (although labor-intensive) approach for quantitatively characterizing the effects of polymorphisms on human variability in tissue dose."		Based on (Gearhart et al., 1994)	(Gentry et al., 2002b)
Soman (pinocolyl methylphosphonofluoridate) (OP)	Rats	i.m. or i.v. injection	PD-model. Inhibition of AChE. 8 compartments	GEAR software	Own model	(Maxwell et al., 1988)

Substances	Species	Route of administration	What do they simulate	Computer program used	Model developed	Reference
Mixture: chlorpyrifos and parathion (OPs)	Rats	S.c. injection, oral	Originally: 2 PBPK models to estimate blood concentration of their respective metabolite. Then linked to submodel of AChE kinetics a) P-450 enzymatic site b) AChE binding sites	Simulink and M-files software of Matlab	Own model	(El-Masri et al., 2004)
Mixture: chlorpyrifos, diazinon (and metabolites of both)	Rats	Dietary, gavage, dermal	Tissue dosimetry + PD (inhibition of ChE). CYP450 interaction: non-competitive (chlorpyrifos and diazinon -> oxon, chlorpyrifos -> 3,5,6-trichloro-2-pyridinol), competitive: (diazinon -> 2-isopropyl-methyl-6-hydroxypyrimidine). B-esterase metabolism described as dose additive. No interactions for hydrolysis of oxon (PON-1)	SimuSolv	Based on (Poet et al., 2004; Timchalk et al., 2002b)	(Timchalk and Poet, 2008)

APPENDIX II

The model code written in Berkeley Madonna for the PBTK/TD model describing chlorpyrifos and chlorpyrifos-oxon in rats are presented below. This is followed by a list of abbreviations used in the model.

MODEL CODE FOR THE PBTK/TD MODEL FOR CHLORPYRIFOS IN RATS

```
Program: PBTK/TD model for chlorpyrifos (CPF) and chlorpyrifos-oxon (CPF-oxon) in rats. Model name: PBTK-TD for CPF.mmd
Model re-build by Trine Klein Reffstrup, DTU-Food, Søborg, Denmark.
Original model developed by Timchalk et al., 2002. A physiologically based pharmacokinetic and pharmacodynamic (PBPK/PD) model for the organophosphate insecticide chlorpyrifos in rats and humans. Toxicological Sciences, 66, 34-53.
Parameters primarily from Timchalk et al. 2002, Gearhart et al 1990, 1994 as indicated.
Vmax3, Vmax4, Km3 and Km4 is from Timchalk et al., 2007


METHOD STIFF;          Rosenbrock (stiff)

STARTTIME = 0;         (hr)
STOPTIME=24;           (hr)
DT = 0.02
```

```
INPUT TO LIVER

PARAMETERS
;Oral absorption parameters, Timchalk et al. 2002
KaS=0.01;    Rate constant, absorption in stomach (1/hr)
KaI=0.5;     Rate constant, absorption in intestine (1/hr)
KsI=0.5;     Rate constant, transfer stomach-intestine (1/hr)
Fa=0.80;     Fractional absorption (80 %)

;Body weight
BW=0.25;     body weight for rats (kg)

;Molecular weight, calculated
Mc=0.350;    Molecular weight for chlorpyrifos (mg/micromol)

EQUATIONS
;Dietary exposure
Dietexp = IF MOD(TIME, 24) <= 12 THEN kzero ELSE 0;   Dietary exposure of chlorpyrifos (micromol/hr)
kzero=Diet*Fa/12; Zero-order uptake rate (micromol/hr). Consumption during 12 hr in a 24 hr interval
Oral_adm=0.1; Dietary administration of chlorpyrifos (mg/kg bw/day)
Diet=Oral_adm*BW/Mc; Dietary administration of chlorpyrifos (recalculation of unit) (micromol/day)

;Repeated dietary exposure of Oral_adm every "R" hr for "repeated" times
Repeat_exp=PULSE(dose,0,R)*SQUAREPULSE(0,repeated); repeated dietary exposure (micromol/hr)
dose_in=1; dose (mg/kg bw/day)
dose=dose_in*BW*Fa/Mc; administered dose of chlorpyrifos (recalculation of units) (micromol/day)
R=24; dosing intervals, 24 hr
```

repeated=648;time over which the dosage is repeated

;Gavage exposure
Stom'=-KaS*Stom - KsI*Stom; Absorption rate in stomach (micromol/hr)
Init Stom=Gavage; Initial amount of chlorpyrifos in stomach (micromol)
Gavage_in=1; Gavage administration of chlorpyrifos (mg/kg bw)
Gavage=Gavage_in*BW/Mc; Gavage administration of chlorpyrifos (recalculation of unit) (micromol)
Intes'=KsI*Stom - KaI*Intes; Absorption rate in intestine (micromol/hr)
Init Intes=0; Initial amount of chlorpyrifos in intestine (micromol)

Oral_abs'=KaS*Stom+KaI*Intes; Rate of oral absorption of chlorpyrifos is equal to sum of absorption rates from Stomach (Stom) and intestine (Intes) (micromol/hr)
Init Oral_abs=0; Initial amount of chlorpyrifos absorbed oral, gavage (micromol)

;Total input to liver from diet and gavage
Input_l'=Oral_abs'+Dietexp+ Repeat_exp; Rate of total input of chlorpyrifos to liver from diet and gavage (micromol/hr)
Init Input_l=0; Initial amount of chlorpyrifos to liver from diet and gavage (micromol)

MODEL FOR CHLORPYRIFOS

PARAMETERS
Physiological Parameters; Data from Gearhart et al. 1990 and 1994
;Tissue as percentage of body weight. (Expresses how much of bw the organ represents (kg/kg bw))
PEbr=1.16; brain as percentage of body weight (%)
PEl=4.00; liver as percentage of body weight (%)
PEr=3.88; rapidly perfused tissues as percentage of body weight (%) (=richly perfused+kidney+lung = 2+0.73+1.15 from Gearhart et al. 1990)
PEf=7.00; fat as percentage of body weight (%)
PEs=68.66; slowly perfused tissues as percentage of body weight (%) (Gearhart et al. 1994)
PEdi=0.30; diaphragm as percentage of body weight (%)
PEbl=6; blood as percentage of body weight (%) (=venous+arterial = 4+2 from Gearhart et al. 1990)

Organ blood flows as percentage of cardiac output; Data from Gearhart et al. 1990
QC=5.4; cardiac output (l/hr)
Qbrc=3; blood flow in brain as percentage of cardiac output (%)
Qdic=0.6; blood flow in diaphragm as percentage of cardiac output (%)
Qfc=9; blood flow in fat as percentage of cardiac output (%)
Qlc=25; blood flow in liver as percentage of cardiac output (%)
Qrc=47.96; blood flow in rapidly perfused tissues as percentage of cardiac output (%) (=richly perf+kidney = 27.96+20 from Gearhart et al. 1990)
Qsc=14.4; blood flow in slowly perfused tissues as percentage of cardiac output (%)

Organ blood flows calculation
Qbr=Qbrc*QC/100; blood flow in brain (l/hr)
Qdi=Qdic*QC/100; blood flow in diaphragm (l/hr)
Qf=Qfc*QC/100; blood flow in fat (l/hr)
Ql=Qlc*QC/100; blood flow in liver (l/hr)
Qr=Qrc*QC/100; blood flow in rapidly perfused tissues (l/hr)
Qs=Qsc*QC/100; blood flow in slowly perfused tissues (l/hr)

Organ volumes as percentage of body weight; Data from Gearhart et al. 1990 and 1994
Vbrc=1.16; volume of brain as percentage of body weight (%)
Vlc=4.00; volume of liver as percentage of body weight (%)
Vrc=3.88; volume of rapidly perfused tissues as percentage of body weight (%) (=richly perfused+kidney+lung = 2+0.73+1.15 from Gearhart et al. 1990)

Vfc=7.00; volume of fat as percentage of body weight (%)
Vsc=68.66; volume of slowly perfused tissues as percentage of body weight (%) (Gearhart et al., 1994)
Vdic=0.30; volume of diaphragm as percentage of body weight (%)
Vvc=4.00; volume of venous blood as percentage of body weight (%)
Vac=2.00; volume of arterial blood as percentage of body weight (%)
Vblc=6; volume of blood as percentage of body weight (%) (=Vvc+Vac = 4+2 from Gearhart et al. 1990)

Organ volume calculation
Vbr=Vbrc*BW/100; volume of brain (l)
Vl=Vlc*BW/100; volume of liver (l)
Vr=Vrc*BW/100; volume of rapidly perfused tissues (l)
Vf=Vfc*BW/100; volume of fat (l)
Vs=Vsc*BW/100; volume of slowly perfused tissues (l)
Vdi=Vdic*BW/100; volume of diaphragm (l)
Vv=Vvc*BW/100; volume of venous blood (l)
Va=Vac*BW/100; volume of arterial blood (l)
Vbl=Vblc*BW/100; volume of blood (l)

Tissue weight calcuation
Wbl=PEbl*BW/100; weight of blood (kg)
Wbr=PEbr*BW/100; weight of brain (kg)
Wdi=PEdi*BW/100; weight of diaphragm (kg)
Wf=PEf*BW/100; weight of fat (kg)
Wl=PEl*BW/100; weight of liver (kg)
Wr=PEr*BW/100; weight of rapidly perfused tissues (kg)
Ws=PEs*BW/100; weight of slowly perfused tissues (kg)

Partition coefficients for chlorpyrifos, Timchalk et al., 2002
PCbrc=33; brain:blood partition coefficient
PCdic=6; diaphragm:blood partition coefficient
PCfc=435; fat:blood partition coefficient
PClc=22; liver:blood partition coefficient
PCrc=10; rapidly perfused tissues:blood partition coefficient
PCsc=6; slowly perfused tissues:blood partition coefficient
PCbl=1; blood:blood partition coefficient

;Plasma protein binding, Timchalk et al., 2002
FBc=97; plasma protein binding for chlorpyrifos (%)

Metabolic parameters, Timchalk et al., 2002
;Chlorpyrifos to chlorpyrifos-oxon
Km1=3.23; Michaelis-Menten constant for metabolism of chlorpyrifos to chlorpyrifos-oxon (liver) by CYP450 (micromol/l) (from Ma & Chambers, 1994)
VmaxC1=80; CYP450 metabolism of chlorpyrifos to chlorpyrifos-oxon (liver) (micromol/hr/kg)
Vmax1=VmaxC1*BW^0.7; Allometric scaling of Vmax1 (as described by El-Masri et al, 1996). Maximum velocity for metabolism of chlorpyrifos to chlorpyrifos-oxon by CYP450 (micromol/hr)

;Chlorpyrifos to TCP
Km2=24.3; Michaelis-Menten constant for metabolism of chlorpyrifos to TCP (liver) by CYP450 (micromol/l) (from Ma & Chambers, 1994)
VmaxC2=273; CYP450 chlorpyrifos metabolism to TCP (liver) (micromol/hr/kg)
Vmax2=VmaxC2*BW^0.7; Allometric scaling of Vmax2 (as described by El-Masri et al, 1996). Maximum velocity for metabolism of chlorpyrifos to TCP by CYP450 (micromol/hr)

EQUATIONS
Mass balance differential equations for each compartment. Concentration of chlorpyrifos in venous blood leaving tissues
;Fat
Cf'=Qf/Vf*(CA_free-CVf_free); rate of change in chlorpyrifos concentration in fat (micromol/l/hr)
Init Cf=0; initial chlorpyrifos concentration (micromol/l)
CVf_free=Cf/PCfc; concentration of free chlorpyrifos in blood leaving fat (micromol/l)

;Slowly perfused tissues
Cs'=Qs/Vs*(CA_free-CVs_free); rate of change in chlorpyrifos concentration in slowly perfused tissues (micromol/l/hr)
Init Cs=0; initial chlorpyrifos concentration (micromol/l)
CVs_free=Cs/PCsc; concentration of free chlorpyrifos in blood leaving slowly perfused tissues (micromol/l)

;Rapid perfused tissues
Cr'=Qr/Vr*(CA_free-CVr_free); rate of change in chlorpyrifos concentration in rapid perfused tissues (micromol/l/hr)
Init Cr=0; initial chlorpyrifos concentration (micromol/l)
CVr_free=Cr/PCrc; concentration of free chlorpyrifos in blood leaving rapid perfused tissues (micromol/l)

;Diaphragm
Cdi'=Qdi/Vdi*(CA_free-CVdi_free); rate of change in chlorpyrifos concentration in diaphragm (micromol/l/hr)
Init Cdi=0; initial chlorpyrifos concentration (micromol/l)
CVdi_free=Cdi/PCdic; concentration of free chlorpyrifos in blood leaving diaphragm (micromol/l)

;Brain
Cbr'=Qbr/Vbr*(CA_free-CVbr_free); rate of change in chlorpyrifos concentration in brain (micromol/l/hr)
Init Cbr=0; initial chlorpyrifos concentration (micromol/l)
CVbr_free=Cbr/PCbrc; concentration of free chlorpyrifos in blood leaving brain (micromol/l)

;Liver
Cl'=(Ql*(CA_free-CVl_free)+Input_l'-AML1'-AML2')/Vl; Rate of change in concentration of chlorpyrifos in liver (micromol/l/hr)
Init Cl=0; Concentration of chlorpyrifos in liver (micromol/l)
AML1'=(Vmax1*Cl)/(Km1+Cl); Rate of change in amount of free chlorpyrifos metabolised to chlorpyrifos-oxon by hepatic CYP450 (micromol/hr)
Init AML1=0; Initial amount of free chlorpyrifos metabolised to chlorpyrifos-oxon by hepatic CYP450 (micromol)
AML2'=(Vmax2*Cl)/(Km2+Cl); Rate of change in amount of free chlorpyrifos metabolised to TCP by hepatic CYP450 (micromol/hr)
Init AML2=0; Amount of free chlorpyrifos metabolised to TCP by hepatic CYP450 (micromol)
CVl_free=Cl/PClc; Concentration of free chlorpyrifos in venous blood draining the liver (micromol/l)

;Concentration of chlorpyrifos in blood
Cbl'=QC/Vbl*(CV-CA); rate of change in chlorpyrifos concentration in mixed blood (micromol/l/hr)
Init Cbl=0; chlorpyrifos concentration in blood (micromol/l)
Cbl_bound=Cbl*FBc/100; concentration of chlorpyrifos bound in mixed blood (micromol/l)
Cbl_free=Cbl*(1-FBc/100); concentration of free chlorpyrifos in mixed blood (micromol/l)

;Concentration of chlorpyrifos in venous blood
CV=CV_free+Cbl_bound; total chlorpyrifos concentration in venous blood (micromol/l)
CV_free=(CVf_free*Qf+CVs_free*Qs+CVr_free*Qr+CVdi_free*Qdi+CVbr_free*Qbr+CVl_free*Ql)/QC;
total concentration of free chlorpyrifos in mixed venous blood from tissues (micromol/l)

;Concentration of chlorpyrifos in arterial blood
CA=Cbl/PCbl; chlorpyrifos concentration in arterial blood (micromol/l)
CA_free=CA*(1-FBc/100); concentration of free chlorpyrifos in arterial blood (micromol/l)

MODEL FOR CHLORPYRIFOS-OXON

PARAMETERS
Partition coefficients for chlorpyrifos-oxon, Timchalk et al., 2002
PCbro=26; brain:blood partition coefficient
PCdio=4.9; diaphragm:blood partition coefficient
PCfo=342; fat:blood partition coefficient
PClo=17; liver:blood partition coefficient
PCro=8.1; rapidly perfused tissue:blood partition coefficient
PCso=4.9; slowly perfused tissue:blood partition coefficient
PCblo=1; blood:blood partition coefficient (from Timchalk et al., 2007 supplemental data)

Pharmacodynamic parameters
;Enzyme turnover rate
TRAChE=1.17*10^(+7); Enzyme turnover rate AChE (enz. hydro./hr) (Wang and Murphy, 1982)
TRBuChE=1.03*10^(+7); Enzyme turnover rate BuChE (enz. hydro./hr) (Main et al. 1972)
TRCaE=1.09*10^(+5); Enzyme turnover rate CaE (enz. hydro./hr) (Maxwell et al. 1987)

;Enzyme activity (Maxwell et al. 1987)
EAChEbr=4.4*10^(+5); Enzyme activity brain AChE (micromol/kg/hr)
EAChEdi=7.74*10^(+4); Enzyme activity diaphragm AChE (micromol/kg/hr)
EAChEl=1.02*10^(+4); Enzyme activity liver AChE (micromol/kg/hr)
EAChEp=1.32*10^(+4); Enzyme activity plasma AChE (micromol/kg/hr)
EBuChEbr=4.68*10^(+4); Enzyme activity brain BuChE (micromol/kg/hr)
EBuChEdi=2.64*10^(+4); Enzyme activity diaphragm BuChE (micromol/kg/hr)
EBuChEl=3.0*10^(+4); Enzyme activity liver BuChE (micromol/kg/hr)
EBuChEp=1.56*10^(+4); Enzyme activity plasma BuChE (micromol/kg/hr)
ECaEbr=6.0*10^(+4); Enzyme activity brain CaE (micromol/kg/hr)
ECaEdi=3.18*10^(+5); Enzyme activity diapgragm CaE (micromol/kg/hr)
ECaEl=1.94*10^(+6); Enzyme activity liver CaE (micromol/kg/hr)
ECaEp=4.56*10^(+5); Enzyme activity plasma CaE (micromol/kg/hr)

;Enzyme degradation rate (Gearhart et al. 1990 and Timchalk et al. 2002)
Kd1=0.01; Brain AChE (1/hr) (from Gearhart et al. 1990)
Kd2=0.01; diaphragm AChE (1/hr)
Kd3=0.1; Liver AChE (1/hr)
Kd4=0.1; Plasma AChE (1/hr) (from Gearhart et al. 1990)
Kd5=0.008; RBC AChE (1/hr)
Kd6=0.01; Brain BuChE (1/hr)
Kd7=0.01; diaphragm BuChE (1/hr)
Kd8=0.1; Liver BuChE (1/hr)
Kd9=0.1; Plasma BuChE (1/hr)
Kd10=7.54*10^(-4); Brain CaE (1/hr)
Kd11=0.001; diaphragm CaE (1/hr)
Kd12=0.001; Liver CaE (1/hr)
Kd13=0.0033; Plasma CaE (1/hr)

;Bimolecular inhibition rate (Gearhart et al. 1990 and Timchalk et al. 2002)
Ki1=243; All tissues AChE (1/(microM*hr))
Ki5=100; RBC AChE (1/(microM*hr))
Ki6=2000; All tissues BuChE (1/(microM*hr))
Ki10=20; Brain CaE (1/(microM*hr))
Ki11=20; diaphragm CaE (1/(microM*hr))
Ki12=20; Liver CaE (1/(microM*hr))
Ki13=20; Plasma CaE (1/(microM*hr))

;Reactivation rate (Carr and Chambers, 1996 and Timchalk et al. 2002)
Kr1=1.403*10^(-2); AChE (1/hr)
Kr5=4.0*10^(-2); RBC AChE (1/hr)
Kr6=1.403*10^(-2); BuChE (1/hr)
Kr10=1.403*10^(-2); CaE (1/hr)

;Aging time (Carr and Chambers, 1996)
Ka1=1.13*10^(-2); AChE (1/hr)
Ka6=1.13*10^(-2); BuChE (1/hr)
Ka10=1.13*10^(-2); CaE (1/hr)

Metabolic parameters; Data from Timchalk et al., 2007
;A-EST chlorpyrifos-oxon to TCP (liver)
Km3=577; Michaelis-Menten constant for saturable process (micromol/l)
VmaxC3=38002; Maximum metabolism rate of chlorpyrifos-oxon to TCP in liver per kg body weight (micromol/hr/kg)
Vmax3=VmaxC3*BW^0.7; Allometric scaling of Vmax3 (as described by El-Masri et al, 1996). Maximum velocity for metabolism to TCP by CYP450 (micromol/hr)

;A-EST chlorpyrifos-oxon to TCP (blood)
Km4=464; A-EST chlorpyrifos-oxon to TCP (blood) (micromol/l)
VmaxC4=40377; Maximum metabolism rate of chlorpyrifos-oxon to TCP in blood per kg body weight (micromol/hr/kg)
Vmax4=VmaxC4*BW^0.7; Allometric scaling of Vmax4 (as described by El-Masri et al, 1996). Maximum velocity for metabolism to TCP by CYP450 (micromol/hr)

;TCP model parameters (Timchalk et al., 2002)
Vd=35; Volume of distribution (l)
Ke=0.017; 1. order elimination constant(1/hr)

;Plasma protein binding, Timchalk et al., 2002
FBo=98; plasma protein binding for chlorpyrifos-oxon (%)

EQUATIONS
Mass balance differential equations for each compartment
;Fat
Cfo'=Qf/Vf*(CAo_free-CVfo_free); Rate of change in chlorpyrifos-oxon concentration in fat (micromol/l/hr)
Init Cfo=0; Initial chlorpyrifos-oxon concentration (micromol/l)
CVfo_free=Cfo/PCfo; concentration of free chlorpyrifos-oxon in blood leaving fat (micromol/l)

;Slowly perfused tissues
Cso'=Qs/Vs*(CAo_free-CVso_free); Rate of change in chlorpyrifos-oxon concentration in slowly perfused tissues (micromol/l/hr)
Init Cso=0; Initial chlorpyrifos-oxon concentration (micromol/l)
CVso_free=Cso/PCso; concentration of free chlorpyrifos-oxon in blood leaving slowly perfused tissues (micromol/l)

;Rapid perfused tissues
Cro'=Qr/Vr*(CAo_free-CVro_free); Rate of change in chlorpyrifos-oxon concentration in rapid perfused (micromol/l/hr)
Init Cro=0; Initial chlorpyrifos-oxon concentration (micromol/l)
CVro_free=Cro/PCro; concentration of free chlorpyrifos-oxon in blood leaving rapid perfused (micromol/l)

;Diaphragm
Cdio'=(Qdi*(CAo_free-CVdio_free)-(AML4di'+AML5di'+AML6di'))/Vdi; rate of change in chlorpyrifos-oxon concentration in diaphragm (micromol/l/hr)
Init Cdio=0; Initial chlorpyrifos-oxon concentration (micromol/l)
CVdio_free=Cdio/PCdio; concentration of free chlorpyrifos-oxon in blood leaving diaphragm (micromol/l)
AML4di'=AAChEdi*Ki1*Cdio; Rate of metabolism of chlorpyrifos-oxon to TCP by AChE in diaphragm (micromol/hr)
Init AML4di=0; Initial amount of chlorpyrifos-oxon metabolised to TCP by AChE in diaphragm (micromol)
AML5di'=ABuChEdi*Ki6*Cdio; Rate of metabolism of chlorpyrifos-oxon to TCP by BuChE in diaphragm (micromol/hr)
Init AML5di=0; Initial amount of chlorpyrifos-oxon metabolised by BuChE to TCP in diaphragm (micromol)
AML6di'=ACaEdi*Ki11*Cdio; Rate of metabolism of chlorpyrifos-oxon to TCP by CaE in diaphragm (micromol/hr)
Init AML6di=0; Initial amount of chlorpyrifos-oxon metabolised by CaE to TCP in diaphragm (micromol)

;Brain
Cbro'=(Qbr*(CAo_free-CVbro_free)-(AML4br'+AML5br'+AML6br'))/Vbr; rate of change of chlorpyrifos-oxon concentration in brain (micromol/l/hr)
Init Cbro=0; Initial chlorpyrifos-oxon concentration (micromol/l)
CVbro_free=Cbro/PCbro; concentration of free chlorpyrifos-oxon in blood leaving brain (micromol/l)
AML4br'=AAChEbr*Ki1*Cbro; Rate of metabolism of chlorpyrifos-oxon to TCP by AChE in brain (micromol/hr)
Init AML4br=0; Initial amount of chlorpyrifos-oxon metabolised to TCP by AChE in brain (micromol)
AML5br'=ABuChEbr*Ki6*Cbro; Rate of metabolism of chlorpyrifos-oxon to TCP by BuChE in brain (micromol/hr)
Init AML5br=0; Initial amount of chlorpyrifos-oxon metabolised to TCP by BuChE in brain (micromol)
AML6br'=ACaEbr*Ki10*Cbro;Rate of metabolism of chlorpyrifos-oxon to TCP by CaE in brain (micromol/hr)
Init AML6br=0; Initial amount of chlorpyrifos-oxon metabolised to TCP by CaE in brain (micromol)

;Liver
Clo'=(Ql*(CAo_free-CVlo_free)+AML1'-AML3l'-(AML4l'+AML5l'+AML6l'))/Vl; Rate of change in concentration of chlorpyrifos-oxon in liver (micromol/l/hr)
Init Clo=0; Initial concentration of chlorpyrifos-oxon in liver (micromol/l)
CVlo_free=Clo/PClo; Concentration of free chlorpyrifos-oxon in venous blood draining the liver (micromol/l)
AML3l'=(Vmax3*Clo)/(Km3+Clo); Rate of A-EST metabolism, chlorpyrifos-oxon -> TCP
Init AML3l=0; Initial amount of chlorpyrifos-oxon metabolised to TCP by A-EST in liver (micromol)
AML4l'=AAChEl*Ki1*Clo; Rate of metabolism of chlorpyrifos-oxon to TCP by AChE in liver (micromol/hr)
Init AML4l=0; Initial amount of chlorpyrifos-oxon metabolised to TCP by AChE in liver (micromol)
AML5l'=ABuChEl*Ki6*Clo; Rate of metabolism of chlorpyrifos-oxon to TCP by BuChE in liver (micromol/hr)
Init AML5l=0; Initial amount of chlorpyrifos-oxon metabolised to TCP by BuChE in liver (micromol)
AML6l'=ACaEl*Ki12*Clo; Rate of metabolism of chlorpyrifos-oxon to TCP by CaE in liver (micromol/hr)
Init AML6l=0; Initial amount of chlorpyrifos-oxon metabolised to TCP by CaE in liver (micromol)

;Blood
Cblo'=QC*(CVo-CAo)/Vbl-AML3bl'/Vbl-(AML4bl'+AML5bl'+AML6bl')/Vbl; Rate of change in concentration of chlorpyrifos-oxon in blood (micromol/l/hr)
Init Cblo=0; Initial concentration of chlorpyrifos-oxon in blood (micromol/l)
Cblo_bound=Cblo*FBo/100; Concentration of bound chlorpyrifos-oxon in mixed blood compartment (micromol/l)
Cblo_free=Cblo*(1-FBo/100);Concentration of free chlorpyrifos-oxon in blood (micromol/l)
AML3bl'=(Vmax4*Cblo_free)/(Km4+Cblo_free); Rate of A-EST metabolism, chlorpyrifos-oxon -> TCP (micromol/hr)

Init AML3bl=0; Initial amount of chlorpyrifos-oxon metabolised to TCP by A-EST in blood (micromol)
AML4bl'=AAChEp*Ki1*Cblo; Rate of metabolism of chlorpyrifos-oxon to TCP by AChE in blood (micromol/hr)
Init AML4bl=0; Initial amount of chlorpyrifos-oxon metabolised to TCP by AChE in blood (micromol)
AML5bl'=ABuChEp*Ki6*Cblo; Rate of metabolism of chlorpyrifos-oxon to TCP by BuChE in blood (micromol/hr)
Init AML5bl=0; Initial amount of chlorpyrifos-oxon metabolised to TCP by BuChE in blood (micromol)
AML6bl'=ACaEp*Ki13*Cblo; Rate of metabolism of chlorpyrifos-oxon to TCP by CaE in blood (micromol/hr)
Init AML6bl=0; Initial amount of chlorpyrifos-oxon metabolised to TCP by CaE in blood (micromol)

;RBC
AML4rbc'=AAChErbc*Ki5*Cblo; Rate of metabolism of chlorpyrifos-oxon to TCP by AChE in RBC (micromol/hr)
Init AML4rbc=0; Initial amount of chlorpyrifos-oxon metabolised to TCP by AChE in RBC (micromol)
AML5rbc'=ABuChErbc*Ki6*Cblo; Rate of metabolism of chlorpyrifos-oxon to TCP by BuChE in RBC (micromol/hr)
Init AML5rbc=0; Initial amount of chlorpyrifos-oxon metabolised to TCP by BuChE in RBC (micromol)
AML6rbc'=ACaEl*Ki13*Cblo; Rate of metabolism of chlorpyrifos-oxon to TCP by CaE in RBC (micromol/hr)
Init AML6rbc=0; Initial amount of chlorpyrifos-oxon metabolised to TCP by CaE in RBC (micromol)

;Venous blood
CVo=CVo_free+Cblo_bound; total concentration of chlorpyrifos-oxon in venous blood (micromol/l)
CVo_free=(CVfo_free*Qf+CVso_free*Qs+CVro_free*Qr+CVdio_free*Qdi+CVbro_free*Qbr+CVlo_free*Ql)/QC; total concentration of free chlorpyrifos-oxon in mixed venous blood from tissues (micromol/l)

;Arterial blood
CAo=Cblo/PCblo; concentration of chlorpyrifos-oxon in arterial blood (micromol/l)
CAo_free=CAo*(1-FBo/100); concentration of free chlorpyrifos-oxon in arterial blood (micromol/l)
CAo_bound=CAo*FBo/100; concentration of bound chlorpyrifos-oxon in arterial blood (micromol/l)

B-EST tissue inhibition by chlorpyrifos-oxon

;BRAIN
;Equations describing AChE inhibition in the brain compartment:
IAAChEbr=EAChEbr*Wbr/TRAChE; initial amount of esterase binding sites brain, AChE (micromol)
KsAChEbr=IAAChEbr*Kd1; zero order synthesis rate of brain AChE (micromol/hr)
AAChEbr'=KsAChEbr-AAChEbr*(Kd1+Ki1*Cbro)+INactive_AChEbr*Kr1; rate of change in brain AChE enzyme (micromol/hr)
Init AAChEbr=IAAChEbr; initial amount of esterase binding sites brain, AChE (micromol)
INactive_AChEbr'=AAChEbr*Ki1*Cbro-INactive_AChEbr*(Ka1+kr1); rate of change in amount of AChE that is inactivated (micromol/hr)
Init INactive_AChEbr=0; initial amount of inactivated AChE (micromol)
Inhib_AChEbr=AAChEbr*100/IAAChEbr; % AChE inhibition in brain

;Equations describing BuChE inhibition in the brain compartment:
IABuChEbr=EBuChEbr*Wbr/TRBuChE; initial amount of esterase binding sites brain, BuChE (micromol)
KsBuChEbr=IABuChEbr*Kd6; zero order synthesis rate of brain BuChE (micromol/hr)
ABuChEbr'=KsBuChEbr-ABuChEbr*(Kd6+Ki6*Cbro)+INactive_BuChEbr*Kr6; rate of change in brain BuChE enzyme (micromol/hr)
Init ABuChEbr=IABuChEbr; initial amount of esterase binding sites brain, BuChE (micromol)
INactive_BuChEbr'=ABuChEbr*Ki6*Cbro-INactive_BuChEbr*(Ka6+kr6); rate of change in amount of BuChE that is inactivated (micromol/hr)
Init INactive_BuChEbr=0; initial amount of inactivated BuChE (micromol)
Inhib_BuChEbr=ABuChEbr*100/IABuChEbr; % BuChE inhibition in brain

;Equations describing CaE inhibition in the brain compartment:
IACaEbr=ECaEbr*Wbr/TRCaE; initial amount of esterase binding sites brain, CaE (micromol)
KsCaEbr=IACaEbr*Kd10; zero order synthesis rate of brain CaE (micromol/hr)
ACaEbr'=KsCaEbr-ACaEbr*(Kd10+Ki10*Cbro)+INactive_CaEbr*Kr10; rate of change in brain CaE enzyme (micromol/hr)
Init ACaEbr=IACaEbr; initial amount of esterase binding sites brain, CaE (micromol)
INactive_CaEbr'=ACaEbr*Ki10*Cbro-INactive_CaEbr*(Ka10+kr10); rate of change in amount of CaE that is inactivated (micromol/hr)
Init INactive_CaEbr=0; initial amount of inactivated CaE (micromol)
Inhib_CaEbr=ACaEbr*100/IACaEbr; % CaE inhibition in brain

;Total B-esterase inhibition in brain
B_EST_total_br=AAChEbr+ABuChEbr+ACaEbr; total B-EST in brain (micromol)
Inhib_tot_br=B_EST_total_br*100/(IAAChEbr+IABuChEbr+IACaEbr); % total B-EST inhibition in brain

;DIAPHRAGM
;Equations describing AChE inhibition in the diaphragm compartment:
IAAChEdi=EAChEdi*Wdi/TRAChE; initial amount of esterase binding sites diaphragm, AChE (micromol)
KsAChEdi=IAAChEdi*Kd2; zero order synthesis rate of diaphragm AChE (micromol/hr)
AAChEdi'=KsAChEdi-AAChEdi*(Kd2+Ki1*Cdio)+INactive_AChEdi*Kr1; rate of change of diaphragm AChE enzyme (micromol/hr)
Init AAChEdi=IAAChEdi; initial amount of esterase binding sites diaphragm, AChE (micromol)

INactive_AChEdi'=AAChEdi*Ki1*Cdio-INactive_AChEdi*(Ka1+Kr1); rate of change in amount of AChE that is inactivated (micromol/hr)
Init INactive_AChEdi=0; initial amount of inactivated AChE (micromol)
Inhib_AChEdi=AAChEdi*100/IAAChEdi; % AChE inhibition in diaphragm

;Equations describing BuChE inhibition in the diaphragm compartment:
IABuChEdi=EBuChEdi*Wdi/TRBuChE; initial amount of esterase binding sites diaphragm, BuChE (micromol)
KsBuChEdi=IABuChEdi*Kd7; zero order synthesis rate of diaphragm BuChE (micromol/hr)
ABuChEdi'=KsBuChEdi-ABuChEdi*(Kd7+Ki6*Cdio)+INactive_BuChEdi*Kr6; rate of change of diaphragm BuChE enzyme (micromol/hr)
Init ABuChEdi=IABuChEdi; initial amount of esterase binding sites diaphragm, BuChE (micromol)

INactive_BuChEdi'=ABuChEdi*Ki6*Cdio-INactive_BuChEdi*(Ka6+Kr6); rate of change in amount of BuChE that is inactivated (micromol/hr)
Init INactive_BuChEdi=0; initial amount of inactivated BuChE (micromol)
Inhib_BuChEdi=ABuChEdi*100/IABuChEdi; % BuChE inhibition in diaphragm

;Equations describing CaE inhibition in the diaphragm compartment:
IACaEdi=ECaEdi*Wdi/TRCaE; initial amount of esterase binding sites diaphragm, CaE (micromol)
KsCaEdi=IACaEdi*Kd11; zero order synthesis rate of diaphragm CaE (micromol/hr)
ACaEdi'=KsCaEdi-ACaEdi*(Kd11+Ki11*Cdio)+INactive_CaEdi*Kr10; rate of change of diaphragm CaE enzyme (micromol/hr)
Init ACaEdi=IACaEdi; initial amount of esterase binding sites diaphragm, CaE (micromol)
INactive_CaEdi'=ACaEdi*Ki11*Cdio-INactive_CaEdi*(Ka10+Kr10); rate of change in amount of CaE that is inactivated (micromol/hr)
Init INactive_CaEdi=0; initial amount of inactivated CaE (micromol)
Inhib_CaEdi=ACaEdi*100/IACaEdi; % CaE inhibition in diaphragm

;Total B-esterase inhibition in diaphragm
B_EST_total_di=AAChEdi+ABuChEdi+ACaEdi; total B-EST in diaphragm (micromol)
Inhib_tot_di=B_EST_total_di*100/(IAAChEdi+IABuChEdi+IACaEdi); % total B-EST inhibition in diaphragm

;LIVER
;Equations describing AChE inhibition in the liver compartment:
IAAChEl=EAChEl*Wl/TRAChE; initial amount of esterase binding sites liver, AChE (micromol)
KsAChEl=IAAChEl*Kd3; zero order synthesis rate of liver AChE (micromol/hr)
AAChEl'=KsAChEl-AAChEl*(Kd3+Ki1*Clo)+INactive_AChEl*Kr1; rate of change of liver AChE enzyme (micromol/hr)
Init AAChEl=IAAChEl; initial amount of esterase binding sites liver, AChE (micromol)
INactive_AChEl'=AAChEl*Ki1*Clo-INactive_AChEl*(Ka1+Kr1); rate of change in amount of AChE that is inactivated (micromol/hr)
Init INactive_AChEl=0; initial amount of inactivated AChE (micromol)
Inhib_AChEl=AAChEl*100/IAAChEl; % AChE inhibition in liver

;Equations describing BuChE inhibition in the liver compartment:
IABuChEl=EBuChEl*Wl/TRBuChE; initial amount of esterase binding sites liver, BuChE (micromol)
KsBuChEl=IABuChEl*Kd8; zero order synthesis rate of liver BuChE (micromol/hr)
ABuChEl'=KsBuChEl-ABuChEl*(Kd8+Ki6*Clo)+INactive_BuChEl*Kr6; rate of change of liver BuChE enzyme (micromol/hr)
Init ABuChEl=IABuChEl; initial amount of esterase binding sites liver, BuChE (micromol)
INactive_BuChEl'=ABuChEl*Ki6*Clo-INactive_BuChEl*(Ka6+Kr6); rate of change in amount of BuChE that is inactivated (micromol/hr)
Init INactive_BuChEl=0; initial amount of inactivated BuChE (micromol)
Inhib_BuChEl=ABuChEl*100/IABuChEl; % BuChE inhibition in liver

;Equations describing CaE inhibition in the liver compartment:
IACaEl=ECaEl*Wl/TRCaE; initial amount of esterase binding sites liver, CaE (micromol)
KsCaEl=IACaEl*Kd12; zero order synthesis rate of liver CaE (micromol/hr)
ACaEl'=KsCaEl-ACaEl*(Kd12+Ki12*Clo)+INactive_CaEl*Kr10; rate of change of liver CaE enzyme (micromol/hr)
Init ACaEl=IACaEl; initial amount of esterase binding sites liver, CaE (micromol)
INactive_CaEl'=ACaEl*Ki12*Clo-INactive_CaEl*(Ka10+Kr10); rate of change in amount of CaE that is inactivated (micromol/hr)
Init INactive_CaEl=0; initial amount of inactivated CaE (micromol)
Inhib_CaEl=ACaEl*100/IACaEl; % CaE inhibition in liver

;Total B-esterase inhibition in liver
B_EST_total_l=AAChEl+ABuChEl+ACaEl; total B-EST in liver (micromol)
Inhib_tot_l=B_EST_total_l*100/(IAAChEl+IABuChEl+IACaEl); % total B-EST inhibition in liver

;PLASMA
;Equations describing AChE inhibition in the plasma:
IAAChEp=EAChEp*Wbl/TRAChE; initial amount of esterase binding sites plasma, AChE (micromol)
KsAChEp=IAAChEp*Kd4; zero order synthesis rate of plasma AChE (micromol/hr)
AAChEp'=KsAChEp-AAChEp*(Kd4+Ki1*Cblo)+INactive_AChEp*Kr1; rate of change of plasma AChE enzyme (micromol/hr)
Init AAChEp=IAAChEp; initial amount of esterase binding sites plasma, AChE (micromol)
INactive_AChEp'=AAChEp*Ki1*Cblo-INactive_AChEp*(Ka1+Kr1); rate of change in amount of AChE that is inactivated (micromol/hr)
Init INactive_AChEp=0; initial amount of inactivated AChE (micromol)
Inhib_AChEp=AAChEp*100/IAAChEp; % AChE inhibition in plasma

;Equations describing BuChE inhibition in the plasma:
IABuChEp=EBuChEp*Wbl/TRBuChE; initial amount of esterase binding sites plasma, BuChE (micromol)
KsBuChEp=IABuChEp*Kd9; zero order synthesis rate of plasma BuChE (micromol/hr)
ABuChEp'=KsBuChEp-ABuChEp*(Kd9+Ki6*Cblo)+INactive_BuChEp*Kr6; rate of change of plasma BuChE enzyme (micromol/hr)

Init ABuChEp=IABuChEp; initial amount of esterase binding sites plasma, BuChE (micromol)
INactive_BuChEp'=ABuChEp*Ki6*Cblo-INactive_BuChEp*(Ka6+Kr6); rate of change in amount of BuChE that is inactivated (micromol/hr)
Init INactive_BuChEp=0; initial amount of inactivated BuChE (micromol)
Inhib_BuChEp=ABuChEp*100/IABuChEp; % BuChE inhibition in plasma

;Equations describing CaE inhibition in the plasma:
IACaEp=ECaEp*Wbl/TRCaE; initial amount of esterase binding sites plasma, CaE (micromol)
KsCaEp=IACaEp*Kd13; zero order synthesis rate of plasma CaE (micromol/hr)
ACaEp'=KsCaEp-ACaEp*(Kd13+Ki13*Cblo)+INactive_CaEp*Kr10; rate of change of plasma CaE enzyme (micromol/hr)
Init ACaEp=IACaEp; initial amount of esterase binding sites plasma, CaE (micromol)
INactive_CaEp'=ACaEp*Ki13*Cblo-INactive_CaEp*(Ka10+Kr10); rate of change in amount of CaE that is inactivated (micromol/hr)
Init INactive_CaEp=0; initial amount of inactivated CaE (micromol)
Inhib_CaEp=ACaEp*100/IACaEp; % CaE inhibition in plasma

;Total B-esterase inhibition in plasma
B_EST_total_p=AAChEp+ABuChEp+ACaEp; total B-EST in plasma (micromol)
Inhib_tot_p=B_EST_total_p*100/(IAAChEp+IABuChEp+IACaEp); % total B-EST inhibition in plasma

;Total cholinesterase (AChE+BuChE)
Inhib_ChEp_total=(AAChEp+ABuChEp)*100/(IAAChEp+IABuChEp); % total cholinesterase inhibition in plasma

;RBC
;Equations describing AChE inhibition in the RBC
IAAChErbc=EAChEp*Wbl/TRAChE; initial amount of esterase binding sites RBC, AChE (micromol)
KsAChErbc=IAAChErbc*Kd5; zero order synthesis rate of RBC AChE (micromol/hr)
AAChErbc'=KsAChErbc-AAChErbc*(Kd5+Ki5*Cblo)+INactive_AChErbc*Kr5; rate of change of RBC AChE enzyme (micromol/hr)
Init AAChErbc=IAAChErbc; initial amount of esterase binding sites RBC, AChE (micromol)
INactive_AChErbc'=AAChErbc*Ki5*Cblo-INactive_AChErbc*(Ka1+Kr5); rate of change in amount of AChE that is inactivated (micromol/hr)
Init INactive_AChErbc=0; initial amount of inactivated AChE (micromol)
Inhib_AChErbc=AAChErbc*100/IAAChErbc;% AChE inhibition in RBC

;Equations describing BuChE inhibition in the RBC:
IABuChErbc=EBuChEp*Wbl/TRBuChE; initial amount of esterase binding sites RBC, BuChE (micromol)
KsBuChErbc=IABuChErbc*Kd9; zero order synthesis rate of RBC BuChE (micromol/hr)
ABuChErbc'=KsBuChErbc-ABuChErbc*(Kd9+Ki6*Cblo)+INactive_BuChErbc*Kr6; rate of change of RBC BuChE enzyme (micromol/hr)
Init ABuChErbc=IABuChErbc; initial amount of esterase binding sites RBC, BuChE (micromol)
INactive_BuChErbc'=ABuChErbc*Ki6*Cblo-INactive_BuChErbc*(Ka6+Kr6); rate of change in amount of BuChE that is inactivated (micromol/hr)
Init INactive_BuChErbc=0; initial amount of inactivated BuChE (micromol)
Inhib_BuChErbc=ABuChErbc*100/IABuChErbc; % BuChE inhibition in RBC

;Equations describing CaE inhibition in the RBC:
IACaErbc=ECaEp*Wbl/TRCaE; initial amount of esterase binding sites RBC, CaE (micromol)
KsCaErbc=IACaErbc*Kd13; zero order synthesis rate of RBC CaE (micromol/hr)
ACaErbc'=KsCaErbc-ACaErbc*(Kd13+Ki13*Cblo)+INactive_CaErbc*Kr10; rate of change of RBC CaE enzyme (micromol/hr)
Init ACaErbc=IACaErbc; initial amount of esterase binding sites RBC, CaE (micromol)
INactive_CaErbc'=ACaErbc*Ki13*Cblo-INactive_CaErbc*(Ka10+Kr10); rate of change in amount of CaE that is inactivated (micromol/hr)
Init INactive_CaErbc=0; initial amount of inactivated CaE (micromol)

Inhib_CaErbc=ACaErbc*100/IACaErbc; % CaE inhibition in RBC

;Total B-esterase inhibition in RBC
B_EST_total_rbc=AAChErbc+ABuChErbc+ACaErbc; total B-EST in RBC (micromol)
Inhib_tot_rbc=B_EST_total_rbc*100/(IAAChErbc+IABuChErbc+IACaErbc); % total B-EST inhibition in RBC

;Total cholinesterase (AChE+BuChE)
Inhib_ChErbc_total=(AAChErbc+ABuChErbc)*100/(IAAChErbc+IABuChErbc); % total cholinesterase inhibition in RBC

One-compartment model for TCP
TCP_form'=AML2'+AML3bl'+AML3l'+AML4br'+AML5br'+AML6br'+AML4di'+AML5di'+AML6di'+AML4l'+AML5l'+AML6l'+AML4bl'+AML5bl'+AML6bl'+AML4rbc'+AML5rbc'+AML6rbc'; rate of formation of TCP (micromol/hr)
Init TCP_form=0; initial amount of TCP formed (micromol)
TCPexc'=ATCP*Ke; rate of urinary excretion of TCP (micromol/hr)
Init TCPexc=0; inital urinary excretion of TCP (micromol)
ATCP'=TCP_form'-TCPexc'; rate of change in amount of TCP (i.e. TCP formation from all sources (i.e. CYP450, A-EST, B-EST) minus urinary elimination of TCP) (micromol/hr)
Init ATCP=0; initial amount of TCP (micromol)
CTCPbl=ATCP/Vd; blood concentration of TCP (micromol/hr), where Vd (liter) is volume of distribution

Mass balances for chlorpyrifos, chlorpyrifos-oxon and TCP
;Mass balance chlorpyrifos
total_massCPF=Input_l+Cf*Vf+Cs*Vs+Cr*Vr+Cdi*Vdi+Cbr*Vbr+Cl*Vl+Cbl*Vbl; total mass of chlorpyrifos (micromol)

;Mass balance chlorpyrifos-oxon
total_massOxon=Cfo*Vf+Cso*Vs+Cro*Vr+Cdio*Vdi+Cbro*Vbr+Clo*Vl+Cblo*Vbl; total mass of chlorpyrifos-oxon (micromol)

;Mass balance TCP
total_massTCP= ATCP+TCPexc; total mass of TCP (micromol)

;Total mass balance
Mass balance check; Total amount of chlorpyrifos delivered in experiment should equal to the amount calculated by the code. This means that the equation below for TOTAL (which is the total amount delivered) should equal total_massCPF
TOTAL=total_massOxon+total_massTCP; total amount of chlorpyrifos delivered to tissues or excreted (micromol)

ABBREVIATIONS IN THE MODEL CODE

AAChEbr: initial amount of esterase binding sites brain, AChE (micromol)
AAChEbr': rate of change in brain AChE enzyme (micromol/hr)
AAChEdi: amount of esterase binding sites diaphragm, AChE (micromol)
AAChEdi': rate of change of diaphragm AChE enzyme (micromol/hr)
AAChEl: amount of esterase binding sites liver, AChE (micromol)
AAChEl': rate of change of liver AChE enzyme (micromol/hr)
AAChEp: amount of esterase binding sites plasma, AChE (micromol)
AAChEp': rate of change of plasma AChE enzyme (micromol/hr)
AAChErbc: amount of esterase binding sites RBC, AChE (micromol)
AAChErbc': rate of change of RBC AChE enzyme (micromol/hr)

ABuChEbr: initial amount of esterase binding sites brain, BuChE (micromol)
ABuChEbr': rate of change in brain BuChE enzyme (micromol/hr)
ABuChEdi: amount of esterase binding sites diaphragm, BuChE (micromol)
ABuChEdi': rate of change of diaphragm BuChE enzyme (micromol/hr)
ABuChEl: amount of esterase binding sites liver, BuChE (micromol)
ABuChEl': rate of change of liver BuChE enzyme (micromol/hr)
ABuChEp: amount of esterase binding sites plasma, BuChE (micromol)
ABuChEp': rate of change of plasma BuChE enzyme (micromol/hr)
ABuChErbc: amount of esterase binding sites RBC, BuChE (micromol)
ABuChErbc': rate of change of RBC BuChE enzyme (micromol/hr)
ACaEbr: initial amount of esterase binding sites brain, CaE (micromol)
ACaEbr': rate of change in brain CaE enzyme (micromol/hr)
ACaEdi: amount of esterase binding sites diaphragm, CaE (micromol)
ACaEdi': rate of change of diaphragm CaE enzyme (micromol/hr)
ACaEl: amount of esterase binding sites liver, CaE (micromol)
ACaEl': rate of change of liver CaE enzyme (micromol/hr)
ACaEp: amount of esterase binding sites plasma, CaE (micromol)
ACaEp': rate of change of plasma CaE enzyme (micromol/hr)
ACaErbc: amount of esterase binding sites RBC, CaE (micromol)
ACaErbc': rate of change of RBC CaE enzyme (micromol/hr)
AML1': rate of change in amount of free chlorpyrifos metabolised to chlorpyrifos-oxon by hepatic CYP450 (micromol/hr)
AML2': rate of change in amount of free chlorpyrifos metabolised to TCP by hepatic CYP450 (micromol/hr)
AML3bl': rate of A-EST metabolism, chlorpyrifos-oxon -> TCP (micromol/hr)
AML3l': rate of A-EST metabolism, chlorpyrifos-oxon -> TCP
AML4bl': rate of metabolism of chlopyrifos-oxon to TCP by AChE in blood (micromol/hr)
AML4br': rate of metabolism of chlopyrifos-oxon to TCP by AChE in brain (micromol/hr)
AML4di': rate of metabolism of chlopyrifos-oxon to TCP by AChE in diaphragm (micromol/hr)
AML4l': rate of metabolism of chlopyrifos-oxon to TCP by AChE in liver (micromol/hr)
AML4rbc': rate of metabolism of chlopyrifos-oxon to TCP by AChE in RBC (micromol/hr)
AML5bl': rate of metabolism of chlopyrifos-oxon to TCP by BuChE in blood (micromol/hr)
AML5br': rate of metabolism of chlopyrifos-oxon to TCP by BuChE in brain (micromol/hr)
AML5di': rate of metabolism of chlopyrifos-oxon to TCP by BuChE in diaphragm (micromol/hr)
AML5l': rate of metabolism of chlopyrifos-oxon to TCP by BuChE in liver (micromol/hr)
AML5rbc': rate of metabolism of chlopyrifos-oxon to TCP by BuChE in RBC (micromol/hr)
AML6bl': rate of metabolism of chlopyrifos-oxon to TCP by CaE in blood (micromol/hr)
AML6br': rate of metabolism of chlopyrifos-oxon to TCP by CaE in brain (micromol/hr)
AML6di': rate of metabolism of chlopyrifos-oxon to TCP by CaE in diaphragm (micromol/hr)
AML6l': rate of metabolism of chlopyrifos-oxon to TCP by CaE in liver (micromol/hr)
AML6rbc': rate of metabolism of chlopyrifos-oxon to TCP by CaE in RBC (micromol/hr)
ATCP: amount of TCP (micromol)
ATCP': rate of change for TCP formation from all sources (i.e. CYP450, A-EST, B-EST) (micromol/hr)
B_EST_total_br: Total B-EST in brain (micromol)
B_EST_total_di: Total B-EST in diaphragm (micromol)
B_EST_total_l: Total B-EST in liver (micromol)
B_EST_total_p: Total B-EST in plasma (micromol)
B_EST_total_rbc: Total B-EST in RBC (micromol)
BW: body weight for rats (kg)
CA: chlorpyrifos concentration in arterial blood (micromol/l)
CA_free: concentration of free chlorpyrifos in arterial blood (micromol/l)
CAo: concentration of chlorpyrifos-oxon in arterial blood (micromol/l)
CAo_bound: concentration of bound chlorpyrifos-oxon in arterial blood (micromol/l)
CAo_free: concentration of free chlorpyrifos-oxon in arterial blood (micromol/l)
Cbl: chlorpyrifos concentration in blood (micromol/l)
Cbl': rate of change in mixed blood.

Cblo: concentration of chlorpyrifos-oxon in blood (micromol/l)
Cblo': rate of change in concentration of chlorpyrifos-oxon in blood (micromol/l/hr)
Cblo_bound: Concentration of bound chlorpyrifos-oxon in mixed blood compartment (micromol/l)
Cblo_free: concentration of free chlorpyrifos-oxon in blood (micromol/l)
Cbr: chlorpyrifos concentration in brain (micromol/l)
Cbr': rate of change of chlorpyrifos concentration in brain (micromol/l/hr)
Cbro: chlorpyrifos-oxon concentration in brain (micromol/l)
Cbro': rate of change of chlorpyrifos-oxon concentration in brain (micromol/l/hr)
Cdi: chlorpyrifos concentration in diaphragm (micromol/l)
Cdi': rate of change in chlorpyrifos concentration in diaphragm (micromol/l/hr)
Cdio: chlorpyrifos-oxon concentration diaphragm (micromol/l)
Cdio': rate of change in chlorpyrifos-oxon concentration in diaphragm (micromol/l/hr)
Cf: chlorpyrifos concentration in fat (micromol/l)
Cf': rate of change in chlorpyrifos concentration in fat (micromol/l/hr)
Cfo: chlorpyrifos-oxon concentration in fat (micromol/l)
Cfo': rate of change in chlorpyrifos-oxon concentration in fat (micromol/l/hr)
Cl: concentration of chlorpyrifos in liver (micromol/l)
Cl': rate of change in concentration of chlorpyrifos in liver (micromol/l/hr)
Clo: concentration of chlorpyrifos-oxon in liver (micromol/l)
Clo': rate of change in concentration of chlorpyrifos-oxon in liver (micromol/l/hr)
Cr: chlorpyrifos concentration in rapidly perfused tissues (micromol/l)
Cr': rate of change in chlorpyrifos concentration in rapid perfused (micromol/l/hr)
Cro: chlorpyrifos-oxon concentration in rapidly perfused tissues (micromol/l)
Cro': rate of change in chlorpyrifos-oxon concentration in rapid perfused (micromol/l/hr)
Cs: chlorpyrifos concentration in slowly perfused tissues (micromol/l)
Cs': rate of change in chlorpyrifos concentration in slowly perfused tissues (micromol/l/hr)
Cso: chlorpyrifos-oxon concentration in slowly perfused tissues (micromol/l)
Cso': rate of change in chlorpyrifos-oxon concentration in slowly perfused tissues (micromol/l/hr)
CTCPbl: blood concentration of TCP (micromol/hr)
CV: total in chlorpyrifos concentration in venous blood (micromol/l)
CV_bound: in chlorpyrifos concentration bound in mixed blood (micromol/l)
CV_free: total concentration of free chlorpyrifos in mixed venous blood from tissues (micromol/l)
CVbr_free: concentration of free chlorpyrifos in blood leaving brain (micromol/l)
CVbro_free: concentration of free chlorpyrifos-oxon in blood leaving brain (micromol/l)
CVdi_free: concentration of free chlorpyrifos in blood leaving diaphragm (micromol/l)
CVdio_free: concentration of free chlorpyrifos-oxon in blood leaving diaphragm (micromol/l)
CVf_free: concentration of free chlorpyrifos in blood leaving fat (micromol/l)
CVfo_free: concentration of free chlorpyrifos-oxon in blood leaving fat (micromol/l)
CVl_free: Concentration of free chlorpyrifos in venous blood draining the liver (micromol/l)
CVlo_free: Concentration of free chlorpyrifos-oxon in venous blood draining the liver (micromol/l)
CVo: total concentration of chlorpyrifos-oxon in venous blood (micromol/l)
CVo_free: total concentration of free chlorpyrifos-oxon in mixed venous blood from tissues (micromol/l)
CVr_free: concentration of free chlorpyrifos in blood leaving rapid perfused tissues (micromol/l)
CVro_free: concentration of free chlorpyrifos-oxon in blood leaving rapid perfused tissues (micromol/l)
CVs_free: concentration of free chlorpyrifos in blood leaving slowly perfused tissues (micromol/l)
CVso_free: concentration of free chlorpyrifos-oxon in blood leaving slowly perfused tissues (micromol/l)
Diet: Dietary administration of chlorpyrifos (micromol/day)
Dietexp: Dietary exposure of chlorpyrifos (micromol/hr)
dose: administered dose of chlorpyrifos (recalculation of units) (micromol/day)
dose_in: administered dose of chlorpyrifos (mg/kg bw/day)
EAChEbr: Enzyme activity brain AChE (micromol/kg/hr)
EAChEdi: Enzyme activity diaphragm AChE (micromol/kg/hr)
EAChEl: Enzyme activity liver AChE (micromol/kg/hr)
EAChEp: Enzyme activity plasma AChE (micromol/kg/hr)
EBuChEbr: Enzyme activity brain BuChE (micromol/kg/hr)

EBuChEdi: Enzyme activity diaphragm BuChE (micromol/kg/hr)
EBuChEl: Enzyme activity liver BuChE (micromol/kg/hr)
EBuChEp: Enzyme activity plasma BuChE (micromol/kg/hr)
ECaEbr: Enzyme activity brain CaE (micromol/kg/hr)
ECaEdi: Enzyme activity diaphragm CaE (micromol/kg/hr)
ECaEl: Enzyme activity liver CaE (micromol/kg/hr)
ECaEp: Enzyme activity plasma CaE (micromol/kg/hr)
Fa: Fractional absorption (%)
FBc: plasma protein binding for chlorpyrifos (%)
FBo: plasma protein binding for chlorpyrifos-oxon (%)
Gavage: Gavage administration of chlorpyrifos (micromol)
Gavage_in: Gavage administration of chlorpyrifos (mg/kg bw)
IAAChEbr: initial amount of esterase binding sites brain, AChE (micromol)
IAAChEdi: Initial amount of esterase binding sites diaphragm, AChE (micromol)
IAAChEl: Initial amount of esterase binding sites liver, AChE (micromol)
IAAChEp: Initial amount of esterase binding sites plasma, AChE (micromol)
IAAChErbc: Initial amount of esterase binding sites RBC, AChE (micromol)
IABuChEbr: initial amount of esterase binding sites brain, BuChE (micromol)
IABuChEdi: Initial amount of esterase binding sites diaphragm, BuChE (micromol)
IABuChEl: Initial amount of esterase binding sites liver, BuChE (micromol)
IABuChEp: Initial amount of esterase binding sites plasma, BuChE (micromol)
IABuChErbc: Initial amount of esterase binding sites RBC, BuChE (micromol)
IACaEbr: initial amount of esterase binding sites brain, CaE (micromol)
IACaEdi: Initial amount of esterase binding sites diaphragm, CaE (micromol)
IACaEl: Initial amount of esterase binding sites liver, CaE (micromol)
IACaEp: Initial amount of esterase binding sites plasma, CaE (micromol)
IACaErbc: Initial amount of esterase binding sites RBC, CaE (micromol)
INactive_AChEbr: amount of inactivated AChE in brain (micromol)
INactive_AChEbr': rate of change in amount of AChE that is inactivated in brain (micromol/hr)
INactive_AChEdi: amount of inactivated AChE in diaphragm (micromol)
INactive_AChEdi: rate of change in amount of AChE that is inactivated in diaphragm (micromol/hr)
INactive_AChEl: amount of inactivated AChE in liver (micromol)
INactive_AChEl': rate of change in amount of AChE that is inactivated in liver (micromol/hr)
INactive_AChEp: amount of inactivated AChE in plasma (micromol)
INactive_AChEp': rate of change in amount of AChE that is inactivated in plasma (micromol/hr)
INactive_AChErbc: amount of inactivated AChE in red blood cells (micromol)
INactive_AChErbc': rate of change in amount of AChE that is inactivated in RBC (micromol/hr)
INactive_BuChEbr: amount of inactivated BuChE in brain (micromol)
INactive_BuChEbr: rate of change in amount of BuChE that is inactivated in brain (micromol/hr)
INactive_BuChEdi: amount of inactivated BuChE in diaphragm (micromol)
INactive_BuChEdi': rate of change in amount of BuChE that is inactivated in diaphragm (micromol/hr)
INactive_BuChEl: amount of inactivated BuChE in liver (micromol)
INactive_BuChEl': rate of change in amount of BuChE that is inactivated in liver (micromol/hr)
INactive_BuChEp: amount of inactivated BuChE in plasma (micromol)
INactive_BuChEp': rate of change in amount of BuChE that is inactivated in plasma (micromol/hr)
INactive_BuChErbc: amount of inactivated BuChE in RBC (micromol)
INactive_BuChErbc': rate of change in amount of BuChE that is inactivated in RBC (micromol/hr)
INactive_CaEbr: amount of inactivated CaE in brain (micromol)
INactive_CaEbr': rate of change in amount of CaE that is inactivated in brain (micromol/hr)
INactive_CaEdi: amount of inactivated CaE in diaphragm (micromol)
INactive_CaEdi': rate of change in amount of CaE that is inactivated in diaphragm (micromol/hr)
INactive_CaEl: amount of inactivated CaE in liver (micromol)
INactive_CaEl': rate of change in amount of CaE that is inactivated in liver (micromol/hr)
INactive_CaEp: amount of inactivated CaE in plasma (micromol)
INactive_CaEp': rate of change in amount of CaE that is inactivated in plasma (micromol/hr)

INactive_CaErbc: amount of inactivated CaE in RBC (micromol)
INactive_CaErbc': rate of change in amount of CaE that is inactivated in RBC (micromol/hr)
Inhib_AChEbr: % AChE inhibition in brain
Inhib_AChEdi: % AChE inhibition in diaphragm
Inhib_AChEl: % AChE inhibition in liver
Inhib_AChEp: % AChE inhibition in plasma
Inhib_AChErbc: % AChE inhibition in RBC
Inhib_BuChEbr: % BuChE inhibition in brain
Inhib_BuChEdi: % BuChE inhibition in diaphragm
Inhib_BuChEl: % BuChE inhibition in liver
Inhib_BuChEp: % BuChE inhibition in plasma
Inhib_CaEbr: % CaE inhibition in brain
Inhib_CaEdi: % CaE inhibition in diaphragm
Inhib_CaEl: % CaE inhibition in liver
Inhib_CaEp: % CaE inhibition in plasma
Inhib_ChEp_total: % total cholinesterase inhibition in plasma
Inhib_ChErbc_total: % total cholinesterase inhibition in RBC
Inhib_tot_br: % total B-EST inhibition in brain
Inhib_tot_di: % total B-EST inhibition in diaphragm
Inhib_tot_l: % total B-EST inhibition in liver
Inhib_tot_p: % total B-EST inhibition in plasma
Inhib_tot_rbc: % total B-EST inhibition in RBC
Init AAChEbr: initial amount of esterase binding sites brain, AChE (micromol)
Init AAChEdi: Initial amount of esterase binding sites diaphragm, AChE (micromol)
Init AAChEl: Initial amount of esterase binding sites liver, AChE (micromol)
Init AAChEp: Initial amount of esterase binding sites plasma, AChE (micromol)
Init AAChErbc: Initial amount of esterase binding sites RBC, AChE (micromol)
Init ABuChEbr: initial amount of esterase binding sites brain, BuChE (micromol)
Init ABuChEdi: Initial amount of esterase binding sites diaphragm, BuChE (micromol)
Init ABuChEl: Initial amount of esterase binding sites liver, BuChE (micromol)
Init ABuChEp: Initial amount of esterase binding sites plasma, BuChE (micromol)
Init ABuChErbc: Initial amount of esterase binding sites RBC, BuChE (micromol)
Init ACaEbr: initial amount of esterase binding sites brain, CaE (micromol)
Init ACaEdi: Initial amount of esterase binding sites diaphragm, CaE (micromol)
Init ACaEl: Initial amount of esterase binding sites liver, CaE (micromol)
Init ACaEp: Initial amount of esterase binding sites plasma, CaE (micromol)
Init ACaErbc: Initial amount of esterase binding sites RBC, CaE (micromol)
Init AML1: Initial amount of free chlorpyrifos metabolised to chlorpyrifos-oxon by hepatic CYP450 (micromol)
Init AML2: Initial amount of free chlorpyrifos metabolised to TCP by hepatic CYP450 (micromol)
Init AML3bl: Initial amount of chlorpyrifos-oxon metabolised to TCP by A-EST in blood (micromol)
Init AML3l: Initial amount of chlorpyrifos-oxon metabolised to TCP by A-EST in liver (micromol)
Init AML4bl: Initial amount of chlorpyrifos-oxon metabolised to TCP by AChE in blood (micromol)
Init AML4br: Initial amount of chlorpyrifos-oxon metabolised to TCP by AChE in brain (micromol)
Init AML4di: Initial amount of chlorpyrifos-oxon metabolised to TCP by AChE in diaphragm (micromol)
Init AML4l: Initial amount of chlorpyrifos-oxon metabolised to TCP by AChE in liver (micromol)
Init AML4rbc: initial amount of TCP from metabolism by AChE in RBC (micromol)
Init AML5bl: Initial amount of chlorpyrifos-oxon metabolised to TCP by BuChE in blood (micromol)
Init AML5br: Initial amount of chlorpyrifos-oxon metabolised to TCP by BuChE in brain (micromol)
Init AML5di: Initial amount of chlorpyrifos-oxon metabolised to TCP by BuChE in diaphragm (micromol)
Init AML5l: Initial amount of chlorpyrifos-oxon metabolised to TCP by BuChE in liver (micromol)
Init AML5rbc: initial amount of TCP from metabolism by BuChE in RBC (micromol)
Init AML6bl: Initial amount of chlorpyrifos-oxon metabolised to TCP by CaE in blood (micromol)
Init AML6br: Initial amount of chlorpyrifos-oxon metabolised to TCP by CaE in brain (micromol)
Init AML6di: Initial amount of chlorpyrifos-oxon metabolised to TCP by CaE in diaphragm (micromol)
Init AML6l: Initial amount of chlorpyrifos-oxon metabolised to TCP by CaE in liver (micromol)

Init AML6rbc: initial amount of TCP from metabolism by CaE in RBC (micromol)
Init ATCP: Initial amount of TCP (micromol)
Init C: initial in chlorpyrifos concentration (micromol/l)
Init Cbl: initial chlorpyrifos concentration in blood (micromol/l)
Init Cblo: Initial concentration of chlorpyrifos-oxon in blood (micromol/l)
Init Cbr: initial chlorpyrifos concentration in brain (micromol/l)
Init Cbro: initial chlorpyrifos-oxon concentration in brain (micromol/l)
Init Cdi: initial chlorpyrifos concentration in diaphragm (micromol/l)
Init Cdio: Initial chlorpyrifos-oxon concentration diaphragm (micromol/l)
Init Cf: initial chlorpyrifos concentration in fat (micromol/l)
Init Cfo: initial chlorpyrifos-oxon concentration in fat (micromol/l)
Init Cl: initial concentration of chlorpyrifos in liver (micromol/l)
Init Clo: initial concentration of chlorpyrifos-oxon in liver (micromol/l)
Init Cr: initial chlorpyrifos concentration in rapidly perfused tissues (micromol/l)
Init Cro: initial chlorpyrifos-oxon concentration in rapidly perfused tissues (micromol/l)
Init Cs: initial chlorpyrifos concentration in slowly perfused tissues (micromol/l)
Init Cso: initial chlorpyrifos-oxon concentration in slowly perfused tissues (micromol/l)
Init INactive_AChEbr: initial amount of inactivated AChE in brain (micromol)
Init INactive_AChEdi: initial amount of inactivated AChE in diaphragm (micromol)
Init INactive_AChEl: initial amount of inactivated AChE in liver (micromol)
Init INactive_AChEp: initial amount of inactivated AChE in plasma (micromol)
Init INactive_AChErbc: initial amount of inactivated AChE in red blood cells (micromol)
Init INactive_BuChEbr: initial amount of inactivated BuChE in brain (micromol)
Init INactive_BuChEdi: initial amount of inactivated BuChE in diaphragm (micromol)
Init INactive_BuChEl: initial amount of inactivated BuChE in liver (micromol)
Init INactive_BuChEp: initial amount of inactivated BuChE in plasma (micromol)
Init INactive_BuChErbc: initial amount of inactivated BuChE in RBC (micromol)
Init INactive_CaEbr: initial amount of inactivated CaE in brain (micromol)
Init INactive_CaEdi: initial amount of inactivated CaE in diaphragm (micromol)
Init INactive_CaEl: initial amount of inactivated CaE in liver (micromol)
Init INactive_CaEp: initial amount of inactivated CaE in plasma (micromol)
Init INactive_CaErbc: initial amount of inactivated CaE in RBC (micromol)
Init Input_l: initial amount of chlorpyrifos to liver from diet and gavage (micromol)
Init Intes: initial amount absorbed in intestine (micromol)
Init Oral: initial amount absorbed in liver from gastrointestinal tract (micromol)
Init Oral_abs: Initial amount of chlorpyrifos absorbed oral, gavage (micromol)
Init Stom: initial amount absorbed in stomach (micromol)
Init TCP_form: initial amount of TCP formed (micromol)
Init TCPexc: initial urinary excretion of TCP (micromol)
Input_l': rate of total input of chlorpyrifos to liver from diet and gavage (micromol/hr)
Intes': Absorption rate in intestine (micromol/hr)
Ka1: aging time, AChE (1/hr)
Ka10: aging time, CaE (1/hr)
Ka6: aging time, BuChE (1/hr)
KaI: rate constant, absorption in intestine (1/hr)
KaS: rate constant, absorption in stomach (1/hr)
Kd1: enzyme degradation rate brain AChE (1/hr)
Kd10: enzyme degradation rate brain CaE (1/hr)
Kd11: enzyme degradation rate diaphragm CaE (1/hr)
Kd12: enzyme degradation rate liver CaE (1/hr)
Kd13: enzyme degradation rate plasma CaE (1/hr)
Kd2: enzyme degradation rate diaphragm AChE (1/hr)
Kd3: enzyme degradation rate liver AChE (1/hr)
Kd4: enzyme degradation rate plasma AChE (1/hr)
Kd5: enzyme degradation rate RBC AChE (1/hr)

Kd6: enzyme degradation rate brain BuChE (1/hr)
Kd7: enzyme degradation rate diaphragm BuChE (1/hr)
Kd8: enzyme degradation rate liver BuChE (1/hr)
Kd9: enzyme degradation rate plasma BuChE (1/hr)
Ke: 1. order elimination constant, urinary elimination of TCP (1/hr)
Ki1: bimolecular inhibition rate all tissues AChE (1/(microM*hr))
Ki10: bimolecular inhibition rate brain CaE (1/(microM*hr))
Ki11: bimolecular inhibition rate diaphragm CaE (1/(microM*hr))
Ki12: bimolecular inhibition rate liver CaE (1/(microM*hr))
Ki13: bimolecular inhibition rate all plasma CaE (1/(microM*hr))
Ki5: bimolecular inhibition rate RBC AChE (1/(microM*hr))
Ki6: bimolecular inhibition rate all tissues BuChE (1/(microM*hr))
Km1: Michaelis-Menten constant for metabolism of chlorpyrifos to chlorpyrifos-oxon (liver) by CYP450 (micromol/l)
Km2: Michaelis-Menten constant for metabolism of chlorpyrifos to TCP (liver) by CYP450 (micromol/l)
Km3: Michaelis-Menten constant for saturable process. A-EST chlorpyrifos-oxon to TCP (liver) (micromol/l)
Km4: Michaelis-Menten constant for saturable process. A-EST chlorpyrifos-oxon to TCP (blood) (micromol/l)
Kr1: reactivation rate, AChE (1/hr)
Kr10: reactivation rate, CaE (1/hr)
Kr5: reactivation rate, RBC AChE (1/hr)
Kr6: reactivation rate, BuChE (1/hr)
KsAChEbr: zero order synthesis rate of brain AChE (micromol/hr)
KsAChEdi: zero order synthesis rate of diaphragm AChE (micromol/hr)
KsAChEl: zero order synthesis rate of liver AChE (micromol/hr)
KsAChEp: zero order synthesis rate of plasma AChE (micromol/hr)
KsAChErbc: zero order synthesis rate of RBC AChE (micromol/hr)
KsBuChEbr: zero order synthesis rate of brain BuChE (micromol/hr)
KsBuChEdi: zero order synthesis rate of diaphragm BuChE (micromol/hr)
KsBuChEl: zero order synthesis rate of liver BuChE (micromol/hr)
KsBuChEp: zero order synthesis rate of plasma BuChE (micromol/hr)
KsBuChErbc: zero order synthesis rate of RBC BuChE (micromol/hr)
KsCaEbr: zero order synthesis rate of brain CaE (micromol/hr)
KsCaEdi: zero order synthesis rate of diaphragm CaE (micromol/hr)
KsCaEl: zero order synthesis rate of liver CaE (micromol/hr)
KsCaEp: zero order synthesis rate of plasma CaE (micromol/hr)
KsCaErbc: zero order synthesis rate of RBC CaE (micromol/hr)
KsI: rate constant, transfer stomach-intestine (1/hr)
kzero: zero-order uptake rate (micromol/hr)
Mc: molecular weight for chlorpyrifos (mg/micromol)
Oral_abs': rate of oral absorption of chlorpyrifos is equal to sum of absorption rates from Stomach (Stom) and intestine (Intes) (micromol/hr)
Oral_adm: Dietary administeration of chlorpyrifos (mg/kg bw/day)
PCbl: blood:blood partition coefficient for chlorpyrifos
PCblo: blood:blood partition coefficient for chlorpyrifos-oxon (from Timchalk et al., 2007 supplemental data)
PCbrc: brain:blood partition coefficient
PCbro: brain:blood partition coefficient for chlorpyrifos-oxon
PCdic: diaphragm:blood partition coefficient
PCdio: diaphragm:blood partition coefficient for chlorpyrifos-oxon
PCfc: fat:blood partition coefficient
PCfo: fat:blood partition coefficient for chlorpyrifos-oxon
PClc: liver:blood partition coefficient
PClo: liver:blood partition coefficient for chlorpyrifos-oxon
PCrc: rapidly perfused tissue:blood partition coefficient
PCro: rapidly perfused tissue:blood partition coefficient for chlorpyrifos-oxon
PCsc: slowly perfused tissue:blood partition coefficient

PCso: slowly perfused tissue:blood partition coefficient for chlorpyrifos-oxon
PEbl: blood percentage of body weight (%)
PEbr: brain percentage of body weight (%)
PEdi: diaphragm percentage of body weight (%)
PEf: fat percentage of body weight (%)
PEl: liver percentage of body weight (%)
PEr: rapidly perfused tissues percentage of body weight (%)
PEs: slowly perfused tissues percentage of body weight (%)
Qbr: blood flow to brain (l/hr)
Qbrc: blood flow in brain as percentage of cardiac output (%)
QC: cardiac output (l/hr)
Qdi: blood flow to diaphragm (l/hr)
Qdic: blood flow in diaphragm as percentage of cardiac output (%)
Qf: blood flow to fat (l/hr)
Qfc: blood flow in fat as percentage of cardiac output (%)
Ql: blood flow to liver (l/hr)
Qlc: blood flow in liver as percentage of cardiac output (%)
Qr: blood flow to rapidly perfused tissues (l/hr)
Qrc: blood flow in rapidly perfused tissues as percentage of cardiac output (%)
Qs: blood flow to slowly perfused tissues (l/hr)
Qsc: blood flow in slowly perfused tissues as percentage of cardiac output (%)
R: dosing intervals
Repeat_exp: repeated dietary exposure (micromol/hr)
Repeated: time over which the dosage is repeated
Stom': absorption rate in stomach (micromol/hr)
Stom: amount of chlorpyrifos in stomach (micromol)
TCP_form': rate of formation of TCP (micromol/hr)
TCPexc': rate of urinary excretion of TCP (micromol/hr)
TCPexc: urinary excretion of TCP (micromol)
TOTAL: total amount of chlorpyrifos delivered to tissues or excreted (micromol)
total_massCPF: total mass of chlorpyrifos (micromol)
total_massOxon: total mass of chlorpyrifos-oxon (micromol)
total_massTCP: total mass of TCP (micromol)
TRAChE: enzyme turnover rate AChE (enzyme hydrolysed/hr)
TRBuChE: enzyme turnover rate BuChE (enzyme hydrolysed/hr)
TRCaE: enzyme turnover rate CaE (enzyme hydrolysed/hr)
Va: volume of arterial blood (l)
Vac: volume of arterial blood as percentage of body weight (%)
Vbl: volume of blood (l)
Vblc: volume of blood as percentage of body weight (%)
Vbr: volume of brain (l)
Vbrc: volume of brain as percentage of body weight (%)
Vd: volume of distribution (l)
Vdi: volume of diaphragm (l)
Vdic: volume of diaphragm as percentage of body weight (%)
Vf: volume of fat (l)
Vfc: volume of fat as percentage of body weight (%)
Vl: volume of liver (l)
Vlc: volume of liver as percentage of body weight (%)
Vmax1: Maximum rate (velocity) for metabolism of chlorpyrifos to chlorpyrifos-oxon by CYP450 (micromol/hr)
Vmax2: Maximum rate (velocity) for metabolism of chlorpyrifos to TCP by CYP450 (micromol/hr)
Vmax3: Maximum rate (velocity) for metabolism of chlorpyrifos-oxon to TCP by CYP450 in liver (micromol/hr)
Vmax4: Maximum rate (velocity) for metabolism of chlorpyrifos-oxon to TCP by CYP450 in blood (micromol/hr)

VmaxC1: Maximum rate for metabolism of chlorpyrifos to chlorpyrifos-oxon per kg body weight (liver) (micromol/hr/kg)
VmaxC2: Maximum rate for metabolism of chlorpyrifos to TCP per kg body weight (liver) (micromol/hr/kg)
VmaxC3: Maximum rate for metabolism of chlorpyrifos-oxon to TCP in liver per kg body weight (micromol/hr/kg)
VmaxC4: Maximum rate for metabolism of chlorpyrifos-oxon to TCP in blood per kg body weight (micromol/hr/kg)
Vr: volume of rapidly perfused tissue (l)
Vrc: volume of rapidly perfused tissue as percentage of body weight (%)
Vs: volume of slowly perfused tissues (l)
Vsc: volume of slowly perfused tissues as percentage of body weight (%)
Vv: volume of venous blood (l)
Vvc: volume of venous blood as percentage of body weight (%)
Wbl: weight of blood (kg)
Wbr: weight of brain (kg)
Wdi: weight of diaphragm (kg)
Wf: weight of fat (kg)
Wl: weight of liver (kg)
Wr: weight of rapidly perfused tissues (kg)
Ws: weight of slowly perfused tissues (kg)

APPENDIX III. REVIEW PAPER

Trine Klein Reffstrup, John Christian Larsen, Otto Meyer, 2010. Risk assessment of mixtures of pesticides. Current approaches and future strategies. Regul. Toxicol. Pharmacol., 56, 174-192.

Regulatory Toxicology and Pharmacology 56 (2010) 174–192

Contents lists available at ScienceDirect

Regulatory Toxicology and Pharmacology

journal homepage: www.elsevier.com/locate/yrtph

Risk assessment of mixtures of pesticides. Current approaches and future strategies

Trine Klein Reffstrup *, John Christian Larsen, Otto Meyer

National Food Institute, Technical University of Denmark, Mørkhøj Bygade 19, DK-2860 Søborg, Denmark

ARTICLE INFO

Article history:
Received 3 April 2009
Available online 24 September 2009

Keywords:
Risk assessment
Mixture
Pesticide
PBTK
Combined action
Interaction

ABSTRACT

The risk assessment of pesticide residues in food is based on toxicological evaluation of the single compounds and no internationally accepted procedure exists for evaluation of cumulative exposure to multiple residues of pesticides in crops, except for a few groups of pesticides sharing a group ADI. However, several attempts have been suggested during the last decade. This paper gives an overview of the various approaches. It is of paramount importance to consider whether there will be either no interaction or interaction between the compounds in the mixture. When there are no interactions several approaches are available for the risk assessment of mixtures of pesticides. However, no single simple approach is available to judge upon potential interactions at the low doses that humans are exposed to from pesticide residues in food. In these cases, PBTK models could be useful as tools to assess combined tissue doses and to help predict potential interactions including thresholds for such effects. This would improve the quality of the risk assessment.

1. Introduction

During the last decades there has been increasing focus on the fact that humans are concurrently exposed to a number of chemicals via food and environment. These chemicals may have a combined action that causes a lower or higher toxic effect than would be expected from knowledge about the single compounds (Larsen et al., 2003). Consequently, combined actions need to be addressed in the risk assessment process. This paper will focus on risk assessment of combined actions of pesticide residues in food.

Ideally, the evaluation of the toxicological properties of a pesticide mixture requires detailed information on the composition of the mixture and the mechanism of action of each of the individual compounds. In order to perform a risk assessment, proper exposure data are also needed, however, such detailed information is normally not available. The mixture of pesticide residues that a person would be exposed to via the food chain may change over time in composition and quantity. Adequate testing of mixtures is often not possible because the number of theoretical possible combinations is enormous and furthermore the use of a sufficient number of dose levels is not feasible. A full study design would require $2^n - 1$ test groups to identify interactions between all compounds of interest (n is the number of chemicals in the mixture). In addition, high-dose levels of a pesticide mixture as used in toxicological studies may have different types of effects than low dose levels.

One of the main points to consider is whether there will be either no interaction or interaction in the form of either synergism or antagonism. These basic principles of combined actions of chemical mixtures are purely theoretical and one often has to deal with more than one of the concepts at the same time when mixtures consist of more than two compounds and when the toxicity targets are more complex.

During the last two decades several suggestions have been published on how to perform risk assessment on mixtures of pesticides. In 1986 the Environmental Protection Agency in USA (US EPA) published a guideline for health risk assessment of chemical mixtures (US EPA, 1986). However, what really put focus on this topic was the Food Quality Protection Act of 1996 which in relation to pesticide residues requires US EPA to consider "available information concerning the cumulative effects of such residues and other substances that have a common mechanism of toxicity" (United States of America in Congress, 1996). Since then US EPA has published several reports and guidelines on health risk assessment of chemical mixtures (US EPA, 1999a, 2000, 2002, 2003).

The Agency for Toxic Substances and Disease Registry in USA (ATSDR) has published two guidelines with instructions to users on how to apply current methodologies for risk assessment of combined actions of chemicals (ATSDR, 2001, 2004). In 2002 the Health Council of The Netherlands as well as the Committee on Toxicity of Chemicals in Food, Consumer Products and the Environment in United Kingdom published advisory reports (Committee

* Corresponding author. Fax: +45 3588 7699.
E-mail addresses: tkre@food.dtu.dk (T.K. Reffstrup), jchla@food.dtu.dk (J.C. Larsen), oame@food.dtu.dk (O. Meyer).

0273-2300/$ - see front matter © 2009 Elsevier Inc. All rights reserved.
doi:10.1016/j.yrtph.2009.09.013

on Toxicity, 2002; Feron et al., 2004; Health Council of the Netherlands, 2002).

The Danish Veterinary and Food Administration has published the reports "Combined Actions of Pesticides in Food" (Reffstrup, 2002) and "Combined Actions and Interactions of Chemicals in Mixtures" (Larsen et al., 2003) which summarised and evaluated the present knowledge about combined toxic effects of mixtures of chemicals. One of the main conclusions was that the existing methods were uncertain and rough.

Since then, several international initiatives have been taken in order to more closely explore what approaches can be used to evaluate chemical mixtures. Most notably, the European Food Safety Authority (EFSA) organised a workshop on cumulative risk assessment in 2006 (EFSA, 2007) and more recently the Norwegian Scientific Committee for Food Safety and EFSA have published opinions on risk assessment of combined actions on chemicals (EFSA, 2008; Norwegian Scientific Committee for Food Safety, 2008).

These organizations and workshops recommended to introduce physiologically based toxicokinetic (PBTK) modelling as a tool in the risk assessment of chemical mixtures. These models can be used as a technique for prediction of internal dose levels and thereby it can be useful in for instance predicting kinetic overload and levels at the target site. The models require a large amount of data for construction and therefore they should only be used for higher tier assessment. However, when the models are constructed and evaluated they can reduce the need for data on specific scenarios.

2. Types of combined actions

The basic types of combined action of compounds are either no interaction in the form of simple similar action (dose addition) and simple dissimilar action (response addition) or combined effect with interaction (antagonism, synergism). Many terms have been used for additivity, but it seems as the terminology that has become fairly common includes the terms simple similar action and simple dissimilar action to describe additivity (Teuschler, 2007).

2.1. No interactions

The model for simple similar action (synonyms: dose additivity, Loewe additivity) assumes that the compounds in the mixture behave as if they are dilutions of each other (Krishnan et al., 1997; Svendsgaard and Hertzberg, 1994). This means that the compounds act on the same biological site by the same mechanism/mode of action and differ only in their potencies. The dose–response curves for the single compounds in a mixture are allowed to be nonparallel (on a linear-log graph). (Svendsgaard and Greco, 1995).

The theoretical basis for the simple dissimilar action (synonyms: response additivity, Bliss independence) is probabilistic independence. This means that the compounds in the mixture do not interfere with each other but they all contribute to a common result. The model assumes that the compounds in the mixture do not act by the same mode of action and the nature and site of action may also differ among the compounds.

2.2. Interactions

Interactions are defined as combined actions resulting in a stronger (synergism) or weaker (antagonism) effect than would be expected based on the assumption of additivity. Interactions can be divided into direct chemical–chemical, toxicokinetic or toxicodynamic actions (ATSDR, 2001; Norwegian Scientific Committee for Food Safety, 2008).

In direct chemical–chemical interactions, one chemical interacts directly with another chemical causing a chemical change which will lead to a change in the toxicity causing a stronger or weaker effect. Toxicokinetic-based interactions may result in effects on absorption, distribution, metabolism or elimination of the compounds. Toxicokinetic-based interaction is of particular concern when it results in an increase in the internal dose of the active form of another compound. Toxicodynamic interactions occurs when the presence of two (or more) compounds change the response without affecting the tissue dose of each of the compounds. They occur at the cellular receptor site, or target molecule, or among receptor sites or targets. When interaction takes place at the same receptor site this usually results in antagonism.

It is difficult to predict interactions leading to toxicity at very low exposure levels. Knowledge about combined actions has normally been obtained for considerably higher concentrations than for the levels actually found in food and it is often unclear whether knowledge about the combined action at higher concentrations are relevant for the low exposure level. For example a combined toxic action observed at high dose level may be based on mechanism that is not relevant at low dose levels and high to low-dose extrapolation may be meaningless (Borgert et al., 2004). Overall, interactions appear less often at relatively low exposure levels compared to high exposure levels since they are primarily caused by various thresholds and saturation phenomenon (saturation of activating, detoxification or reparative processes). The main mode of toxicologic interaction is the alteration of the toxicokinetic process, which strongly depends on the exposure levels of the compounds in the mixture (US EPA, 2000). Slikker et al. (2004) have given examples in which dose-dependent transition in the underlying kinetic and/or dynamic factors behind the toxicity occurs. It is often difficult to interpret effects at high dose levels in animal studies and the results may not reflect the actual toxicity at relevant human exposure levels. This is particularly the case if dose-dependent transitions in the principal mechanism of toxicity occur (Slikker et al., 2004).

2.3. Early experimental work on mixture toxicology

From the results of experimental short-term toxicity studies Feron and co-workers concluded that combined exposure to arbitrarily chosen chemicals demonstrated less than an additive effect when all chemicals in the mixture were administrated at their own individual no observed adverse effect levels (NOAELs) whereas no clear evidence of toxicity was found at slightly lower dose levels. The examined compounds had either different target organs and/or differed in the mode of action. Exposure levels at or below the individual NOAELs of the compounds in a mixture are therefore not expected to be associated with a greater hazard than exposure to the individual chemicals. However, both synergistic and antagonistic effects may be seen at exposure levels higher than the NOAELs (Feron et al., 1995b; Groten et al., 1997; Jonker et al., 1990, 1993, 1996).

The Dutch research group was of the opinion that the use of the "dose addition" approach to the risk assessment of chemical mixtures is only scientifically justifiable when the chemicals in the mixture act in the same way, by the same mechanism and thus differ only in their potencies. Application of the "dose addition" model to mixtures of chemicals that act by mechanisms for which the additivity assumptions are invalid could greatly overestimate the risk (Cassee et al., 1998; Feron et al., 1995a). This group found it reasonable to use the approaches based on toxicological similarity and toxicological independency for risk assessment of pesticide residues in food since these compounds are found at levels well below the NOAELs for the compounds.

However, the group did not define the criteria used to judge whether two compounds in a mixture share a common mode of action. This means that when looking on the same data other scientists may come to another conclusion as to whether the compounds are similar with respect to mode of action. Therefore the results from these studies are not totally unambiguous.

3. Methods for risk assessment of mixtures of pesticides in foods

Various approaches have been suggested in the scientific literature for use in the evaluation of the health risks from exposure to mixtures of chemicals but there is no internationally accepted procedure. The most important approaches are summarised in this section.

The first step in the cumulative risk assessment of mixtures is to identify a group of compounds that induce a common toxic effect by a common mechanism of toxicity. US EPA has described a procedure for that in "Guidance for identifying pesticide chemicals and other substances that have a common mechanism of toxicity" (US EPA, 1999a). In this guidance US EPA defined a common mechanism to be caused "by the same, or essentially the same, sequence of major biochemical events". This definition is equivalent to the definition of the term mode of action (US EPA, 2002). In other reports US EPA distinguished between mechanism of action and mode of action: The term mode of action describes the key events and processes starting with interaction of a compound with a cell via operational and anatomical changes, resulting in the toxic effect. Mechanism of action implies a more detailed understanding and description of steps at the molecular level (US EPA, 2000, 2005).

The International Life Sciences Institute (ILSI) convened a group of experts to consider the definition of the term common mechanism. They concluded that chemicals act via a common mechanism of toxicity if they cause the same critical effect, act on the same molecular target issue, act by the same biochemical mechanism of action, or share a common toxic intermediate (Botham et al., 1999; Mileson et al., 1998).

ATSDR do not define the terms mode of action and mechanism of action. However, they point out that for mixtures of compounds that have an effect on the same endpoint by the same mode of action dose addition is the most appropriate method (ATSDR, 2001, 2004).

The requirement of knowledge on the mode of action is an assumption made for the purpose of being able to perform the risk assessment process for mixtures. However, the theoretical and empirical basis for the term mode of action has yet to be established. Thus, Borgert et al. (2004) have questioned the use of the mode of action to predict combined actions of mixtures. They stated that in order to use mechanistic information for predicting combined action on a scientific basis more research is needed to better understand how mode of action for individual compounds is related to the toxicity of the whole mixture and they concluded that until then the use of mode of action to predict mixture toxicity will remain tenuous (Borgert et al., 2004). Berenbaum (1989) described why interactions cannot usefully be defined as departures from what is expected from mechanism of action and how one instead should analyse a mixture for departure from additivity rather than for specific interactions by comparing dose–response information for the compounds in the mixture to the observed responses induced by a specific mixture (Berenbaum, 1989).

Ideally the identification of a group of pesticides for cumulative risk assessment should be based on criteria providing the best and most robust grouping such as chemical structure, mechanism of action, common toxic mode of action or common toxic effect. Unfortunately, such data are seldom available for all of the compounds of concern. Therefore, EFSA has suggested to group compounds for cumulative assessment even in the absence of such detailed data and make cumulative assessment groups (CAG) based on less refined evaluation of the mode of action e.g. only on target organ toxicity (EFSA, 2008).

The next step is to select an appropriate method and dataset for combining the risks of the compounds in the group. In 1986, the US EPA recommended three approaches for health risk assessment of chemical mixtures (Mumtaz, 1995; US EPA, 1986): (1) the mixture of concern approach, (2) the similar mixture approach and (3) the single compounds approach.

The choice of method depends on the toxic effect, the available data on toxicity of the mixture or the compounds in the mixture, the predicted interactions among the compounds in the mixture and on the quality of the exposure data. However, the US EPA points out that it is ideal to conduct all three assessments when possible in order to make the best risk assessment and to use all the available data—in particular the incorporation of interaction data when available. The uncertainties for the risk assessment should be clearly discussed and the overall quality of the risk assessment should be characterised (US EPA, 1986).

3.1. Mixture approaches

The guidance was supplemented in 2000 (US EPA, 2000) and the flow chart for the different types of mixture assessments shown in Fig. 1 was suggested. In this new guidance three methods for whole mixture assessment and four compound-based methods were presented. The first step in the flow chart is to assess the quality of the available data of the compounds of interest. When the data are adequate for an assessment, it should be decided whether there are data available for an assessment on the whole mixture or only on the single compounds.

The assessment based on data on whole mixtures can be done on the mixture of concern, on a sufficiently similar mixture (almost the same compounds and in almost the same proportions as in the mixture of concern) or on a group of similar mixtures (same compounds but slightly different ratios, or lacking one or more compounds or having one or more additional compounds compared with the mixture one wants to evaluate). These assessments would be the most appropriate for risk assessment of pesticide residues in food; however, they are very data intensive and data for these methods are rarely available.

3.2. Single compound approaches

US EPA has proposed guidance on how to perform a risk assessment on a mixture of pesticides that act by a common mechanism (US EPA, 2002). For mixtures of compounds that are toxicologically similar, US EPA suggested three methods based on simple similar action: the hazard index method (HI), the relative potency factor method (RPF) and the special type of the relative potency factor method named the toxicity equivalency factor method (TEF) (US EPA, 2000).

The point of departure index (PODI) has also been suggested for estimating the risk of a group of compounds which are toxicologically similar. Also the margin of exposure (MOE) as wells as the cumulative risk index (CRI) have been suggested. These two methods are reciprocals of the point of departure and the hazard index, respectively (US EPA, 2003).

These six methods based on simple similar action differ by the required data on toxicological processes but in all cases the exposure levels are added after having been multiplied by a scaling factor that accounts for differences in the toxicological potency (for instance acceptable daily intake (ADI) or reference dose (RfD)) or

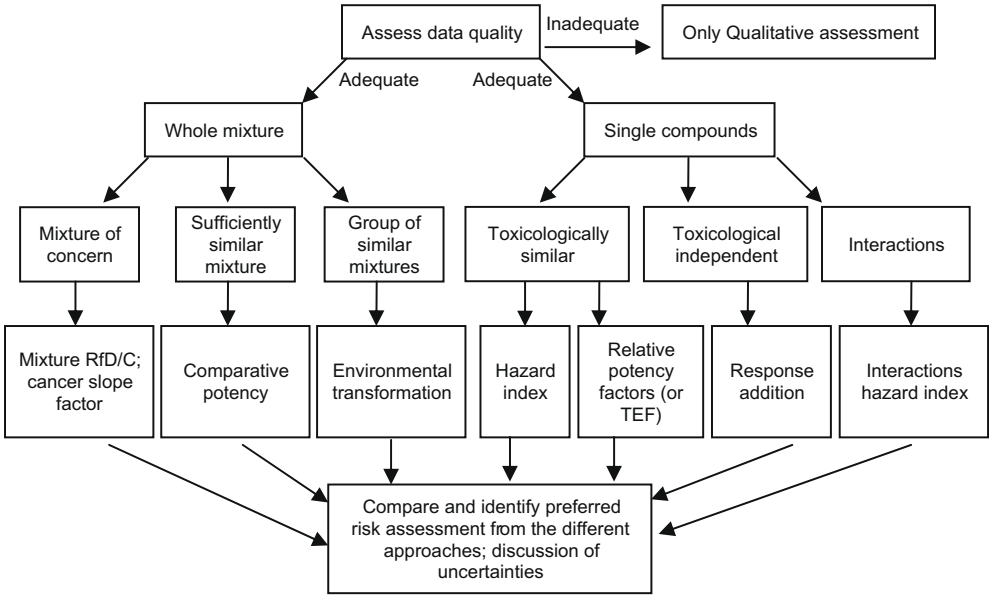

Fig. 1. Flow chart of the risk assessment approach used by US EPA. Modified from (US EPA, 2000).

point of departure doses (e.g. benchmark dose at 10% effect level, BMD_{10}). For compounds acting independently by simple dissimilar action the response addition (Bliss independence) approach may be used, and for compounds that interact, use of interaction hazard index is applicable (US EPA, 2000).

When making a risk assessment of exposure to a mixture the need to perform a comprehensive risk assessment should be determined early in the process and the most appropriate method should be used (US EPA, 2002). The single compound approaches are described in more details in the following.

3.3. Hazard index

In the hazard index approach the doses are standardised by using health-based values such as the ADI. The hazard index is calculated by the following equation:

$$\mathrm{HI} = \frac{E_1}{\mathrm{AL}_1} + \frac{E_2}{\mathrm{AL}_2} + \cdots + \frac{E_n}{\mathrm{AL}_n} = \sum_{i=1}^{n} \frac{E_i}{\mathrm{AL}_i} \quad (1)$$

where E_1, E_2, E_n and E_i are the levels of exposure of each individual compound (i) in a mixture of n compounds. AL_1, AL_2, AL_n and AL_i are the maximum acceptable level for each compound. The "acceptable level" is often a regulatory goal for exposure to the ith compound e.g. ADI or RfD (as used by US EPA) (US EPA, 1986, 2000). If the hazard index exceeds 1, the mixture has exceeded the maximum acceptable level (e.g. ADI or RfD) and there might thus be a risk. The fractions (E_1/AL_1 etc.) are sometimes called the hazard quotients, HQ. Since this method is based on an assumption of additivity it can lead to errors if a synergistic or antagonistic action occurs.

As an example of how to use the HI method we have examined a mixture of three pesticides, see Table 1. Chlorpyrifos, methidathion and malathion are chosen for the example as they are the three most frequently found pesticides in the Danish monitoring programme (Jensen et al., 2003). All three compounds can be found in oranges and the residues used in the calculations are the highest amount found in oranges in the latest Danish survey from 2005 (Christensen et al., 2006). The same uncertainty factor (UF = 100) was used to derive the ADI for the three compounds. The hazard index is then calculated from the values of exposure levels and ADIs given:

$$\mathrm{HI} = \frac{2.6 \times 10^{-5}}{0.01} + \frac{6.8 \times 10^{-6}}{0.001} + \frac{1.7 \times 10^{-5}}{0.3} \cong 0.0095$$

The calculated HI is well below one and the mixture is therefore not expected to constitute a risk.

3.4. Relative potency factor and toxicity equivalency factor Approach

The relative potency factor method has been applied to mixtures of a single class of chemicals for which extensive information are available for one of the chemicals in the group but less for the other members. The method assumes simple similar action and that the potency ratios between each chemical in the group remain constant at all dose levels. It requires toxicological similarity for specific conditions i.e. endpoint, route of exposure and duration. In cases where data indicate that different modes of action may apply to different target organs or under different exposure conditions or in cases where data are insufficient, endpoint specific RPFs may be derived for each effect or exposure condition (Advisory Committee on Hazardous Substances, 2007; US EPA, 2000).

The potency of each compound is expressed in relation to the potency of an index chemical which is typically the most exten-

Table 1
Data on three pesticides found as residues in oranges imported to Denmark. The residues are the highest amount found in oranges in the latest Danish survey from 2005 (Christensen et al., 2006).

Compound	Residue (mg/kg)	Exposure[a] (mg/kg bw/day)	NOAEL (mg/kg bw/day)	ADI (mg/kg bw)	Acute RfD (mg/kg bw)	TEF (Jensen et al., 2003)
Chlorpyrifos	0.19	2.6×10^{-5}	1	0.01[b]	0.1[b]	1
Methidathion	0.049	6.8×10^{-6}	0.1	0.001[c]	0.01[c]	0.2
Malathion	0.12	1.7×10^{-5}	29	0.3[d]	2[d]	2

[a] Exposure = (residue × intake)/(weight of person), where "weight of person" = 72 kg and "intake" (of orange) is 0.01 kg/day (Jensen et al., 2003).
[b] Chlorpyrifos: ADI and Acute RfD from JMPR (JMPR, 2000).
[c] Methidathion: ADI from JMPR (JMPR, 1993); Acute RfD from JMPR (JMPR, 1998).
[d] Malathion: ADI from JMPR (JMPR, 1998); Acute RfD from JMPR (JMPR, 2004). It should be noted that an ADI for malathion of 0.03 mg/kg bw and an ARfd = 0.3 mg/kg bw in EU have been set more recently based on the same study but with an uncertainty factor for 1000 and 100, respectively (EFSA, 2006).

sively studied chemical in the mixture. To evaluate a set of data of combined effects it is necessary to know the dose–response curve for the index compound and to know the effect of the other compounds in the mixture (Seed et al., 1995; US EPA, 2000).

Recently the RPF method has been used in cumulative risk assessment of effects of pesticides by combining it with an Integrated Probabilistic Risk Assessment (IPRA) model. The RPF values were estimated with the use of one or two index compounds and the RPF for each compound were used to calculate the cumulative residue level of each sample expressed as equivalents of the index compound. Then the probabilistic approach was used to calculate the distribution of the cumulative dietary exposure from consumption data and residue data of a group of pesticides in a population. The use of this approach has been demonstrated for a group of 40 acetylcholinesterase inhibiting pesticides (Boon and van Klaveren, 2003), for a group of 31 organophosphorus pesticides (Bosgra et al., 2009) as well as in a study of three anti-androgenic pesticides (Müller et al., 2009). This method makes it possible to better describe the uncertainties that are present in the data (Advisory Committee on Hazardous Substances, 2007).

The toxicity equivalency factor method is a special case of RPF in which a single TEF is derived for each chemical in the mixture across all endpoints and all exposure conditions. Therefore it requires a strong degree of toxicologically similarity as well as toxicological equivalence across all endpoints, i.e. it is assumed that all the toxic effects of concern share a common mode of action (US EPA, 2000). Other assumptions are that the effects of each compound in the mixture are essentially additive at sub-maximal levels of exposure and that the dose–response curves are parallel (Advisory Committee on Hazardous Substances, 2007; Safe, 1998; US EPA, 2000). The assumptions for the TEF model imply that a large amount of data is collected for the group of compounds under evaluation. So far the TEF approach has only been implied for a few mixtures of pesticides e.g. for assessment of combined risk from exposure to mixtures of organophosphorus compounds and carbamates (Boon and van Klaveren, 2003; Jensen et al., 2003; Mileson et al., 1999; National Research Council, 1993).

The TEF method was originally developed during the 1980s to express the toxicological potency of mixtures of polychlorinated dibenzo-*p*-dioxins and dibenzofurans by several authorities (US EPA, 1989a). According to Safe (1990) TEF values should be derived from data available for more than one response. These criteria were used by Safe for deriving TEF values for polychlorinated biphenyls, dibenzo-*p*-dioxins, dibenzofurans ("dioxins") and related compounds (Safe, 1990). Based on the experience from the development of TEFs for dioxins in the beginning of the 1990s seven guiding criteria were developed for the TEF approach for application to dioxins and dioxin-like compounds (US EPA, 2000). In this report EPA also described a procedure for developing a RPF approach for more general use. Similar criteria was used by an expert meeting organised by WHO in 1997 with the purpose to derive consensus TEF values for polychlorinated dibenzo-*p*-dioxins, dibenzofurans and dioxinlike polychlorinated biphenyls. They followed a ranking order for weighting different types of studies: *in vivo* studies were higher ranked than *in vitro* studies and/or quantitative structural activity relationship (QSAR) data. In accordance with the approach used by Safe the studies were then further ranked due to the type of study (chronic > subchronic > subacute > acute) (Van den Berg et al., 1998). The TEF values for "dioxins" were re-evaluated at another WHO meeting in 2005 (Van den et al., 2006).

The toxicity equivalent (TEQ) concentration is calculated by multiplying the concentration of each compound (C_i) in a mixture with the TEF value of the individual compounds in the mixture (TEF_i):

$$\mathrm{TEQ} = \sum C_i \times \mathrm{TEF}_i \tag{2}$$

The resulting TEQ is assumed to be an equivalent concentration of the index compound and it can therefore be compared to the RfD of the index compound (Botham et al., 1999). If the TEQ is greater than the RfD, the mixture may constitute a risk.

In order to improve the application of relative potency factors to pesticide mixtures US EPA has published a report with information concerning biological concepts and statistical procedures (US EPA, 2003).

In the following the mixture of three pesticides in Table 1 in Section 3.3 is used in an example of use of the TEF method. The TEQ is calculated by the above equation in which the exposure data (from Table 1) are inserted as the concentration of each compound:

$$\mathrm{TEQ} = ((2.6\times10^{-5}\times1)+(6.8\times10^{-6}\times0.2) + (1.7\times10^{-5}\times2))\mathrm{mg/kg\,bw/day} \cong 6.1\times10^{-5}\mathrm{mg/kg\,bw/day}$$

The ADI for the index compound chlorpyrifos is 0.01 mg/kg bw/day (see Table 1) and the TEQ is then a factor of 165 below ADI. Therefore the mixture is not expected to constitute a risk. In this example the uncertainty factor is the same for the three compounds and therefore the result does not depend on the index compound chosen. However, if the uncertainty factor differs the choice of index compound will affect the result in the way that a higher uncertainty factor will result in a higher combined risk.

3.5. Point of departure, margin of exposure, cumulative risk index

In the point of departure index (PODI) method the exposures of each compound in the mixture are summed and expressed as a fraction of their respective PODs.

$$\mathrm{PODI} = \frac{E_1}{\mathrm{POD}_1} + \frac{E_2}{\mathrm{POD}_2} + \cdots + \frac{E_n}{\mathrm{POD}_n} = \sum_{i=1}^{n} \frac{E_i}{\mathrm{POD}_i} \tag{3}$$

The point of departure can be a data point (typically the NOAEL) or an estimated point derived from observed dose response data (e.g. benchmark dose at 10% effect level, BMD_{10}). Thus in contrast to the HI method the PODI method does not employ an uncertainty factor. The point of departure for the index chemical is used for extrapolating the risk of the cumulative assessment group. The point of departure on each compound's dose–response curve can be determined as the toxic potency of the compound relative to the other compounds (Larsen et al., 2003; US EPA, 2002).

An EFSA colloquium (EFSA, 2007) recommended the use of the PODI instead of the less transparent HI method because it does not involve a policy driven uncertainty factor. However, they state that HI is a practical tool for screening purposes.

EFSA uses the term reference point (RP or RfP) to replace the term point of departure (EFSA, 2008). Barlow et al. distinguish between the term reference point and point of departure in the way that the reference point is used in description of the margin of exposure approach and the point of departure is used in descriptions of extrapolation approaches (Barlow et al., 2006).

Data from Table 1 in Section 3.3 is used to calculate PODI with the NOAEL as the POD:

$$\mathrm{PODI} = \frac{1}{2.6\times10^{-5}} + \frac{0.1}{6.8\times10^{-6}} + \frac{29}{1.7\times10^{-5}} \cong 9.5\times10^{-5}$$

No international consensus exists on how to valuate the PODI. However, the PODI can be converted into a "risk cup" unit by multiplying with a group UF. A suggestion could be to use a group UF of 100 and an acceptable risk cup unit should be below 1. In the above example a risk cup unit of 0.0095 is obtained which is well below 1 and therefore is considered acceptable.

In the margin of exposure (MOE) method the point of departure (POD) is divided by the measured or estimated exposure (E) from a given route:

$$\mathrm{MOE} = \frac{\mathrm{POD}}{E} \tag{4}$$

The margin of exposure approach has been used by EPA to determine the acceptability of acute risks for single chemicals and MOEs of >10 or >100 are usually considered acceptable when derived from toxicological data from human and animal studies. These levels are chosen since they are numerically the same as the typical uncertainty factors that are used in calculating e.g. a RfD from NOAEL (Wilkinson et al., 2000).

The combined margin of exposure ($\mathrm{MOE_T}$) is the reciprocal of the sum of the reciprocal of MOEs of each compound in the mixture (Wilkinson et al., 2000):

$$\mathrm{MOE_T} = \frac{1}{1/\mathrm{MOE}_1 + 1/\mathrm{MOE}_2 + \cdots + 1/\mathrm{MOE}_n} = \sum_{i=1}^{n} \frac{1}{1/\mathrm{MOE}_i} \tag{5}$$

That is $\mathrm{MOE_T}$ is the reciprocal of PODI. A $\mathrm{MOE_T}$ higher than 100 is usually considered acceptable when derived from toxicological data from animal studies (Wilkinson et al., 2000).

For the example in Table 1 (Section 3.3) the $\mathrm{MOE_T}$ can be calculated by inserting MOE from each of the three compounds in the above equation:

$$\mathrm{MOE_T} = \frac{1}{\mathrm{POD}_1/E_1 + \mathrm{POD}_2/E_2 + \mathrm{POD}_3/E_3} = \frac{1}{\mathrm{PODI}} = \frac{1}{9.5 \times 10^{-5}} \cong 10,500$$

As $\mathrm{MOE_T}$ is higher than 100 it is considered acceptable.

US EPA has suggested to derive a cumulative risk index from the MOE for compounds with different uncertainty factors. The risk index (RI) can be calculated as follows:

$$\mathrm{RI} = \frac{\mathrm{POD}}{E \times \mathrm{UF}} = \frac{\mathrm{RfD}}{E} = \frac{1}{\mathrm{HQ}} \tag{6}$$

The cumulative risk index is the reciprocal of the sum of the reciprocal of the RIs and thereby of HI:

$$\mathrm{CRI} = \frac{1}{1/\mathrm{RI}_1 + 1/\mathrm{RI}_2 + \cdots + 1/\mathrm{RI}_n} = \frac{1}{E_1/\mathrm{RfD}_1 + E_2/\mathrm{RfD}_2 + \cdots + E_n/\mathrm{RfD}_n} = \sum_{i=1}^{n} \frac{1}{E_i/\mathrm{RfD}_n} \tag{7}$$

The risk increases as the CRI falls below 1, that is exposure is higher than the RfD (Larsen et al., 2003; US EPA, 1999b; Wilkinson et al., 2000).

The data from Table 1 in Section 3.3 will be used in this example showing how to calculate the cumulative risk index for the three compounds:

$$\mathrm{CRI} = \frac{1}{E_1/\mathrm{RfD}_1 + E_2/\mathrm{RfD}_2 + E_3/\mathrm{RfD}_3} = \frac{1}{2.6 \times 10^{-5}/0.1 + 6.8 \times 10^{-6}/0.01 + 1.7 \times 10^{-5}/2} \cong 1050$$

This is well above one and therefore the mixture is not expected to constitute a risk.

3.6. Simple dissimilar action, response addition

The model for simple dissimilar action assumes that the compounds in the mixture do not act by the same mode of action and the model does not assume that the dose–response curves have a similar shape. The nature and site of action may also differ among the compounds and every compound in the mixture is thought to provoke effects (response) independent of the presence of other compounds present i.e. the effect of one compound is the same whether or not another compound is present. An example of simple dissimilar action is the combined risk of any kind of reproductive toxicity for a set of chemicals with different modes of action (US EPA, 2000).

If we look at a mixture of two compounds: compound 1 has a probability for adverse effect, p_1, then compound 2 can act only on the remaining fraction $1 - p_1$ assuming that the maximum fraction of total possible effect is 1 (Svendsgaard and Hertzberg, 1994). Then the probability for adverse effect of compound 2 will be $p_2 \times (1 - p_1)$ and the expected probability for an adverse effect from the mixture according to the model of Bliss independence, p_{mix}, at the doses d_1 and d_2, respectively, will be:

$$p_{\mathrm{mix}}(d_1, d_2) = p_1(d_1) + p_2(d_2) \times (1 - p_1(d_1)) = p_1(d_1) + p_2(d_2) - p_1(d_1) \times p_2(d_2) \tag{8}$$

Bliss independence occurs if the measured effect of the mixture (stated as a probability for an adverse effect) equals $p_{\mathrm{mix}}(d_1,d_2)$ (Bliss, 1939; Könemann and Pieters, 1996; National Research Council, 1989; US EPA, 2000).

In a more general form, the probability for an adverse effect to arise from a mixture with more than two compounds is 1 minus the probability of not responding to any of the single compounds:

$$p_{\mathrm{mix}}(d_1, \ldots, d_n) = 1 - [(1 - p(d_1)) \times (1 - p(d_2)) \ldots \times \ldots (1 - p(d_n))] = 1 - \prod_{i=1}^{n} (1 - p_i) \tag{9}$$

(Advisory Committee on Hazardous Substances, 2007; US EPA, 2000).

The response to a mixture depends on the dose and on the correlation of tolerances. This correlation can vary between −1 and 1. The equation above corresponds to no correlation of tolerances and it is the standard formula for statistical independence (Könemann and Pieters, 1996). If the organisms most sensitive to chemical 1 are also most sensitive to compound 2 then the compounds are completely positively correlated. In case of complete positive correlation ($r = 1$) the effect of the mixture will depend on the most toxic compound in the mixture, that is:

$$\begin{aligned} p_{\mathrm{mix}} &= p_1(d_1) \quad \text{if} \quad p_1(d_1) > p_2(d_2) \\ p_{\mathrm{mix}} &= p_2(d_2) \quad \text{if} \quad p_1(d_1) < p_2(d_2) \end{aligned} \tag{10}$$

In case of complete negative correlation ($r = -1$), the probability of an adverse effect from a mixture of compounds 1 and 2 equal to the sum of the individual responses:

$$p_{\mathrm{mix}} = p_1(d_1) + p_2(d_2) \quad \text{if} \quad p_{\mathrm{mix}} \leqslant 1 \tag{11}$$

In this case the organisms most sensitive to compound 1 is least sensitive to compound 2 and vice versa (ATSDR, 2004; Könemann and Pieters, 1996; US EPA, 2000).

The last equation is the most conservative approach to describe simple dissimilar action and US EPA has recommended it to be used in risk assessment of mixtures of carcinogens. They use the following equation to estimate the risk (unit-less probability that an individual will develop cancer) for the mixture:

$$\mathrm{Risk} = \sum_{i=1}^{n} \mathrm{Risk}_i = \sum_{i=1}^{n} d_i B_i \tag{12}$$

where Risk_i is the risk estimate for the ith compound, d_i is the dose and B_i is the potency parameter for the ith carcinogen (US EPA, 1986). According to US EPA the equation is appropriate when the risks of the individual compounds are less than 0.01 and the sum of the individual risks is less than 0.1 (ATSDR, 2004; US EPA, 1989b, 2000).

In the following we look at an example of a hypothetical mixture of four compounds, I, II, III and IV. The compounds are present in the mixture at concentrations providing the following doses: 1.5, 2.0, 2.5 and 3.0 mg/kg/day. The corresponding responses are derived from the hypothetical dose–response curves in Fig. 2: 0.3, 0.16, 0.11 and 0.

The probability for an adverse effect to arise from the mixture is calculated:

$$p_{mix} = 1 - (1 - 0.3) \times (1 - 0.16) \times (1 - 0.11) \times (1 - 0) = 0.48$$

This is called the "true response" by US EPA (US EPA, 2000).

If we use the more conservative method we get an unadjusted mixture risk (corresponding to complete negative correlation) of:

$$p_{mix} = 0.3 + 0.16 + 0.11 + 0 = 0.57$$

This gives a relative error of:

$$(0.57 - 0.48)/(0.48) = 20\%$$

The results from using the two different approaches give a relative error of 20%. In both cases the risk of an adverse effect arising from the mixture is around 50%.

The response addition is based on the principle that each organism will have a certain level of susceptibility to each compound and the threshold of susceptibility has to be exceeded in order to perform a response. This means that the response addition method cannot estimate a toxic effect from a mixture when the individual compounds in the mixture do not lead to an effect. Based on this assumption EFSA concluded that response addition will rarely if ever be relevant for pesticide residues in food since they generally are found at levels well below their respective toxic levels (EFSA, 2008).

3.7. Interactions

US EPA has suggested the interaction hazard index approach for mixtures consisting of interacting compounds in order to take antagonistic and synergistic interactions into account in the derivation of a hazard index. The interaction-based hazard index uses the weight of evidence (WOE) approach as a quantitative modifier to the hazard index in risk assessments involving interactions of multiple compounds (Mumtaz and Durkin, 1992; Mumtaz et al., 1998; US EPA, 2000). It assumes that binary interactions are the most important and information on binary interactions is used to modify the hazard index using binary weight of evidence (BINWOE). It is also assumed that compounds in a mixture act by similar mechanisms (US EPA, 2000).

There are four important features in the interaction hazard index approach (Seed et al., 1995). Firstly, the interaction mechanism should be well understood. Secondly, the data from other related compounds should be consistent with the proposed mechanism. Thirdly, the toxicological significance of this interaction should be demonstrated and fourthly, the *in vivo* data of the interaction should be available from long-term studies using a route of exposure relevant for humans.

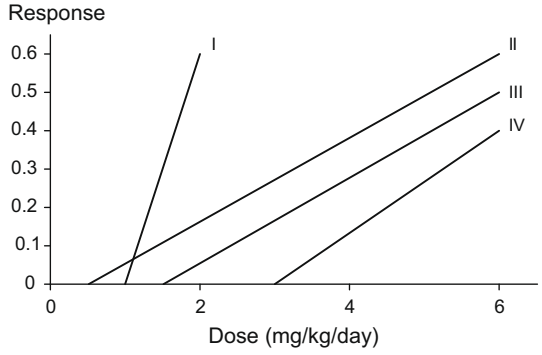

Fig. 2. Hypothetical dose–response curve for the four compounds I, II, III and IV.

In the first steps of the interaction-based hazard index approach the mechanistic understanding and the toxicological significance is connected. This forms the basis of the risk assessment. Thereafter the binary mixtures are grouped in three modifying categories used to alter the rating of the risk assessment. The three modifying categories are duration/sequence of exposure, *in vivo*/*in vitro* and route of exposure.

This classification is used to set up a quantitative interaction matrix by the aid of a set of default weighting factors and many calculations. The calculations include the hazard index and interaction factors for each binary mixture. The normalised site-specific weight of evidence is calculated and used to adjust the hazard index for the uncertainty of interactions. And finally the adjusted hazard index can be evaluated.

The dose-additive hazard index can be modified by using a scaled BINWOE (WOE_N) giving the interaction hazard index, HI_I:

$$HI_I = HI_{ADD}(UF_I)^{WOE_N} \quad (13)$$

where HI_{ADD} is the non-interactive HI based on dose addition and UF_I is the uncertainty factor for the interactions (Mumtaz and Durkin, 1992; US EPA, 2000).

US EPA has pointed out some very important weaknesses of the interaction hazard index approach (US EPA, 2000): There is no guidance for selection of the uncertainty factors for interactions used in the method and the steps in determining the BINWOE are complex. The weighting factors used in the method lack support from empirical assessments of key experimental variables. Further the interaction hazard index approach is supposed to account for (pair wise) interactions, but the method may be too simple in that the interaction information is only represented by the uncertainty factor, which is multiplied with the entire additive hazard index. The magnitude of the interaction is not included in the method. The fact that a qualitative/subjective evaluation of data is used as the basis for quantitative modelling makes this model less applicable.

Neither the approaches for toxicologically similar compounds nor the approach for toxicologically independent compounds presented earlier in the text will accurately predict risks for compounds that exhibit toxicological interactions. The interaction-based hazard index approach introduced by Mumtaz and Durkin (1992) seems to be the only method at present that take toxicological interactions into account. However, this method is complicated to use and it requires a great deal of data, calculations and assumptions concerning the interactions of the compounds. Conolly has stated that one of the greatest dangers in trying to describe mechanisms quantitatively is the use of speculative assumptions about the mechanisms rather than the lack of knowledge as such (Conolly, 2001).

The method described by Mumtaz and Durkin requires an evaluation of data quality for mechanistic information however it does not provide guidance on evaluating interactions data themselves. Borgert et al. (2001) has presented five criteria to evaluate the quality of data and interpretations in studies of chemical mixtures. The criteria are intended to assist the risk assessor in the evaluation of interactions studies for use in risk assessment of chemical mixtures (Borgert et al., 2001). EPA has also pointed out statistical deficiencies in handling and interpretation of data from interaction studies (US EPA, 1988).

The quality of studies and the uncertainty in the interpretation of studies on combined actions of compounds in mixtures is a very important point since it makes the basis for deciding whether there

will be no interaction or interaction between the compounds in the mixture and that again is used for deciding which method to use in the evaluation process.

4. Advantages and disadvantages of the methods

Eight methods for risk assessment of mixtures based on data on single compounds are shown in Table 2. The required data, applicability, assumptions, advantages and disadvantages of each method are summarised.

5. Proposed flow charts for risk assessment of mixtures of chemicals

In 2001 ATSDR published the report "Guidance for the Preparation of an Interaction Profile" including flow charts for a step-by-step procedure for assessing effects (including carcinogenicity) (ATSDR, 2001). These flow charts were revised in the report "Guidance Manual for the Assessment of Joint Toxic Action of Chemical Mixtures" in 2004 (ATSDR, 2004). The flow charts are shown in Fig. 3 and 4. The two guidelines are especially concerned with how exposure to chemical mixtures at hazardous waste sites affects public health.

The two flow charts for non-carcinogenic and carcinogenic effects, respectively, are similar. In the first steps it is considered which information is available on the mixture:—an interaction profile?—A toxicological profile?—A minimal risk level (MRL)?—Other health guideline values? If no such information is available the single compounds approach should be used. ATSDR recommends using PBPK/PD models, if available, to predict the potential for interactions or effects from the mixture. The hazard index method is recommended to be used for screening for non-cancer hazards

Table 2
Advantages and disadvantages of the methods. Overview of eight methods for risk assessment of mixtures based on data on single compounds.

Procedure	Required data	Applicability	Assumptions	Advantages	Disadvantages
Hazard index (HI)	Maximum acceptable level for each compound (e.g. RfD or ADI). Exposure data	Compounds having adequate dose–response data, as well as exposure data at low levels. HI is also used for compounds with similar target organ	Simple similar action—toxicological similarity	Transparent, understandable, relates directly to long-used and well-understood measure of acceptable risk e.g. RfD or ADI	RfD (or ADI) is not an appropriate point of departure—it involves an UF (subjective). If the UFs are not the same for all compounds in mixture this will affect the result
Relative potency factor (RPF)	Toxicity data for each compound, dose–response data for the index compound. Exposure data	Some data available—restricted by similarity and to specific conditions	Simple similar action—toxicological similarity, but for specific conditions (end point, route, duration). It is supposed to account for mixtures with different mode of action	Transparent, understandable, relates directly to real exposure and toxicity data	Complicated to use. Relies on the availability of dose–response data for the index compound
Toxicity equivalency factor (TEF)	Toxicity data for each compound, dose–response data for the index compound. Exposure data	Data seldom available. A TEF value is applied to all end points; therefore method restricted to mixtures of compounds with strong similarity—few chemical classes will qualify	Simple similar action—toxicological similarity across endpoints	Transparent, understandable, relates directly to real exposure and toxicity data	In some cases complicated to use. Relies on the availability of dose–response data for the index compound
Margin of exposure for mixtures (MOE_T)	Point of departure (e.g. NOAEL or BMD_{10}). Exposure data.	Compounds having adequate dose–response data, as well as exposure	Simple similar action—toxicological similarity	Relates directly to real exposure and toxicity data—not based on a policy driven parameter like ADI	No criteria for defining the magnitude for an acceptable MOE_T
Point of departure index (PODI)	Point of departure (e.g. NOAEL or BMD_{10}). Exposure data.	Compounds having adequate dose–response data, as well as exposure	Simple similar action—toxicological similarity	Relates directly to real exposure and toxicity data—not based on a policy driven parameter like ADI	No criteria for defining the magnitude for an acceptable PODI
Cumulative risk index (CRI)	Point of departure (e.g. NOAEL or BMD_{10}) or maximum acceptable level for each compound (e.g. RfD or ADI). Exposure data	Compounds having adequate dose–response data, as well as exposure	Simple similar action—toxicological similarity	Combines MOEs for chemicals with different UFs	RfD (or ADI) is not an appropriate POD—it involves an UF (subjective). Not as transparent and understandable as the HI. Complex calculations
Response addition	Toxicity data measured as a fraction of responding. Good dose–response data. Exposure data	Data seldom if ever available	Simple dissimilar action—Bliss independence	Mathematically easy	Data applicability is low
Interaction hazard index (HI_I)	Maximum acceptable level for each compound, a number of weighting factors. Exposure data	Data seldom available: limited data on interactions	Binary interactions are most important. Magnitude of interaction depends on proportions of the compounds—ot dose dependent	Supposed to account for interactions (binary)	Complex to determine the BINWOE. Weighting factors are not supported by experimental data. No guidance for selecting UFs for interactions and interactions are only represented by these

from potential additivity of the compounds in the mixture (Fig. 3). In case of carcinogenic effects the compounds in the mixture are summed to screen for hazards from potential additivity (Fig. 4). The potential impact of interactions on non-cancer and cancer health effects is evaluated by a weight of evidence method.

In 2002 a committee of the Health Council of The Netherlands published an advisory report which included a flow chart for safety evaluation of combined exposures using the so-called "top n" and "pseudo top n" approaches in which the most toxic compounds in the mixture are selected and assessed for toxicity, see Fig. 5 (Feron et al., 2004; Health Council of the Netherlands, 2002). This approach is especially suitable for the toxicological evaluation of workplace and hazardous waste site atmospheres. The report recommends use of Mumtaz–Durkin weight of evidence method for prioritisation of the combined exposures according to their potential risk (Feron et al., 2004). The intention is that the flow chart should be walked through in its entirety in order to select the best method. In the upper part of Fig. 5 it is decided whether the data on toxicity is available on a mixture or on single compounds, that is to say corresponding with the upper part of the flow chart suggested by US EPA shown in Fig. 1. The lower part of Fig. 5 is intended for specified mixtures of compounds concentrating on pairs of compounds in the mixture. The first step is to consider whether the compounds in the mixture act by similar action or dissimilar action and thereafter consider whether interactions occur or not. If the compounds act by similar action without interaction the scheme

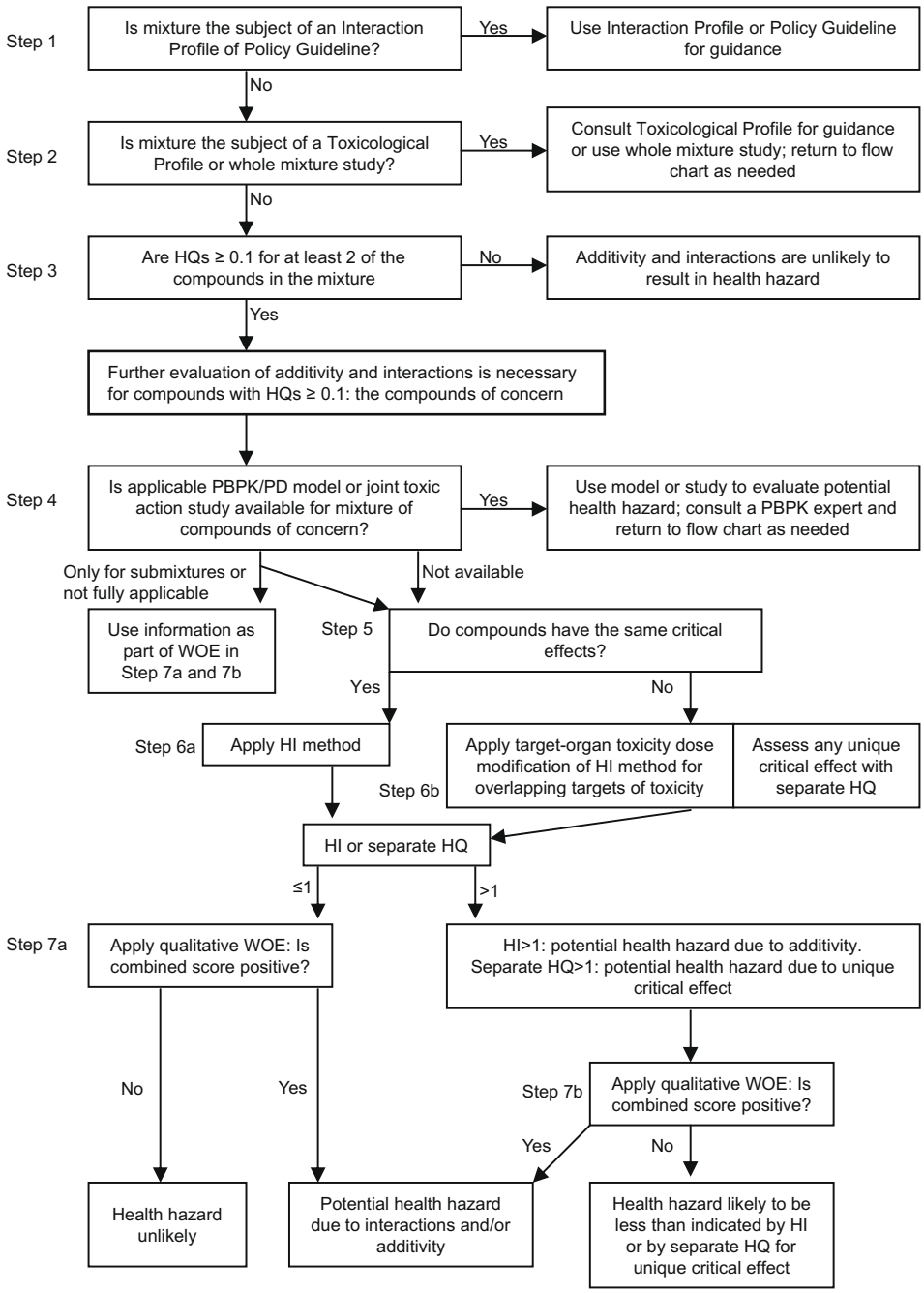

Fig. 3. Flow chart proposed by ATSDR for a step-by-step procedure for assessment of combined action of mixtures of non-carcinogenic chemicals. Modified from (ATSDR, 2004).

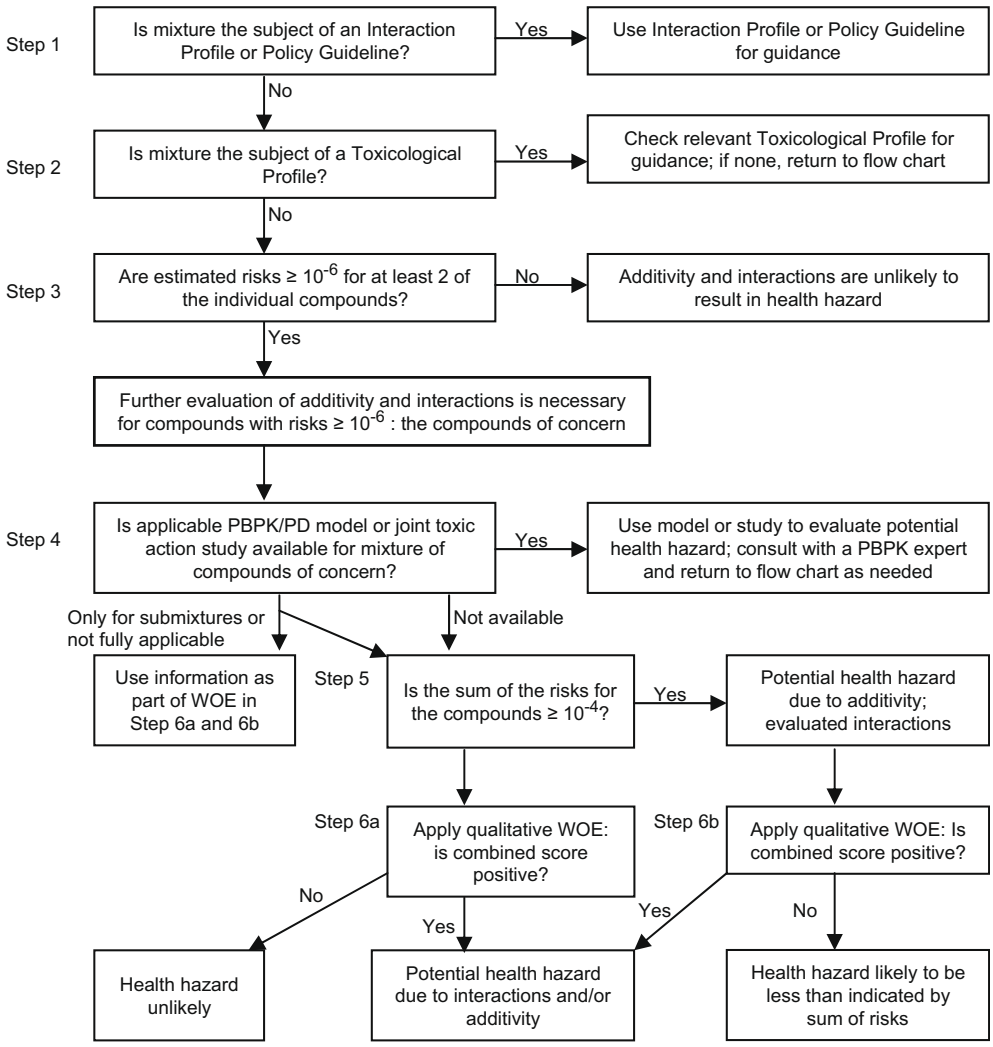

Fig. 4. Flow chart proposed by ATSDR for a step-by-step procedure for assessment of combined action of mixtures of carcinogenic chemicals. Modified from (ATSDR, 2004).

recommends dose addition and toxicity equivalency factor for assessing the joint toxicity. If the compounds act by dissimilar action without interaction, response addition should be used.

Use of a hazard index is also recommended for mixtures of compounds without interactions: in the case of similar action the hazard quotients are added and in the case of dissimilar action the highest hazard quotient is chosen even though the latter is not following the theory stringent (Health Council of the Netherlands, 2002). In cases with similar action with interactions or dissimilar action with interactions it is necessary to examine whether the data available can be used for a quantitative conclusion; the Committee concluded that it is not able to give universal criteria for this.

The flow chart in Fig. 6 is an expansion of the method proposed by US EPA in Fig. 1: one method has been added to the single compound-based methods. In the case of a mixture of compounds having different modes of action but causing the same toxic effect it is suggested to combine the response and dose addition methods in what they call the cumulative relative potency factors (CRPF). The compounds in the mixture which have the same mode of action are put together in subclasses. Then the RPF can be used to estimate the risk of each subclass. These subclasses are expected to act independently of each other (that is simple dissimilar action) and therefore the calculated RPFs can be added to give the total mixture risk (Teuschler, 2007).

The Norwegian Scientific Committee for Food Safety has suggested a step-wise case-by-case evaluation of the toxicological data on the compounds and the exposure data, see Fig. 7 (Norwegian Scientific Committee for Food Safety, 2008). They assume that if exposure to compounds is below the individual NOAELs and they act by similar mode of action then no more than an additive effect is expected. If exposure to compounds is above the NOAELs, interaction may occur. Interactions are taken into account in the two boxes with dotted lines in the figure.

On the left hand side in Fig. 7, it should be considered whether the compounds act on the same target organ, whether the compounds in the mixture act by the same mode of action and finally in the refinement it should be considered whether the compounds act by the same mechanism of action. If data are available and indicate that the compounds act by the same mechanism of action the toxicity equivalency factor method should be used, otherwise (i.e. the compounds act by the same mode of action) the hazard index, the margin of safety or the point of departure index method should be used. On the right hand side it should be considered whether the compounds in the mixture act by simple dissimilar action.

In 2002, the Danish Veterinary and Food Administration suggested to use the flow chart shown in Fig. 8 for risk assessment of pesticide mixtures found as residues in food (Reffstrup, 2002). The risk assessment must be done on a case-by-case evaluation in which the available chemical and toxicological data on the

pesticides are evaluated in a weight of evidence process. Then the hazard index with the ADI as the acceptable level in the denominator should be used. However, in cases where the weight of evidence points out that the compounds in the mixture share a common mechanism the toxicity equivalency factor should be used instead of the hazard index. This concerns for instance the organophosphorus pesticides, the chloroacetanilides, the dithiocarbamates and the thiocarbamates. This is a rough and pragmatic method. In Denmark, we have used this method for evaluating mixtures of pesticides in crops since 2002. In most cases, the hazard index was used with ADI as the acceptable level. In only a few cases the ADI were exceeded and this was often due to only one compound in the mixture.

The Scientific Panel on Plant Protection Products and their Residues (PPR Panel) has recommended the flow chart shown in Fig. 9 mentioning what they consider the most useful methods (EFSA,

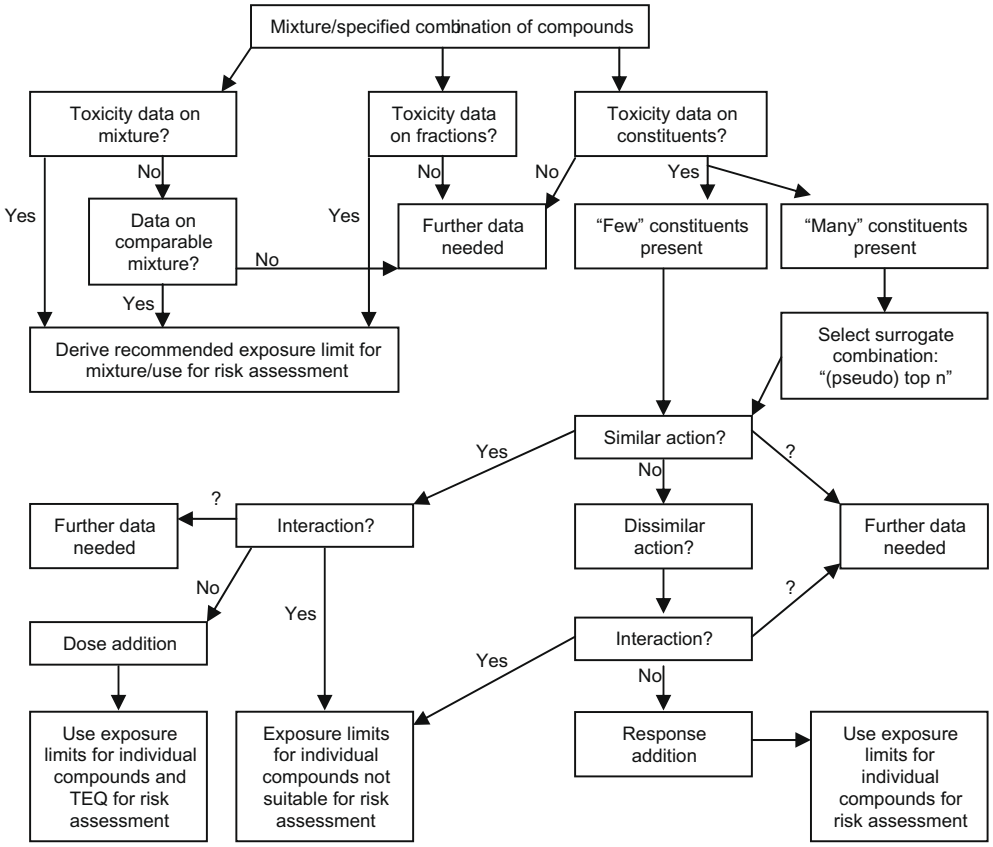

Fig. 5. Flow chart suggested by Health Council of The Netherlands for assessing combined actions of two compounds. Modified from (Feron et al., 2004; Health Council of the Netherlands, 2002).

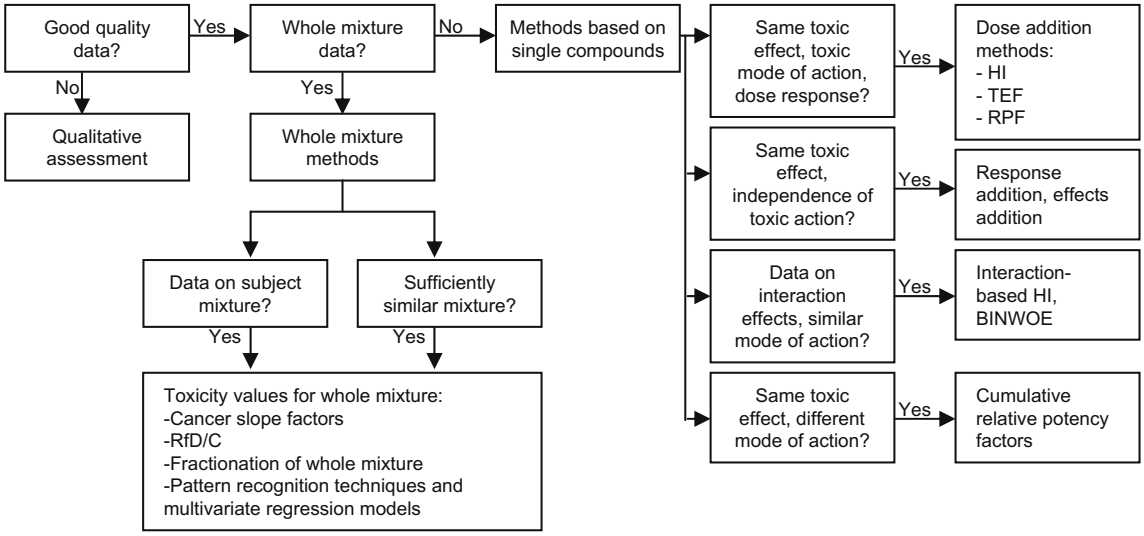

Fig. 6. Flow chart for assessment of combined actions of chemical mixtures. Adapted from (Teuschler, 2007).

2008). Going from the top and down through the flow chart there are an increasing level of complexity and refinement: the hazard index, the reference point index, the relative potency factor method and physiologically based toxicokinetic modelling.

An overview of the required data and assumptions for these eight flow charts are shown in Table 3 as well as the advantages and disadvantages of the different strategies.

6. Defined cumulative assessment groups/common mechanism groups for pesticides

As mentioned earlier the Food Quality Protection Act of 1996 requires US EPA to take cumulative effects into account in the risk assessment of mixtures of pesticide residues in food. On that background US EPA has up till now evaluated data on four common mechanism groups (CMGs): organophosphates (US EPA, 2006c), *N*-methyl carbamates (US EPA, 2007), triazines (US EPA, 2006d) and chloroacetanilides (US EPA, 2006b):

- Evaluation of the group of organophosphorus pesticides was prioritized as they are expected to be one of the classes of pesticides that pose the greatest risk. In the group of organophosphorus compounds methamidophos was selected as the index chemical to standardize the toxic potencies of the compounds. US EPA used the relative potency factor method to determine the cumulative risk. Benchmark dose estimates at a level of 10% brain acetylcholinesterase inhibition in studies on female rats was used to determine relative potencies for the organophosphorus compounds (US EPA, 2006c).
- US EPA has defined a group of chloroacetanilides consisting of acetochlor, alachlor and butachlor based on the common mode of action that cause nasal olfactory epithelium tumours in rats. Due to knowledge on the capacity to induce adverse effects by a common mechanism of toxicity this group of pesticides was prioritized. Alachlor was selected as the index chemical. Butachlor was excluded from the risk assessment since there was no registered use of the compound in US. The point of departure has been calculated for each compound and the margin of exposure for the cumulative exposure using relative potency factor (US EPA, 2006b).
- Six triazines (atrazine, propazine, simazine and three of their metabolites) have been defined as a group based on a common mechanism causing neuroendocrine and endocrine-related developmental, reproductive and carcinogenic effects. The compounds were included in the cumulative assessment group based on use patterns and the likelihood of exposure. The pri-

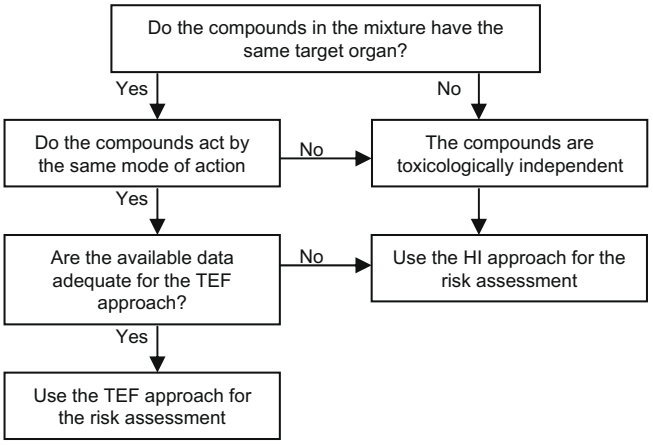

Fig. 8. Flow chart of the risk assessment approach for pesticide mixtures found in food (Reffstrup, 2002).

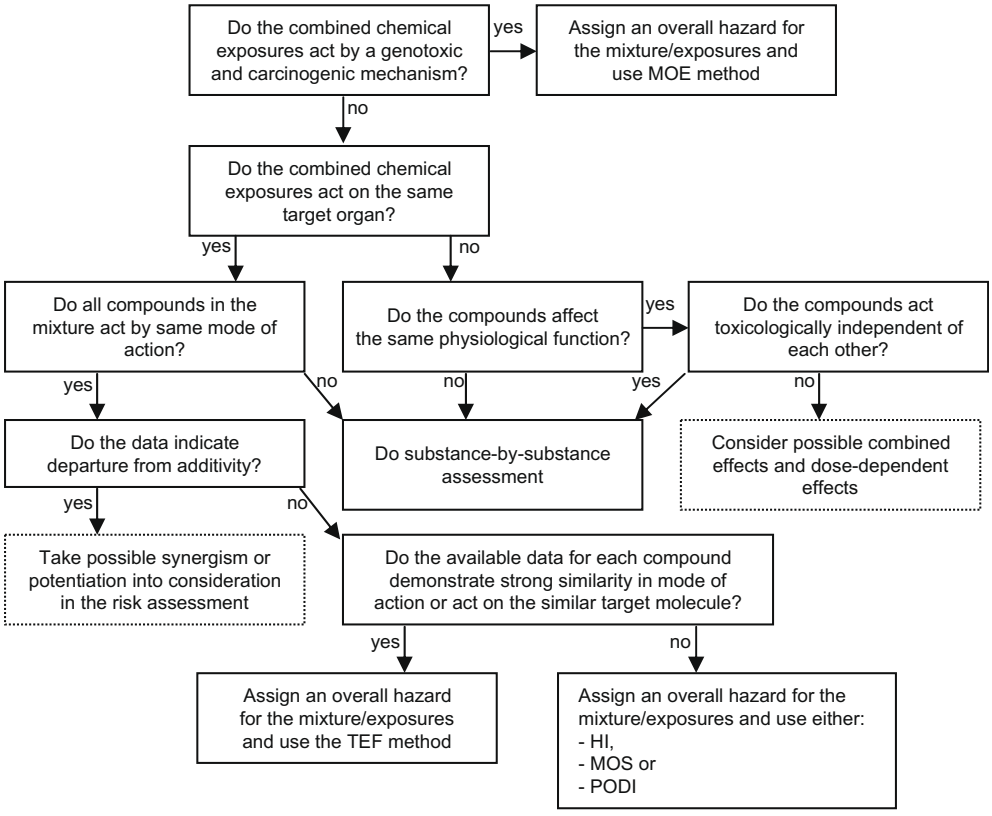

Fig. 7. Flow chart proposed by Norwegian Scientific Committee for Food Safety. Adapted from (Norwegian Scientific Committee for Food Safety, 2008).

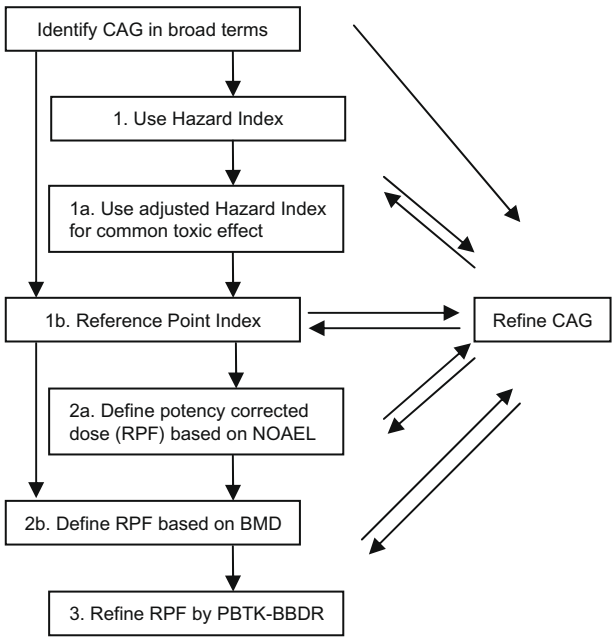

Fig. 9. Tiered hazard assessment proposed by EFSA. Modified from (EFSA, 2008). BBDR = biologically based dose response modelling.

mary exposure route for these triazines is drinking water. Propazine, simazine and the three metabolites in the group are considered to be equivalent in toxicity to atrazine, per se, based on the evaluation of endocrine-related data on the triazines demonstrating either equal potency or potency less than atrazine (US EPA, 2006d).

- The *N*-methyl carbamate pesticides were found to share a common mechanism of action. The ten carbamates all inhibit acetylcholinesterase. In this group, oxamyl was selected as the index chemical. Benchmark dose estimates at a level of 10% brain acetylcholinesterase inhibition was used to estimate the relative potencies for the compounds (US EPA, 2007).

EFSA has evaluated data on 25 compounds with a triazole-ring as a cumulative assessment group. From the literature they found that concerning acute toxicity seven of the compounds were producing crania facial malformation via a common mechanism of toxicity. Further, for chronic assessment 11 compounds were found to cause hepatotoxicity as a common effect (EFSA, 2009).

7. Newer approaches in the risk assessment of mixtures

In the area of pharmacology, physiologically based pharmacokinetic/pharmacodynamic (PBPK/PD) modelling is used as a technique for prediction of the absorption, distribution, metabolism and excretion (ADME) of a compound in humans and other species. The development of PBPK models arose from the need to relate doses of a chemical (pharmaceutical) to an animal or human with the actual internal concentration at the target site.

In the area of pharmacology Teorell used physiological considerations as the basis for a pharmacokinetic description (Rowland et al., 2004). However, his work was done in the 1930s and the computational resources necessary for solving the differential equations were not available at that time. Therefore the equations were replaced with simpler ones and for many years these simple pharmacokinetic approaches continued to be in use even after the computational resources became available.

In the area of toxicology several scientists have used the term physiologically based toxicokinetic/toxicodynamic (PBTK/TD); however the principles of the models are the same as for PBPK/PD models. Several scientists, organizations and workshops have recommended using PBTK/TD modelling as a tool in the risk assessment of chemical mixtures. The European Food Safety Authority (EFSA) organised a workshop on cumulative risk assessment of pesticides which strongly encouraged the introduction of PBTK/TD models in the cumulative risk assessment (EFSA, 2007). In the EFSA opinion concerning risk assessment of pesticide mixtures PBTK modelling is mentioned as the most refined model (EFSA, 2008).

Simmons (1996) mentioned that there is a clear need for the development of PBTK/TD models for mixtures. And this development should be performed for the same mixtures by several laboratories in order to determine inter-laboratory consistency and variability. Scientists should also focus on extrapolation across species and development of human PBTK models for mixtures (Simmons, 1996).

The US National Research Council has provided "guidance on new directions in toxicity testing, incorporating new technologies such as genomics and computational systems biology into a new vision for toxicity testing" (Andersen and Krewski, 2009). They recommend further development and use of *in vitro* methods instead of *in vivo* studies as well as improvement and use of computational methods to extrapolate from *in vitro* to *in vivo* systems to predict tissue and blood concentrations in humans after exposure to chemicals in specific circumstances. PBTK models are a good answer to this.

Teuschler pointed out the necessity to develop PBPK models for common mixtures of concern in order to use such models routinely in future risk assessments (Teuschler, 2007). As a helping tool for risk assessors and PBPK modellers US EPA has published a report describing different aspects of use and evaluation of PBPK models in risk assessment (US EPA, 2006a). Further, some basic considerations for evaluation of PBTK models intended for risk assessment are nicely described by Chiu et al. (2007).

In a physiologically based toxicokinetic model the animal or man is described as a set of tissue compartments which is combined by mathematical descriptions of biological tissues and physiological processes in the body. Thereby it is possible to quantitatively simulate the absorption, distribution, metabolism and excretion of chemicals.

A PBTK model can predict tissue concentrations and true toxicokinetic parameter values under a variety of conditions. It is useful to predict internal dose levels for hypothetical exposure regimens which will reduce the uncertainty in risk assessment. It is also possible to predict overload of toxicokinetic pathways and to do high-dose to low-dose extrapolation. The models are mathematically complex and require extensive data on disposition of the chemical and physiological parameters-related data.

PBTK models are increasingly being used in deriving RfDs for use in risk assessment. In the absence of adequate human data to assess the risk for humans directly, the RfD is typically derived from animal data. Uncertainty factors are then used to fill in the data gaps between the species as well as the intra-species variability. When a PBTK model is developed and tested adequately, it will provide a more scientifically supportable result than the use of uncertainty factors, will give (DeWoskin and Thompson, 2008).

Exposure to multiple chemicals may cause alterations in the toxicokinetics of the individual chemicals resulting in a change in the predicted toxicity based on the summation of the effects of the single compounds. As described earlier, toxicokinetic interactions occur as a result of one compound altering the absorption, distribution, metabolism or elimination of other compounds. They

Table 3
Overview of the required data, assumptions, advantages and disadvantages for the eight flow charts/assessment strategies shown in this paper.

Flow chart	Required data	Methods suggested	Assumptions	Advantages	Disadvantages
Fig. 1. Flow chart of the risk assessment approach used by US EPA (US EPA, 2000). Developed for environmental contaminant mixtures	Either data on mixture or on single compounds	Mixture: RfD/C, cancer slope factor, comparative potency, environmental transformation Single compounds: HI, RPF/TEF, response addition, interaction based HI	For single compound approaches (except interaction based HI): no or insignificant interaction effects at low dose levels. In some cases the requirement of similar mode of action is relaxed to require only same target organ	Flow chart is straight forward. Very broad flow chart that covers many approaches/ situations and can therefore be used in many cases. Allows risk assessment based on whole mixtures as well as single compounds with a wide range of methods suggested	Comprehensiveness makes the flow chart complicated. Some of the methods are complicated and requires many data. In case of interaction no universal criteria for deciding whether the data permits a quantitative conclusion to be drawn
Fig. 3. Flow chart proposed by ATSDR for assessment of non-carcinogenic chemicals from hazardous waste sites (ATSDR, 2004)	Either data on mixture or on single compounds	Mixture: use of interaction profile (if available) incl. MRL. Single compounds: HI, PBTK/PD, BIN-WOE, target organ toxicity dose (TTD) modification of HI (for compounds not having same critical effect but have overlapping target organ)	The mechanism of toxicity is well enough known to assume which compounds will be additive and which will not (McCarty and Borgert, 2006). If two or more compounds have HQ $\geqslant 0.1$ the mixture requires more evaluation of additivity and interactions	Flow chart is comprehensive and allows use of different approaches including newer modelling techniques. Depending on the available data and exposure level the risk assessment can stop after only a few steps	Criteria for judging whether the compounds act additively or not are not defined or validated (McCarty and Borgert, 2006). Comprehensiveness makes the flow chart complicated. Some of the methods are complicated and requires many data
Fig. 4. Flow chart proposed by ATSDR for assessment of carcinogenic chemicals from hazardous waste sites (ATSDR, 2004)	Either data on mixture or on single compounds	Mixture: use of interaction profile (if available). Single compounds: cancer risk estimates (cancer slope factors times exposure of the population of concern)	Cancer is regarded as same critical effect not considering the tumour type or location. The mechanism of toxicity is well enough known to assume which compounds will be additive and which will not (McCarty and Borgert, 2006). If two or more compounds have estimated risk $\geqslant 10^{-6}$ the mixture requires more evaluation of additivity and interactions	Flow chart easily understandable although it requires many data. Depending on the available data and exposure level the risk assessment can stop after only a few steps	Criteria for judging whether the compounds act additively or not are not defined or validated (McCarty and Borgert, 2006). Some of the methods are complicated and requires many data
Fig. 5. Flow chart suggested by Health Council of The Netherlands for assessing risk from contaminated soil, but the Committee recommends use in e.g. consumption of contaminated food or inhalation of polluted air (Health Council of the Netherlands, 2002; Feron et al., 2004)	Either data on mixture or on single compounds	Mixture: recommended exposure limits for mixture. Single compounds: TEQ, exposure limits for individual compounds. HI (not shown in flow chart) is also recommended in the report for similar and dissimilar acting compounds even though the latter is not following the theory stringent	Assesses the combined effect per pair in the mixture. Concerning exposure limits: harmfulness only manifests itself above a certain concentration	Flow chart straight forward. Broad flow chart that covers many approaches/situations and can therefore be used in many cases. Allows risk assessment based on whole mixtures as well as single compounds	Even though flow chart is broad it does not directly concretize many methods (e.g. method(s) for dissimilar acting compounds). The Committee concludes that in case of interaction there are no universal criteria for deciding whether the data permits a quantitative conclusion to be drawn
Fig. 6. Flow chart for assessment of combined actions from environmental contaminant mixtures (Teuschler, 2007)	Either data on mixture or on single compounds	Mixture: RfD/C, cancer slope factor, fractionation of whole mixture, pattern recognition techniques and multivariate regression Single compounds: HI, TEF, RPF, response addition, interaction based HI, BIN-WOE, cumulative relative potency factors	Departure from additivity is more likely at "high" concentrations than at "low"	Flow chart is straight forward – even though this is not always the case for the answers (Teuschler, 2007). Very broad flow chart that covers many approaches/situations and can therefore be used in many cases. Allows risk assessment based on whole mixtures as well as single compounds with a wide range of methods suggested	Comprehensiveness makes the flow chart complicated. Some of the methods are complicated and requires many data. Missing criteria to assess whether mixtures are sufficiently similar (Teuschler, 2007). In case of interaction data for a group of compounds with different modes of action there is no quantitative method

(*continued on next page*)

Table 3 (*continued*)

Flow chart	Required data	Methods suggested	Assumptions	Advantages	Disadvantages
Fig. 7. Flow chart proposed by Norwegian Scientific Committee for Food Safety for risk assessment of chemical mixtures in food, feed and cosmetics (Norwegian Scientific Committee for Food Safety, 2008)	Data on single compounds	MOE, HI, MOS, PODI, TEF, response addition	Uses the term "same mode of action" which does not require knowledge about precise molecular mechanism, but dose addition may be used anyway. No more than additive effect is expected for compounds at concentrations below individual NOAELs; above NOAEL interactions may occur	Flow chart straight forward. Can be used for many types of compounds/situations. The first step sorts out genotoxic and carcinogenic chemicals	Does not suggest methods in case of data on mixtures, if compounds act independently and in case of interactions (but report suggests: case-by-case basis – ideally based on test on the mixture). Flow chart introduces to consider whether the compounds affect the same physiological function but do not explain what is meant by that and how to deal with it
Fig. 8. Flow chart for risk assessment of pesticide mixtures found as residues in food (Reffstrup, 2002)	Data on single compounds	HI, TEF	No more than additive effect is expected since pesticides are present in food at concentrations below individual NOAELs, and available evidence supports the view that significant toxic interactions are less likely to occur at these levels than at higher	Very simple to use – few and simple steps in the flow chart. Simplified to cover pesticide residues in food. Valuable as a first step in the risk assessment	Pragmatic. Deals only with compounds present at low concentrations. Not scientific comprehensive, e.g. do not take interactions and dissimilar actions into account. Do not deal with data on whole mixtures (however seldom available for mixtures of pesticides)
Fig. 9. Flow chart proposed by EFSA for risk assessment of pesticide mixtures found as residues in food (EFSA, 2008)	Data on single compounds	HI, reference point index (PODI), RPF, PBTK-BBDR	No more than additive effect (similar action) is expected since pesticides are present in food at concentrations below individual NOAELs, and available evidence supports the view that significant toxic interactions are less likely to occur at these levels than at higher	Flow chart straight forward. Simplified to cover pesticide residues in food	Deals only with compounds present at low concentrations. Do not take interactions and dissimilar actions into account. Do not deal with data on whole mixtures (however seldom available for mixtures of pesticides) Some of the methods are complicated and requires many data

may affect the relationship between the administered dose and the dose delivered to the target site (Krishnan et al., 1994, 2002).

The PBTK model can be used to investigate hypotheses regarding mechanisms of interaction between chemicals and to define the doses at which interactions become significant (the interaction threshold). However, predictions of such thresholds should be validated with data from experiments (Simmons, 1996). For example, a PBTK model can make it possible to analyse the competition for an enzyme or a transport protein. A PBTK model describing interactions consists of sets of identical equations, one set for each chemical as well as an equation that specifically accounts for the interactions (e.g., competitive inhibition for metabolism in liver or induction of hepatic metabolism) (ATSDR, 2001).

In the risk assessment the PBTK models could be even more useful if the tissue dose metrics from the PBTK models are combined with toxicodynamic models which would make it possible to better characterise the dose–response relationships. The output of a PBTK model is linked to a toxicodynamic model by mathematical description of the hypothesis of how compounds contribute in the initiation of cellular changes leading to the toxic responses. Such a model is sometimes called a biologically based dose–response model (BBDR) (EFSA, 2008; US EPA, 2006a). As mentioned earlier interactions can also take place at the toxicodynamic level and when the PBTK models are expanded by a toxicodynamic part, the model could make it possible to predict deviations from additivity at the toxicodynamic level.

A PBTK model for the two organophosphorus pesticides chlorpyrifos and parathion and their metabolites chlorpyrifos-oxon and paraoxon, respectively, were developed by El-Masri and coworkers in order to simulate the interaction threshold for the joint toxicity of the two pesticides in rats (El-Masri et al., 2004). A schematic overview of the model is shown in Fig. 10. At first a model for each of the parent compounds was developed in order to estimate the blood concentrations of their metabolites. Then the output from these models i.e. the concentrations of metabolite in blood was linked to a sub-model describing the kinetic of acetylcholinesterase. The overall model describes the interactions between the pesticides at the P450 enzymatic bio-activation site and at the acetylcholinesterase binding sites. The simulations showed an interaction threshold (at oral dose: 0.08 mg/kg of each compound) below which additivity was shown. Above this threshold it was found that antagonism by enzymatic competitive inhibition is the mode of interaction.

The steps in developing a PBTK model for estimating tissue dose metrics for use in chemical risk assessment is as follows (see also Fig. 11) (Andersen, 2003; Clewell and Clewell, 2008; US EPA, 2006a):

(1) Identify toxic effects in animals (and humans) and determine the critical effects.
(2) Search the literature and organise available data in order to determine the mode of action, metabolism, as well as physiological constants for the relevant animal.
(3) Suggest relationships between response and tissue dose.
(4) Model formulation: develop a PBTK model to estimate the tissue dose metric at various doses.

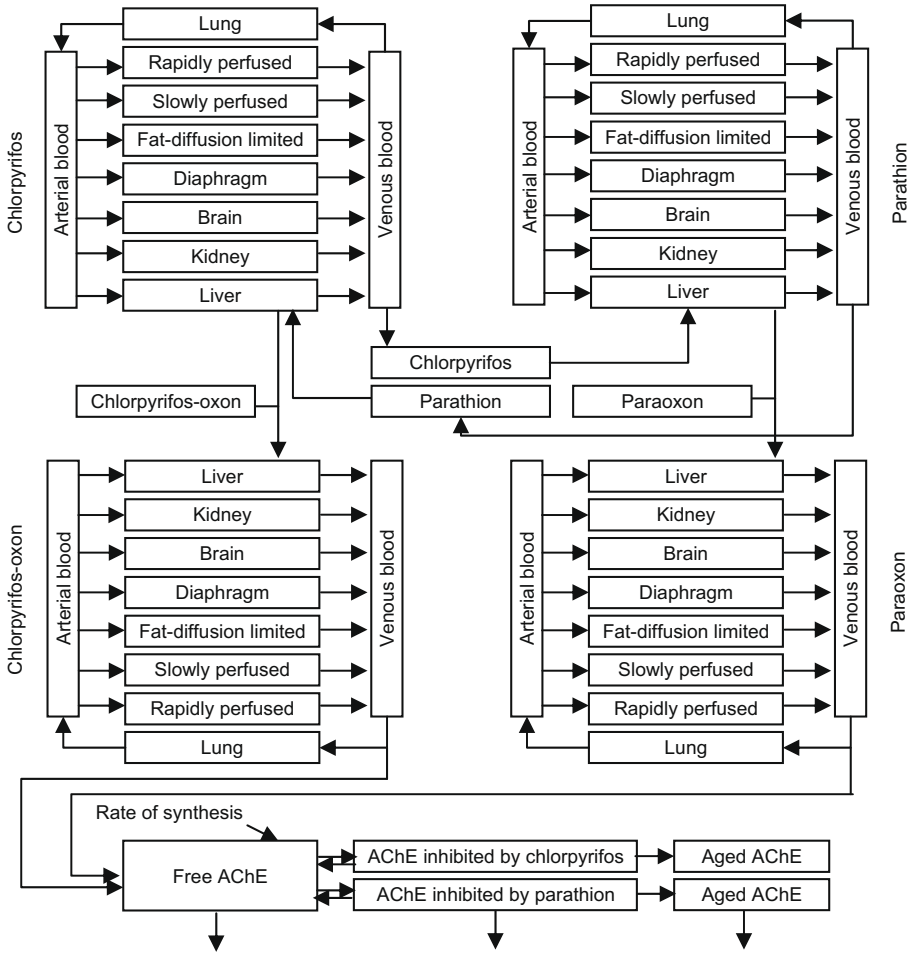

Fig. 10. Schematic overview of a PBTK model for the two pesticides chlorpyrifos and parathion and their metabolites chlorpyrifos-oxon and paraoxon, respectively. The model consists of five sub-models, one for each parent compound and metabolite, as well as one sub-model describing the kinetic of acetylcholinesterase (AChE) linked to the two sub-models for the metabolites. Adapted from (El-Masri et al., 2004).

(5) Run the model.
(6) Compare output from the model-simulation with available experimental data. If the result from the simulation deviates from the data go to point (7) otherwise go to point (9).
(7) Refine the model.
(8) Repeat point (5) and (6).
(9) Application in risk assessment.

Before using the model in risk assessment the model should be evaluated. The purpose of this is to assess the available toxicokinetic and dose–response data of the chemical-biological system and also to depict the uncertainty associated with the parameter values. Further, in the context of risk assessment the suitability and the applicability of the model for regulatory purposes should be assessed (US EPA, 2006a). Model evaluation consist of validation and verification, that is whether the model is correctly build and whether it is the right model, respectively (Balci, 1997; US EPA, 2006a).

When a model has been built and evaluated in for instance rats the model is ready for extrapolation to other species including humans. The steps in developing a PBTK model for interspecies extrapolation is as follows: (1) the model is built for the appropriate species (e.g. rats), (2) the a priori predictions are compared with experimental data and the structure and the parameters in the model are evaluated. If necessary the parameters may be adjusted. (3) The species-specific or allometrically scaled physiological parameters should be replaced by appropriate estimates for the species of interest (e.g. humans) (US EPA, 2006a).

Haddad et al. have shown how estimates from PBTK models can be used in the risk assessment. They used the PBTK model approach to account for interactions in occupational inhalation exposure of mixtures of five volatile organic chemicals (Haddad et al., 2001). This approach is similar to the one proposed by the same group for calculating biological hazard index for chemical mixtures to be used in biological monitoring of worker exposure (Haddad et al., 1999). The interaction-based hazard index for systemic toxicant mixtures was calculated from target tissue dose levels in a similar way as the hazard index in Section 3.3:

$$HI_I = \sum_{i=1}^{n} \frac{TM_i}{TR_i} \quad (14)$$

where TR_i and TM_i are estimates of tissue dose levels derived from PBTK models. TR_i is the tissue dose levels calculated (by PBTK models) based on guideline values of individual compounds in the mixture (in this case they use threshold limit values; but as the background equation just requires the "maximum acceptable level" ADI or RfD may also be used). TM_i is the estimated tissue dose levels of each compound in the mixture during human exposure calculated in PBTK models which take interactions into account. In cases were the compounds in the mixture act by different mechanisms or

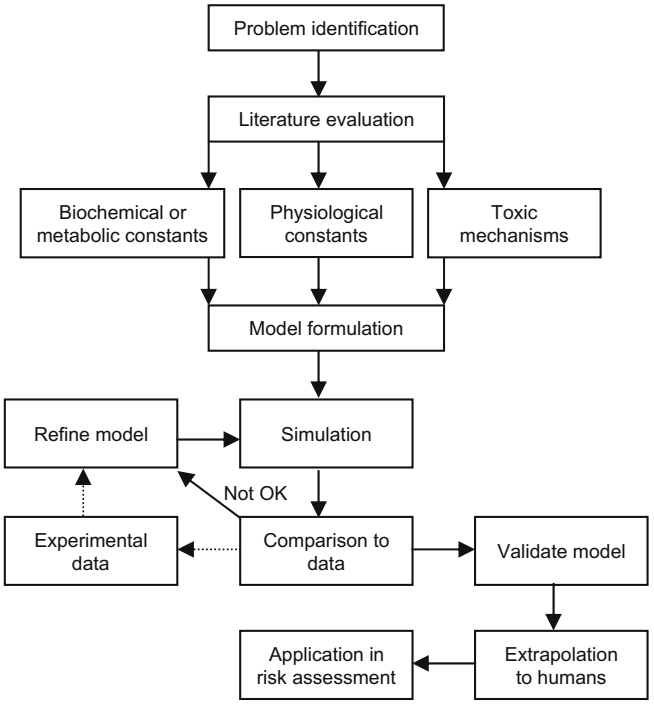

Fig. 11. Flow chart for development of a PBTK model. Modified from (Clewell and Clewell, 2008; US EPA, 2006).

affect different target organs, the interaction-based hazard index should be calculated for each end point.

The same group of scientists suggested a similar approach for mixtures of carcinogenic compounds in that they revised the following equation for calculation of the carcinogenic risk related to mixture exposure (CRM):

$$\mathrm{CRM} = \sum_{i=1}^{n} (E \times q_i^*) \tag{15}$$

where q^*_i is the carcinogenic potential of compound i expressed as risk per unit dose.

Rewriting this equation gives

$$\mathrm{CRM} = \sum_{i=1}^{n} (\mathrm{TM}_i \times q^*_{\mathrm{tt}} i) \tag{16}$$

where $q^*_{\mathrm{tt}} i$ is the tissue dose based unit risk for each carcinogenic compound in the mixture and this level is estimated in PBTK models for the individual compounds in the mixture. TM_i is defined above.

Overall, development of PBTK models for the most common chemical mixtures of concern to be used routinely would be of great importance in the future risk assessment. Validation of the models and development of principles and guidance for good modelling practice (Loizou et al., 2008) as well as statistical research to support model assumptions is needed. Teuschler has specified the statistical research to "include testing for similar shapes of component dose–response curves, determining whether additivity assumptions are applicable or not for describing mixture risk, and using algorithms to form groups of similar components or similar mixtures" (Teuschler, 2007).

In addition, developments in the area of toxicogenomics have also been suggested as a way of increasing our knowledge of mechanism of toxicity in order to better understand and improve the approaches for risk assessment of combined actions of chemicals (Andersen and Krewski, 2009; El-Masri, 2007; Groten et al., 2001).

8. Conclusion

Of the various approaches for risk assessment of mixtures of chemicals discussed in this paper, the whole mixture approaches would be the ideal choice for assessment of pesticide residues in food. However, they are normally not applicable since they require a large number of experimental data that are rarely available. This leaves the single compound approaches as the more realistic ones.

In the risk assessment of multiple residues in food, the individual compounds will be considered for possible candidates in one (or more) cumulative assessment groups. When adequate data are available a common mechanism group should be established. The cumulative risk assessment of this group will then be performed assuming simple similar action using preferably the PODI, but in practice the HI based on the reference value i.e. ADI/RfD would normally be sufficient. Sometimes a refinement i.e. using the NOAEL for the relevant toxicological effect is required as the reference value can be based on a critical toxicological effect different from the CAG based effect.

Where more than one common mechanism group based on simple similar actions is identified, they should be assessed separately as indicated above. In addition, the potential for interactions between the groups (or single compounds) have to be considered. If interaction between the groups/compounds can be ruled out, simple dissimilar action can be anticipated, and the effect of the mixture should be assessed by response addition. However, it is a common perception that at very low doses, where none of the compounds in the mixture have any toxic effect, no adverse effect of the mixture will be anticipated as well.

In many cases it can be predicted that evaluators will tend to use very pragmatic approaches, such as assuming that all compounds in the mixture show simple similar actions, and thus use HI or PODI, such evaluations would be more convincing if lack of interaction between the compounds at the actual dose level had been demonstrated.

Therefore, a crucial point in the assessment is whether there is interaction or no interaction between the compounds in the mixture. Although interactions among chemicals at high doses are well-known, there is currently no single simple approach to judge upon potential interactions at the low doses that humans are exposed to from pesticide residues in food. For this purpose, PBTK models could be useful as tools to assess combined tissue doses and to help predict potential interactions including thresholds for such effects.

The use of PBTK modelling in the risk assessment of mixtures is an upcoming challenge. PBTK models are complex and should of course only be used when it is considered essential. However, they will provide better knowledge and understanding of the effects of mixtures on biological systems and provide improved information on tissue dose levels and variations between species and within a population. Moreover, scientifically supportable results in the risk assessment of mixtures of pesticides would help the risk managers in making more weighty decisions. If the PBTK models are expanded by a toxicodynamic part, the model could be even better and make it possible to identify deviations from additivity at the toxicodynamic level.

Conflict of Interest statement

The authors declare that there are no conflicts of interest.

References

Advisory Committee on Hazardous Substances, 2007. Chemical mixtures: a framework for assessing risks. In: Liu, Q. (Ed.). Version 6.

Andersen, M.E., 2003. Toxicokinetic modeling and its applications in chemical risk assessment. Toxicol. Lett. 138, 9–27.
Andersen, M.E., Krewski, D., 2009. Toxicity testing in the 21st century: bringing the vision to life. Toxicol. Sci. 107, 324–330.
ATSDR, 2001. Guidance for the preparation of an interaction profile. In: Pohl, H., Hansen, H., Wilbur, S., Odin, M., Ingerman, L., Bosch, S., McClure, P., Coleman, J. (Eds.), US Department of Health and Human Services. Public Health Service. Agency for Toxic Substances and Disease Registry. Division of Toxicology.
ATSDR, 2004. Guidance manual for the assessment of joint toxic action of chemical mixtures. In: Wilbur, S., Hansen, H., Pohl, H., Colman, J., Stiteler, W. (Eds.), US Department of Health and Human Services. Public Health Service. Agency for Toxic Substances and Disease Registry. Division of Toxicology.
Balci, O., 1997. Verification, validation and accreditation of simulation models. In: Andradóttir, S., Healy, K.J., Withers, D.H., Nelson, B.L. (Eds.), Proceedings of the 1997 Winter Simulation Conference. IEEE Xplore. pp. 135–141.
Barlow, S., Renwick, A.G., Kleiner, J., Bridges, J.W., Busk, L., Dybing, E., Edler, L., Eisenbrand, G., Fink-Gremmels, J., Knaap, A., Kroes, R., Liem, D., Muller, D.J., Page, S., Rolland, V., Schlatter, J., Tritscher, A., Tueting, W., Wurtzen, G., 2006. Risk assessment of substances that are both genotoxic and carcinogenic report of an international conference organized by EFSA and WHO with support of ILSI Europe. Food Chem. Toxicol. 44, 1636–1650.
Berenbaum, M.C., 1989. What is synergy? Pharmacol. Rev. 41, 93–141.
Bliss, C.I., 1939. The toxicity of poisons applied jointly. Ann. Appl. Biol. 26, 585–615.
Boon, P.E., van Klaveren, J.D., 2003. Cumulative exposure to acetylcholinesterase inhibiting compounds in the Dutch population and young children. Toxic equivalency approach with acephate and phosmet as index compounds. RIKILT—Institute of Food Safety.
Borgert, C.J., Price, B., Wells, C.S., Glenn, S., 2001. Evaluating chemical interaction studies for mixture risk assessment. Hum. Ecol. Risk Assess. 7, 259–306.
Borgert, C.J., Quill, T.F., McCarty, L.S., Mason, A.M., 2004. Can mode of action predict mixture toxicity for risk assessment? Toxicol. Appl. Pharmacol. 201, 85–96.
Bosgra, S., van der Voet, H., Boon, P.E., Slob, W., 2009. An integrated probabilistic framework for cumulative risk assessment of common mechanism chemicals in food: an example with organophosphorus pesticides. Regul. Toxicol. Pharmacol. 54, 124–133.
Botham, P., Chambers, J., Kenyon, E., Matthews, H.B.S., Sultatos, L., Van Pelt, C., Zeise, L., Faustman, E., Mileson, B., 1999. Report of the toxicology breakout group (BOG). In: Mileson, B.E., Faustman, E., Olin, S., Ryan, P.B., Ferenc, S., Burke, T. (Eds.), A Framework for Cumulative Risk Assessment. International Life Sciences Institute, pp. 5–23.
Cassee, F.R., Groten, J.P., van Bladeren, P.J., Feron, V.J., 1998. Toxicological evaluation and risk assessment of chemical mixtures. Crit. Rev. Toxicol. 28, 73–101.
Chiu, W.A., Barton, H.A., Dewoskin, R.S., Schlosser, P., Thompson, C.M., Sonawane, B., Lipscomb, J.C., Krishnan, K., 2007. Evaluation of physiologically based pharmacokinetic models for use in risk assessment. J. Appl. Toxicol. 27, 218–237.
Clewell, R.A., Clewell III, H.J., 2008. Development and specification of physiologically based pharmacokinetic models for use in risk assessment. Regul. Toxicol. Pharmacol. 50, 129–143.
Committee on Toxicity, 2002. Risk assessment of mixtures of pesticides and similar substances. Chairman: Professor Hughes, I., Chairman of the working group on risk assessment of pesticides and similar substances: Professor Woods, H.F. (Eds.), Committee on Toxicity of Chemicals in Food, Consumer Products and the Environment. FSA/0691/0902.
Conolly, R.B., 2001. Biologically motivated quantitative models and the mixture toxicity problem. Toxicol. Sci. 63, 1–2.
Christensen, H.B., Petersen, A., Poulsen, M.E., Grossmann, A., Holm, M., 2006. Pesticide residues in food 2005—results from the Danish pesticide survey [Pesticidrester i fødevarer 2005—resultater fra den danske pesticidkontrol]. Report in Danish. Danish Veterinary and Food Administration. FødevareRapport. p. 23.
DeWoskin, R.S., Thompson, C.M., 2008. Renal clearance parameters for PBPK model analysis of early lifestage differences in the disposition of environmental toxicants. Regul. Toxicol. Pharmacol. 51, 66–86.
EFSA, 2006. Conclusion regarding the peer review of the pesticide risk assessment of the active substance malathion. Finalised 13 January 2006. EFSA Scientific Report 63, pp. 1–86.
EFSA, 2007. EFSA scientific colloquium. 28–29 November 2006—Parma, Italy. Summary report. Cumulative risk assessment of pesticides to human health: the way forward.
EFSA, 2008. Scientific opinion of the Panel on Plant Protection products and their Residues (PPR Panel) on a request from the EFSA evaluate the suitability of existing methodologies and, if appropriate, the identification of new approaches to assess cumulative and synergistic risks from pesticides to human health with a view to set MRLs for those pesticides in the frame of Regulation (EC) 396/2005 (Question No. EFSA-Q-2006-160). EFSA J. 704.
EFSA, 2009. Scientific opinion of the Panel on Plant Protection Products and their Residues (PPR Panel) on a request from European Food Safety Authority on risk assessment for a selected group of pesticides from the triazole group to test possible methodologies to assess cumulative effects from exposure throughout food from these pesticides on human health. EFSA J. 7, 1167.
El-Masri, H.A., Moiz, M., Mumtaz, M.L., Yushak, L., 2004. Application of physiologically-based pharmacokinetic modeling to investigate the toxicological interaction between chlorpyrifos and parathion in the rat. Environ. Toxicol. Pharmacol. 16, 57–71.
El-Masri, H.A., 2007. Experimental and mathematical modeling methods for the investigation of toxicological interactions. Toxicol. Appl. Pharmacol. 223, 148–154.
Feron, V.J., Groten, J.P., Jonker, D., Cassee, F.R., van Bladeren, P.J., 1995a. Toxicology of chemical mixtures: challenges for today and the future. Toxicology 105, 415–427.
Feron, V.J., Groten, J.P., van Zorge, J.A., Cassee, F.R., Jonker, D., van Bladeren, P.J., 1995b. Toxicity studies in rats of simple mixtures of chemicals with the same or different target organs. Toxicol. Lett. 82–83, 505–512.
Feron, V.J., van Vliet, P.W., Notten, W.R.F., 2004. Exposure to combinations of substances: a system for assessing health risks. Environ. Toxicol. Pharmacol. 18, 215–222.
Groten, J.P., Schoen, E.D., van Bladeren, P.J., Kuper, C.F., van Zorge, J.A., Feron, V.J., 1997. Subacute toxicity of a mixture of nine chemicals in rats: detecting interactive effects with a fractionated two-level factorial design. Fundam. Appl. Toxicol. 36, 15–29.
Groten, J.P., Feron, V.J., Suhnel, J., 2001. Toxicology of simple and complex mixtures. Trends Pharmacol. Sci. 22, 316–322.
Haddad, S., Tardif, R., Viau, C., Krishnan, K., 1999. A modeling approach to account for toxicokinetic interactions in the calculation of biological hazard index for chemical mixtures. Toxicol. Lett. 108, 303–308.
Haddad, S., Beliveau, M., Tardif, R., Krishnan, K., 2001. A PBPK modeling-based approach to account for interactions in the health risk assessment of chemical mixtures. Toxicol. Sci. 63, 125–131.
Health Council of the Netherlands, 2002. Exposure to combinations of substances: a system for assessing health risks. Health Council of the Netherlands.
Jensen, A.F., Petersen, A., Granby, K., 2003. Cumulative risk assessment of the intake of organophosphorus and carbamate pesticides in the Danish diet. Food Add. Contam. 20, 776–785.
JMPR, 1993. Pesticide residues in food—1992. Evaluations. Part II—Toxicology. Joint FAO/WHO Meeting on Pesticide Residues. Rome 21–30 September 1992. WHO, Geneva. WHO/PCS/93.34.
JMPR, 1998. Pesticide residues in food—1997. Evaluations. Part II—Toxicological and Environmental. Joint FAO/WHO Meeting on Pesticide Residues. Lyon 22 September–1 October 1997. WHO, Geneva. WHO/PCS/98.6.
JMPR, 2000. Pesticide residues in food—1999. Evaluations. Part II—Toxicological. Joint FAO/WHO Meeting on Pesticide Residues. Rome 20–29 September 1999. WHO, Geneva. WHO/PCS/00.4.
JMPR, 2004. Pesticide residues in food—2003. Evaluations. Part II—Toxicological. Joint FAO/WHO Meeting on Pesticide Residues. Geneva 15–24 September 2003. WHO, Geneva. WHO/PCS/04.1.
Jonker, D., Woutersen, R.A., Feron, V.J., 1996. Toxicity of mixtures of nephrotoxicants with similar or dissimilar mode of action. Food Chem. Toxicol. 34, 1075–1082.
Jonker, D., Woutersen, R.A., van Bladeren, P.J., Til, H.P., Feron, V.J., 1993. Subacute (4-wk) oral toxicity of a combination of four nephrotoxins in rats: comparison with the toxicity of the individual compounds. Food Chem. Toxicol. 31, 125–136.
Jonker, D., Woutersen, R.A., van Bladeren, P.J., Til, H.P., Feron, V.J., 1990. 4-Week oral toxicity study of a combination of eight chemicals in rats: comparison with the toxicity of the individual compounds. Food Chem. Toxicol. 28, 623–631.
Könemann, W.H., Pieters, M.N., 1996. Confusions of concepts in mixture toxicology. Food Chem. Toxicol. 34, 1025–1031.
Krishnan, K., Haddad, S., Béliveau, M., Tardif, R., 2002. Physiological modeling and extrapolation of pharmacokinetic interactions from binary to more complex chemical mixtures. Environ. Health Perspect. 110, 989–994.
Krishnan, K., Paterson, J., Williams, D.T., 1997. Health risk assessment of drinking water contaminants in Canada: the applicability of mixture risk assessment methods. Regul. Toxicol. Pharmacol. 26, 179–187.
Krishnan, K., Andersen, M.E., Clewell III, H.J., Yang, R.S.H., 1994. Physiologically based pharmacokinetic modeling of chemical mixtures. In: Yang, R.S.H. (Ed.), Toxicology of Chemical Mixtures. Academic Press, New York, pp. 399–437.
Larsen, J.C., Binderup, M.-L., Dalgaard, M., Dragsted, L.O., Hossaini, A., Ladefoged, O., Lam, H.R., Madsen, C., Meyer, O., Rasmussen, E.S., Reffstrup, T.K., Søborg, I., Vinggaard, A.M., Østergård, G., 2003. Combined actions and interactions of chemicals in mixtures. The toxicological effects of exposure to mixtures of industrial and environmental chemicals. In: Larsen, J.C. (Ed.). Danish Veterinary and Food Administration. FødevareRapport 12.
Loizou, G., Spendiff, M., Barton, H.A., Bessems, J., Bois, F.Y., d'Yvoire, M.B., Buist, H., Clewell III, H.J., Meek, B., Gundert-Remy, U., Goerlitz, G., Schmitt, W., 2008. Development of good modelling practice for physiologically based pharmacokinetic models for use in risk assessment: the first steps. Regul. Toxicol. Pharmacol. 50, 400–411.
McCarty, L.S., Borgert, C.J., 2006. Review of the toxicity of chemical mixtures: theory, policy, and regulatory practice. Regul. Toxicol. Pharmacol. 45, 119–143.
Mileson, B.E., Chambers, J.E., Chen, W.L., Dettbarn, W., Ehrich, M., Eldefrawi, A.T., Gaylor, D.W., Hamernik, K., Hodgson, E., Karczmar, A.G., Padilla, S., Pope, C.N., Richardson, R.J., Saunders, D.R., Sheets, L.P., Sultatos, L.G., Wallace, K.B., 1998. Common mechanism of toxicity: a case study of organophosphorus pesticides. Toxicol. Sci. 41, 8–20.
Mileson, B.E., Faustman, E., Olin, S., Ryan, P.B., Ferenc, S., Burke, T., 1999. A framework for cumulative risk assessment. In: Mileson, B.E., Faustman, E., Olin, S., Ryan, P.B., Ferenc, S., Burke, T. (Eds.), International Life Sciences Institute. An ILSI Risk Science Institute Workshop Report. pp. 1–55.
Mumtaz, M.M., 1995. Risk assessment of chemical mixtures from a public health perspective. Toxicol. Lett. 82–83, 527–532.

Mumtaz, M.M., De Rosa, C.T., Groten, J., Feron, V.J., Hansen, H., Durkin, P.R., 1998. Estimation of toxicity of chemical mixtures through modeling of chemical interactions. Environ. Health Perspect. 106 (Suppl. 6), 1353–1360.

Mumtaz, M.M., Durkin, P.R., 1992. A weight-of-evidence approach for assessing interactions in chemical mixtures. Toxicol. Ind. Health 8, 377–406.

Müller, A.K., Bosgra, S., Boon, P.E., van der Voet, H., Nielsen, E., Ladefoged, O., 2009. Probabilistic cumulative risk assesment of anti-androgenic pesticides in food. Food Chem. Toxicol., doi:10.1016/j.fct.2009.07.039.

National Research Council, S.D.W.C., 1989. Drinking Water and Health. Selected Issues in Risk Assessment. National Academy Press, Washington, DC.

National Research Council, 1993. Pesticides in the Diets of Infants and Children. National Academy Press, Washington, DC.

Norwegian Scientific Committee for Food Safety, 2008. Combined toxic effects of multiple chemical exposures. In: Alexander, J., Hetland, R.B., Vikse, R., Dybing, E., Eriksen, G.S., Farstad, W., Jenssen, B.M., Paulsen, J.E., Skåre, J.U., Steffensen, I.-L., Øvrebø, S. (Eds.), Vitenskapskomiteen for Mattrygghet/Norwegian Scientific Committee for Food Safety. Report 1.

Reffstrup, T.K., 2002. Combined Actions of Pesticides in Food. Danish Veterinary Food Administration. FødevareRapport 19.

Rowland, M., Balant, L., Peck, C., 2004. Physiologically based pharmacokinetics in drug development and regulatory science: a workshop report (Georgetown University, Washington, DC, May 29–30, 2002). AAPS PharmSci. 6, 1–12.

Safe, S., 1990. Polychlorinated biphenyls (PCBs), dibenzo-*p*-dioxins (PCDDs), dibenzofurans (PCDFs), and related compounds: Environmental and mechanistic considerations which support the development of toxic equivalency factors (TEFs). Crit. Rev. Toxicol. 21, 51–88.

Safe, S.H., 1998. Hazard and risk assessment of chemical mixtures using the toxic equivalency factor approach. Environ. Health Perspect. 106, 1051–1058.

Seed, J., Brown, R.P., Olin, S.S., Foran, J.A., 1995. Chemical mixtures: current risk assessment methodologies and future directions. Regul. Toxicol. Pharmacol. 22, 76–94.

Simmons, J.E., 1996. Application of physiologically based pharmacokinetic modelling to combination toxicology. Food Chem. Toxicol. 34, 1067–1073.

Slikker Jr., W., Andersen, M.E., Bogdanffy, M.S., Bus, J.S., Cohen, S.D., Conolly, R.B., David, R.M., Doerrer, N.G., Dorman, D.C., Gaylor, D.W., Hattis, D., Rogers, J.M., Woodrow, S.R., Swenberg, J.A., Wallace, K., 2004. Dose-dependent transitions in mechanisms of toxicity. Toxicol. Appl. Pharmacol. 201, 203–225.

Svendsgaard, D.J., Greco, W.R., 1995. Session summary: experimental designs, analyses and quantitative models. Toxicology 105, 157–160.

Svendsgaard, D.J., Hertzberg, R.C., 1994. Statistical methods for the toxicological evaluation of the additivity assumption as used in the environmental protection agency chemical mixture risk assessment guidelines. In: Yang, R.S.H. (Ed.), Toxicology of Chemical Mixtures. Academic Press, New York, pp. 599–642.

Teuschler, L.K., 2007. Deciding which chemical mixtures risk assessment methods work best for what mixtures. Toxicol. Appl. Pharmacol. 223, 139–147.

US EPA, 1986. Guidance for health risk assessment of chemical mixtures. Federal Register 51(185). Risk Assessment Forum, US Environmental Protection Agency, Washington, DC. EPA/630/R-98/002. pp. 34014–34025.

US EPA, 1988. Technical Support Document on Risk Assessment of Chemical Mixtures. US Environmental Protection Agency, Environmental Criteria and Assessment Office, Cincinnati. EPA/600/8-90/064.

US EPA, 1989a. Interim Procedures for Estimating Risks Associated with Exposures to Mixtures of Chlorinated Dibenzo-P-Dioxins and-Dibenzofurans (CDDs and CDFs) and 1989 Update. US Environmental Protection Agency, Risk Assessment Forum, Washington DC. EPA/625/3-89/016 (NTIS PB90145756).

US EPA, 1989b. Risk Assessment. Guidance for Superfund, volume 1, Human Health Evaluation Manual (Part A). Interim Final. Risk Assessment Forum, US Environmental Protection Agency, Washington, DC. EPA/540/1-89-002.

US EPA, 1999a. Guidance for Identifying Pesticide Chemicals and Other Substances that have a Common Mechanism of Toxicity. Docket Number: OPP-00542 (Acessed 29-1-1999a).

US EPA, 1999b. Guidance for Performing Aggregate Exposure and Risk Assessments. Office of Pesticide Programs, Environmental Protection Agency. Item: 6043.

US EPA, 2000. Supplementary Guidance for Conducting Health Risk Assessment of Chemical Mixtures. US Environmental Protection Agency. Risk Assessment Forum Technical Panel. Office of EPA/630/R-00/002.

US EPA, 2002. Guidance on Cumulative Risk Assessment of Pesticide Chemicals that have a Common Mechanism of Toxicity. Office of Pesticide Programs. US Environmental Protection Agency. Washington, DC. 20460.

US EPA, 2003. Developing Relative Potency Factors for Pesticide Mixtures: Biostatistical Analyses of Joint Dose-response. National Center for Environmental Assessment. Office of Research and Development. US Environmental Protection Agency. Cincinnati, OH 45268. EPA/600/R-03/052.

US EPA, 2005. Guidelines for Carcinogen Risk Assessment. Risk Assessment Forum. US Environmental Protection Agency. EPA/630/P-03/001F, March 2005.

US EPA, 2006a. Approaches for the application of physiologically based pharmacokinetic (PBPK) models and supporting data in risk assessment. In: Barton, H., Chiu, W., DeWoskin, R., Foureman, G., Krishnan, K., Lipscomb, J., Schlosser, P., Sonawane, B., Thompson, C. (Eds.), National Center for Environmental Assessment. Office of Research and Development. US Environmental Protection Agency, Washington, DC. EPA/600/R-05/043F.

US EPA, 2006b. Cumulative Risk from Chloroacetanilide Pesticides. US Environmental Protection Agency Office of Pesticide Programs Health Effects Division.

US EPA, 2006c. Organophosphorus Cumulative Risk Assessment 2006 update. US Environmental Protection Agency Office of Pesticide Programs.

US EPA, 2006d. Triazine Cumulative Risk Assessment. US Environmental Protection Agency Office of Pesticide Programs Health Effects Division.

US EPA, 2007. Revised *N*-methyl Carbamate Cumulative Risk Assessment. US Environmental Protection Agency Office of Pesticide Programs.

United States of America in Congress, 1996. Food Quality Protection act of 1996. Public Law. 104–170. pp. 1489–1538.

Van den Berg, M., Birnbaum, L., Bosveld, A.T.C., Brunström, B., Cook, P., Feeley, M., Giesy, J.P., Hanberg, A., Hasegawa, R., Kennedy, S.W., Kubiak, T., Larsen, J.C., van Leuwen, F.X.R., Liem, D., Nolt, C., Peterson, R.E., Poellinger, L., Safe, S., Shrenk, D., Tillitt, D., Tysklind, M., Younes, M., Wærn, F., Zacharewski, T., 1998. Toxic equivalency factors (TEFs) for PCBs, PCDDs, PCDFs for humans and wildlife. Environ. Health Perspect. 106, 775–792.

Van den, B.M., Birnbaum, L.S., Denison, M., De, V.M., Farland, W., Feeley, M., Fiedler, H., Hakansson, H., Hanberg, A., Haws, L., Rose, M., Safe, S., Schrenk, D., Tohyama, C., Tritscher, A., Tuomisto, J., Tysklind, M., Walker, N., Peterson, R.E., 2006. The 2005 World Health Organization reevaluation of human and Mammalian toxic equivalency factors for dioxins and dioxin-like compounds. Toxicol. Sci. 93, 223–241.

Wilkinson, C.F., Christoph, G.R., Julien, E., Kelley, J.M., Kronenberg, J., McCarthy, J., Reiss, R., 2000. Assessing the risks of exposures to multiple chemicals with a common mechanism of toxicity: how to cumulate? Regul. Toxicol. Pharmacol. 31, 30–43.